Directed, *Meta*-Selective C–H Functionalisation of Aryl Boronic Acid MIDA Esters

Alexander Williams

Imperial College London

Department of Chemistry

January 2020

A Thesis submitted in Partial Fulfilment for the degree of Ph.D

Declaration of originality

I hereby declare that the content of this thesis is my own work. All additional sources of information have been cited accordingly. Parts excepted are corrections of form and content by both Professor Alan C. Spivey and Dr Christopher Cordier.

Copyright declaration

The copyright of this thesis rests with the author. Unless otherwise indicated, its contents are licensed under a Creative Commons Attribution-Non Commercial 4.0 International Licence (CC BY-NC).

Under this licence, you may copy and redistribute the material in any medium or format. You may also create and distribute modified versions of the work. This is on the condition that: you credit the author and do not use it, or any derivative works, for a commercial purpose.

When reusing or sharing this work, ensure you make the licence terms clear to others by naming the licence and linking to the licence text. Where a work has been adapted, you should indicate that the work has been changed and describe those changes.

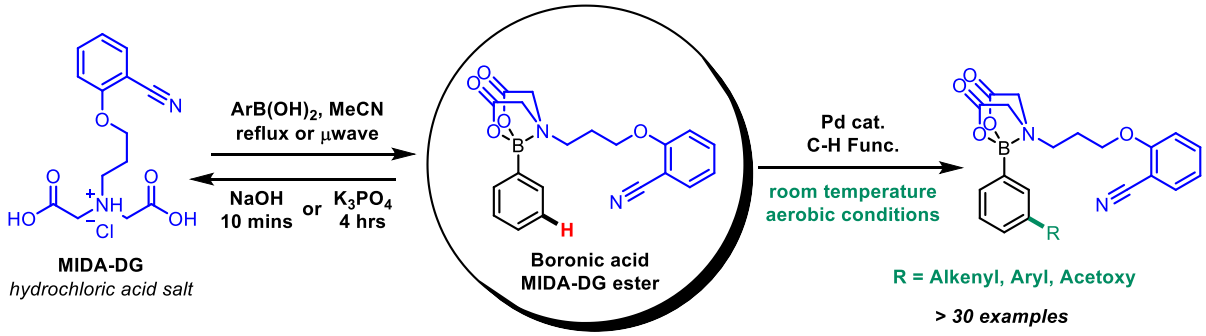
Please seek permission from the copyright holder for uses of this work that are not included in this licence or permitted under UK Copyright Law.

Abstract

Directed C(sp^2)–H functionalisation has emerged as a powerful and economical method for the synthesis of complex aromatic systems. Despite the broad range of directing groups (DGs) developed, those bound by boronic acid functional groups remain limited in number, despite the ubiquity and versatility of aryl boronic acids in organic synthesis. Issues with the reactivity of the functionalities to transition metal catalysts and instability under forcing reaction conditions have hampered their development.

Herein is described the modification of *N*-methyliminodiacetic acid (MIDA) with the tethering of directing motifs for the protection and C–H functionalisation of aryl boronic acids. Initial designs focused on strongly co-ordinating heterocyclic DGs in attempts to achieve *ortho*-C–H functionalisation of phenylboronic acid. Though ultimately unsuccessful, the first generation designs provided valuable information used in the development of a different, second approach.

Changing focus to *meta*-C–H functionalisations and embracing the design principles elucidated during initial investigations allowed the development of a successful, nitrile based, MIDA tethered DG (MIDA-DG).



The MIDA-DG proved simple to install and remove by condensation and hydrolysis respectively, with full recovery of the DG after C–H functionalisation. The development of alkenylation and acetoxylation reactions are described, as is initial work towards the development of C–H arylations.

The benefits of using a boronic acid tethered DG are exemplified, by the removal of the MIDA-DG and diverse derivatisation of the functionalised boronic acid. Using established transformations of boronic acids, a range of functional groups were accessed, including those difficult to prepare using previously available DGs.

Finally, the development of an iterative C–H functionalisation/cross-coupling pathway is outlined, with the expedient synthesis of a 1,3,4,5,-tetrasubstituted aromatic system in just 3 catalytic steps and with one chromatographic purification.

Acknowledgements

I would first like to thank my supervisors Dr Chris Cordier and Prof. Alan Spivey for all the support, advice and wisdom they have imparted over the three years. I would especially like to thank Chris for the amazing opportunity to work on this project, and Alan for helping me to continue this work.

I would also like to thank both of their group members past and present, including, but not limited to, Alex Brown, Kari Mosleh, Richard Thistlewaite, Mahesh Mohan, Josh Linfoot, Stas Piletsky and Alex Swan. Special mention must go to Chris Nielsen who provided an endless source of discussion and kindly proof read this thesis. I would also like to thank Alex Boddy, Ed Briggs, Daniele Antermite, Philipp Natho and the many others who made my time at Imperial College so enjoyable.

I am grateful to the academic and technical staff at Imperial College including Phil Parsons, Peter Haycock, Lisa Haigh and Andrew White for providing helpful discussion and aiding in the collection of data during the project.

I must mention my housemates Ted Rowntree, Tom Corkett, Xavier White de Groote, Simon Vinall, Steve Brzezicki, Nick Bantick and Luke Shermer for providing endless entertainment as well as endless 5-a-side trophies (with the help of one Daniel Cartland) over the three years. Special mention also to my very brief housemates Jack Barber, Amelia Kenneth and Isla Featherstone-Clarke. I must thank Tom Claessens for organising such excellent holidaying experiences and finally all of the Fun-done-in London bunch, who are too many to name, but to whom I am eternally grateful.

Lastly, I would like to thank the lovely Charlie Pickering and my family, Sarah, Tim, Becca and Rory Williams for all their love, encouragement and support.

Finally, this thesis is dedicated to my good friend Greg McHugh who will always be missed.

Abbreviations

AAM	Anthranilamide
Ac	Acetyl
Ac-Gly-OH	*N*-Acetylglycine
Ac-Phe-OH	*N*-Acetylphenylalanine
AcOH	Acetic acid
Ad	Adamantyl
AIBN	Azobisisobutyronitrile
AQ	8-Aminoquinoline
Bn	Benzyl
Boc	*tert*-Butyloxycarbonyl
BQ	Benzoquinone
CAN	Ceric ammonium nitrate
cf.	Short for the Latin: *confer/conferatur*, both meaning 'compare'
CMD	Concerted metalation deprotonation
cod	Cyclooctadiene
Cy	Cyclohexyl
dan	1,8-Diaminonapthalene
DCC	*N,N'*-Dicyclohexylcarbodiimide
DCE	1,2-Dichloroethane
DCM	Dichloromethane
DEA	diethanolamine
DFT	Density functional theory
DG	Directing group
DIAD	Diisopropyl azodicarboxylate
DIPEA	*N,N,N*-Diisopropylethylamine

DMF	*N,N*-dimethylformamide
DMSO	Dimethylsulfoxide
DOE	Design of experiment
Eq.	Equivalents
Et	Ethyl
GC	Gas chromatography
H	hours
HFIP	1,1,1,3,3,3-Hexafluoroisopropanol
IDA	Iminodiacetic acid
LiTMP	Lithium tetramethylpiperidine
Me	Methyl
MeCN	Acetonitrile
MeOH	Methanol
Mes	Mesityl
MIDA	*N*-Methyliminodiacetic acid
mom	Methoxymethyl ether
MPAA	Mono-protected amino acid
MS	Molecular sieves
NCS	*N*-Chlorosuccinimide
NMR	Nuclear Magnetic Resonance
PA	Picolinamide
PIDA	Pinene derived iminodiacetic acid
Pin	Pinacol
Piv	Pivalate
PMB	*para*-Methoxybenzene
ppm	Parts per million

PZA	2-Pyrazol-5-ylaniline
RMSE	Root mean square error
r.t.	Room temperature
SAR	Structure activity relationship
S_NAr	Nucleophilic aromatic substitution
TBAI	Tetrabutylammonium iodide
$TBAPF_6$	Tetrabutylammonium hexafluorophosphate
TEA	Triethylamine
Tf	Triflate
TFA	Trifluoroacetic acid
TFE	2,2,2-Trifluoroethanol
THF	Tetrahydrofuran
TS	Transition state
TsOH	*p*-Toluenesulfonic acid
VT	Variable temperature
Z-Gly-OH	*N*-Carbobenzyloxyglycine

Contents

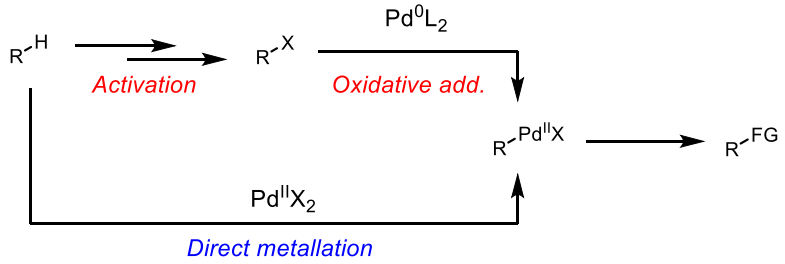
Declaration of originality 1
Copyright declaration 1
Abstract 2
Acknowledgements 3
Abbreviations 4
1. Introduction 9
1.1 Palladium Catalysed C(sp^2)–H Functionalisation 9
1.1.1 Mechanistic Insights 10
1.1.2 Pyridyl, Picolinamide and 8-Amidoquinoline DGs 16
1.1.3 Weakly Coordinating DG Strategies 21
1.2 Boronic Acid Based DGs in C–H Functionalisation 28
1.3 *N*-Methyliminodiacetic Acid (MIDA) Boronate Esters 34
1.3.1 Structure and Properties 34
1.3.2 Synthetic Applications of Boronic Acid MIDA esters 38
1.4 Aims and Objectives 44
2. First Generation Designs 46
2.1 Design of DGs 46
2.2 Synthesis of the First Generation DGs 48
2.2.1 Synthesis of PhB(IDA-AQ) 187 48
2.2.2 Synthesis of PhB(IDA-PA) 188 52
2.3 Investigations into *ortho*-C(sp^2)–H Arylation Reactions 54
2.3.1 Method Development 54
2.3.2 Screening of Reagents and Conditions 56
2.3.3 Investigations into PhB(IDA-PA) 188 and PhB(IDA-AQ) 187 Stability 59
3. Second Generation Designs 62
3.1 A Different Approach 62
3.1.1 Design of the Second Generation DGs 65
3.2 Synthesis of the Second Generation DGs 69
3.2.1 *Meta*-Selective DGs 69
3.2.2 *Para*-Selective DG 75
3.3 Screening of the Second Generation DGs 76
4. C–H Alkenylations Using the MIDA-DG Boronate Ester 82
4.1 Optimisations 82
4.1.1 Design of Experiment (DOE) Optimisation of Reaction Conditions 82

4.1.2 Optimisation of the MIDA-DG Synthesis 90
4.2 Investigating the Scope of the C–H Alkenylation Reaction 91
4.2.1 Varying Aryl Boronic Acids 91
4.2.2 Varying the Alkene Coupling Partner 95
4.2.3 Protecting Group Conversion of the Alkenylated Products 97
5. C–H Acetoxylations and C–H Arylations Using the MIDA-DG Boronate Ester 99
5.1 Development of C–H Acetoxylations 99
5.1.1 Reaction Discovery and Optimisation 99
5.1.2 Scope of the C–H Acetoxylation Reaction 102
5.1.3 Oxidation of the C–H Acetoxylated Products 105
5.2 Development of C–H Arylations 106
6. Derivatisations and Applications of C–H Functionalised Boronic Acids 112
6.1 Derivatisation of Functionalised Boronic Acids 112
6.1.1 Large Scale C–H Alkenylation 112
6.1.2 Deprotection and Recovery of the MIDA-DG 113
6.1.3 Derivatisation of the Deprotected Boronic Acids 114
6.2 Applications of MIDA-DG Boronate Esters 117
6.2.1 MIDA-DG as a Protecting Group For Boronic Acids 117
6.2.2 Iterative Synthetic Pathways Using MIDA-DG Boronate Esters 120
7. Conclusions 123
Experimental 129
General Experimental Details 129
Chapter 2 130
Chapter 3 138
Chapter 4 152
Chapter 5 195
Chapter 6 206
X-Ray Crystallisation Data 214
References 225

1. Introduction

1.1 Palladium Catalysed C(sp²)–H Functionalisation

Palladium catalysed carbon–hydrogen (C–H) functionalisation involves the activation of a carbon-hydrogen bond by palladium, allowing subsequent conversion to a carbon-carbon (C–C) or carbon-heteroatom bond.[1,2] Classical cross-coupling approaches for forming these bonds involve the formation of a reactive organometallic species (R–Pd^{II}), after oxidative addition into an activated carbon-halogen or pseudo-halogen bond.[3,4] C–H functionalisation chemistry aims to access these valuable R–Pd^{II} intermediates directly from less activated C–H bonds, which are ubiquitous within organic frameworks (**Scheme 1**).[5]



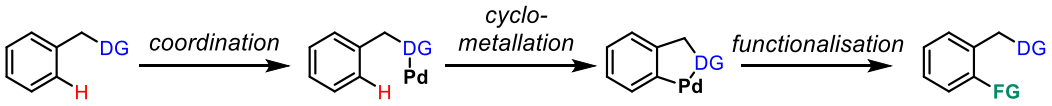
Scheme 1: A comparison between different routes to the key R–Pd^{II} intermediate in aryl functionalisation reactions — via a classical cross-coupling sequence and a C–H functionalisation reaction.

The resulting transformations allow economical and sustainable routes to complex chemicals such as natural products, pharmaceuticals, agrochemicals, and fine chemicals.[6,7,8]

The activation of C–H bonds involves a number of challenges. The ubiquity of C–H bonds within organic molecules raises issues of both regio- and chemo-selectivity,[9,10] while the combined low bond dissociation energies and polarities of C–H bonds make insertion energetically problematic.[11]

It has been known since the 1960s that palladium and other transition metals can insert into C(sp²)–H bonds when facilitated by co-ordination to a proximal Lewis base 'directing group' (DG).[12] Palladium is particularly suited to C–H functionalisation chemistry for a number of reasons. The chemistry of organo-palladium(II) species is well established and Pd^{II} is compatible with numerous oxidants and often with aerobic and hydrous conditions.[3,13] Lastly, cyclometallation with palladium has been shown to be directed by numerous Lewis-basic functional groups.[5]

These characteristics have since been exploited to address the challenges associated with selective activation of C–H bonds.[9] Numerous methods have been developed using Lewis basic functionalities to ligate a Pd catalyst, bringing it into close proximity with the targeted bond and allowing regioselective activation and functionalisation (**Scheme 2**).[5]

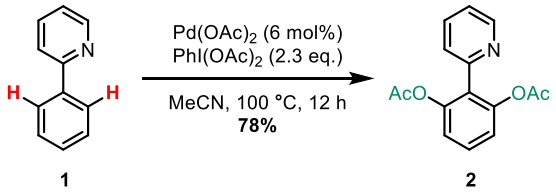


Scheme 2: The role of a DG in facilitating the C–H insertion of palladium to allow access to valuable organopalladium species for diverse functionalisation.

1.1.1 Mechanistic Insights

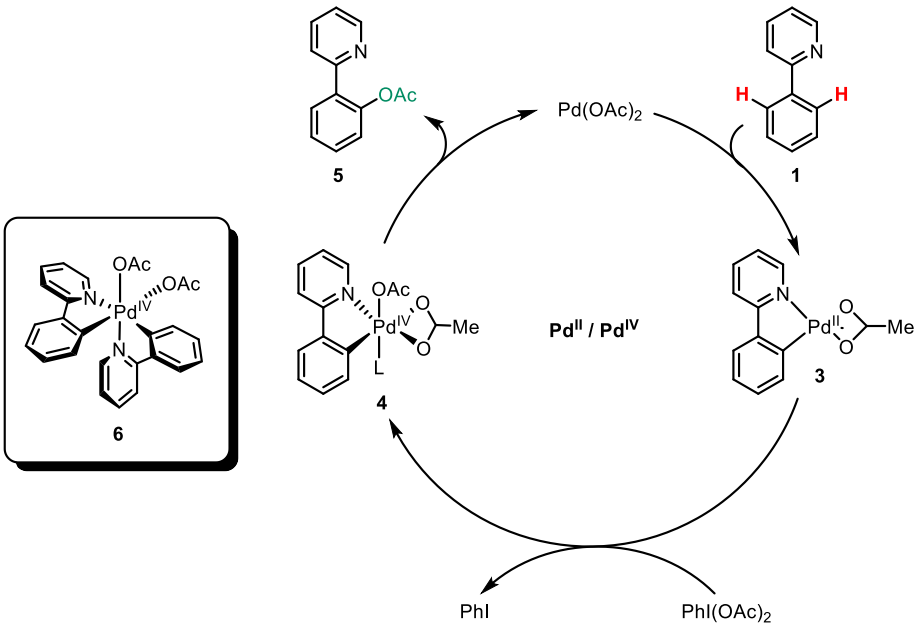
A classic model system in palladium catalysed C(sp^2)–H activation is 2-phenylpyridine **1**. By judicious choice of reagents and conditions, different mechanistic pathways have been invoked to achieve a variety *ortho* of C–H functionalisations in the phenyl ring using the pyridine nitrogen as the directing motif. The insights derived from these studies were applied when investigating palladium catalysed C–H functionalisation processes employing other more complex systems.

For example, Sandford employed $PhI(OAc)_2$ with catalytic $Pd(OAc)_2$ to achieve *bis* C–H acetoxylation at the *ortho* position; it was proposed that this was occurring *via* a Pd^{II}/Pd^{IV} catalytic cycle (**Scheme 3**).[14,15]



Scheme 3: Sanford's C(sp^2)-H oxidation using a pyridyl DG.[14,15]

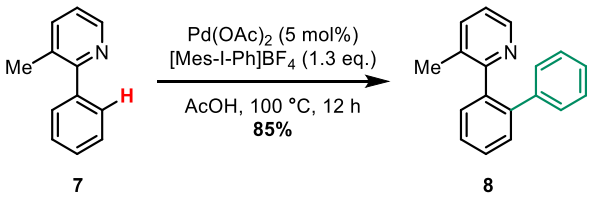
The suggested mechanism begins with the formation of a 5-membered metallocycle **3** after C–H 'insertion'. Two electron oxidation of the Pd^{II} to Pd^{IV} by $PhI(OAc)_2$ then generates the octahedral intermediate **4** which can undergo reductive elimination to yield the mono-acetoxylated product **5**. A second acetoxylation, by the same mechanism, subsequently yields the final product **2** (**Scheme 4**).



Scheme 4: Sanford's proposed mechanism for C-H acetoxylation involving a Pd^{II}/Pd^{IV} catalytic cycle.[14,15]

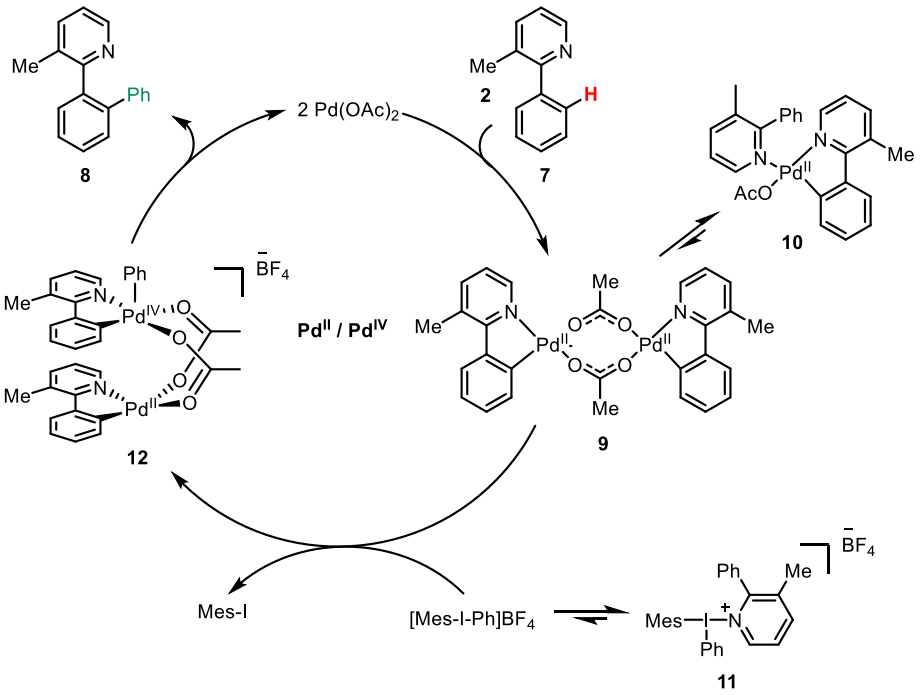
The proposed mechanism has been investigated in some detail. Kinetic isotope effects indicate that the initial cyclopalladation step is rate limiting,[16] while synthesis and isolation of an analogous [Pd^{IV}(2-phenylpyridine)$_2$(OAc)$_2$] species **6** (**Scheme 4**, boxed structure) provided evidence that the two electron oxidation to Pd^{IV} is feasible.[17] On heating, the compound **6** also underwent quantitative reductive elimination to give the acetoxylated product **5**.

A similar Pd^{II}/Pd^{IV} catalytic cycle has been invoked in C(sp^2)–H arylations using diaryliodonium salts (**Scheme 5**).[18,19]



Scheme 5: C–H arylation using diaryliodonium salts.[18,19] *The 3-methyl substituent prevents di-arylation. Mes = mesityl.*

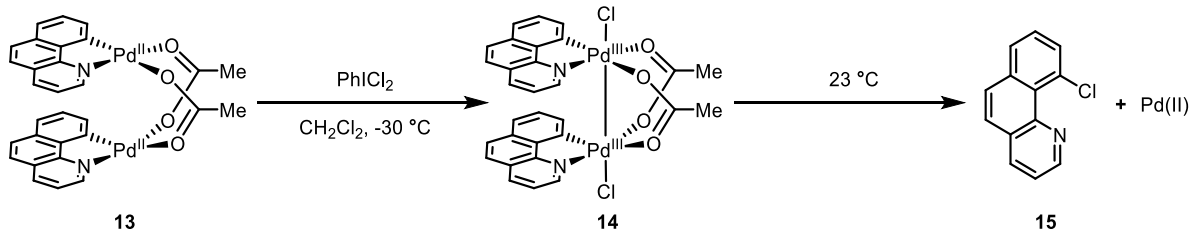
Interestingly, mechanistic work elucidated the presence of two off-cycle species (**10** and **11**) and the involvement of two dimeric palladium species (**9** and **12**).[20] The modified catalytic cycle is shown in **Scheme 6**.



Scheme 6: Mechanism for C-H arylation showing dimeric palladium species and off-cycle intermediates.[18,19]

The key individual steps remain broadly the same to those proposed for C–H acetoxylations (i.e **Scheme 4**). $Pd(OAc)_2$ insertion, facilitated by co-ordination to the DG, is followed by oxidation to a Pd^{IV} intermediate, followed by reductive elimination to yield the desired product. However, in contrast to the acetoxylation reaction, the C–H arylation was observed to be second order in [Pd], indicating an acetate bridged Pd^{IV}–Pd^{II} dimer **12** as a key intermediate. Proton NMR studies also indicated the presence of intermediates **10** and **11** as the off-cycle resting states of the oxidant and catalyst. The Pd^{VI}–Pd^{II} dimeric species could potentially have been described as a Pd^{III}–Pd^{III} dimer. However, DFT calculations suggested that the Pd–Pd interaction in this structure was minimal, disfavouring the symmetrical Pd^{III}–Pd^{III} species.[5]

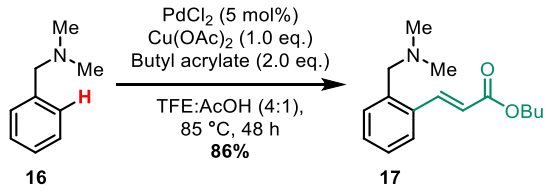
Significant Pd–Pd interactions suggesting the presence of Pd^{III}–Pd^{III} dimeric species have been observed in other, similar systems however.[21,22] Two electron oxidation employing NCS or $PhICl_2$ of the bicyclopalladated species **13** leads to formation of the dimeric Pd^{III} species **14**, with a synergistic relationship between the two Pd centres during oxidation and subsequent, bimetallic, reductive elimination (**Scheme 7**).[23,24]



Scheme 7: The synthesis and subsequent bimetallic reductive elimination of a dimeric Pd^{III} species in the chlorination of benzo[H]quinone.[23]

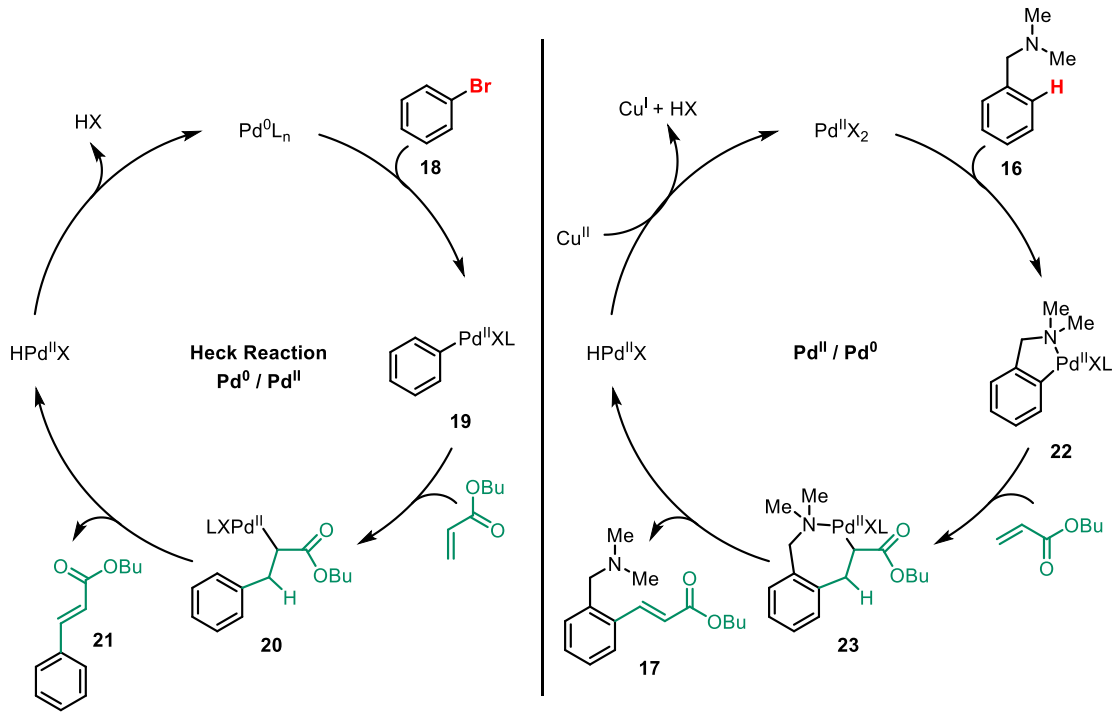
The Pd^{III} dimers were observed when performing C(sp^2)–H chlorinations, brominations and acetoxylations of benzo[*H*]quinone. As such, Pd^{II}/Pd^{III} catalytic cycles must be considered when investigating purported Pd^{II}/Pd^{IV} cycles.

Activation of C(sp^2)–H bonds generally occurs at Pd^{II} centres, leading to cyclopalladated intermediates such as **3**, **9** and **13,** already shown.[5] In contrast to the previously discussed mechanisms, redox neutral processes can also occur at these R–Pd^{II} intermediates, before reductive elimination from the Pd^{II} centre. The resulting Pd^{II}/Pd^{0} catalytic cycles are often invoked in palladium catalysed C(sp^2)–H functionalisations.[25,26] An example of a reaction proposed to involve such a cycle is the alkenylation enabled by a tertiary amine DG shown in **Scheme 8**.



Scheme 8: Alkenylation of N,N-dimethylbenzylamines with $PdCl_2$.[27]

The *ortho*-C(sp^2)–H alkenylation of **16** proceeds in high yield following a mechanism that can be compared to a Heck reaction (**Scheme 9**).[27]

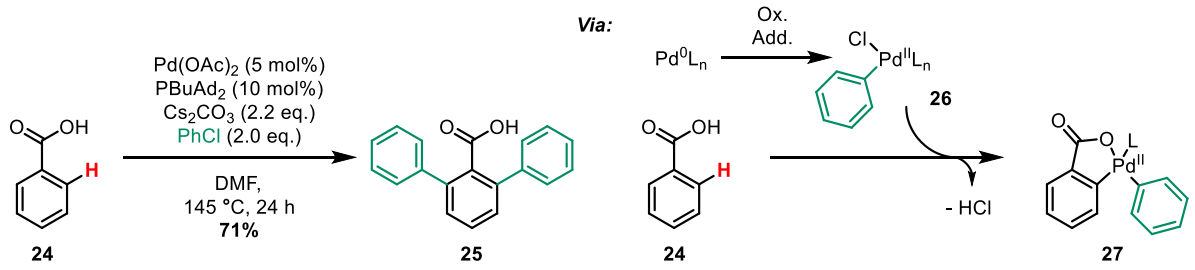


Scheme 9: Comparisons between the mechanism of a Heck reaction and that of a Pd^{II}/Pd^{0} C–H alkenylation reaction. Comparisons can be also drawn between Suzuki-Miyaura cross-coupling mechanisms and that of a C–H arylation using aryl boronic esters.[27]

Crucially, the aryl Pd^{II} species **22** that undergoes migratory insertion is generated from a redox neutral process, not oxidative addition. As such, the Pd^{0} species formed after reductive elimination must be oxidised using an external oxidant, in this case $Cu(OAc)_2$. Other terminal oxidants often used in Pd^{II}/Pd^{0} catalytic cycles include molecular oxygen or silver salts — also commonly employed as halide scavengers.[28,29,30] While the benefit of an external oxidant over a halide-activated arene may be unclear in the simple systems shown in **Scheme 9**, in more complex systems where accessing the halogenated aryl system may be difficult, this represents a distinct improvement.

Similar to the comparisons drawn with the Heck reaction, when employing reagents that undergo facile transmetalation (e.g. boronic esters) similar parallels can be drawn with Suzuki-Miyaura cross-coupling mechanisms.[31,32] Transmetalation to a cyclopalladated intermediate (such as **22**) is followed by reductive elimination to yield the functionalised products and an inactive Pd^{0} species. Oxidation subsequently regenerates the active Pd^{II} catalyst.

By contrast, C(sp^2)–H arylations using aryl chlorides as coupling partners have been proposed to proceed via a Pd^{II}/Pd^{0} mechanism without the need for an external oxidant (**Scheme 10**).[33,34]

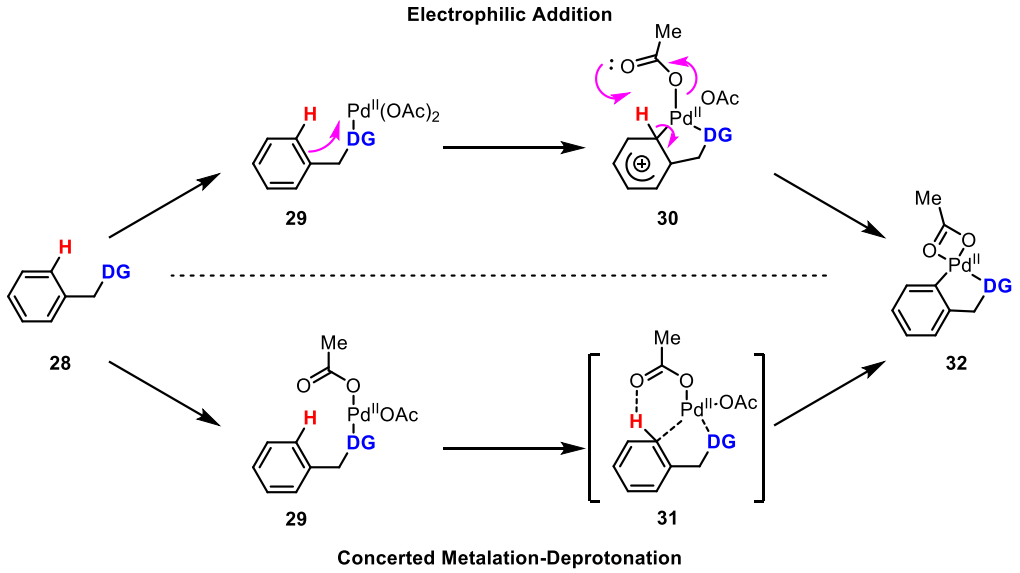


Scheme 10: The C–H arylation of benzoic acids with aryl chlorides showing how oxidation of Pd^{0} to Pd^{II} is achieved by oxidative insertion, without the need for an external oxidant.[33,34]

In these rarer cases, oxidative addition first generates the active organo-Pd^{II} species **26**. Subsequent cyclopalladation, forming complex **27**, and reductive elimination yields the arylated product **25**. When aryl iodides are used in place of aryl chlorides, the mechanism is proposed to switch to a Pd^{II}/Pd^{IV} cycle (analogous to that shown in **Scheme 4**).

Common to both Pd^{II}/Pd^{IV} and Pd^{II}/Pd^{0} cycles discussed is the functionalisation of a C(sp^2)–H bond with a Pd^{II} species. A number of mechanisms have been proposed for this key step including electrophilic addition,[35,36,37] oxidative insertion,[38] a Heck-like process,[39] or a concerted

metalation-deprotonation (CMD) event.[40,41,42] The two mechanistic processes most often invoked, electrophilic addition and CMD, are shown in **Scheme 11**.



Scheme 11: Two potential mechanisms for Pd^{II} insertion into a C–H bond.

The electrophilic addition mechanism begins with nucleophilic attack from the arene to the proximal, coordinated electrophilic Pd^{II} centre.[43] The resulting intermediate **30** is analogous to a Wheland intermediate. Consequently, Hammet analysis has been employed as a key diagnostic for this mode of C–H insertion.[35,] Deprotonation and recovery of aromaticity may be accelerated by 'lone-pair assistance' from carboxylate or heteroatom ligands, or by an external base.[44]

In contrast to the step-wise electrophilic addition mechanism, a concerted metalation-deprotonation event can occur.[45,46] After coordination to the DG, a six-membered transition state **31** can be invoked with a carboxylate (or other)[47] ligand, breaking the C–H and Pd–OAc bonds while concomitantly forming the Pd–H and AcO–H bonds in a concerted manner (transition state **31**).[48,49] This results in minimal build-up of charge on the aryl ring and, as such, transformations proceeding via the CMD pathway may be less susceptible to variations in the electron demand of arene substituents.

In general, electron-rich aromatics and electron-deficient ligands on the Pd^{II} catalyst, such as TFA, will favour an electrophilic addition mechanism, while CMD is preferred in less electron-rich systems.[50]

The regioselectivity of the cyclopalladation event is largely dictated by proximity to the C–H bond and the ring size of the palladacycle formed. Analogous to carbocyclic systems, 5 and 6 membered systems are thermodynamically and kinetically favoured, though not exclusively.[51,52] As such,

palladium catalysed C(sp^2)–H functionalisation protocols generally activate the proximal *ortho* position, with *meta* and *para* activating methods being less well explored.[53]

1.1.2 Pyridyl, Picolinamide and 8-Amidoquinoline DGs

The key requirement for a DG motif is a Lewis-basic functional group that is able to coordinate and selectively direct a palladium catalyst. As such, numerous functional groups have been developed for *ortho*-C(sp^2)–H functionalisations.[9] Among these, monodentate pyridyl **33** and bidentate, monoanionic picolinamide (PA) **34** and 8-aminoquinoline (AQ) **35** DGs have emerged as privileged examples (**Figure 1**).

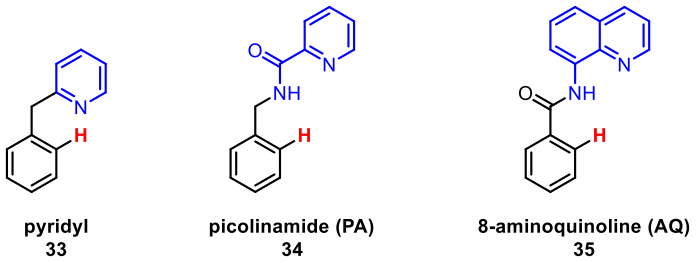
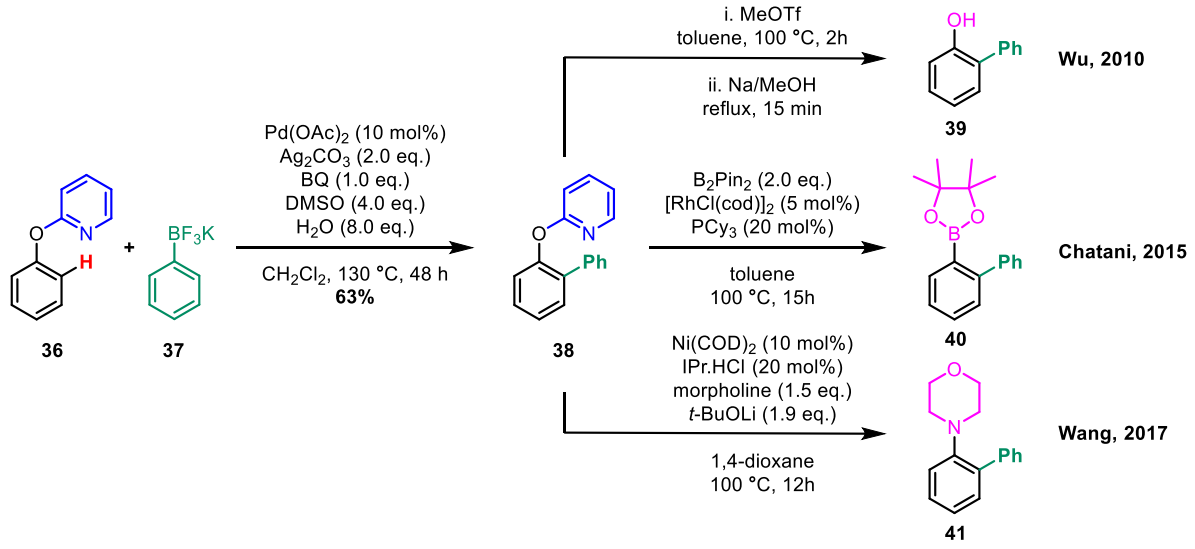


Figure 1: General structures of pyridyl, PA and AQ DGs for ortho C(sp^2)–H functionalisation

Pyridyl DGs were first utilised for Ru-catalysed processes,[54] before their use was extended to palladium catalysed processes by Sanford and Daugulis.[14,55] Since these seminal studies, numerous pyridine-based scaffolds and transformations have been developed. The popularity of pyridine-based DGs has several origins. Pyridine and related aromatic N-heterocycles are often found in bioactive compounds, avoiding the need for their explicit introduction.[56] If not inherent within the molecule of interest, pyridine functional groups are simple to introduce into compounds using cross-coupling chemistry.[57] Lastly, the strong coordination of the pyridine to palladium can often out-compete other coordinating functionalities that could otherwise cause selectivity issues.[58]

Using the 2-phenylpyridine DG **1** previously discussed (see: **Scheme 3** and **Scheme 5**) as an example, since Sanford's seminal oxidation with $PhI(OAc)_2$,[14] *ortho*-C(sp^2)–H arylations,[18,19,55,59] halogenations,[60–62] cyanations,[63] esterifications,[64,65] sulfonylations,[66] and amino and aryl carbonylations have been developed.[67–71] However, the attachment of the DG via a C–C bond represents a synthetic cul-de-sac. It is only useful for compounds inherently containing a 2-phenylpyridine or related moiety. As such, large efforts have been made to design pyridine based DGs that can be removed and further functionalised.

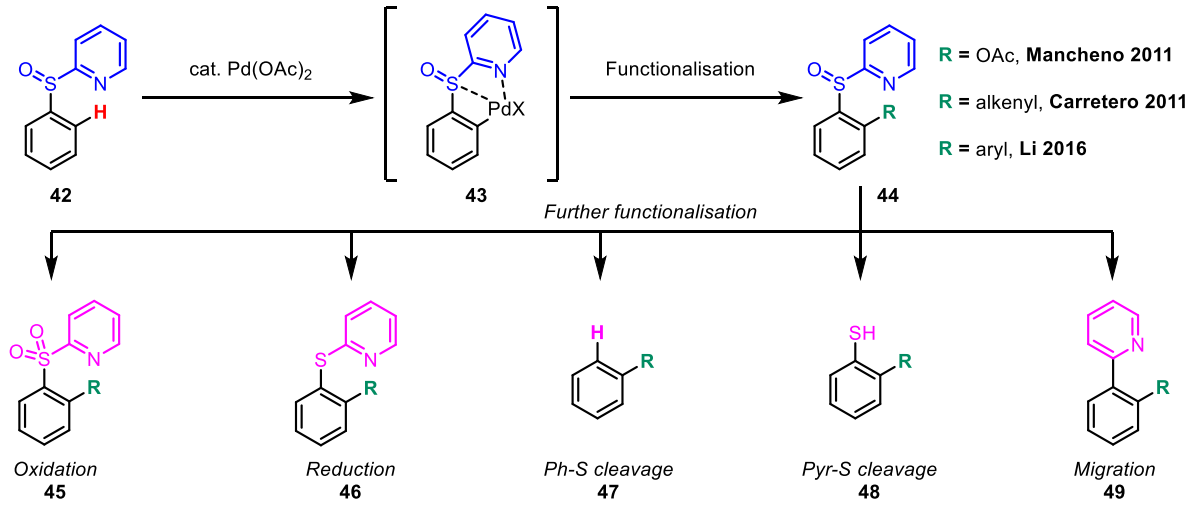
Wu *et al.* recognised that an ether bridged pyridine DG **36** would allow derivatisation of the C–H functionalised product and offer greater synthetic versatility than a classic C–C bonded system (**Scheme 12**).[72]



*Scheme 12: Wu's O-tethered pyridine DG, which offers greater synthetic versatility than C–C bound systems (e.g. 2-phenylpyridine **1**)* [72,73,74,75]

Activation of the pyridine ring using MeOTf allows cleavage to reveal a phenol (**39**) for further elaboration. Building on this work, Chatani developed Rh and Ni catalysed conditions for the borylative cleavage of the DG, installing highly versatile boronic esters (**40**) in the place of the DG.[73,74] Lastly, Wang developed an amination of the DG, again using Ni^0 catalysis (compound **41**).[75]

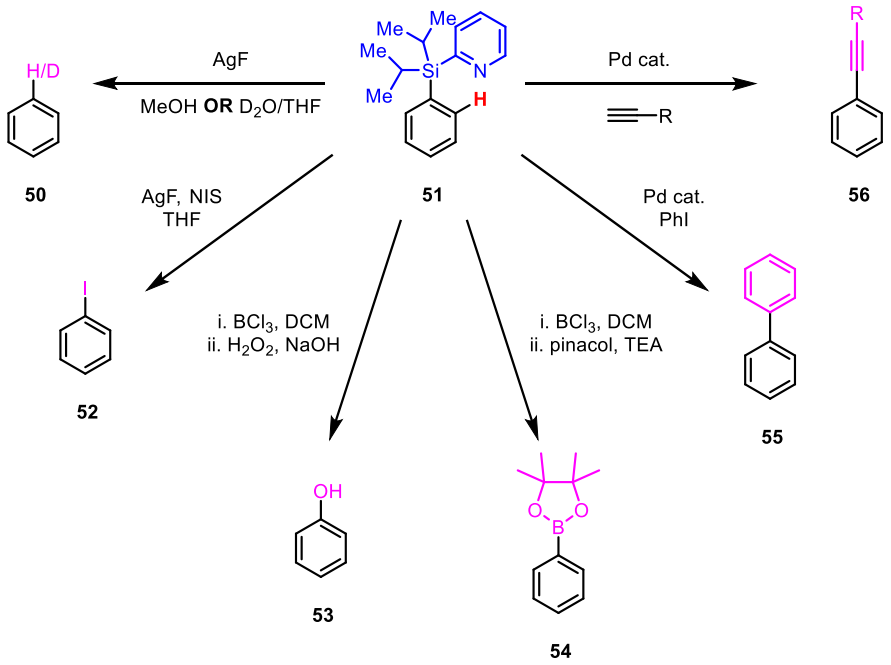
Sulfoxide linked pyridyl systems, developed concurrently by Mancheno and Carretero, also provide a synthetic handle for removal of the pyridine ring whilst aiding in coordination of the catalyst (**Scheme 13**).[76,77]



Scheme 13: Synthetic transformations of sulfoxide linkers showing how a second coordination site can aid C–H insertion, as well as providing a synthetic handle for further functionalisation.[76,77]

The sulfoxide-containing DG **42** proved active in C–H acetoxylations and alkenylations, proceeding via Pd^{II}/Pd^{IV} and Pd^{II}/Pd^{0} mechanisms respectively. This was later expanded to C–H arylations by Li.[78] The sulfoxide linker could subsequently be oxidised (**45**), reduced (**46**), and cleaved at the phenyl–S (**47**) or pyridyl–S bonds (**48**).[76,77] The phenylpyridine **49** was also accessible after C–H functionalisation.

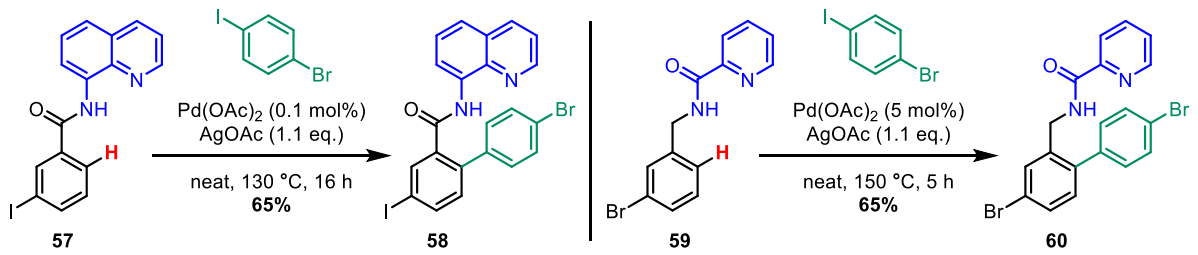
In 2011, Gevorgyan developed an extremely versatile silyl-linked pyridyl DG (**51**), termed PyDipSi, that was amenable to a broad range of transformations after C–H functionalisation (**Scheme 14**).[79]



Scheme 14: Pathways for further functionalisation of Gevorgyan's PyDipSi DG.[79]

Utilising Hiyama-Denmark style cross-coupling conditions,[80] palladium catalysed arylations and alkynylations were possible, yielding structures such as **55** and **56**. The DG could also act in a 'traceless' manner, with cleavage to give simply C–H or C–D bonds (**50**). The C–H functionalisation reaction repertoire was later expanded by Zhang to include alkylations.[81]

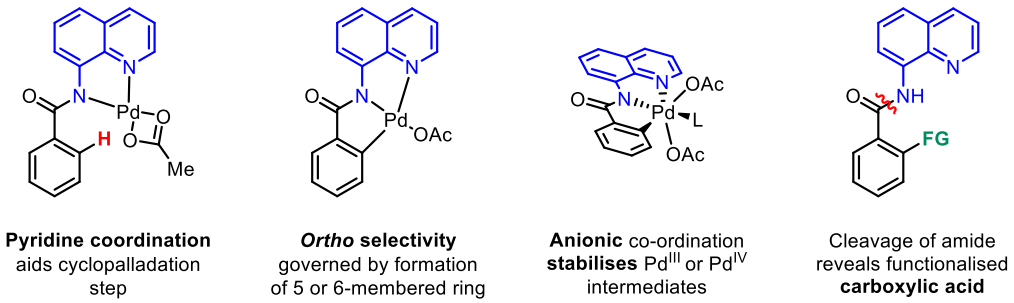
8-Aminoquinoline **35** and picolinamide **34** DGs were first introduced by Daugulis in 2005 for the $C(sp^2)$–H and $C(sp^3)$–H arylation of carboxylic acids and amines (**Scheme 15**).[82]



Scheme 15: Daugulis' 8-aminoquinoline (AQ) and picolinamide (PA) based DGs.[82]

Since Daugulis' seminal work, these scaffolds have been employed in numerous C(sp^2)–H functionalisations, catalysed by palladium and other metals.[9,83,84]

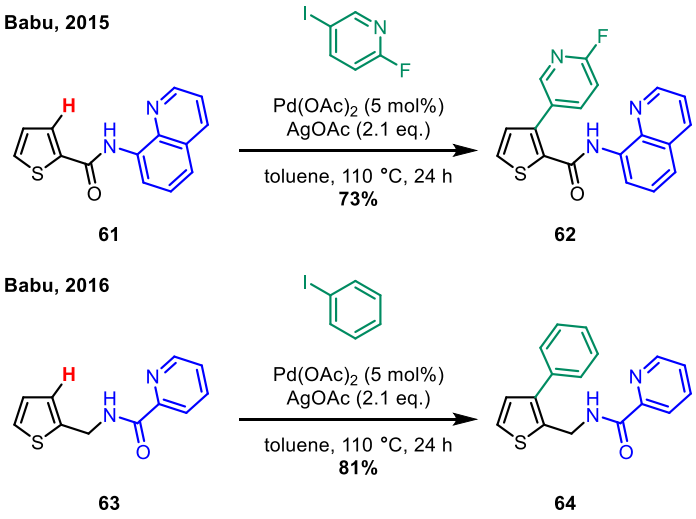
The mono-anionic bidentate groups are privileged scaffolds in C–H functionalisation for a number of reasons. The AQ and PA DG are installed by simple amide coupling to either a carboxylic acid or amine precursor respectively — functionalities often found in complex molecules and chemical building blocks. The pyridyl component of each DG facilitates cyclometallation,[83] while the coordination of the mono-anionic amide is able to stabilise any high-valent Pd^{III} or Pd^{IV} species formed (**Scheme 16**).[85]



Scheme 16: Structural features of the AQ DG that facilitate its role as an efficient DG. These structural features are also found on PA based DGs.

Lastly, unlike C–C bonded pyridyl systems which required modification to increase synthetic utility (*vide supra*), the AQ and PA DGs are attached by amide bonds. Cleavage of these reveals the parent carboxylic acids or amines.

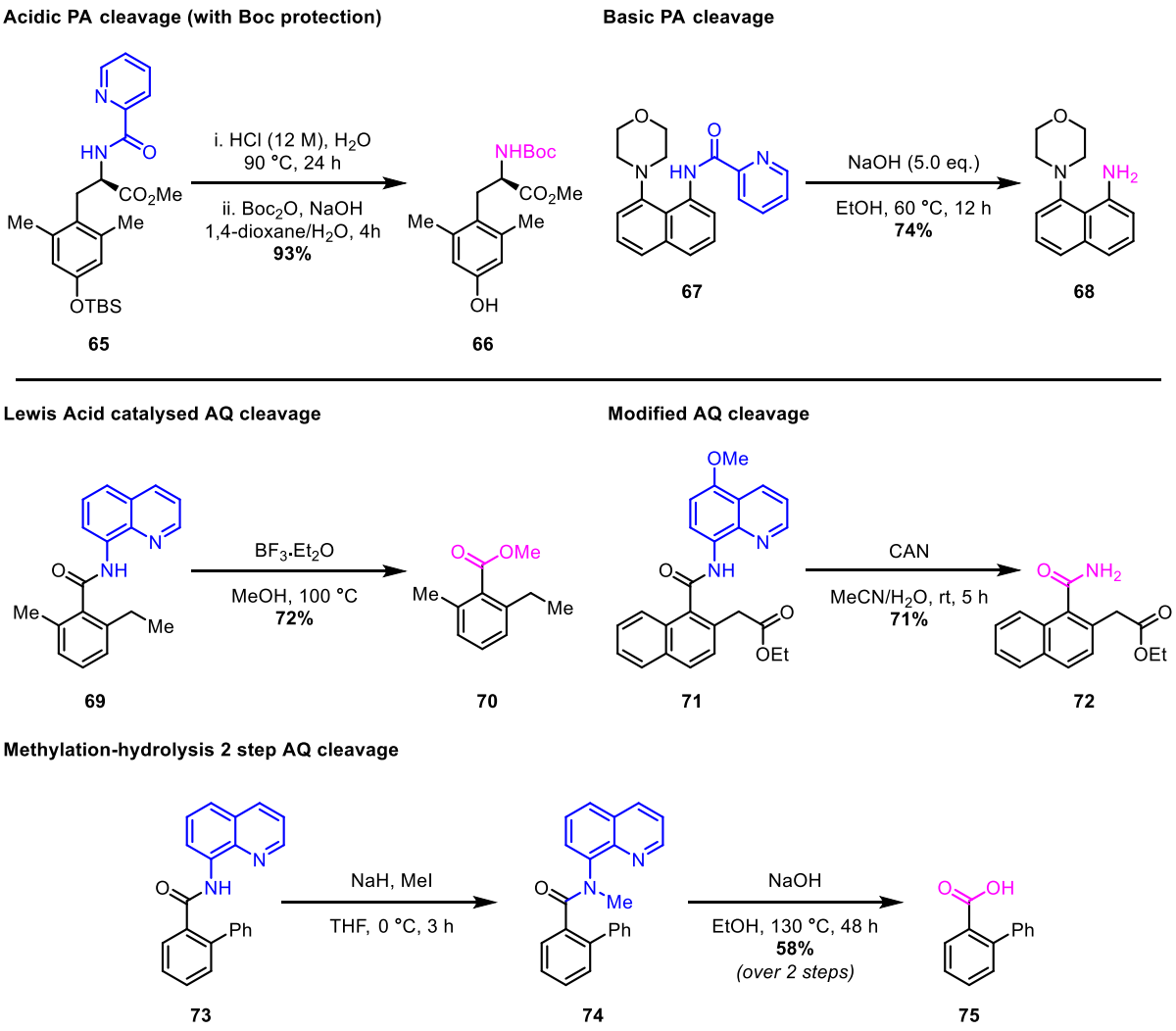
As an example of the utility of the AQ and PA DGs, Babu was able to achieve palladium catalysed C–H (hetero)arylations of thiophenes **61** and **63** at the C3 positions (**Scheme 17**).[86,87]



Scheme 17: C3 arylation of thiophenes developed by Babu.[86,87] The AQ and PA DGs allow complementary arylation of both 2-carboxylic acid and 2-methylamino thiophenes.

The use of these bidentate DGs allowed successful *ortho*-selective C–H activation, despite potential competitive coordination to the thiophene, and activation of the C3 position over the usually more reactive C5 position (by S_EAr chemistry). Other transformations developed using AQ and PA DGs include arylations,[88,89] alkylations,[90,91] alkenylations,[92] and aminations.[93] Considerable effort has also focused on palladium catalysed C(sp^3)–H functionalisations, where AQ and PA DGs have emerged as particularly useful scaffolds for performing these difficult transformations.[83,84]

The removal of the DG scaffolds is key to their synthetic utility. The picolinamide DG can be cleaved under acidic or basic conditions to reveal the desired amine (**Scheme 18**, top).[90,93]



Scheme 18: An overview of the various methods available for removing the AQ and PA DGs. CAN = cerium ammonium nitrate [90,93,91,94,95]

The 8-aminoquinoline DG can require more forcing conditions to remove. As such, methods to facilitate the amide cleavage, or access different functional groups have been developed (**Scheme 18**, bottom). These include Lewis acid assisted esterification, amine methylation then hydrolysis, or modification of the DG itself (compound **71**) to allow transamidation with cerium ammonium nitrate (CAN).[91,94,95]

1.1.3 Weakly Coordinating DG Strategies

Alongside the use of strongly coordinating *N*-heterocyclic DGs, a second, distinct strategy for C(sp^2)–H functionalisation using weakly coordinating DGs has been pioneered by Yu.[96,97] *Ortho*-C–H insertions to form 5 or 6-membered palladacycles are driven by the formation of low energy metalacylic intermediates. These intermediates constitute thermodynamic minima (**Figure 2**,

Int-2) and can have large activation energies to convert them to the functionalised products and to achieve catalyst turn-over via ligand exchange of the coordinated products with starting material (**Figure 2**, **Int-3**). As a result, harsh reaction conditions, such as temperatures in excess of 100 °C, strong oxidants, or acids are often employed (*vide supra*).

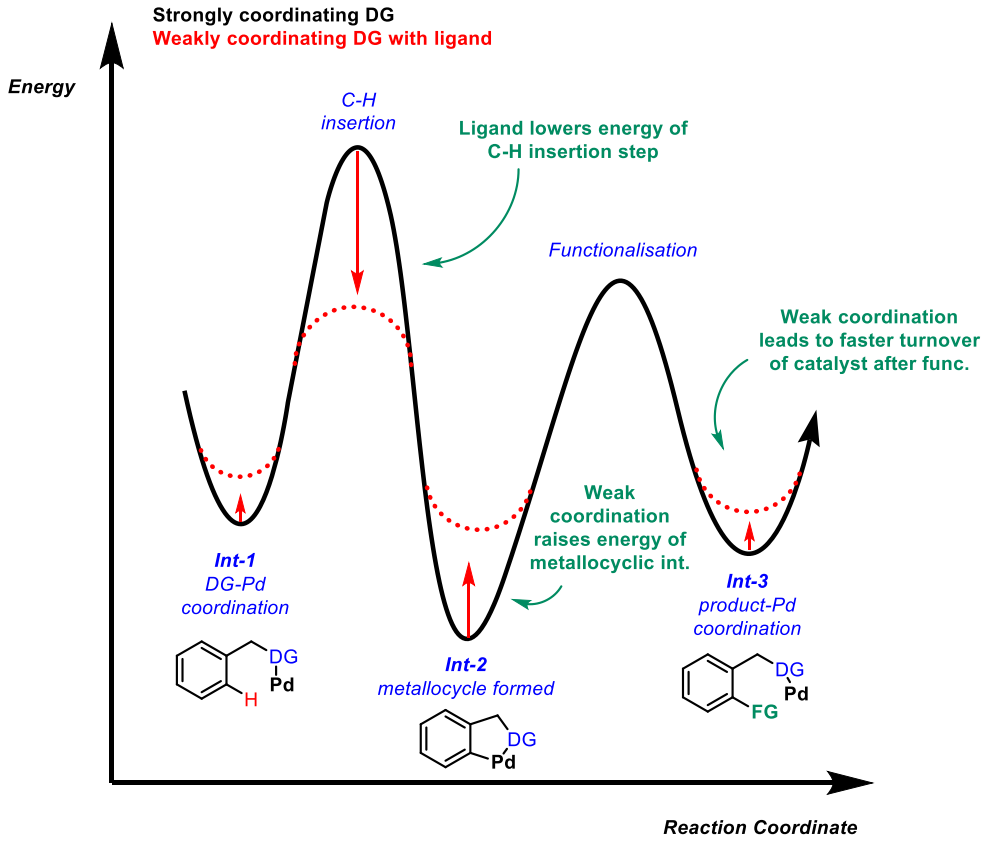


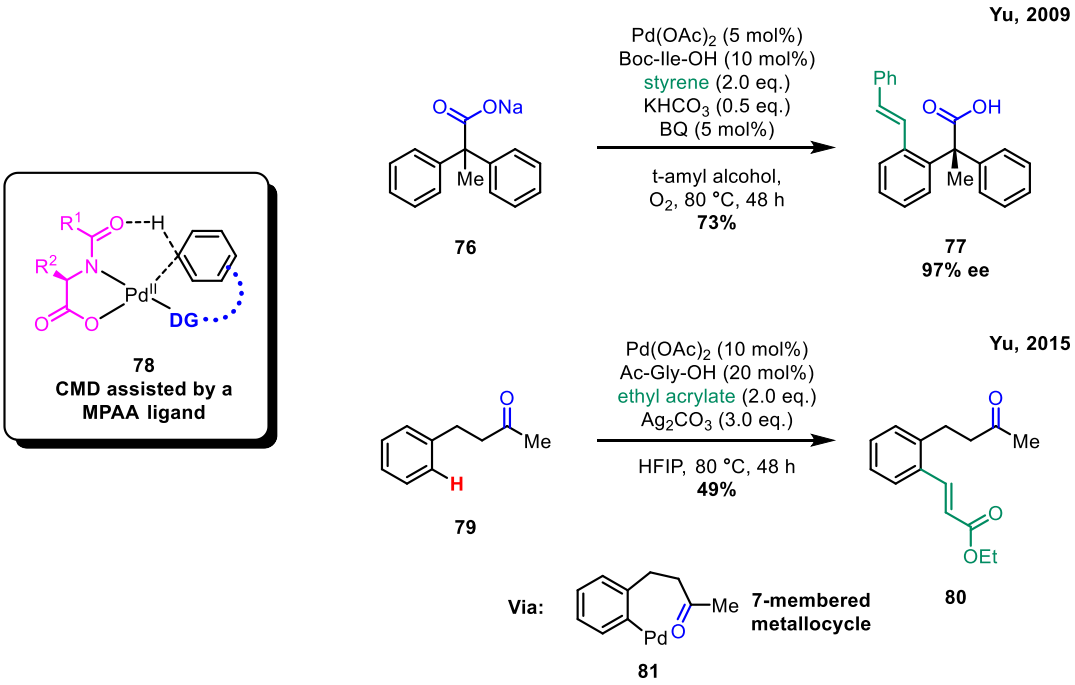
Figure 2: A theoretical reaction coordinate diagram for C–H functionalisation using weakly (red) and strongly (black) coordinating DGs. Adapted from Yu et al.[97]

By combining weakly coordinating DGs with external ligands, Yu has been able to perform C(sp^2)–H functionalisations with native functional groups inherent to molecules, under mild conditions and at distal positions.[96–99] **Figure 2** shows the theoretical reaction coordinate diagrams for palladium catalysed C–H functionalisations, comparing both strong and weakly coordinating groups. A weakly coordinating DG raises the energy of the three intermediates formed after coordination (**Int-1**), cyclopalladation (**Int-2**) and functionalisation (**Int-3**). The introduction of an external ligand acts to lower the energy barrier to the C–H insertion step. The external ligand required is often dependent on the substrate and DG being used.[98] The overall effect is a lowering of the activation energy for each of the steps, allowing milder conditions to be used. Catalyst turn-over can also be increased due to reduced product inhibition through coordination.

The basic reaction manifold developed by Yu has proven effective in numerous palladium catalysed C(sp^2)–H functionalisations. For example, ketones,[97,100] esters,[97,101] carboxylic

acids,[31,102–105] amides,[106,107] alcohols,[108,109] triflamides,[110,111] Weinreb amides,[97,112] nitriles[113] and ethers[114] have all been successfully employed as DGs.

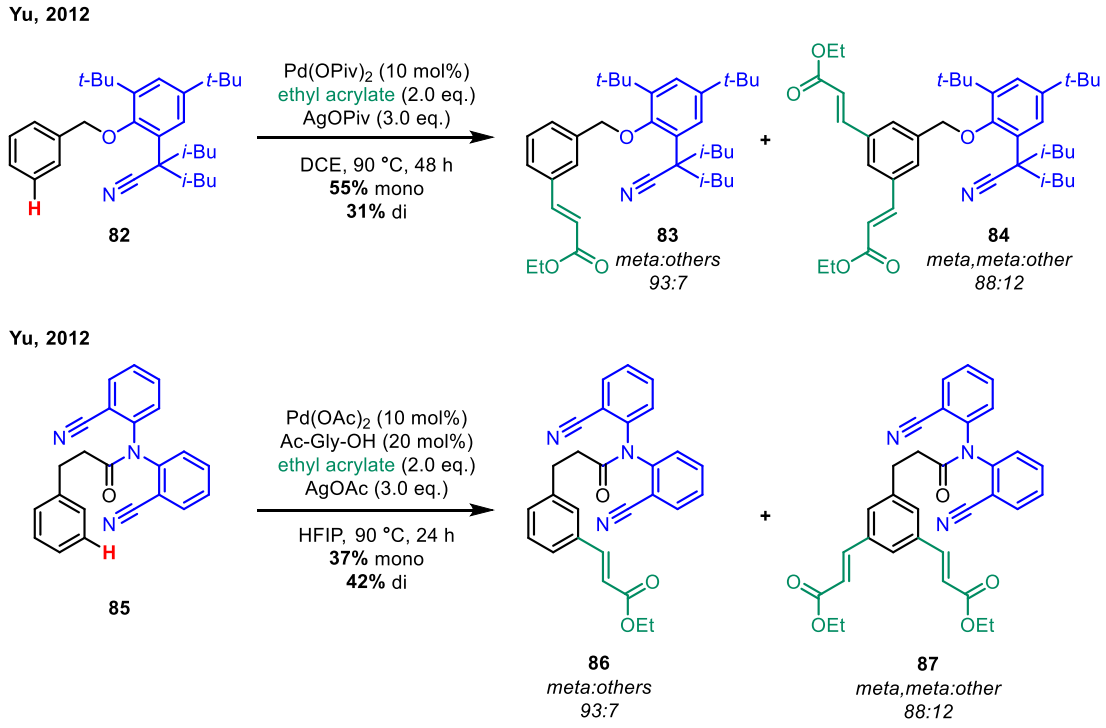
A number of ligands have shown proficiency in C–H functionalisations with weakly coordinating DGs, however the most prominently used are mono-protected amino acid (MPAA) ligands.[98,108,115–117] The ligands are believed to bind in a bidentate manner to the Pd^{II} catalyst and aid in the CMD of the C–H bond (**Scheme 19**, transition state **78**).[118] Hexafluorisopropanol (HFIP) as solvent and silver oxidants are also commonly employed reagents in these processes.[119,120]



Scheme 19: Enantioselective desymmetrizations and distal C–H alkenylations using MPAA ligands.[97,121]

Combinations of these reagents have allowed the development of synthetically powerful transformations. Yu was able to affect enantioselective C–H alkenylations of 2,2-diphenylpropanoic acid derivatives (**76**) using a Boc-protected isoleucine ligand (**Scheme 19**, top). He was also able to achieve the distal functionalisation of 4-phenylbutan-2-one **79** using the native ketone as the DG, proceeding via a rare 7-membered metallocycle **81** (**Scheme 19**, bottom).[97,121]

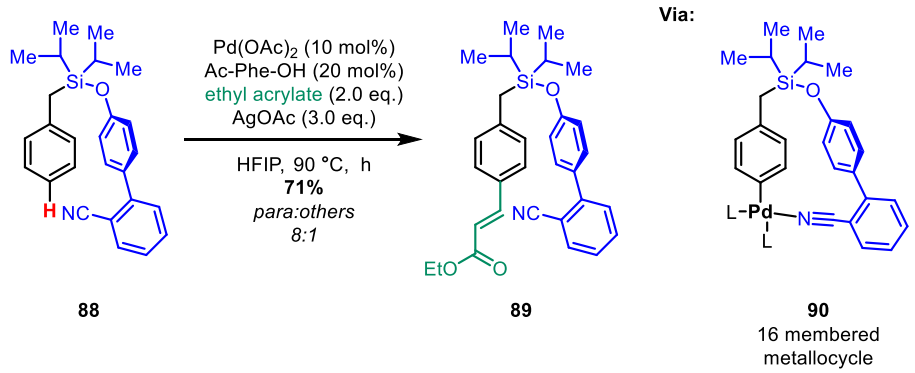
Weakly coordinating DG strategies have been particularly useful in the directed functionalisation of *meta* and *para* C–H bonds.[53,99] Yu was able to achieve highly *meta*-selective C–H alkenylations of benzyl alcohols **82** and hydrocinnamic acids **85** by appending carefully designed, nitrile-based, 'U-shaped' DGs (**Scheme 20**).[122]



Scheme 20: Yu's meta directed C–H functionalisations using U-shaped, 'end on' nitrile templates.[122]

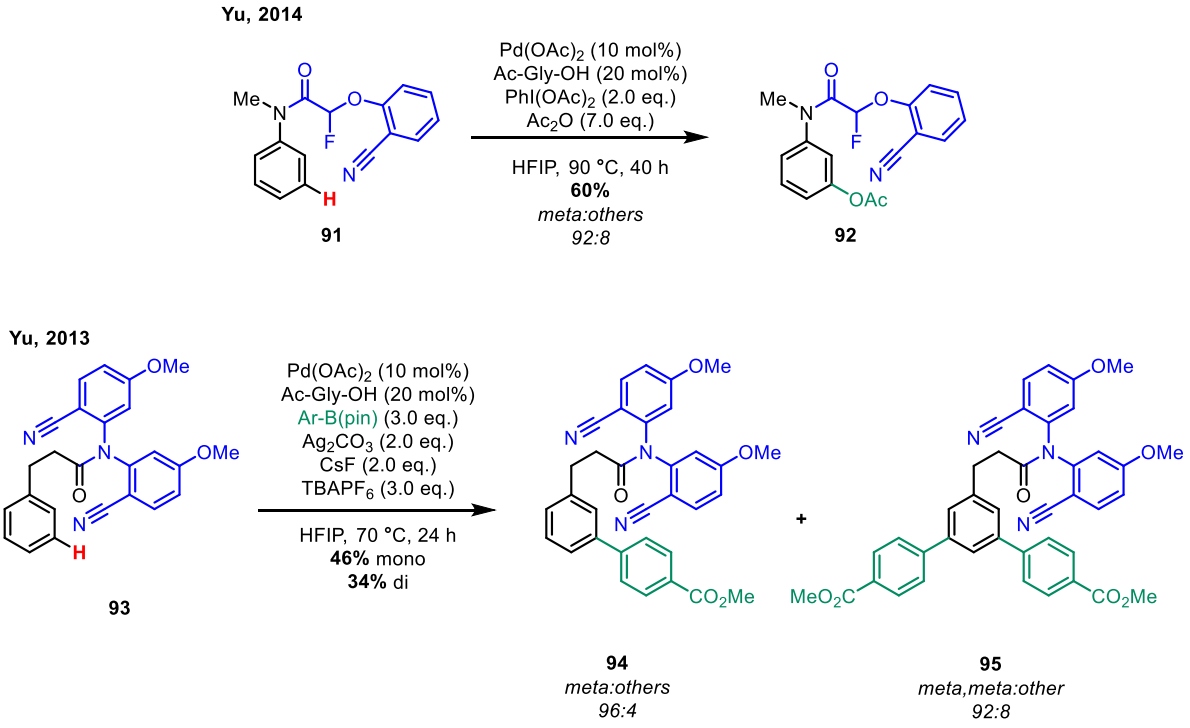
Linear coordination of the Pd^{II} catalysts to the nitrile DGs directed them selectively to the *meta* positions, via 11 and 12-membered cyclophane-like transition states respectively.

Yu's seminal work was subsequently built upon by Maiti, who was able to use the same principles to design a selective *para* directing 'D-shaped' template **88**.[123] Key to the design was the rigid biphenyl scaffold and two isopropyl substituents on the silyl tether, which was proposed to aid cyclometallation by exerting a Thorpe-Ingold effect (**Scheme 21**).[124]



Scheme 21: Maiti's D-shaped template for para *selective C–H alkenylations.*[123]

As well as regioselective C(sp^2)–H alkenylations, *meta* and *para* selective acetoxylations and *meta* selective arylations have been developed using the nitrile-based template strategy (**Scheme 22**).[123,125–127]



Scheme 22: Yu's distal meta *C–H acetoxylations and arylations using nitrile based templates.*[125,127]

Acetoxylations using $PhI(OAc)_2$ proceeding via a Pd^{II}/Pd^{IV} mechanism were developed by Yu for the remote functionalisation of arylamine **91** and subsequently employed by Maiti with his D-shaped template **88** (**Scheme 21**). Arylations of hydrocinnamic acid **93** were performed using arylboronic acid esters and were suggested to proceed by a Pd^{II}/Pd^{0} mechanism (**Scheme 22**, bottom).

The role of the MPAA ligands and silver salts and the origins of the *meta* selectivity have been extensively investigated (**Figure 3**).[118,128,129]

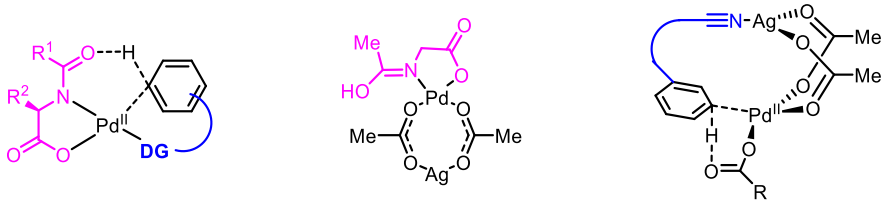


Figure 3: Structures of MPAA and silver salt-containing species postulated to have beneficial roles in the distal functionalisations of aromatic systems.[118,128,129]

The amino acid ligand acts not only as a mono-anionic bidentate ligand, but has been suggested to act as an internal base during concerted metalation-deprotonation by Houk and Yu (**Figure 3**, **78**).[118] In an alternate benzoic acid based system, the MPAA ligand was shown to elicit a four-fold

increase in rate, however computational studies indicated this rate acceleration could be attributed to the stabilisation of a Pd–Ag heterodimeric species **96**, as opposed to reduction of the activation barrier for C–H insertion.[129] DFT calculations indicated the heterodimer **97** was the active species in another, benzyl alcohol based system investigated, with Ag coordinating to the nitrile DG.[128] The *meta* selectivity appears to be derived from this complex (**Figure 3, 97**). As such, silver salts likely play dual roles – improving selectivity by aiding coordination, as well as acting as external oxidants.

While nitrile templates are extremely powerful tools for distal functionalisations, they suffer from similar limitations to the bidentate DGs discussed above (*see chapter 1.1.2*). Unlike other weakly coordinating DGs, they are not native to the molecules being functionalised and require introduction and subsequent cleavage after use. Their synthetic utility is therefore limited by the functional group required for attachment.

In response to this, many bespoke designs have been developed for the *meta* or *para* functionalisation of different aryl systems. These include DGs covalently linked by carbonyl,[122,125,128–134] ether,[122] silyl,[123,135–138] sulfonyl,[126,139–144] and phosphonate[145] functional groups. Pyrimidyl **99** and 2-fluoropyridine **98** based groups have also been developed, allowing *meta* deuterations, cyanations and iodinations (**Figure 4**).[146–153]

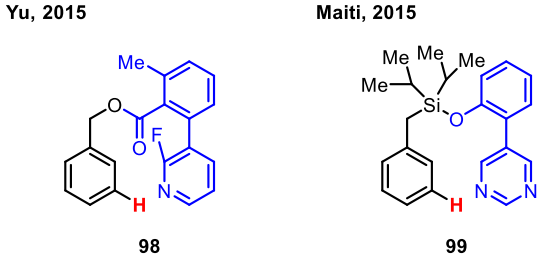
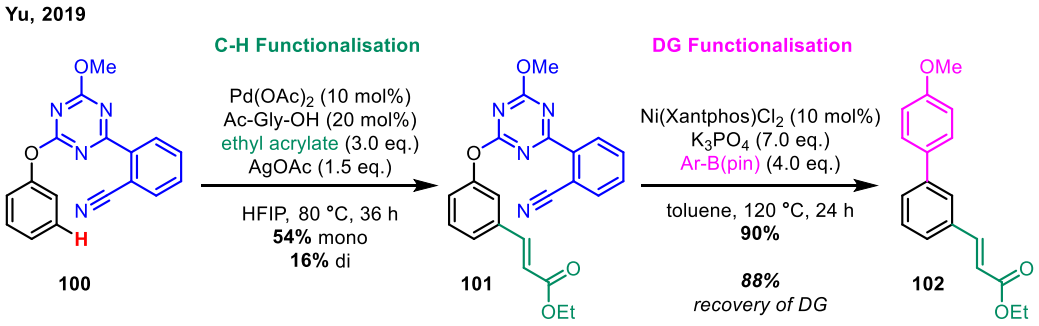


Figure 4: Examples of palladium catalysed pyridyl and pyrimidyl based meta selective DGs.[146–153]

The development of increasingly synthetically useful scaffolds constitutes a current trend. In 2019, a 1,3,5-triazine based DG **100** was developed by Yu, which can be directly cross-coupled using Ni after *meta*-C(sp²)–H functionalisation (**Scheme 23**).[154]

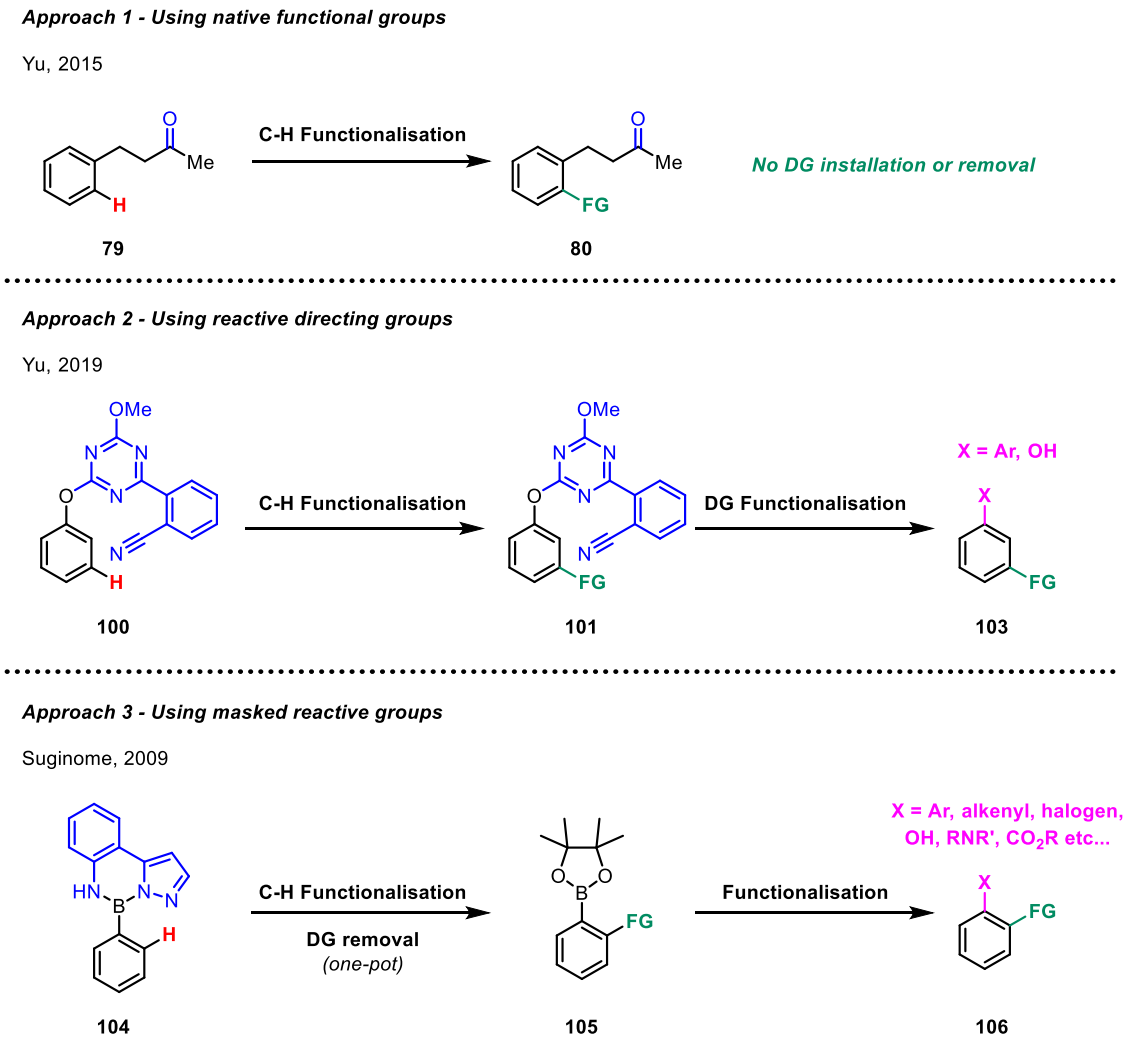


Scheme 23: Direct cross-coupling and recycling of Yu's triazine based DG.[154]

Cleavage to reveal the phenol is also possible, as is the recovery of the DG motif, important when considering the atom economy of this type of transformation.

1.2 Boronic Acid Based DGs in C–H Functionalisation

As indicated above, an emerging theme in the area of directed C(sp^2)–H functionalisation is the design of 'synthetically useful' DGs. In this regard, three main have approaches have been taken to increase the synthetic utility of directed C–H functionalisations (**Scheme 24**).

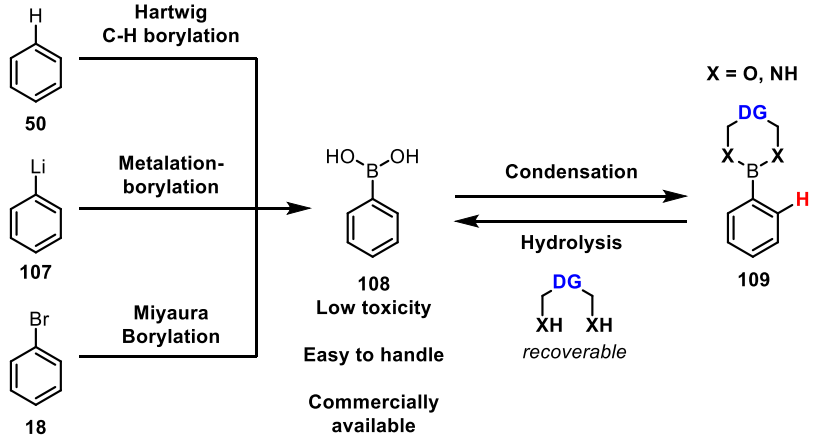


Scheme 24: Examples of the three main approaches to designing synthetically useful C–H functionalisations.[97,154,155]

Firstly, by developing transformations directed by native functionalities, the need for installation and removal of uneconomical, extraneous DGs is avoided (**Scheme 24**, Approach 1). While this approach is often preferred, it is unsuitable for systems lacking the required native functional groups. Secondly, by designing DGs that can be subsequently functionalised themselves (**Scheme 24**, Approach 2), the overall C(sp^2)–H functionalisation process becomes more efficient. However, these DGs are often bespoke and limited in the functionalities they can be converted into. A third approach focuses on using a DG tethered by a synthetically valuable parent functional group (**Scheme 24**, Approach 3). Removal of the DG (ideally allowing it's recovery and reuse) reveals

the parent functionality, which can be subsequently converted to a broad range products. This powerful technique allows the use of one general DG to access a broad range of systems.

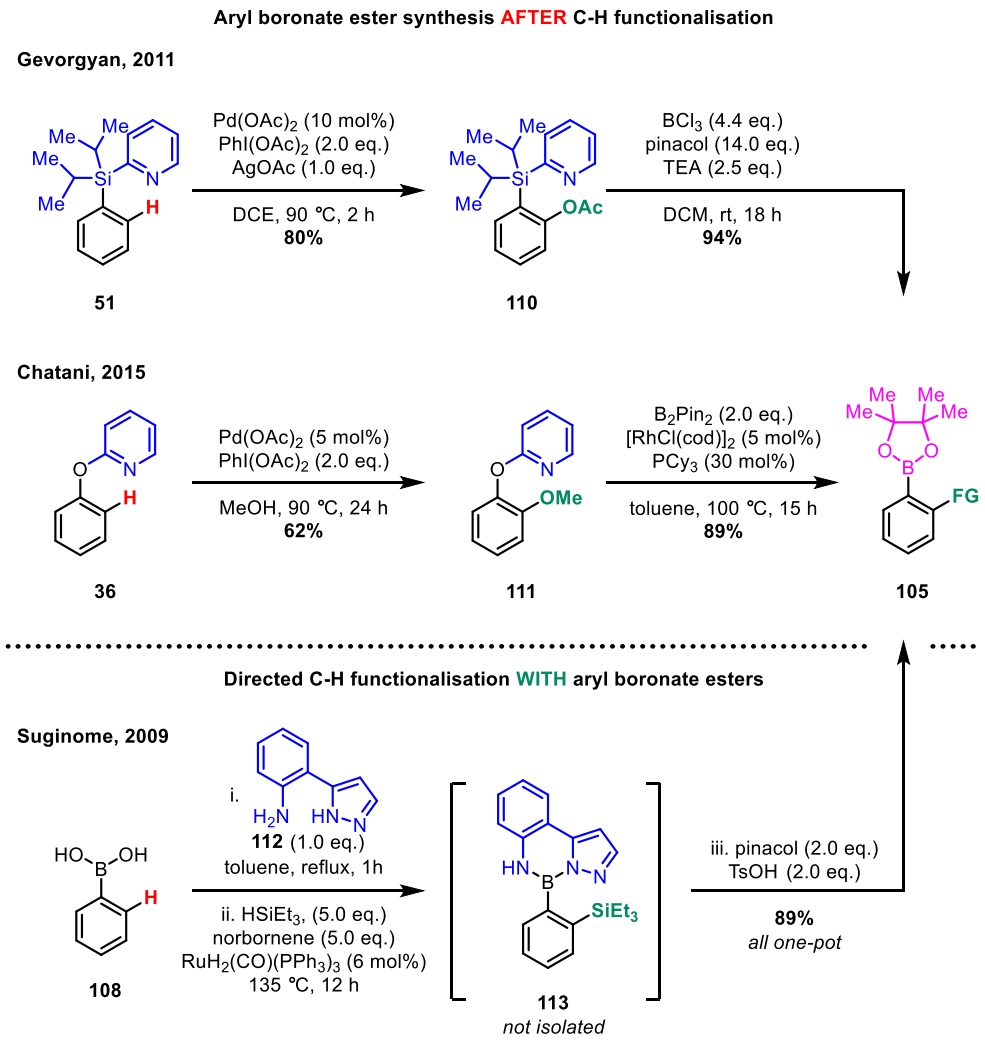
Aryl boronic acids represent ideal functional groups for the third approach (**Scheme 25**).



Scheme 25: Boronic acids as handles for covalently attaching DGs.

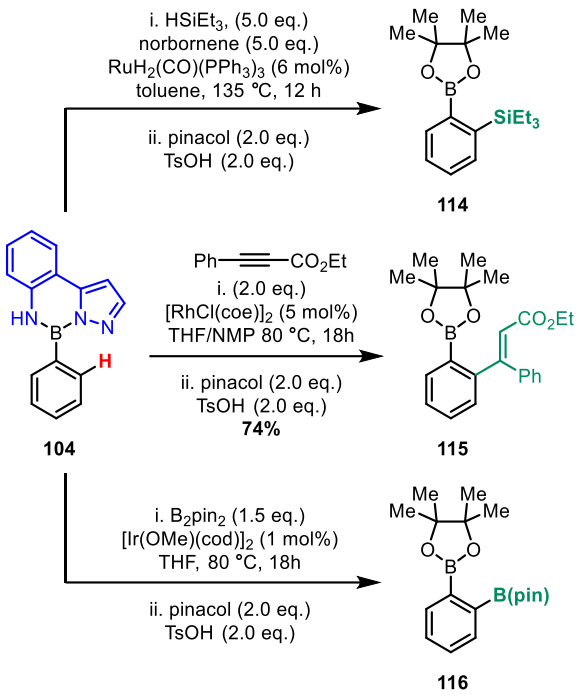
Boronic acids are common building blocks which have low toxicities, are readily available from commercial suppliers and have a number of well-established routes for their synthesis.[156] Accessing different boronate esters from boronic acids is often facile and can be used to modulate the reactivity of the group.[157] In this manner, a DG tethered via a boronate ester could be envisaged to be simple to introduce and remove using condensation and hydrolysis.

Aryl boronic acids are also extremely useful building blocks due to their synthetic versatility.[158,156] Their ability to undergo transmetalation in transition metal catalysed transformations allows their conversion to a broad range of functional groups. The Suzuki-Miyaura coupling, for example, is frequently employed in medicinal chemistry.[159] This was recognised by Gevorgyan and Chatani who developed techniques for the transformation of pyridyl DGs into pinacol boronate esters after C(sp^2)–H functionalisations (**Scheme 26**, top).[73,79]



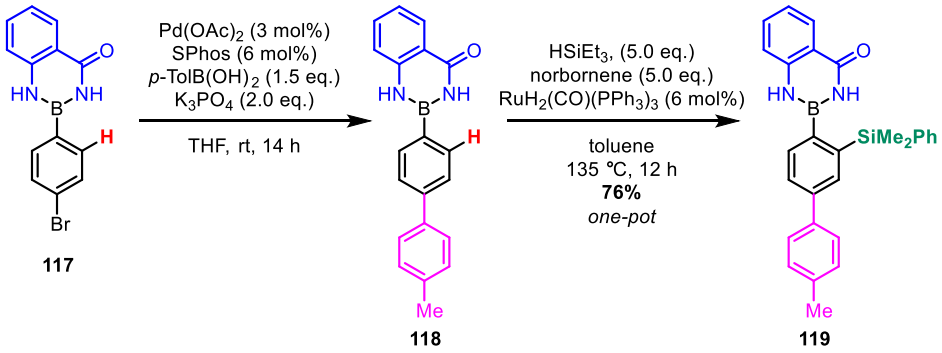
Scheme 26: A comparison of two different methods for accessing C-H functionalised aryl boronic acid pinacol esters. [73,79,155]

In 2009 Suginome took a different approach, developing a 2-pyrazol-5-ylaniline (PZA) DG **112** that allows the direct C(sp²)–H functionalisation of aryl boronic acids (**Scheme 26**, bottom).[155] This approach led to a number of benefits. The ArB(PZA) ester **104** is synthesised by simple condensation, hydrolysed using aqueous acid with recovery of the DG **112**, and is bench stable for over 10 months.[155] This is in contrast to DGs attached by amide bonds for instance, which can require forcing conditions to remove (*see* **Scheme 18**). The PZA DG **112** is also able to direct *ortho*-selective C–H alkenylations and borylations, as well as silylations (**Scheme 27**).[160–163] The utility of the approach is exemplified in **Scheme 26**, with Suginome's approach requiring fewer steps, only one metal catalyst and resulting in higher overall yield than alternate approaches.



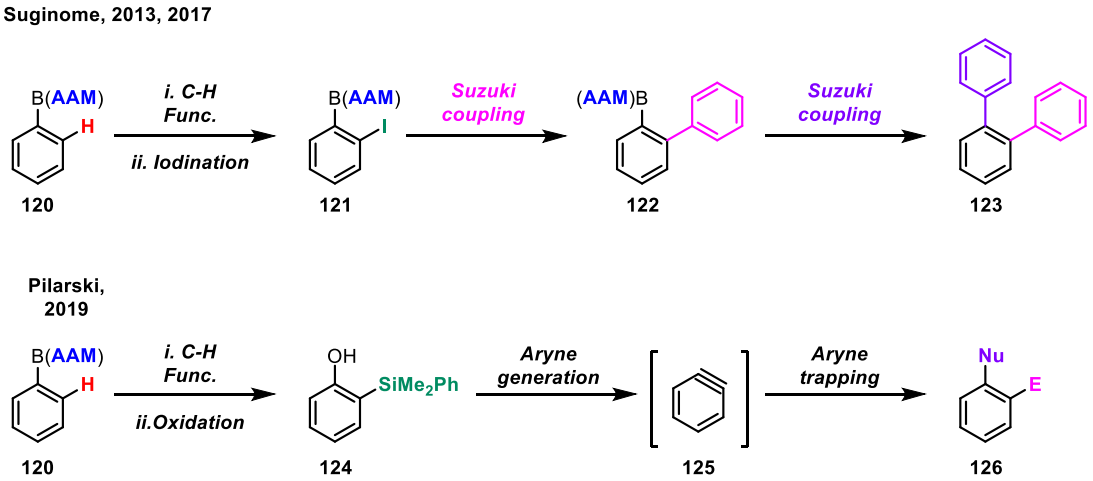
*Scheme 27: Suginome's C-H silylations, alkenylations and borylations using the PZA ester DG **111**.*[155,160–163]

A second DG for arylboronic acids was also designed by Suginome.[164] An anthranilamide (AAM) boronate ester **117** could direct *ortho*-CH silylations, while also providing improved protection for the boronic acid functional group (**Scheme 28**).



Scheme 28: The AAM protecting-DG which allows selective coupling of one organoboron species to another, followed by directed ortho *C–H silylation.*[164]

The dual directing-protecting AAM ligand prevents the parent boronic acid from transmetalating under Suzuki coupling conditions. The conditions for attachment and removal of the AAM DG are identical to those reported for the PZA DG, with full recovery of the DG possible following cleavage. Aryl boronic acid AAM esters have found a number of applications (**Scheme 29**).



Scheme 29: Applications of Suginome's AAM boronate ester to iterative cross-couplings and aryne syntheses.[165–167]

By performing iodination of the arylsilane formed after C–H functionalisation, Suginome was able to use an iterative procedure to form oligo-arenes (such as **123**) and helical oligo-napthalenes.[165,166] Recently, Pilarski employed the C-H functionalisation in a 4-step, telescoped procedure to access and then trap benzyne (**125**).[167] Lastly, novel, silylated ferroceneboronic acids were expediently synthesised using the technique.[168]

The PZA and AAM DGs do however have some limitations. Aryl boronic acid PZA esters are unstable on silica, requiring transesterification prior to chromatographic purification. Although the AAM boronate esters are stable on silica, only directed C(sp^2)–H silylations have been demonstrated using this DG. The stability of Suginome's DG boronate esters, measured by rate of hydrolysis in H_2O:DMSO, are particularly low when compared to other common boronate esters (**Figure 5**).

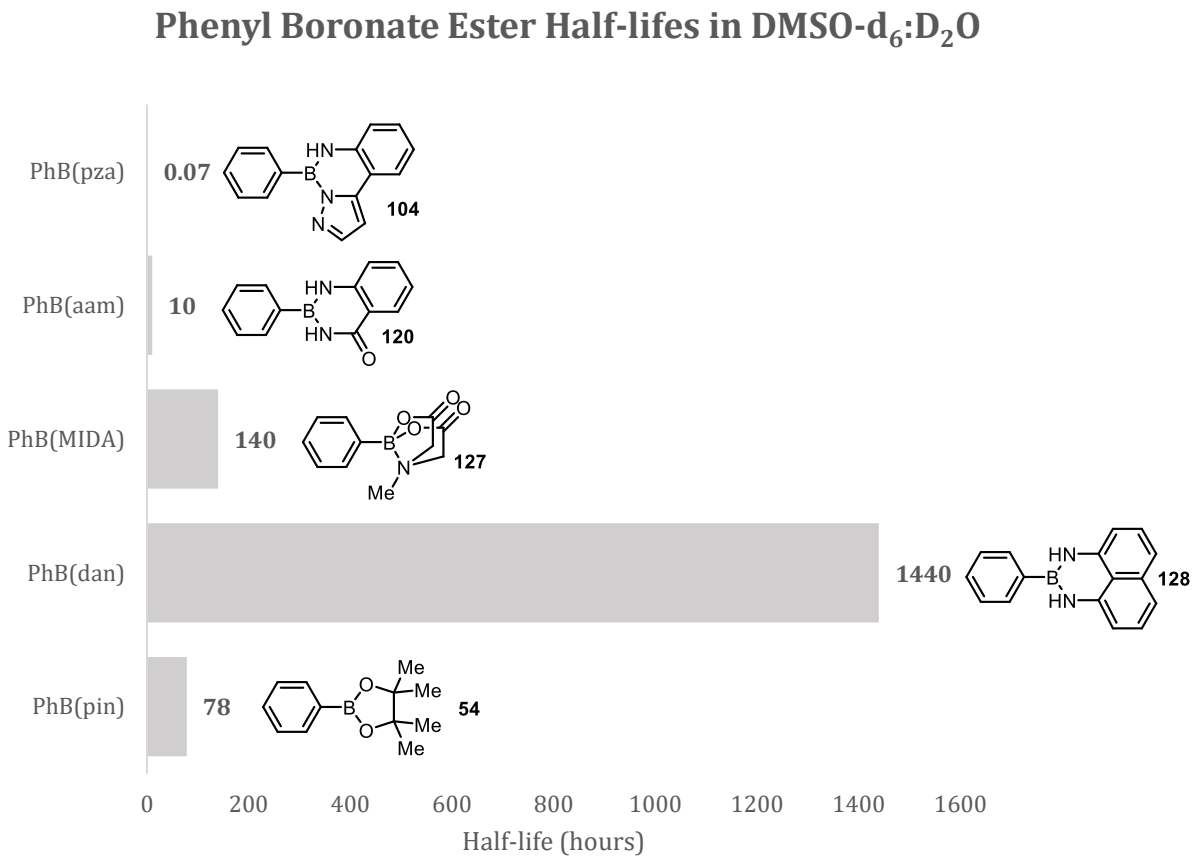


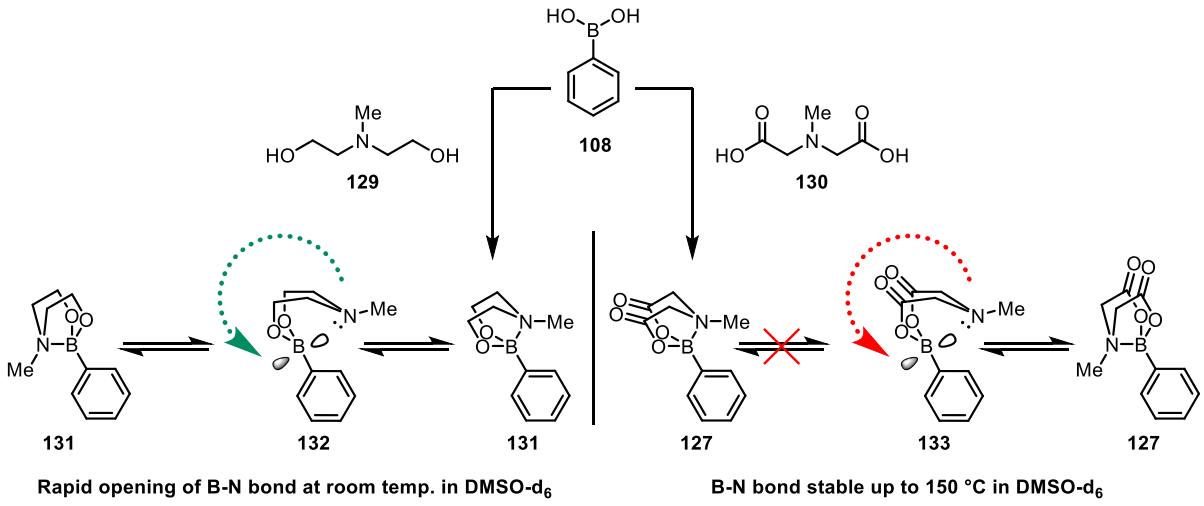
Figure 5: Respective half-lives of the PZA and AAM boronate esters, compared to other commonly used motifs. Measured using NMR spectroscopy in 10:1 DMSO-d_6:D_2O at room temperature.[164]

This lack of hydrolytic stability may limit their use in many transition metal catalysed C–H functionalisations, such as those discussed above using palladium catalysts and often requiring high temperatures (*see chapter 1.1*). A boronic acid tethered DG based on a different boronate ester scaffold may be able to address some of these limitations.

1.3 *N*-Methyliminodiacetic Acid (MIDA) Boronate Esters

1.3.1 Structure and Properties

The phenyl *N*-methyliminodiacetic acid (MIDA) boronate ester **127** was first synthesised and characterised in the 1980s.[169] The carboxyl-containing bicyclic scaffold of this ester derivative, which contains a tetrahedral, sp^3 hybridised, boron centre was found to be remarkably stable, especially in comparison to the corresponding *N*-methyldiethanolamine boronate ester **131** (**Scheme 30**).[170]



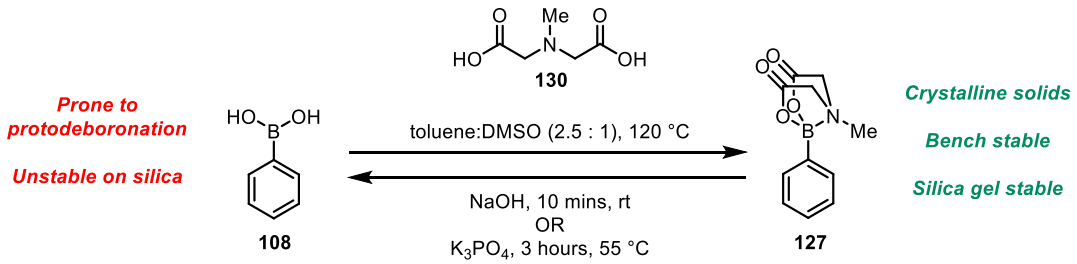
Scheme 30: Comparison of the conformational rigidty of phenyl MIDA boronate ester with its des-carbonyl analogue. [169, 171]

The stability of MIDA boronate esters can be attributed to the carboxyl functionalities in the MIDA backbone **130**. Firstly, the electron-withdrawing effect of the carbonyls increases the Lewis-acidity of the boron centre, allowing a stronger dative nitrogen–boron interaction. Secondly, the planar sp^2-hybridised carbon centres increase the strain accrued when a conformational flip occurs (*via* intermediate **133**). The overarching result is a large increase in the stability of the MIDA system, as demonstrated by a $\Delta G^{\ddagger}$ value of >90 kJ M^{-1} for B–N breakage in MIDA ester **127**, compared to a $\Delta G^{\ddagger}$ of around 49 kJ M^{-1} for *N*-methyldiethanolamine boronate ester **131**.[169] This is manifested in the stability of each of the boronate esters **127** and **131** in DMSO-d_6. Coalescence of the diastereotopic methylene protons in the ^{1}H NMR, indicative of conformational flipping, was observed at room temperatures with boronate ester **131**, however the MIDA equivalent **127** proved stable even at 150 °C (**Scheme 30**).[171]

The tetrahedral, sp^3-hybridised boronate MIDA esters have a number of properties that make them excellent protecting groups for boronic acids. The vast majority of MIDA boronate esters reported to date are crystalline solids, stable to silica gel chromatography and on the bench indefinitely.[157] Consequently, their handling is generally much easier than for unprotected

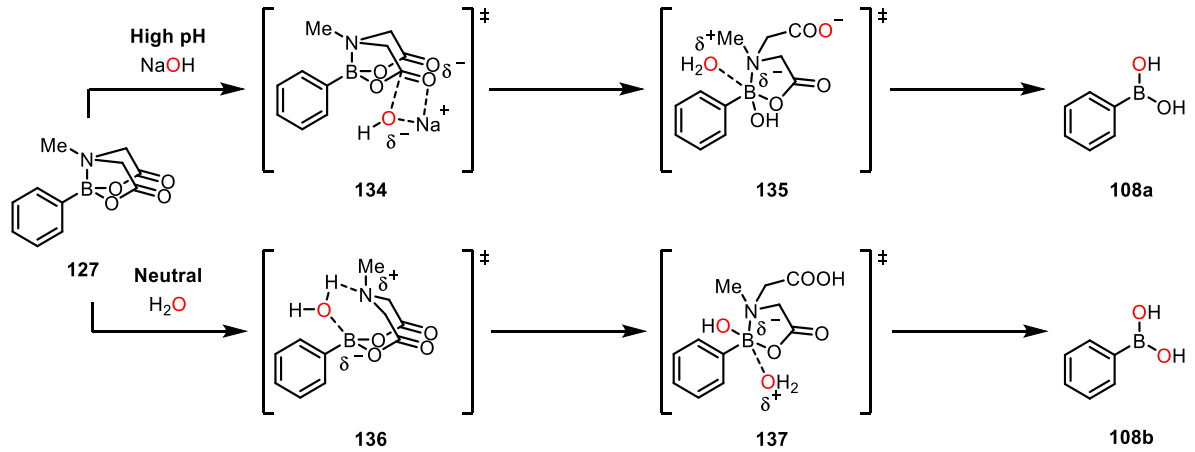
boronic acids, which are often unstable on silica and prone to protodeboronation. Even highly unstable 2-heterocyclic boronic acids are rendered air and bench stable as MIDA derivatives.[172]

Synthesis of arylboronic acid MIDA esters involves a simple condensation reaction between the boronic acid and *N*-methyliminodiacetic acid **130** (**Scheme 31**).



Scheme 31: Installation and removal of MIDA protecting groups via simple condensation and 'fast' or 'slow' hydrolysis.

The reaction is driven to completion by the removal of water, typically using Dean-Stark apparatus, with DMSO co-solvent required to solubilise the zwitterionic MIDA ligand **130**. Hydrolysis of MIDA boronate esters with aqueous base can be performed 'fast' using NaOH, or 'slow' using K_3PO_4. Investigations by Burke and Lloyd-Jones elucidated a difference in the mechanisms of hydrolysis under high pH and neutral conditions (**Scheme 32**).[173]

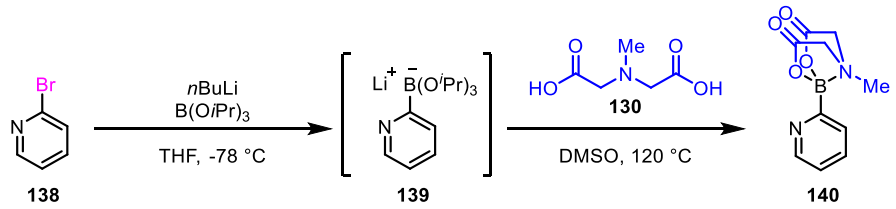


Scheme 32: The two separate mechanisms for hydrolysis of MIDA boronate esters under basic and neutral conditions, as investigated by Lloyd-Jones.[173]

Using ^{18}O labelling experiments and by measuring $^{12/13}C$, $^{10/11}B$, $^{14/15}N$ and $^{1/2}H$ kinetic isotope effects, in conjunction with DFT calculations, Lloyd-Jones *et al.* were able to discern the two prevailing mechanisms which lead to the disparities in rates. When using NaOH, the first step in the hydrolysis is analogous to an ester hydrolysis, with nucleophilic attack by hydroxide at a carbonyl centre (**Scheme 32**, TS **134**). This is followed by attack at the boron and loss of the MIDA, leading to incorporation of one ^{18}O atom in the acid **108a** and the MIDA each, when using labelled NaOH. Conversely, under neutral conditions, attack by water occurs at the boron in both steps,

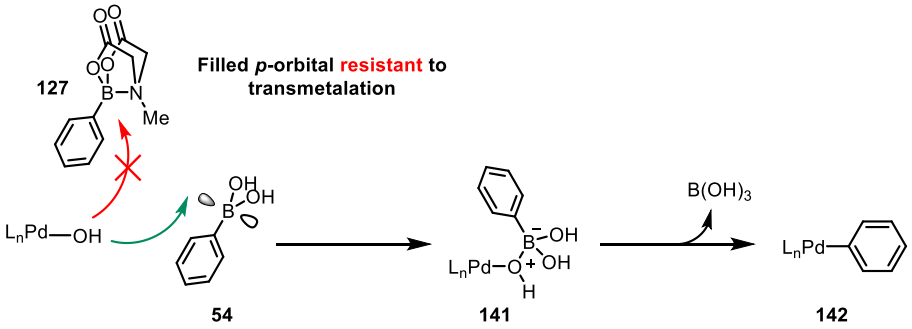
with B–N bond cleavage facilitated by hydrogen bonding to the H_2O nucleophile (**Scheme 32**, TS **136**). Consequently, only the boronic acid product **108b** is fully ^{18}O labelled.

Burke also developed a telescoped procedure to access the MIDA boronate esters of unstable boronic acids (**Scheme 33**).[172]



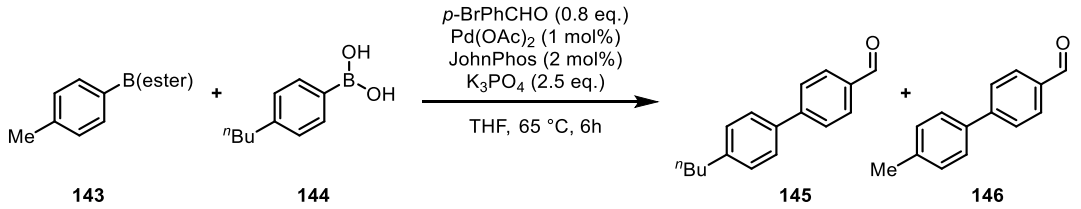
Scheme 33: An example of the telescoped procedure developed by Burke for the synthesis of MIDA boronates from unstable boronic acids.[172]

Lithiation of the corresponding bromide **138** allows nucleophilic attack of $B(O^iPr)_3$ to form the lithium boronate species **139**. This is then added to an anhydrous solution of MIDA **130** in DMSO at 120 °C, forming the desired boronate ester **140**. The *p*-orbital of the boron centre is coordinated to a lone pair of electrons in all the intermediates, first to an alkoxide then to the MIDA ligand, thus minimising the opportunity for protodeboronation.[174] As well as blocking protodeboronation, the sp^3-hybridised boron centre is resistant to transmetalation (**Scheme 34**).[157,175]



Scheme 34: Mechanism of transmetalation of phenyl boronic acid with palladium and comparison with phenyl MIDA boronate for which N to B coordination prevents transmetalation.[176]

The B–N coordination blocks formation of the key $L_nPd–O–B(OR)_2R'$ species **141** required for transmetalation to Pd^{II} species during Suzuki-Miyaura couplings.[176] This was exemplified by Burke, who investigated the competitive coupling of aryl boronic acids in the presence of various *N*-coordinated boronate esters (**Table 1**).[175]



143 **144** **145** **146**

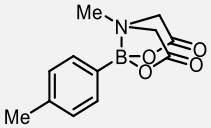
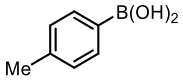
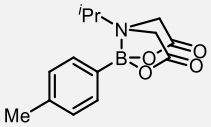
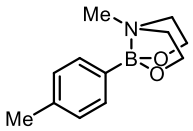
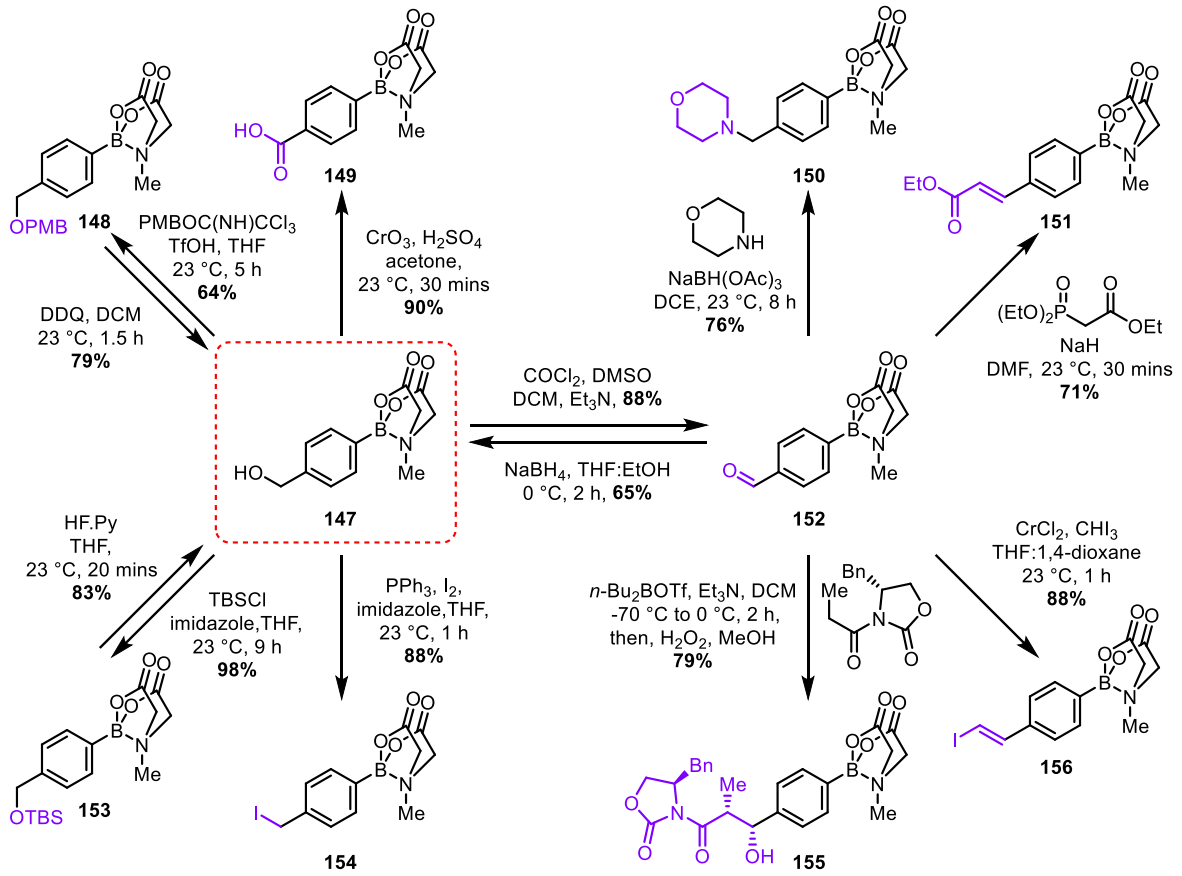
Entry	Compound		145 : 146
1	**143a**		24 : 1
2	**143b**		1 : 1
3	**143c**		26 : 1
4	**143d**		1 : 1

Table 1: A comparison of N-boronate ester stabilities, as measured by competitive Suzuki-Miyaura coupling with a free boronic acid.[175]

Under anhydrous Suzuki-Miyaura coupling conditions, a selectivity of 24 : 1 for coupling of the free boronic acid **144** over the *p*-tolylboronic acid MIDA ester **143a** was achieved. This was increased to 26 : 1 by appending an isopropyl group to the iminodiacetic acid **143c**. The increased steric bulk around the N–B bond further impedes nucleophilic attack (*see* **Scheme 32**, bottom pathway). At 65 °C the rapid conformational flipping of the diethanolamine ester **143d** provides no protection, resulting in a 1 : 1 ratio of products.

Further investigations by Burke found that MIDA boronate esters are remarkably stable under a number of reaction conditions (**Scheme 35**).[171]



*Scheme 35: Reactions of benzyl alcohol **147** under a broad range of reaction conditions, as performed by Burke to demostrate the stability of MIDA boronates.*[171]

Using the simple benzyl alcohol **147** as a starting point, the MIDA boronate protecting group was observed to tolerate strong acids such as TfOH (**148**), reductive conditions using borohydrides (**150**) and even Jones' oxidation conditions (**149**). The MIDA boronates are however susceptible to reaction with hard nucleophiles, such as $LiAlH_4$ or metal alkoxides, which lead to their cleavage consistent with the mechanism for deprotection by NaOH (**Scheme 32**, top pathway). In a similar manner, unsaturated vinyl and ethynyl MIDA boronate esters can be rapidly diversified into complex building blocks.[177–180]

1.3.2 Synthetic Applications of Boronic Acid MIDA esters

In 2007 Burke identified that the orthogonal reactivity of MIDA boronates and unprotected boronic acids could be harnessed for iterative C–C bond coupling sequences (*see* **Table 1**).[175] Analogous to the peptide coupling sequences used in protein chemistry, halide-containing boronic acid building blocks could be utilised to synthesise complex molecules via iterative Suzuki-Miyaura couplings (**Figure 6**).[181]

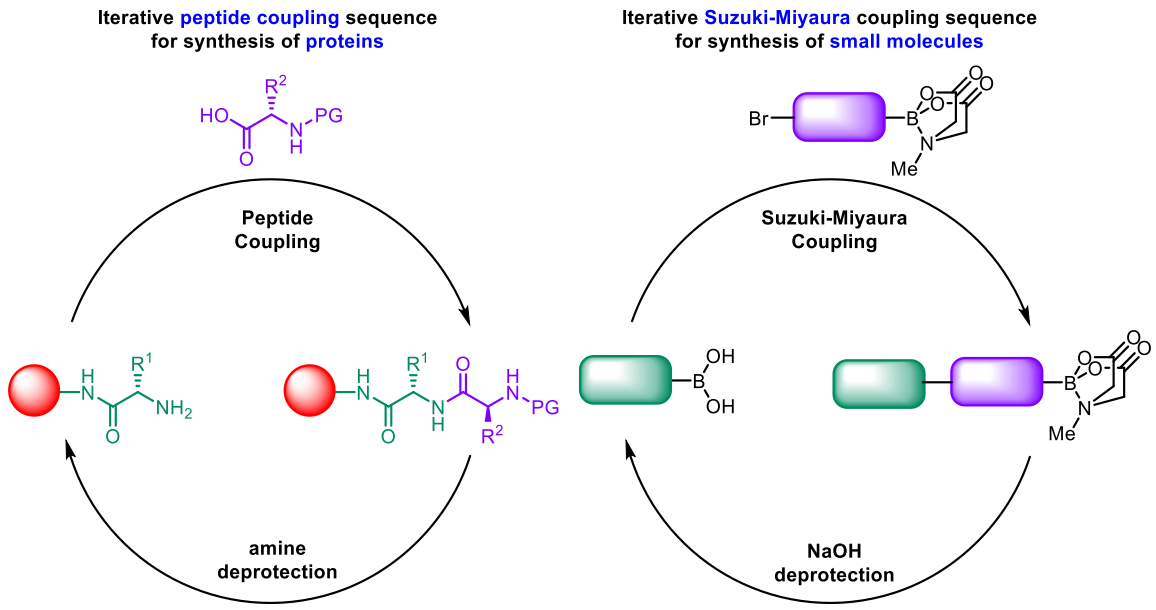


Figure 6: Burke's iterative Suzuki-Miyaura coupling sequence, modelled on an interative peptide coupling sequence which allows the modular synthesis of small molecules.[175]

Burke identified that many small molecule targets are inherently modular in nature. By identifying suitable retrosynthetic disconnections, complex molecules can be assembled in an iterative manner using the cross-coupling/deprotection sequence from simple MIDA boronate building blocks (**Figure 7**).

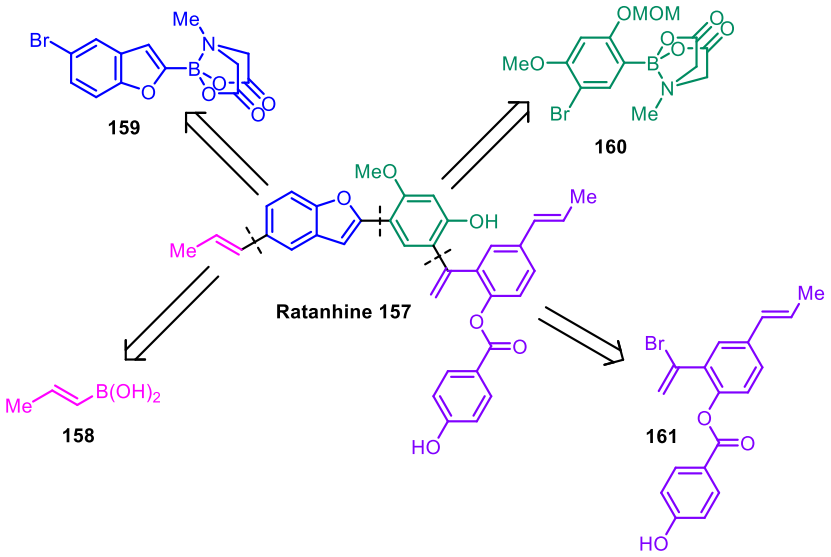
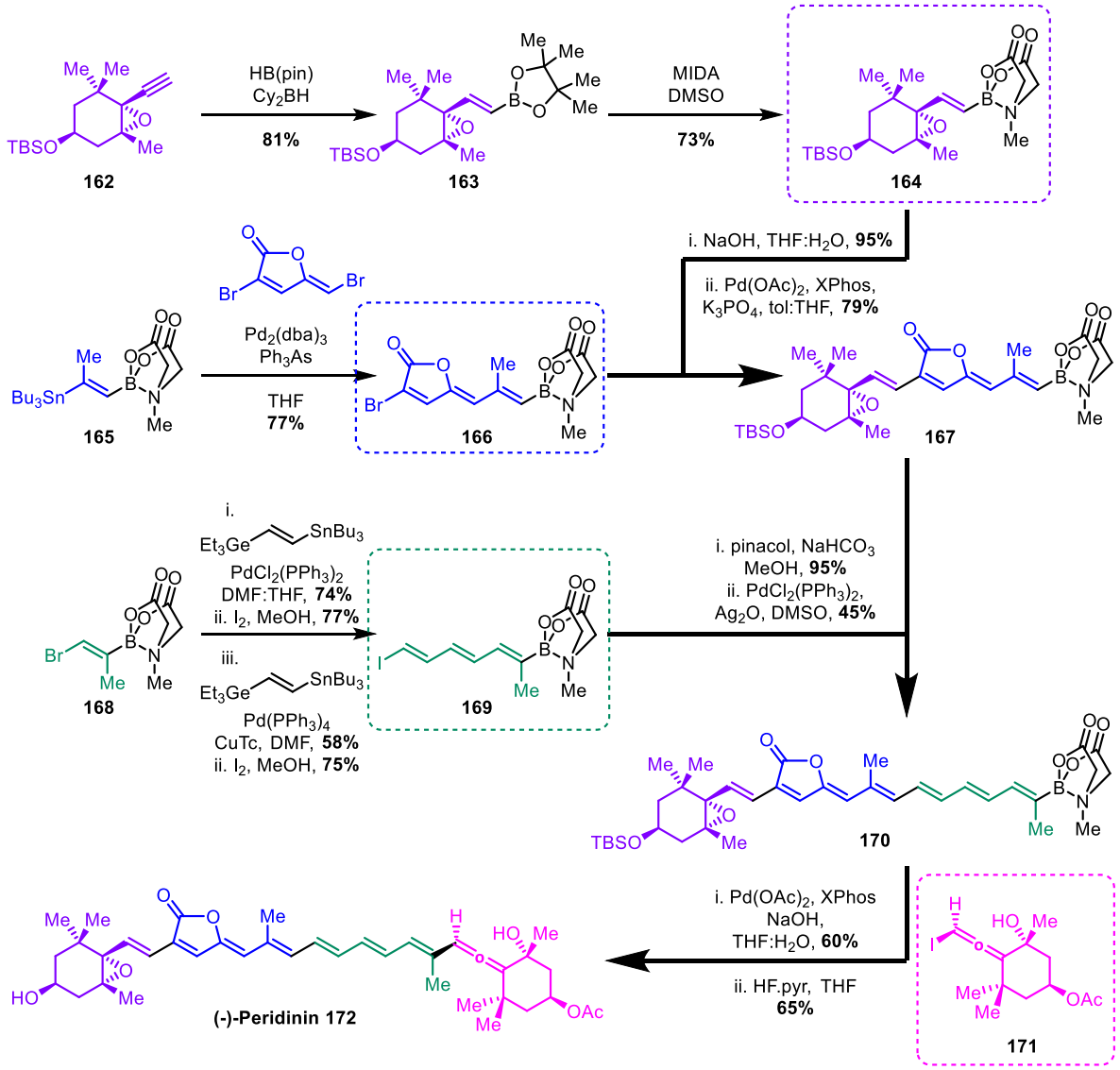


*Figure 7: Burke's synthesis of the natural product Ratanhine **157** – proof of concept for an iterative approach using just three Suzuki-Miyaura couplings and the four building blocks (**158-161**).*[175]

The MIDA boronate building blocks can be expediently accessed from simple boronic acids using synthetic sequences such as those shown in **Scheme 35**. The retention of stereochemistry during the Suzuki-Miyaura couplings of vinyl boronic acids mean that this technique is particularly

powerful for the synthesis of polyene natural products.[182–187] As an example, Burke was also able to achieve an efficient stereoselective synthesis of the norcarotenoid natural product (−)-peridinin **172** (**Scheme 36**).[183]



Scheme 36: Burke's iterative cross-coupling strategy for stereoselective synthesis of (-)-peridinin.[183]

Using the three MIDA boronate building blocks **164**, **166** and **169**, which were themselves accessed from simple MIDA ester starting materials, and three iterative Suzuki-Miyaura couplings the bioactive polyene **172** could be accessed in a modular fashion. The key step involved the stereoretentive coupling of the known iodoallene **171** with the MIDA boronate **170**.[188] The modular approach had major benefits to classical linear syntheses. Peridinin has exhibited potential antilipoperoxidant activity and may be therapeutically relevant.[189] The modular synthesis allows the facile modification of specific areas of the compound for investigation of structure-activity relationships (SARs) in medicinal chemistry campaigns. Indeed, Burke used

this approach to synthesise, investigate the biological function and develop potential therapeutic analogues of the membrane protein amphotericin B.[190] Owing to biosynthetic divergence, Burke also suggested that >75% of all polyene natural product cores should be able to be accessed from just 12 vinyl MIDA boronate building blocks, demonstrating the enormous potential of the iterative Suzuki-Miyaura cross-coupling technique.[187]

The advent of solid-phase peptide synthesis has greatly increased the simplicity and speed of accessing synthetic proteins by allowing for the automation of their isolation and purification.[191,192] Solid-phase synthesis has been applied in the total synthesis of small molecules, however it has proven difficult to apply more broadly due to a lack of commonality in functional groups.[193] The building blocks used in the iterative Suzuki-Miyaura cross-coupling sequence however, universally contain the MIDA boronate functional group.

Burke *et al.* discovered highly unusual, solvent dependent behaviour on silica gel, which was common to all MIDA boronate esters.[194] Namely, all compounds tested which had a MIDA boronate functionality showed no mobility on silica utilising Et_2O:MeOH (98.5:1.5) as eluent. However, the MIDA boronates eluted cleanly when using more polar solvents such as THF. Consequently, reaction by-products can be removed from silica using an Et_2O:MeOH (98.5:1.5) wash, before the desired MIDA boronate is cleanly eluted using THF. This simple 'catch and release' purification allowed the development of a fully automated process for performing iterative Suzuki-Miyaura cross-coupling sequences (**Figure 8**).[194]

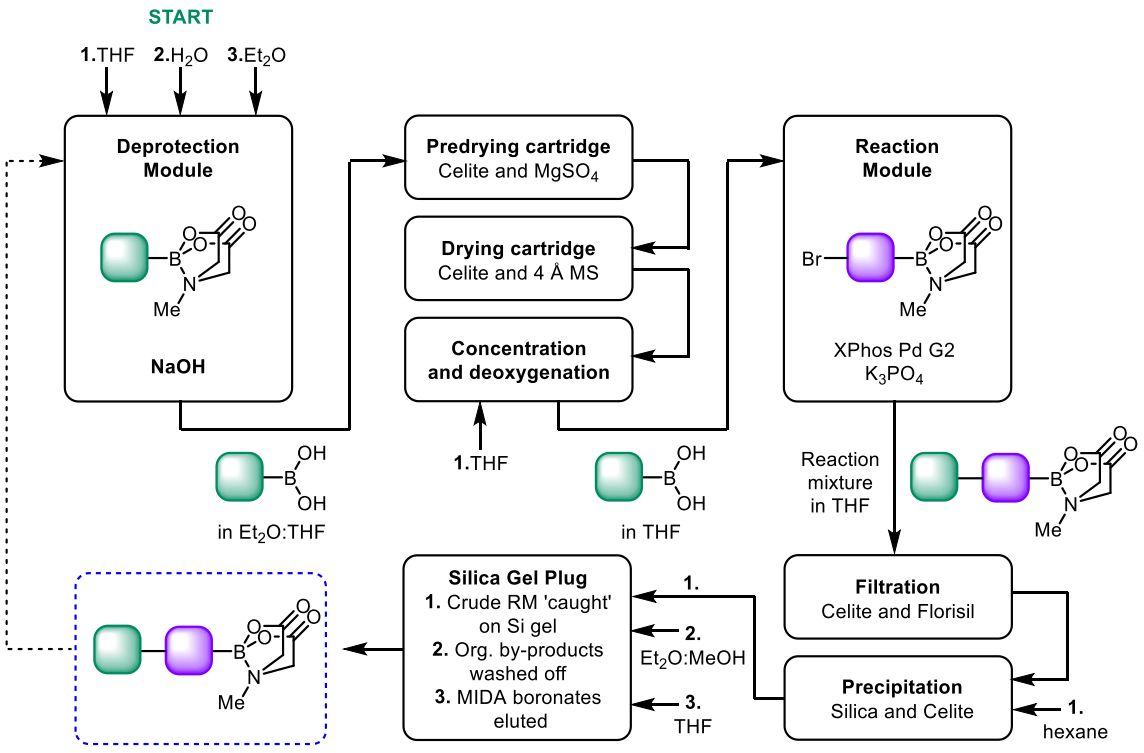
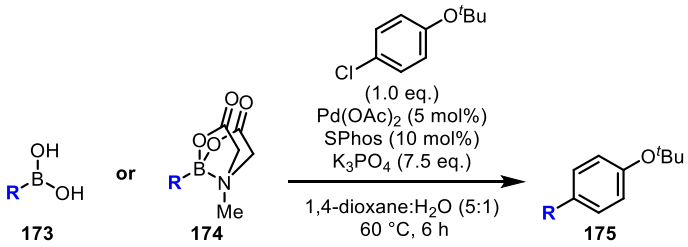


Figure 8: An overview of Burke's automated iterative cross-coupling process.[194]

Using the automated synthesis platform, Burke was able to access 14 diverse small molecules including polyenes, polyaromatics, oligomers and polycylic alkane cores. As well as Suzuki-Miyaura couplings, by varying the reagents added to the Reaction Module Buchwald-Hartwig couplings, alkylations and amidations could also be performed and purified in an automated fashion. Lastly, Burke was able to expediently generate 20 structural analogues of the neolignan natural product **ratanhine** (**157**) by simply varying the MIDA boronate building block inputs (**Figure 7**).

Burke also investigated the efficiencies of cross-coupling of various heterocyclic MIDA boronates compared to their boronic acid parent compounds (**Table 1**).[195]



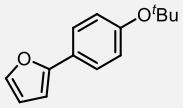
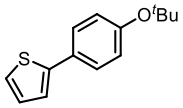
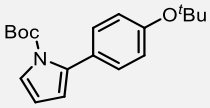
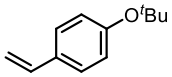
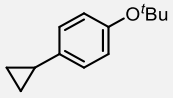
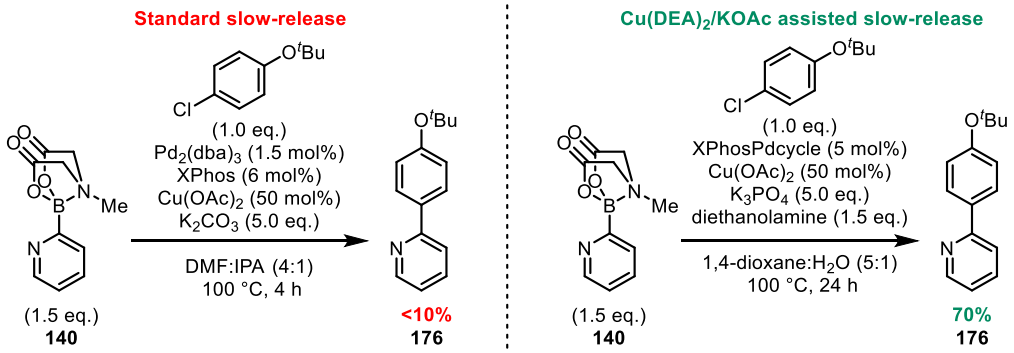
Entry	R	% remaining after benchtop storage: **173a-e** (15 days)	% remaining after benchtop storage: **174a-e** (60 days)	**175a-e**	% isolate yield after cross-coupling: **173a-e**	% isolate yield after cross-coupling: **174a-e**
1		7	>95		68	94
2		80	>95		37	94
3		<5	>95		61	90
4		5	>95		79	98
5		31	>95		95	96

Table 2: A comparison of the stabilities of unstable boronic acids and MIDA boronates towards bench-top storage, and the beneficial effects of MIDA slow-release in Suzuki-Miyaura cross-couplings.[195]

2-Heterocyclic, vinyl and cyclopropyl boronic acids **173a-e** are prone to protodeboronation or oxidation and will rapidly decompose when stored on the bench under air (**Table 2**, column 3).[174,195] This instability often also impacts yields in cross-couplings (**Table 2**, column 6), as under

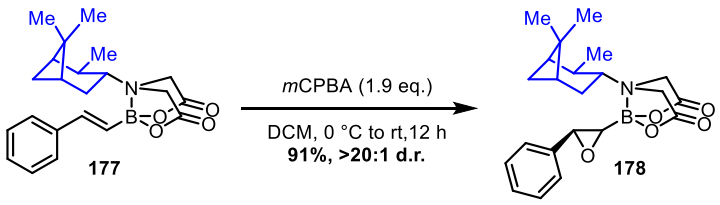
the reaction conditions these processes are accelerated. As has been discussed, the corresponding MIDA boronates **174a-e** are considerably more stable due to the N–B coordination inhibiting protodeboronation or oxidation (**Table 2**, column 4).[172] The MIDA boronate esters can also be slowly hydrolysed by using K_3PO_4 in the presence of water (**Scheme 31**). Burke identified that by performing cross-couplings under hydrous conditions with K_3PO_4 as base, slow-release deprotection occurs *in situ*.[195] Consequently, unstable boronic acids are present only in small quantities and react immediately, reducing side reactions with a requisite increase in yield. As shown in **Table 2**, column 7, yields were increased in all cases using the slow-release method with an array of valuable, unstable boronic acids.

2-Pyridyl boronic acids provided erratic yields under slow-release conditions however, with only some coupling partners suitable. Investigation by Burke identified $Cu(DEA)_2$ and KOAc (both formed *in situ*) as providing reliably high yields in the difficult cross-coupling (**Scheme 37**).[196]



Scheme 37: Burke's use of diethanolamine (DEA) and $Cu(OAc)_2$ to form KOAc and $Cu(DEA)_2$ in situ, allowing increased yields and reliability in Suzuki-Miyaura couplings with 2-pyridyl boronic acids.[196]

As a final application, Burke demonstrated that it was possible to modify the MIDA ligand to further increase its synthetic utility. By appending a (+)-α-pinene derived motif to the nitrogen, the resulting PIDA (pinene-derived iminodiacetic acid) can act as a chiral auxiliary, allowing diastereoselective epoxidations of vinyl boronic acids (**Scheme 38**).[197]



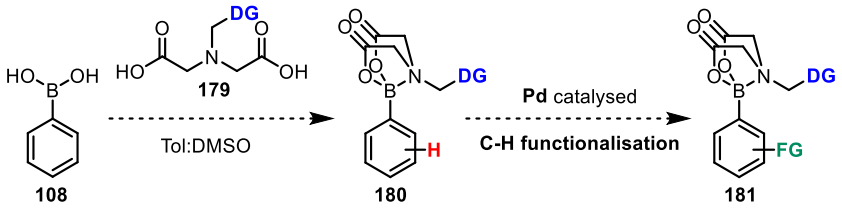
Scheme 38: Burke's pinene-derived iminodiacetic acid (PIDA) chiral auxiliary allows diasteroselective epoxidations while also acting as a protecting group for the parent boronic acid.[197]

The inherently rigid nature of the bicyclic PIDA boronate ester **177** holds the auxiliary in the desired position, allowing excellent diastereoselectivities to be achieved. The PIDA ligand is also simple to install and remove in an identical manner to standard MIDA boronate esters and retains the protecting group ability.

We envisioned that the ability to quickly introduce or remove an auxiliary held in a specific desired rigid conformation would be advantageous properties for a DG in C–H activation chemistry — see next chapter.

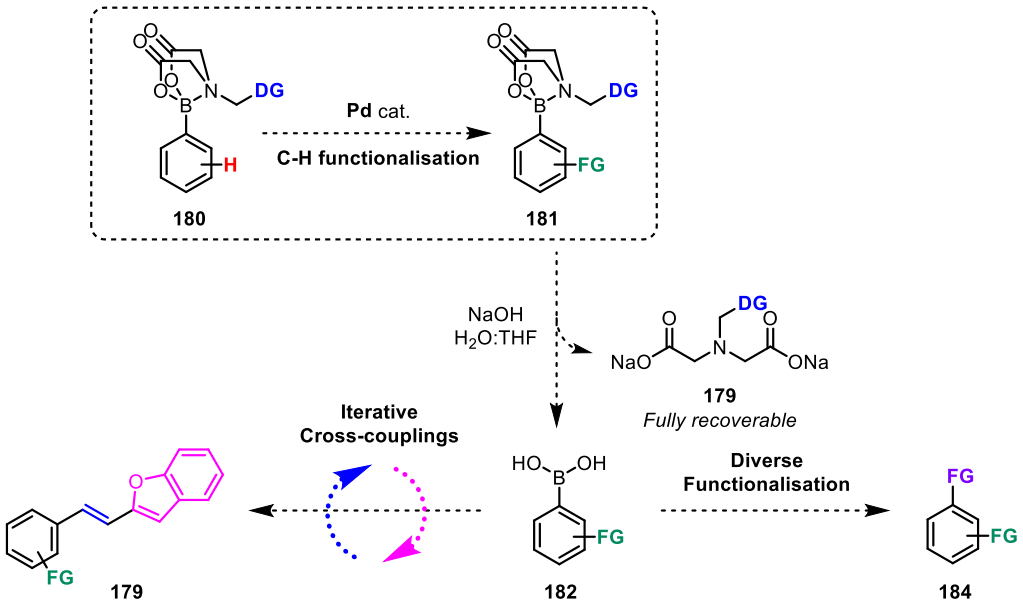
1.4 Aims and Objectives

The aim of the research described in this thesis was to design and synthesise modified iminodiacetic acid ligands that would be able to direct the palladium catalysed C(sp^2)–H functionalisation of aryl boronic acids. The DG-modified iminiodiacetic acids would be designed to retain the beneficial properties of MIDA boronates: ease of installation and removal, excellent protecting group ability and simple 'catch and release' purifications (**Scheme 39**).



Scheme 39: Proposed DG modified iminodiacetic acid, designed to allow the palladium catalysed C–H functionalisation of boronic acids, whilst also acting as a protecting group.

The research was to focus on using palladium catalysts to achieve the C(sp^2)–H functionalisations, with selectivity of *ortho*, *meta,* and *para* positions being of interest. Palladium catalysed C–H functionalisations are well understood mechanistically, with a wealth of viable potential DG scaffolds. Burke's extensive work on Suzuki-Miyaura couplings with MIDA boronates suggests their stability to conditions similar to those employed in C–H functionalisations (*see* **Table 1**). Once successful C–H functionalisation had been achieved, it was envisioned that it would be possible to demonstrate the utility of the aryl boronic acid esters products **181** by immediately diversifying them into numerous functionalities, or directly employing them in iterative cross-couplings, ideally with full recovery of the DG **179** (**Scheme 40**).



Scheme 40: The proposed use of an iminodiacetic acid tethered DG to allow synthesis of diverse boronic acids for further functionalisation or use in iterative cross-coupling sequences.

If succesful, it was hoped that this chemistry would broaden the applications of directed C–H functionalisations in organic synthesis by extending its application to boronic acid building blocks ubiquitous within the field. The dual 'protecting-directing' group developed would provide expedient access to a broad range of novel, highly functionalised boronic acids in an economical manner.

2. First Generation Designs

2.1 Design of DGs

Initial DG designs focused on the 8-aminoquinoline and picolinamide scaffolds commonly utilised in C(sp^2)–H functionalisations. These strongly, coordinating DGs were chosen for a number of reasons:

- The wealth of literature pertaining to C–H functionalisations using these scaffolds[9,83,84]
- The well documented benefits of utilising mono-anionic, bidentate DGs (**Scheme 16**)[83,85]
- The ease of introduction of the scaffolds
- Potential future application of the DGs to C(sp^3)–H functionalisation of alkylboronic acids

The initial designs selected are shown in **Figure 9**.

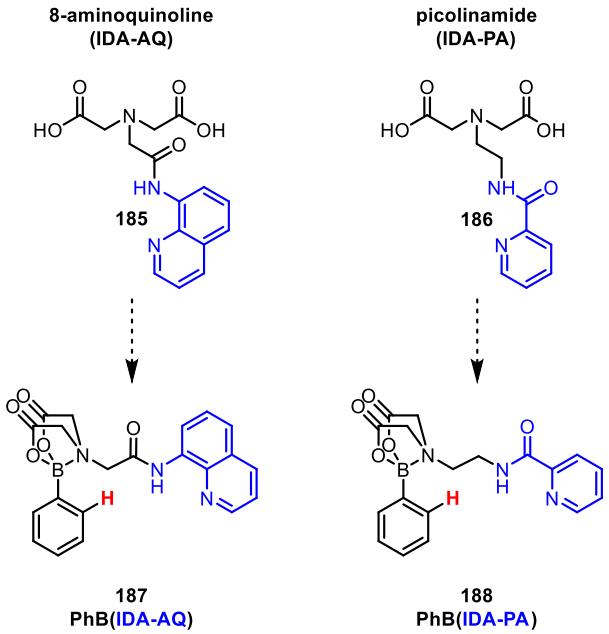


Figure 9: Initial designs for strongly coordinated DGs tethered to iminodiacetic acid to enable the ortho-C–H functionalisation of aryl boronic acids.

The proposed structures **185** and **186** were intended to enable *ortho*-C(sp^2)–H functionalisations and consequently were designed to restrict the size of the metallacycles that could be formed during cyclometalation. However, it was also anticipated that electron-withdrawing groups proximal to the iminodiacetic acid nitrogen would weaken the strength of the B–N coordination and that in turn, these would reduce their ability as protecting groups; clearly a balance would need to be struck.

The potential 8-membered metallacyclic intermediates **189** and **190** that could be formed after directed C–H insertion are shown in **Figure 10**.

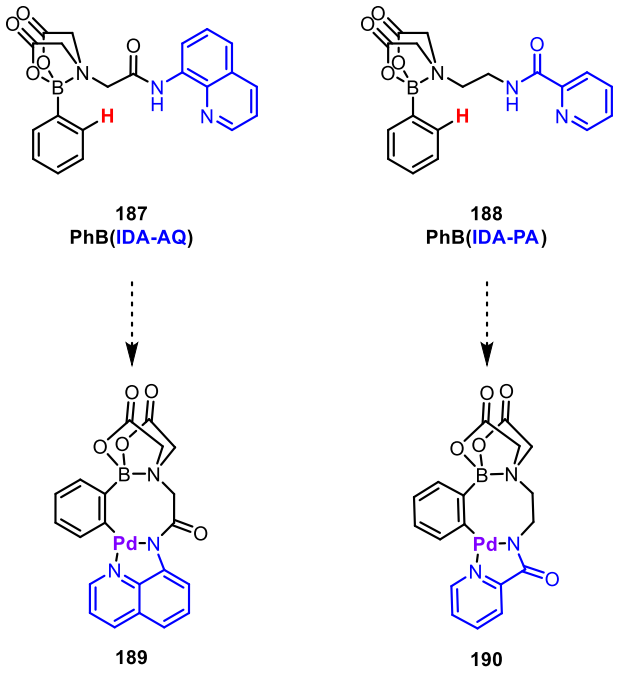


Figure 10: Proposed 8-membered metalacyclic intermediates that could be formed following coordination of Pd to the DGs, followed by C–H insertion.

Although 8-membered metallacycles are rarely invoked in C–H functionalisations, it was hoped that the significant sp^2 character of several of the constituent atoms of the rings would reduce the transannular strain associated with 8-membered systems. The rigid, bicylic boronate IDA functionalities could also aid formation of the metallocycle via the Thorpe-Ingold effect.[124] As such it was believed that these structures **187** and **188** would provide the best balance of proximity to the desired *ortho* position, combined with distance from the B–N bond.

Retrosynthetic analysis provided two possible routes to the iminiodiacetic acid tethered DGs **187** and **188** — synthesis of the modified diacids **185** and **186** then condensation, as used by Burke,[197] or alkylation of phenyl boronic acid iminiodiacetic acid (IDA) ester **195**, as demonstrated by Mancilla (**Figure 11**).[198,199]

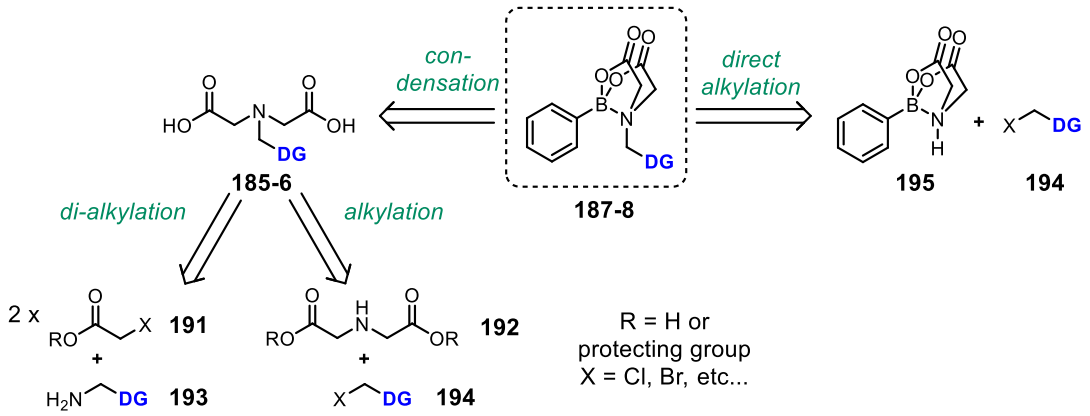
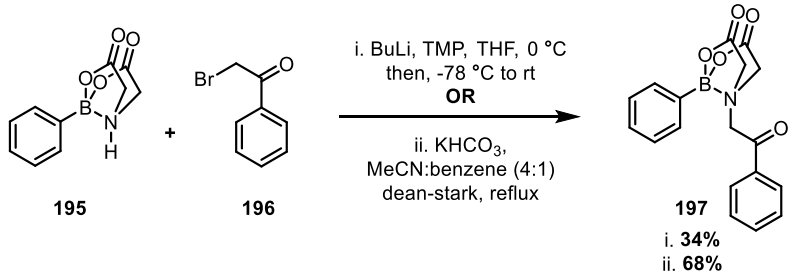


*Figure 11: Two possible routes for the synthesis of the proposed DGs **187** and **188**.*

2.2 Synthesis of the First Generation DGs

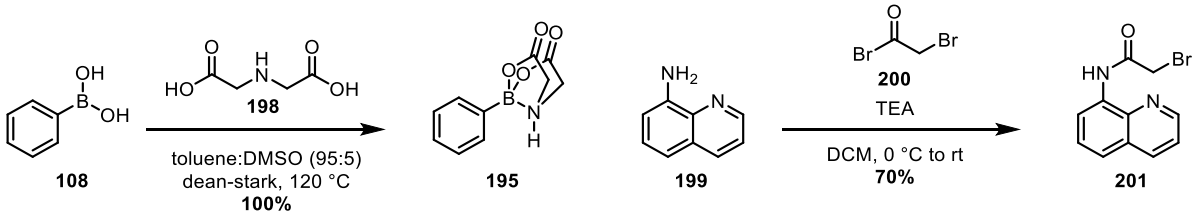
2.2.1 Synthesis of PhB(IDA-AQ) 187

Studies by Mancilla *et al*. demonstrated that the alkylation of PhB(IDA) **195** was possible using both lithium tetramethylpiperidine (LiTMP) and simple $KHCO_3$ in combination with a suitable alkyl bromide (**Scheme 41**).[198,199]



Scheme 41: Conditions developed by Mancilla for the alkylation of PhB(IDA).[198,199]

This synthetic route was first investigated for the synthesis of the PhB(IDA-AQ) **187** as it avoided the need for protection and deprotection of the IDA **198**, and could be applied for the synthesis of both DG designs (**Scheme 42**).



*Scheme 42: Synthesis of the starting materials for the alkylation of PhB(IDA) **195**.*

The PhB(IDA) **195** was first accessed in quantitative yield by adapting the route developed by Burke for the synthesis of MIDA boronates.[200] The requisite α-bromo acetamide **201** was next accessed in one step from bromoacetyl bromide **200** and 8-aminoquinoline **199** in 70% yield.

The reaction conditions used by Mancilla were then attempted (**Table 3**, Entries 1 and 2).



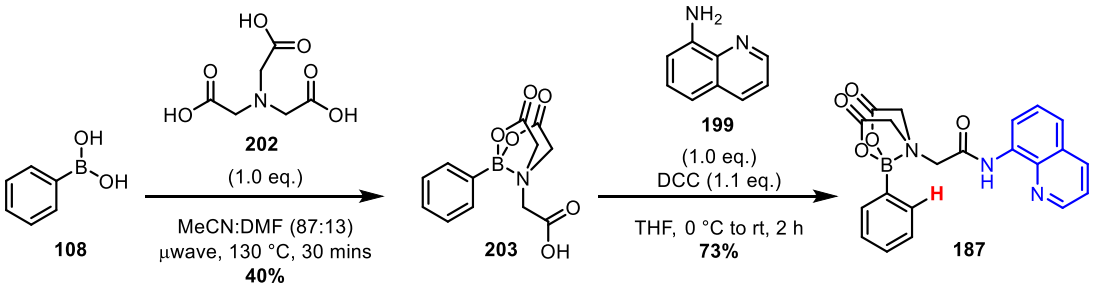
Entry	Conditions	Yield of 187
1	LiTMP (1.0 eq.), THF, -78 °C [198]	0%
2	$KHCO_3$ (3.0 eq.), MeCN:Tol (8:2), 95 °C, dean-stark [199]	0%
3	DIPEA (3.0 eq.), TBAI (20 mol%), MeCN, 90 °C	24%
4	$KHCO_3$ (3.0 eq.), TBAI (20 mol%), MeCN, 90 °C	0%
5	K_2CO_3 (3.0 eq.), TBAI (20 mol%), MeCN, 90 °C	0%
6	Na_2CO_3 (3.0 eq.), TBAI (20 mol%), MeCN, 90 °C	0%
7	DIPEA (3.0 eq.), TBAI (20 mol%), MeCN, room temp.	**49%**

*Table 3: Screening of reaction conditions for the alkylation of PhB(IDA) **195**. All reactions were performed under N_2 for 16 hours, on a 0.1 mmol scale.*

Unfortunately, neither of the conditions yielded any product. Consequently, a screen of bases and conditions was performed to try and achieve the alkylation. Gratifyingly, it was found that DIPEA was a suitable base, in conjunction with a tetrabutylammonium iodide (TBAI) additive and that this combination afforded a 24% yield of the desired product **187** (**Table 3**, Entry 3). Further optimisation was able to double the yield to 49% (**Table 3**, Entry 7).

When attempted on a larger scale however, the alkylation reaction proved unreliable, with yields varying from 49% to 18%. As well as this, several by-products were formed making purification difficult. It became apparent that a different route was required to access the PhB(IDA-AQ) **187** in the quantities required for method development.

It was envisaged that condensation of $PhB(OH)_2$ **54** with nitrilotriacetic acid **202** could be used to access the free carboxylic acid **203**, which in turn could be directly coupled to 8-aminoquinoline **199** using a suitable amide coupling reagent (**Scheme 43**).



*Scheme 43: Two-step synthesis of the PhB(IDA-AQ) **187** using nitrilotriacetic acid **202** and DCC.*

After investigating a number of conditions, a modified version of the microwave mediated procedure developed by Spencer *et al.* allowed access to the nitrilotriacetic acid boronate ester **203** in 40% yield.[201]

The low yield was deemed acceptable due to the cheap, readily available starting materials **108** and **202**, the speed of the reaction and ease of purification using Burke's 'catch and release' conditions.[194] The amide coupling then proceeded smoothly using DCC to yield the IDA-AQ boronate ester **187** in 75% yield.

With the first PhB(IDA-DG) **187** in hand, attention turned to investigations into its stability. Consistent with standard MIDA boronates, the phenyl IDA-AQ boronate **187** was an off-white, free-flowing crystalline solid that was stable on the bench over extended periods.

Phenyl MIDA boronate **127** has been reported as stable in DMSO-d_6 at temperatures in excess of 130 °C.[171] The phenyl boronic acid IDA-AQ ester **187** was subjected to variable temperature (VT) ^{1}H NMR analysis in DMSO-d_6 from 50 °C to 130 °C for comparison (**Figure 12**).

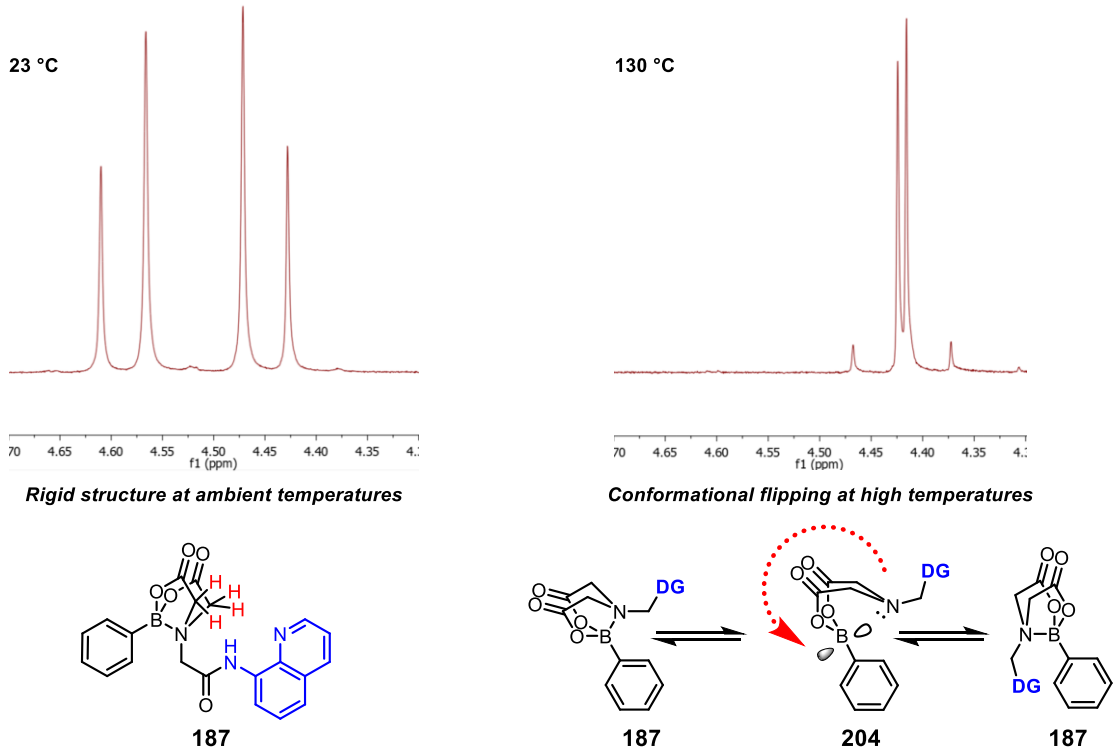


*Figure 12: Variable temperature ^{1}H NMR spectra of compound **187** —showing the chain in chemical shift of the highlighted diastereotopic protons at 130 °C. Spectra recorded in DMSO-d_6 at 400 MHz.*

A considerable change in the chemical shifts of the diastereotopic IDA protons (**Figure 12**, *left spectra*) was observed at 130 °C indicating temperature dependent shifts, with conformational flipping likely occurring slower than the NMR timescale. At temperatures above 80 °C, new peaks in the aryl region were also observed, suggestive of slow disassociation of the IDA-AQ ligand at elevated temperatures however.

The molecular structure of the PhB(IDA-AQ) **187** in the solid phase was obtained by a single crystal X-ray structure analysis (**Figure 13**).

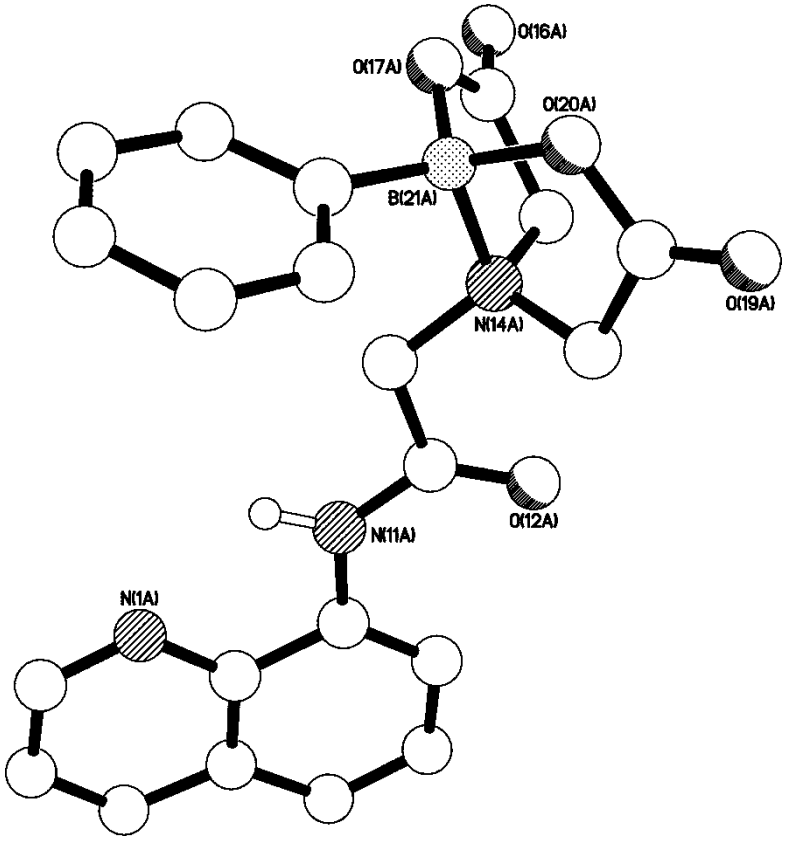
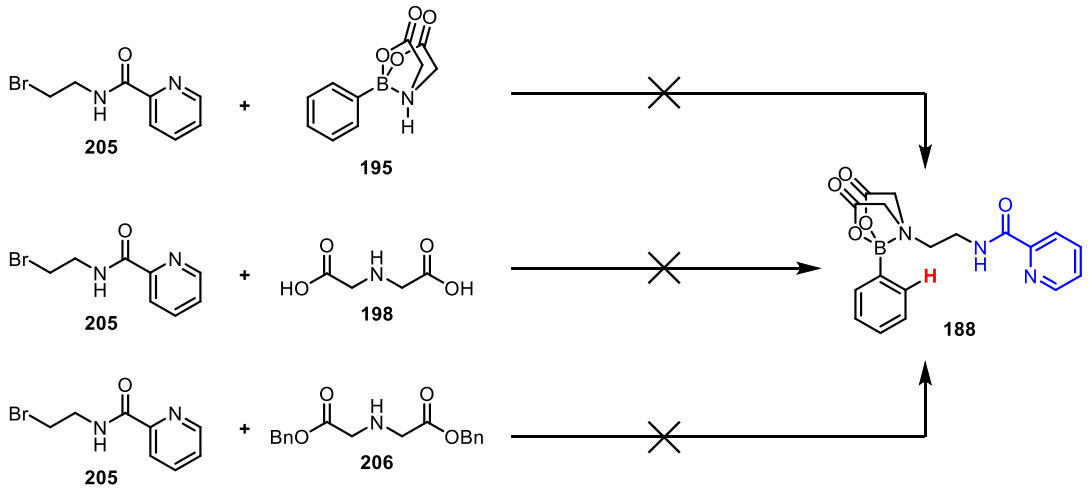


*Figure 13: The molecular structure of PhB(IDA-AQ) **187** obtained by a single crystal X-ray structure analysis.*

The data obtained from this experiment allowed for a comparison of the B–N bond length to be drawn with that in the phenylboronic acid MIDA ester **127** using literature values. The B–N bond lengths of 1.668 and 1.660 Å respectively for the two structural conformations where in accordance with the literature values of 1.662 and 1.673 Å for PhB(MIDA) **127**.[202]

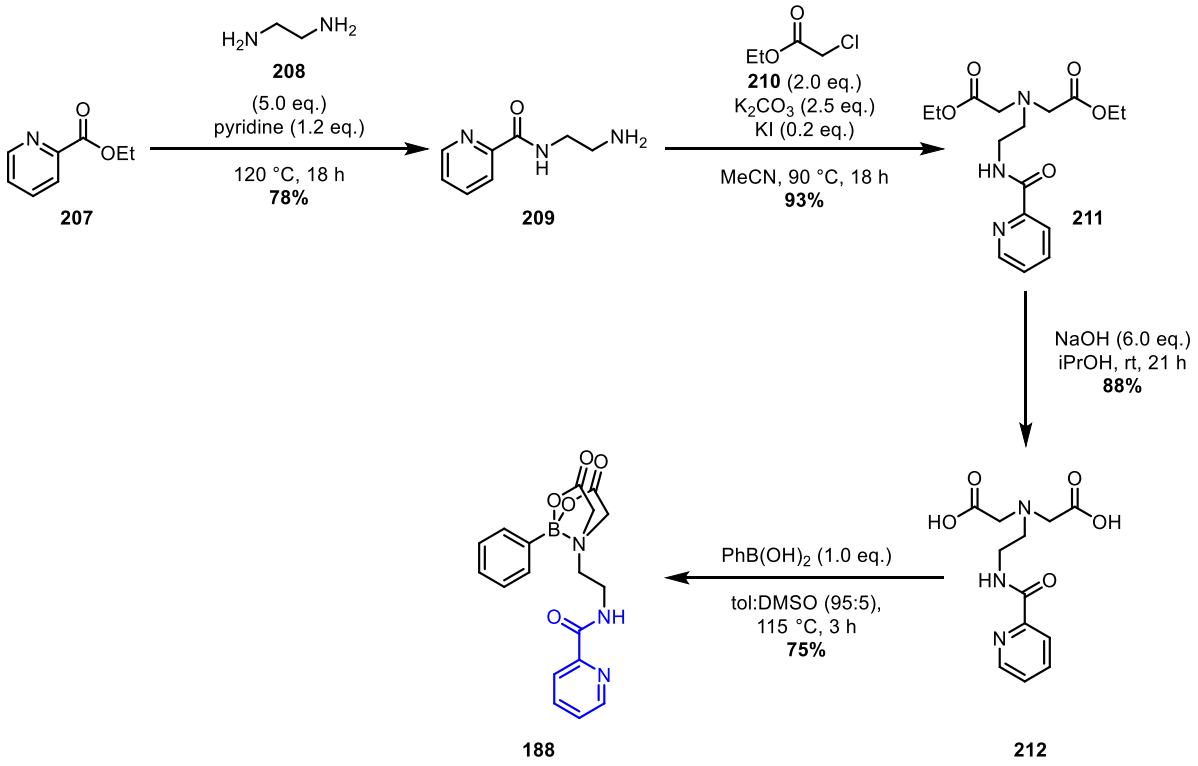
2.2.2 Synthesis of PhB(IDA-PA) 188

The synthesis of the picolinamide based DG **188** proved more challenging than accessing the PhB(IDA-AQ) **187**. Attempts to alkylate PhB(IDA) **195** with the corresponding alkyl bromide **205** were wholly unsuccessful, including using the previously optimised DIPEA conditions. Further attempts to perform the alkylation with IDA **198** and dibenzyl iminodiacetate **206** were also unsuccessful (**Scheme 44**).



*Scheme 44: Unsuccessful attempted alkylations towards the synthesis of PhB(IDA-AQ) **188**.*

As a result, a dialkylation approach was undertaken, beginning from 1,2-diaminoethane **208** (**Scheme 45**).



*Scheme 45: The successful synthetic route to PhB(IDA-PA) **188**, achieving 48% yield over 4 steps after optimisation.*

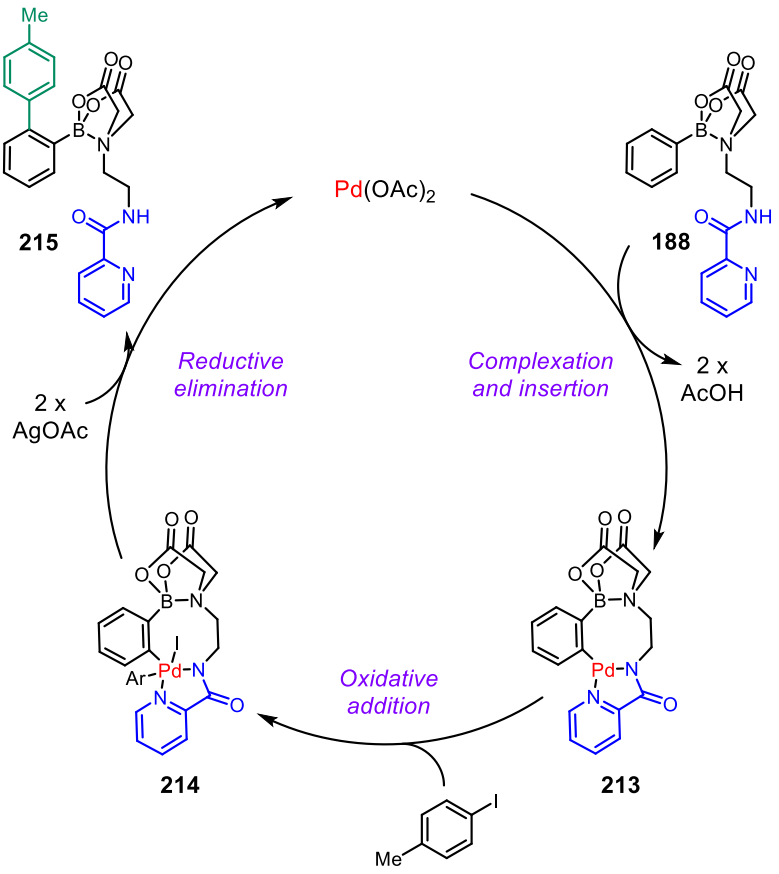
Amidation of ethyl picolinamate **207** proceeded well in an economical manner, requiring no solvent or amide coupling agent. Benzyl ester protecting groups were initially investigated, with an eye to accessing compound **212** as the free zwitterion. It was believed that the pH neutral hydrogenolysis conditions used for deprotection would allow expedient access to **212**. However, in practice, the reductive *bis*-deprotection proved low yielding. Alkylation using ethyl

chloroacetate **210** and subsequent *bis*-deprotection proved a more suitable solution. Purification of the dicarboxylic acid **212** sodium salt after saponification was achieved using a barium assisted precipitation method developed by Burke.[197] Finally, PhB(IDA-PA) **188** was accessed by condensation with $PhB(OH)_2$ (**108**) in just 3 hours and a total yield of 48% over 4 steps. Gratifyingly, Burke's 'catch and release' purification conditions (*see 1.3.2*) could be used to simplify the isolation of **188**.

2.3 Investigations into *ortho*-C(sp^2)–H Arylation Reactions

2.3.1 Method Development

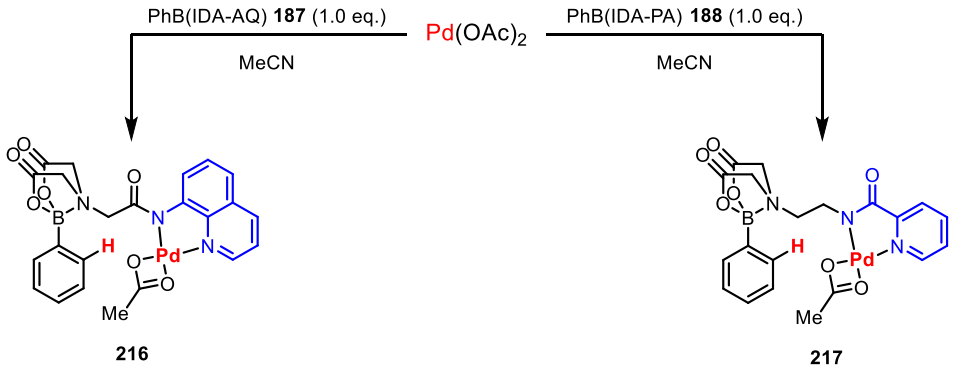
With the DGs **187** and **188** in-hand, interest turned to the development of C–H arylation reactions. Investigations would initially focus on palladium acetate as catalyst, as this compound has been employed widely in C(sp^2)–H arylation reactions when coupled with an aryl iodide or diaryliodonium salt electrophile. It was hypothesised the transformation would proceed via a Pd^{II}/Pd^{IV} mechanism (**Scheme 46**).



*Scheme 46: A hypothetical Pd^{II}/Pd^{IV} mechanism for C–H arylations using the PhB(IDA-PA) **188** DG, $Pd(OAc)_2$, a silver salt and an aryl iodide electrophile.*

Co-ordination of Pd^{II} to the bidentate DG followed by *ortho* C–H metalation would form the 8-membered metallocycle **213**. The catalyst could then undergo oxidation from Pd^{II} to the high energy Pd^{IV} complex **214** by the aryl iodide (or diaryliodonium salt), due to the stabilising effect of the bidentate directing ligand. Finally, reductive elimination and ligand exchange would regenerate the active catalyst and yield the biaryl product **215**.

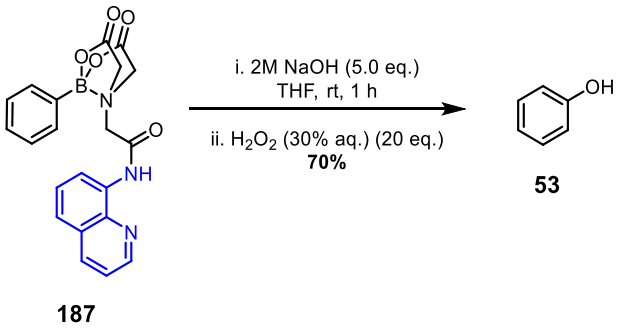
To investigate the interaction between $Pd(OAc)_2$ and the PhB(IDA-DGs) **187** and **188**, attempts to isolate the key C–H inserted palladacycles were performed (**Scheme 47**).



*Scheme 47: Stoichiometric reactions of $Pd(OAc)_2$ with PhB(IDA-AQ) **187** and PhB(IDA-PA) **188** DGs both yielded yellow precipitates, indicative of coordination to yield the putative structures **216** and **217**.*

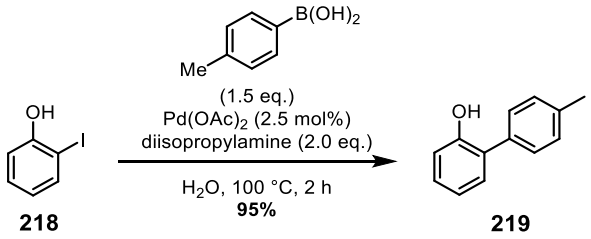
In two separate reactions, stoichiometric amounts of $Pd(OAc)_2$ and each DG were combined in anhydrous MeCN at room temperature. Yellow precipitates were observed forming after several hours with both the 8-AQ and picolinamide based DGs **187** and **188**, indicative of complexation. Unfortunately, ^1H NMR analysis was unable to distinguish whether only complexation or complexation and subsequent C–H insertion had occurred. Multiple efforts to prepare samples for single crystal X-ray crystallography were also unsuccessful.

Next, a method for the high-throughput screening of reaction conditions was developed, that utilised gas chromatography (GC) for analysis of the results. The high polarity and molecular weights of the phenyl IDA-DG boronates made them unsuitable for GC analysis. As such, a one-pot deprotection-oxidation of the IDA-DG boronates was developed to allow for the rapid conversion of the products to the corresponding phenols (**Scheme 48**).



Scheme 48: The deprotection/oxidation of IDA-DG boronate esters — as used to allow rapid analysis of reactions.

The procedure, using NaOH followed by hydrogen peroxide, reliably oxidised the PhB(IDA-AQ) **187** to the corresponding phenol **53** in around 70% yield in just one hour. The relative proportions of phenol **53** and biphenol product **219** could then be analysed using GC analysis with an internal standard to allow calculation of yields. An authentic sample of the 2-(*p*-tolyl)phenol product **219** was synthesised to allow for calibration of the GC. Consequently, the tentative assigning of yields was possible based upon analysis of peaks with retention times matching the authentic sample. Dodecane was chosen as the internal standard (**Scheme 49**).

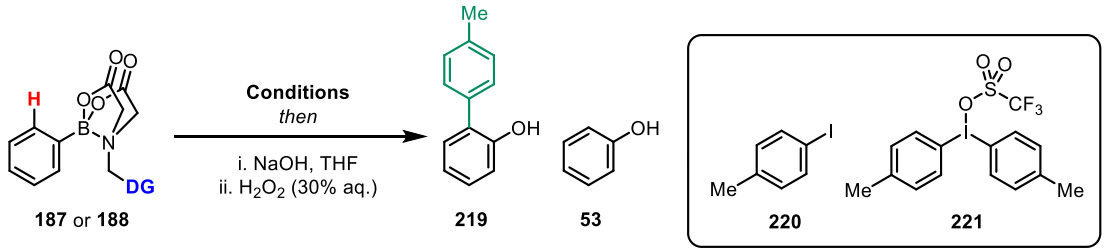


Scheme 49: Synthesis of an authentic sample of the desired product from ortho C–H arylation – deprotection – oxidation, to allow GC calibration.

2.3.2 Screening of Reagents and Conditions

4-Iodotoluene **220** and di(*p*-tolyl)iodonium triflate **221** were chosen as the initial coupling partners for investigation. Methyl-substituted arylating reagents were chosen to allow differentiation between products in the event of deprotection of the IDA-DG boronate starting material and C–H arylation using the phenyl boronic acid **108** formed. The triflate salt of the hypervalent iodine was chosen due to ease of synthesis.[203]

Screening of reagents and conditions focused on the two oxidants (**220** or **221**), inorganic carbonate and acetate bases, high temperatures and tolyl or alcohol solvents. A summary of the successful reactions and variations attempted is given in **Table 4**.



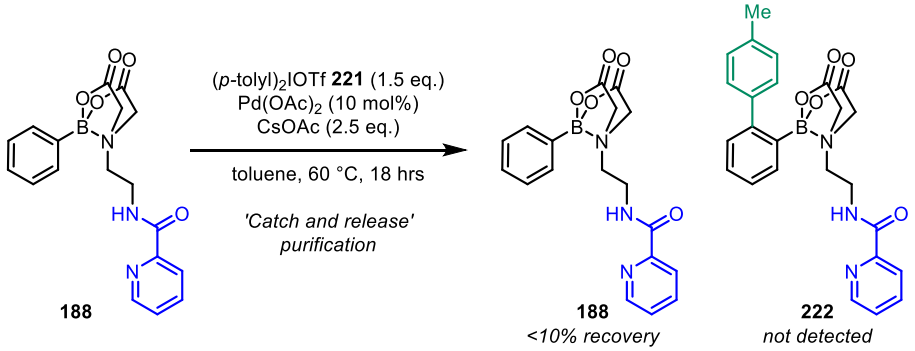
Entry	DG	Conditions[a]	Yield 219[b]	Yield 53[b]
1	AQ **187**	**220**, AgOAc, tol, 110 °C, 72 h	0%	ND
2	AQ **187**	**220**, K_2CO_3, 4-iodotoluene, 110 °C, 72 h	0%	ND
3	AQ **187**	**220**, AgOAc, tol, 60 °C, 48 h	0%	ND
4	AQ **187**	**221**, CsOAc, ^{t}BuOH, 60 °C, 17 h	trace	70%
5	AQ **187**	**221**, AgOAc, tol, 60 °C, 17 h	6%	**46%**
6	PA **188**	**221**, AgOAc, tol, 60 °C, 18 h	5%	37%
7	PA **188**	**221,** CsOAc, tol, 60 °C, 18 h	**9%**	40%
8	PA **188**	**221,** AgOAc, tol, 60 °C, 18 h, H_2O (3 eq.)	**11%**	23%
9	PA **188**	**221**, CsOAc, tol, 60 °C, 18 h, Ac-Gly-OH (0.2 eq)	6%	43%
10	PA **188**	**221**, CsOAc, tol, 60 °C, 18 h, 2,6-lutidine (0.2 eq)	9%	42%
11	PA **188**	**221**, CsOAc, ^{t}amyl-OH, 60 °C, 18 h, 3Å mol sieves	trace	73%
12	PA **188**	**221**, CsOAc, HFIP, 60 °C, 18 h	0%	53%
13	PA **188**	**221**, CsOAc, tol, 100 °C, 36 h	trace	21%

*Table 4: Screening conditions for C(sp^2)–H arylation of compounds **187** and **188**. [a]$Pd(OAC)_2$ (10 mol%), Oxidant (**220** or **221**) (1.5 eq.), Base (2.5 eq.), temp, time, additive, dodecane (1.0 eq.), solvent (0.1M). [b]Yields are tentatively assigned using GC with a dodecane internal standard. Yields of <5% are reported as trace.*

PhB(IDA-AQ) **187** was investigated first leading to a number of key findings (**Table 4,** entries 1-5). At temperatures >60 °C rapid degradation occurred, in accordance with the VT NMR data obtained. Diaryliodonium salt **221** proved to be a suitable oxidant, with no product observed using aryl iodide **220**. Acetate bases, particularly CsOAc (**Table 4,** entry 4) and AgOAc (**Table 4,** entry 5), were essential to obtaining the 2-(*p*-tolyl)phenol (**219**).

The successful conditions were next applied using the picolinamide-based DG **188** (**Table 4,** entries 6-13). Toluene proved to be the most effective solvent, able to achieve 10% yield with CsOAc and with AgOAc when doped with water (**Table 4,** entries 7-8). Despite investigating numerous conditions and additives, no higher yields were achieved.

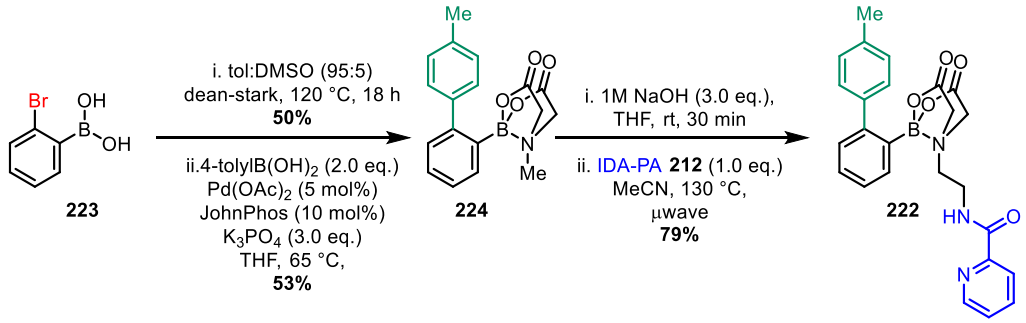
As the oxidation was not quantitative, it was believed that the yields being achieved were higher than those measured by GC analysis. To measure the yield accurately, the reaction conditions yielding the highest amount of both phenols **53** and **219** were repeated on a larger scale (*cf.* **Table 4,** entry 7) and purified using a 'catch and release' purification (**Scheme 50**).



*Scheme 50: Attempted 'catch and release' purification for isolation of the arylated product **222**.*

Unfortunately, only a very small amount of the starting material **188** was recovered with none of the desired product **222**.

With the suspicion of false positives being detected by GC, NMR was enlisted to corroborate the results obtained thus far. To aid NMR analysis, an authentic sample of the product **22** was prepared (**Scheme 51**).



*Scheme 51: Synthesis of an authentic sample of biaryl IDA-PA product **222**, for NMR analysis.*

The diastereotopic protons alpha to the MIDA carbonyl functionalities, previously used to diagnose conformational flipping (*see* **Figure 12**), were also chosen as the key peaks used to monitor the reaction by ^{1}H NMR. This was due to the ease of analysis of the characteristic AB coupling pattern. The effect of the *ortho* tolyl substituent on the chemical shifts of the diagnostic protons was a small upfield shift and increased splitting between the two doublets. While the starting material **188** doublet peaks appear at 4.21 ppm and 4.06 ppm, the biaryl **222** diastereotopic proton system appears at 4.08 ppm and 3.45 ppm, with a consistent *J* value of 17 Hz for all peaks (**Figure 14**).

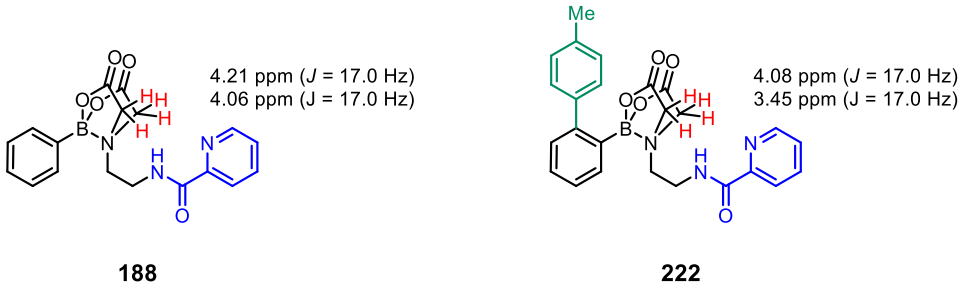


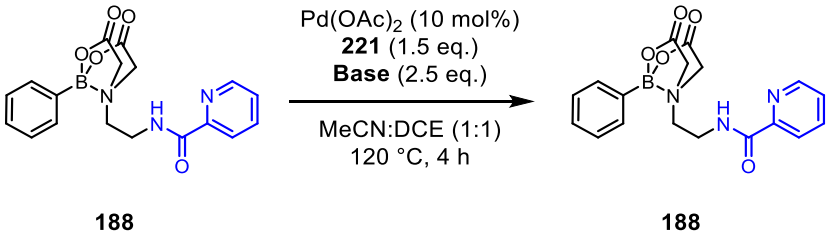
Figure 14: Comparison of the ^{1}H NMR shifts of the key diasterotopic protons used for NMR analysis of reaction mixtures.

Having established a method by which to judge product formation by inspection of key ^{1}H NMR shift values the reaction was repeated under the conditions previously identified (**Table 4,** entries 7-8). Unfortunately, no product peaks were observable in the ^{1}H NMR spectrum of the crude reaction mixture. A possible reason for this is the rapid deprotection of the product **222** to the corresponding boronic acid after arylation. Subsequent oxidation of this species to the biphenol **219** could explain the GC yields observed. Due to congestion in the aromatic region of the reaction ^{1}H NMR spectra, this putative biaryl boronic acid was not conclusively detected. Although, aryl boronic acid peaks in the ^{11}B NMR spectra were observed, it was not possible to differentiate whether these corresponded to phenyl (deprotected starting material) or biaryl (deprotected product) boronic acid peaks.

What was clear during NMR analysis of the reaction mixtures was that a large amount of degradation and by-product formation was occurring during the reactions, with highly complex NMR spectra obtained.

2.3.3 Investigations into PhB(IDA-PA) 188 and PhB(IDA-AQ) 187 Stability

With concerns about the stability of the DGs under the reaction conditions, a number of further investigations into their stability under C–H arylation reaction conditions were performed. Specifically, it was suspected that the base component of the reactions was causing the loss of the DG. This was confirmed with a screen of bases at 120 °C (**Table 5**).

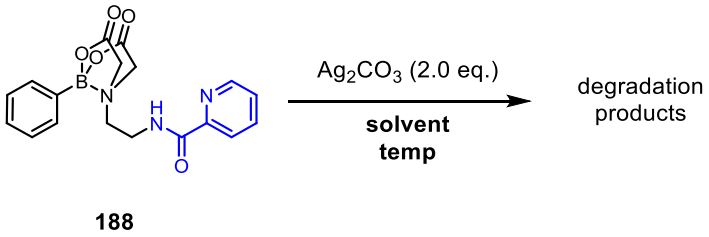


Entry	Base	188 Remaining
1	AgOAc	73%
2	CsOAc	63%
3	K_3PO_4	41%
4	none	97%

*Table 5: The effect of base on the rate of degradation of PhB(IDA-AQ) **188**.*

As was expected, increasing strength of base saw increasing amounts of degradation. The control experiment (**Table 5,** entry 4) also confirmed the stability of the DG **188** to the other reaction components.

The effect of solvent and temperature on stability were next examined. Temperatures of 100 °C and 120 °C were chosen to be examined, as representative of the temperature ranges generally employed for C–H arylations with mono-anionic bidentate DGs (*see Chapter 1.1.2*). MeCN:DCE (1:1) and *tert*-amyl alcohol were chosen as representative high boiling point, non-nucleophilic and nucleophilic solvents respectively, commonly used in C–H functionalisations. A MeCN:DCE mixture was used as the IDA-DG boronates **187** and **188** were only sparingly soluble in DCE. Ag_2CO_3 was not fully soluble in MeCN:DCE or *t*-amyl alcohol. The results are shown in **Figure 15**.



188

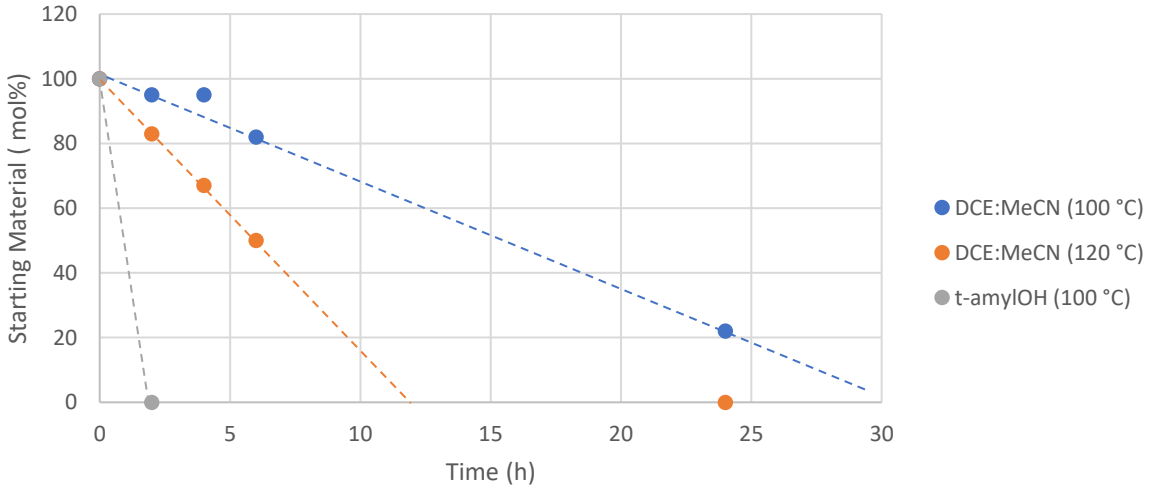
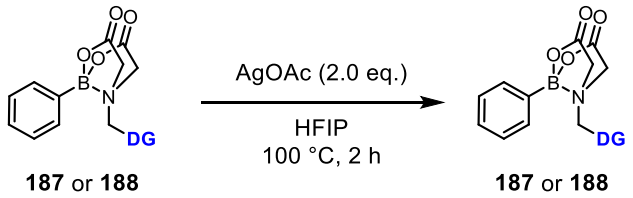


*Figure 15: The effect of solvent and increasing temperature on degradation of the PhB(IDA-PA) **188**.*

Using 2.0 equivalents of Ag_2CO_3 to simulate reaction conditions, almost full degradation was observed within 24 hours under all conditions. *tert*-Amyl alcohol caused almost immediate loss (within 2 h) of the DG, despite the sterically hindered nature of the nucleophilic solvent.

Finally, a comparison of the two DG stabilities was made (**Table 6**).



187 or **188** **187** or **188**

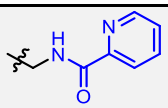
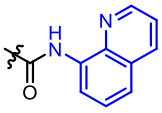
Entry	DG	SM Remaining
1		50%
2		17%

Table 6: Comparison of the stabilities of the two IDA-DG boronate esters.

The weakly, nucleophilic solvent HFIP, a privileged solvent in C–H functionalisations, was used at a temperature of 100 °C.[119,120,204] These conditions were anticipated to cause partial degradation to allow comparisons to be drawn between the two DGs **187** and **188**. It was predicted that the aminoquinoline based DG **187** would be more labile, due to the close proximity of the electron-withdrawing carbonyl to the B–N bond. In practice, the difference in stability was marked, with only 17% of the PhB(IDA-AQ) **187** remaining after 2 hours, compared to 50% PhB(IDA-PA) **188** after the same duration.

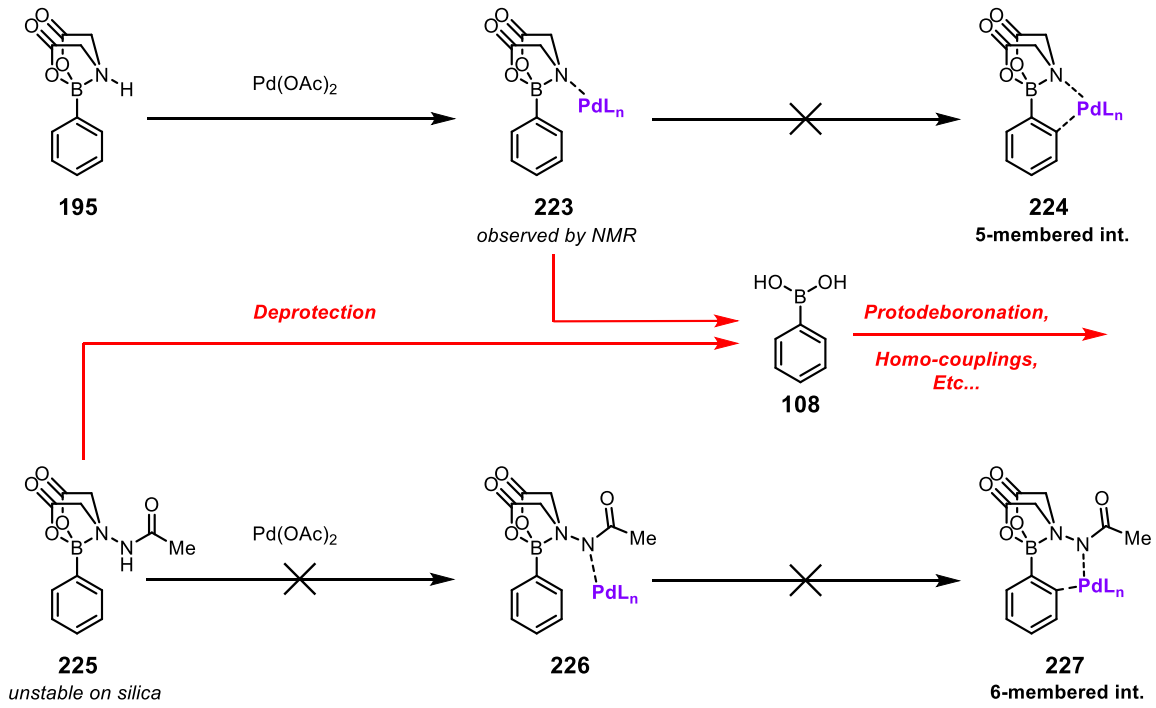
From the stability studies it became apparent that an alternate approach was required. Although coordination to the DGs was likely occurring, at 60 °C little evidence of C–H arylation with retention of the B(IDA-DG) functionality was evident. The higher temperatures likely to be required, especially to access the putative 8-membered palladacycles, resulted in rapid loss of the starting material over the reaction times. Accordingly, the two DG scaffolds, IDA-PA **186** and IDA-AQ **185** were ultimately deemed unsuitable.

3. Second Generation Designs

3.1 A Different Approach

Although the first generation picolinamide and aminoquinoline based DGs **187** and **188** had proved unsuitable for our purposes, the studies on these derivatives had provided valuable data to take into account when looking to design new IDA tethered DGs.

The first design consideration was the size of the metallacyclic intermediate required to form to enable C–H insertion. In this regard, it was believed that the medium ring sizes previously targeted were unsuitable. Preliminary investigations using a simple iminodiacetic acid scaffold **195** and a hydrazide based DG **225** confirmed that 5 or 6 membered metallacylic systems were also unsuitable using the N–B coordinated scaffold (**Scheme 52**).



*Scheme 52: Experiments to access 5- or 6-membered metallocycles using the PhB(IDA) and hydrazide based DGs **195** and **225**. These were unsuitable due to stability issues — coordination of Pd weakened the B–N bond in PhB(IDA) **195** causing deprotection, while the hydrazide based DG **225** was unstable even on silica.*

While evidence of coordination to the nitrogen in PhB(IDA) **195** by $Pd(OAc)_2$ was obtained by ^1H NMR spectroscopy when using stoichiometric palladium, this coordination led to deprotection of the boronic acid even at room temperature. As the weakening of the B–N bond was such that even in the absence of base and elevated temperatures degradation occurred, PhB(IDA) **195** was deemed unsuitable as a directing motif. Similarly, the hydrazide based boronate ester **225** degraded upon silica gel, making it's purification difficult and suggesting a high degree of instability.

These experiments highlighted the need to minimise any electron-withdrawing effects on the B–N bond. Consequently, it was hypothesised that any successful DG would be required to form larger cyclic intermediates during the C–H functionalisation. Electron withdrawing groups proximal to the B–N dative bond would also need to be avoided in the new design. Lastly, 'harsh' reaction conditions, defined as temperatures in excess of 100 °C, nucleophilic solvents and strong bases, needed to be avoided if possible.

The techniques pioneered by Yu for the *meta*- or *para*-selective C(sp^2)–H functionalisation of aryl systems using nitrile DGs seemed to address these requirements (**Figure 16**).[99,122]

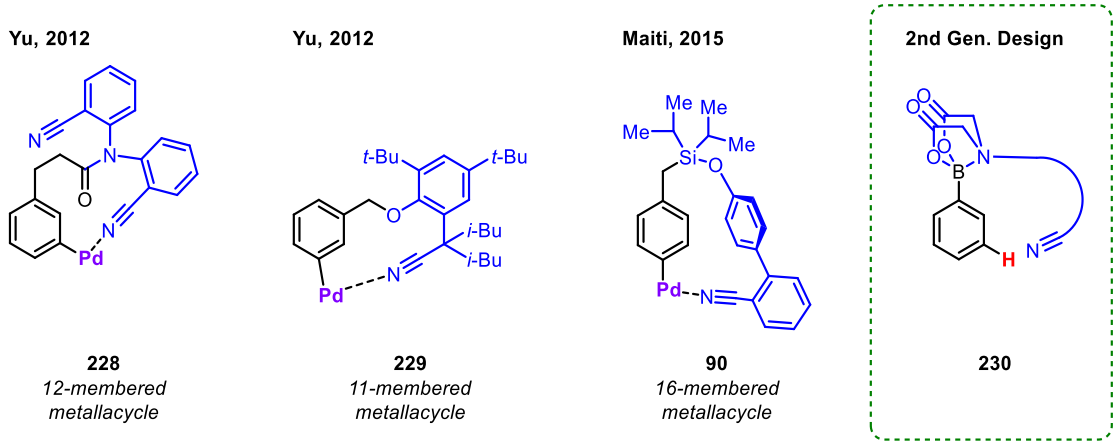
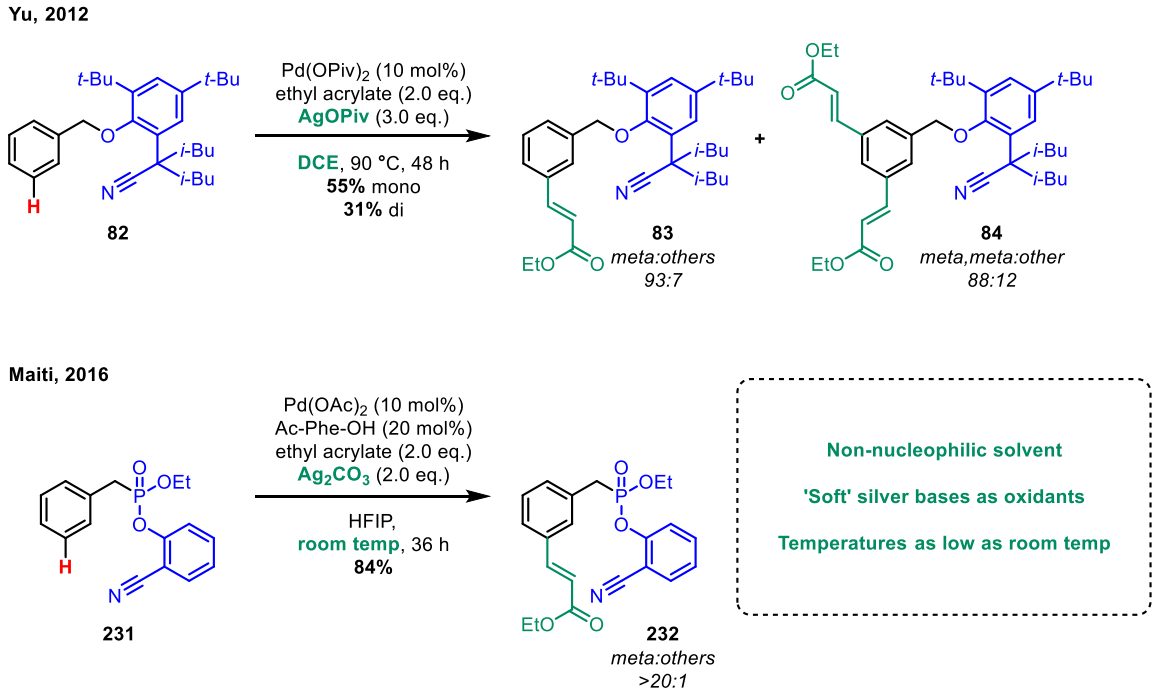


Figure 16: Macrocyclic metallacycles involving linear coordination of Pd to a nitrile DG as proposed to be operative in successful literature C–H functionalisation reactions and a proposed MIDA boronate design inspired by these.[122,123]

The nitrile coordinates to palladium in a linear manner, allowing macrocyclic 'cyclophane-like' transition states to form during C–H insertion.[99] Metallacycles with as many as 16 constituent atoms have been invoked (compound **90**).[123] When applied to the MIDA boronate systems, the distal nature of the DGs would allow for designs with minimal negative electronic effect on the B–N bond.

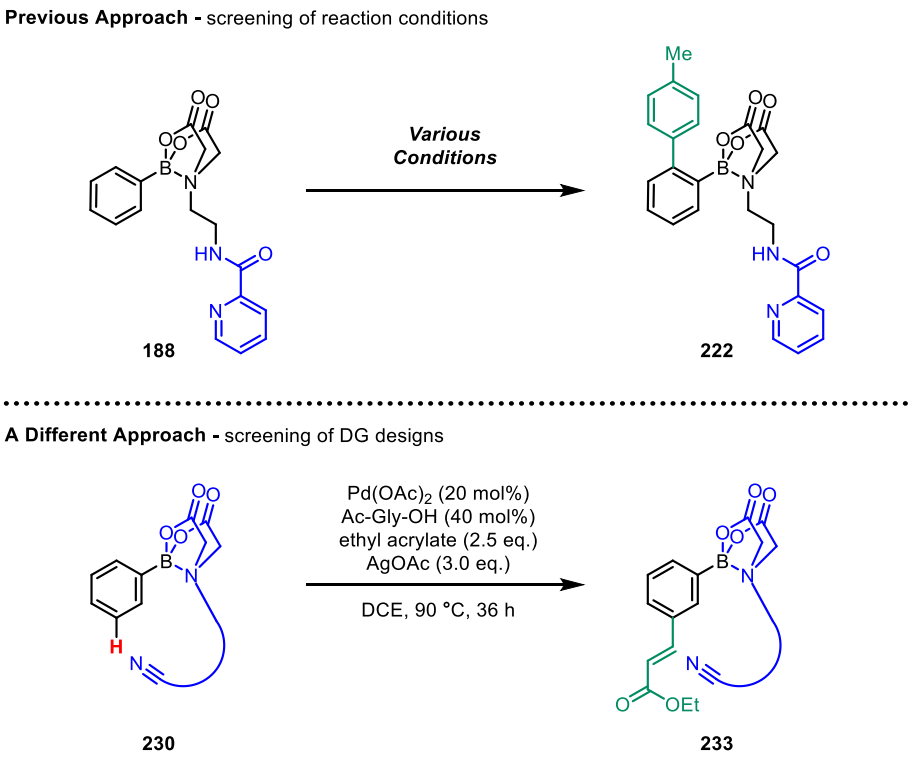
The reaction conditions employed for C–H functionalisations using these systems also appeared amenable to MIDA boronates (**Scheme 53**).



Scheme 53: Two examples of reaction conditions for C–H alkenylations using nitrile DGs, with the possible benefits for use with aryl MIDA boronates highlighted.[122,145]

Using C–H alkenylations as a representative reaction, the factors known to result in boronate deprotection are minimised or avoided. Although the weakly nucleophilic solvent HFIP is often employed, precedent exists for utilising the non-nucleophilic solvent DCE.[122] Weakly basic silver salts are employed as oxidants, avoiding harsh alkali bases. Finally, temperatures as low as room temperature have been previously employed.[145] Interestingly, the conditions are also remarkably general across DG scaffolds employing linear nitrile coordination. In contrast, the DG designs themselves are bespoke, requiring different designs for different aryl systems (*see Chapter 1.1.3*)

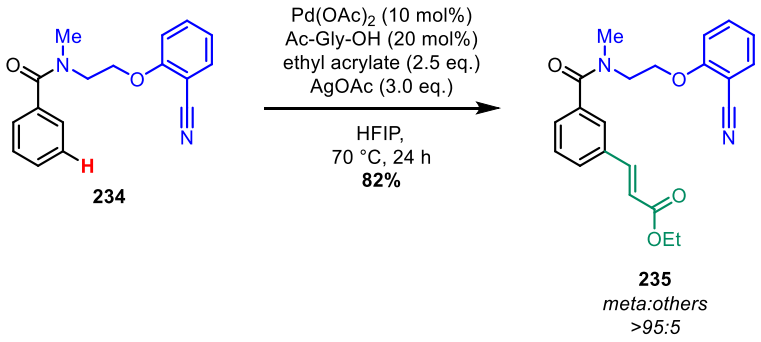
It was concluded that a new approach should be taken. With the first generation designs, method development focused on finding successful conditions for the two DGs synthesised (*see Chapter 2.3.2*). The new approach would instead focus on the screening of DG designs with a set of standard conditions (**Scheme 54**).



Scheme 54: A comparison of the two approaches used for developing novel directed C–H functionalisation methods.

3.1.1 Design of the Second Generation DGs

As indicated above, the plan was to begin with a starting scaffold based on a literature design, and then prepare variations until a successful scaffold was found. As such, a starting point was required that resembled a MIDA boronate, would be simple to synthesise and could be used to synthesise many variants quickly, in a convergent manner. The DG **234** designed by Yu for the *meta*-selective C–H alkenylation of benzoic acid derivatives (**Scheme 55**) was chosen as a suitable starting design.[129]



Scheme 55: Yu's amide tethered, 2-cyanophenol based DG design for the meta*-alkenylation of benzoic acid derivative* ***234****.*[129]

The *N*-methylbenzamide functionality appeared a close surrogate for an aryl MIDA boronate, with only slight differences in conformation anticipated. The aryl ether linkage would minimise negative inductive effects on the B–N bond, while providing a synthetic handle to simplify synthesis. The ethylene bridge could also be lengthened to lessen any detrimental inductive effects. Lastly, the 2-cyanophenol motif could easily be substituted with various steric or electronic modifiers during investigations. In this manner, a library of analogues of the MIDA based DG **236** could be synthesised and screened against standard conditions (**Figure 17**).

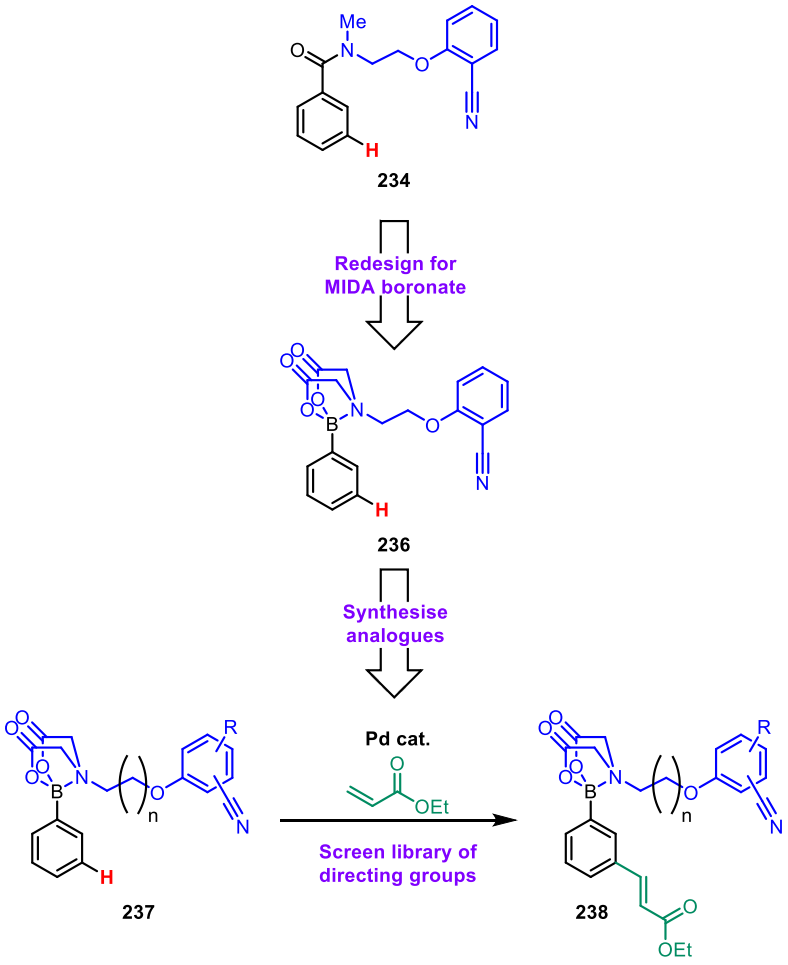
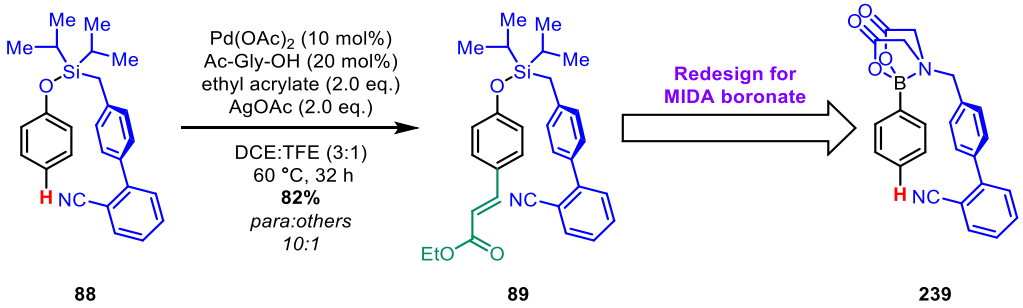


Figure 17: The envisioned approach for designing a meta*-selective DG for MIDA boronates, based on Yu's original scaffold* ***234****.*[129]

The *para* selective motif **88** developed by Maiti and applied in C(sp^2)–H alkenylations, was also suitable for redesign using the MIDA boronate scaffold.[137] It was hypothesised that the quaternary nitrogen centre would prove an excellent mimic for the *bis*-isopropylsilyl linker (**Scheme 56**).



Scheme 56: Maiti's para*-selective DG and the variant* ***239*** *envisioned here for use with a MIDA boronate tether.*[137]

In total, 10 DG designs were envisioned. These would focus mainly on *meta*-functionalisation, with one potential *para* directing design. An overview of the designs and the effects intended for investigation are shown in **Figure 18**.

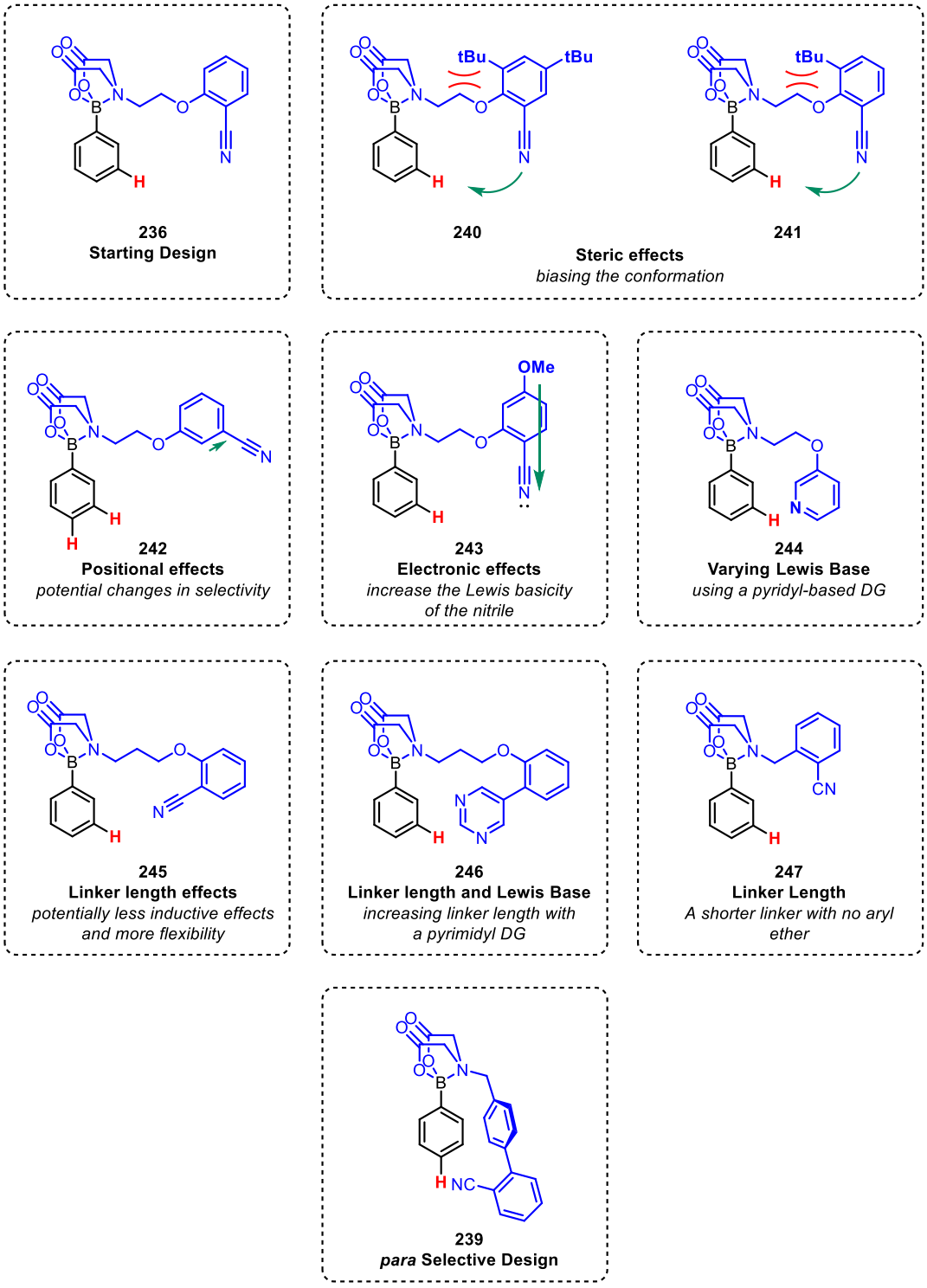
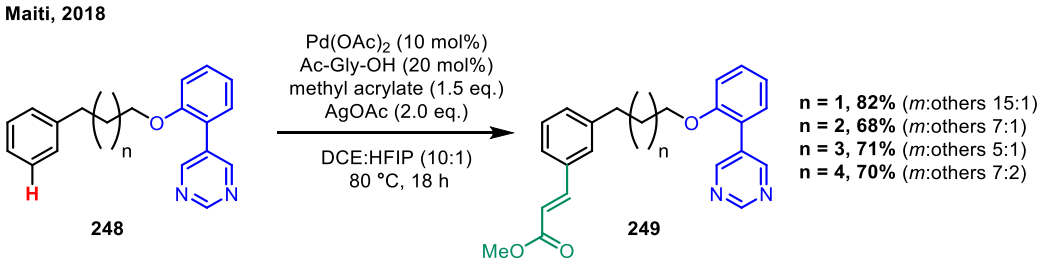


Figure 18: The 10 DG designs selected for synthesis in order to investigate steric, electronic and other factors. The focus was on achieving meta*-selective C–H insertion, however one potentially para directing design was included.*

Comparisons between the 2- and 3-cyanophenols (**Figure 18, 236** and **242**) would provide information on the required directionality, with the 3-cyanophenol potentially activating the *para* C–H position of aryl boronic acids. The two *tert*-butyl substituted cyanophenols (**Figure 18, 240** and **241**) were chosen in an attempt to bias the conformation of the system, pointing the nitrile

towards the parent boronic acid. The methoxy substituent *para* to the nitrile (**Figure 18, 243**) was chosen to strengthen the linear coordination of the nitrile to palladium. The 3-hydroxypyridine derivative (**Figure 18, 244**) was chosen to provide an alternative Lewis basic group to coordinate to the Pd in place of the nitrile DG. Utilising a longer carbon linker (**Figure 18, 245**) would investigate the effect of increased flexibility in the DG, as well as the effect of a slight reduction in the inductive influence of the benzylic oxygen atom on the B–N bond.

Maiti *et al*. were able to achieve *meta* C(sp²)–H alkenylations using a pyrimidyl based DG **248** that could act over extremely long linker lengths, with little effect on yield (**Scheme 57**).[150]



*Scheme 57: The pyrimidyl based DG **248** designed by Maiti which displays* meta *selectivity even over extremely long linker lengths.[150] This work inspired us to test a similar MIDA-based boronate system with a longer linker length.*

As the 2-pyrimidylphenol DG could be easily introduced in the same manner as the cyanophenol motifs, compound **246** was included in the screen.

The shorter, benzyl linked system **247** was included to reduce flexibility and due to its expected ease of synthesis via alkylation of PhB(IDA) **195**. Lastly, scaffold **239** was included as a mimetic of Maiti's *para*-selective systems.[123,137]

3.2 Synthesis of the Second Generation DGs

3.2.1 *Meta*-Selective DGs

When planning the synthetic route to the *meta*-selective DGs, late-stage introduction of the cyanophenol motif was given priority, to expedite the synthesis of the DG library.

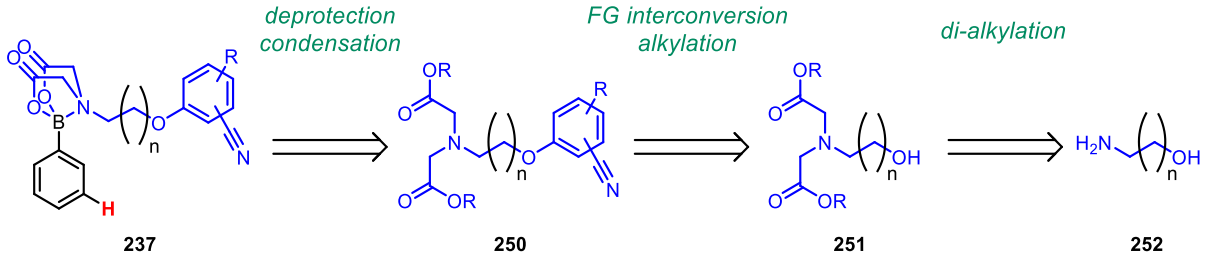
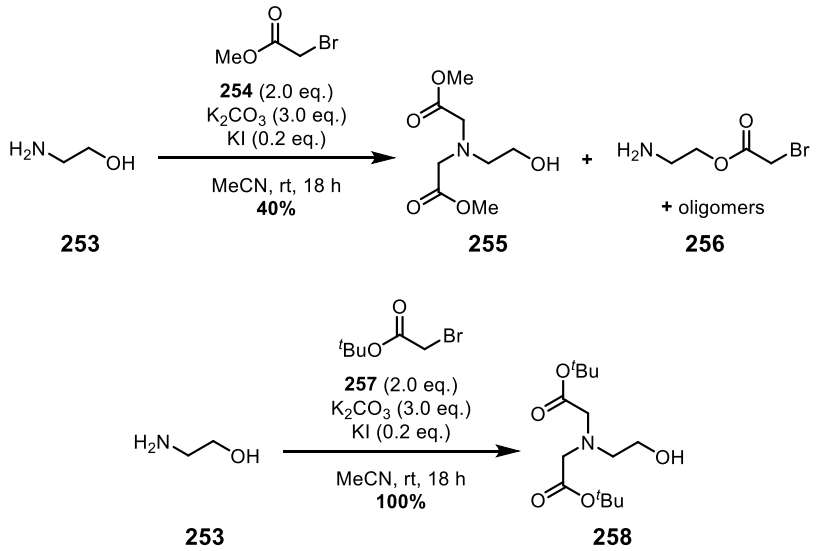


Figure 19: Retrosynthetic analysis of the route for synthesising multiple DG variants. The benzonitrile DG is installed as late as possible to facilitate downstream diversification.

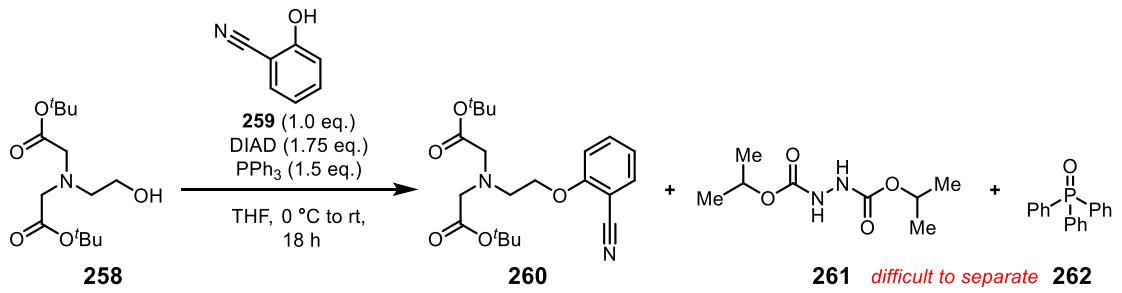
Due to the issues with alkylation of PhB(IDA) **195**, iminodiacetic acid **198,** and benzyl iminodiacetate **206** using the alkyl bromide **205** (*see* **Scheme 44**)**,** the dialkylation of 2-aminoethanol **253** was initially investigated (**Figure 19**). The resulting alcohol could subsequently be activated to nucleophilic attack by conversion to a halide or pseudohalide. Introduction of the desired cyanophenol, deprotection and condensation to phenyl boronic acid **108** would yield the desired PhB(MIDA-DG) analogues for screening.

The synthesis began with the dialkylation of 2-aminoethanol **253**. The conditions used previously (*see* **Scheme 45,** *step 2*) were adapted, with the temperature lowered to try and prevent competing transesterification. Methyl bromoacetate **254** was first employed, as the deprotection of methyl esters is facile using NaOH (**Scheme 58**).



*Scheme 58: Dialkylation of amino alcohol **253** with methyl bromoacetate **254** and with* tert*-butyl analogue **257**.*

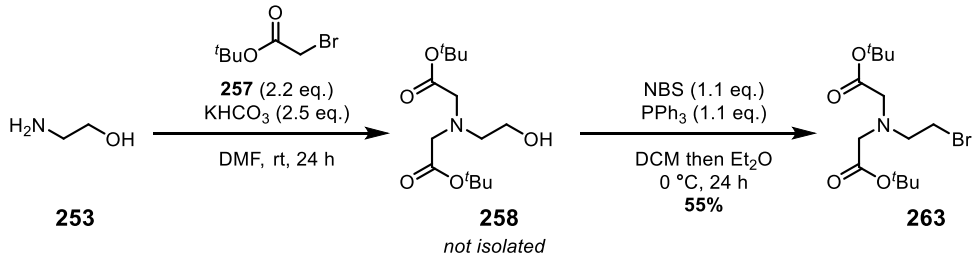
Unfortunately, despite the lowered temperature, large amounts of transesterification was observed, giving various oligomeric by-products (**256**). This led to a disappointing yield of only 40%, compared to the 93% previously achieved (*see* **Scheme 45,** *step 2*). To prevent the transesterification, methyl bromoacetate **254** was exchanged for the sterically hindered *tert*-butyl bromoacetate **257**, resulting in quantitative yield of the desired alcohol **258**.



*Scheme 59: The Mitsunobu reaction of alcohol **258** with phenol **259** showing by-products **261** and **262** which made purification of **260** tedious..*

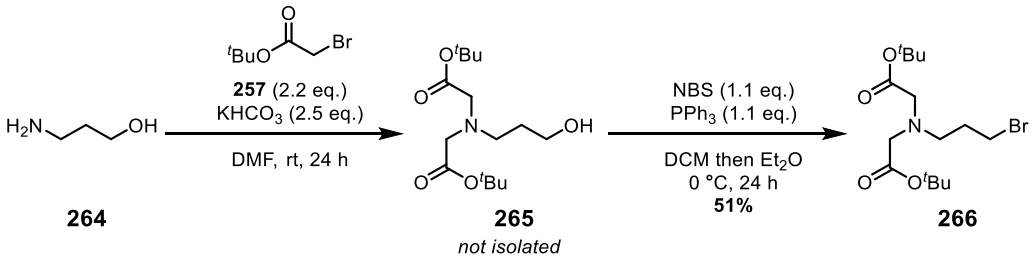
A Mitsunobu reaction was next investigated to form the aryl ether linkage, using 2-cyanophenol **259** as model substrate. Although the yield appeared to be high (approximately 90%) by ^{1}H NMR analysis, the by-products generated during the process were problematic. Removal of the diisopropyl hydrazine-1,2-dicarboxylate **261** and triphenylphosphine oxide **262** by-products proved difficult due to them having similar polarity to the aryl ether **260**. The purification was considered particularly egregious when it was considered that it would have to be repeated for each DG.

Activation of the alcohol **258** by bromination was next considered. Though formally adding an extra step, it was believed it would greatly simplify the subsequent, divergent nucleophilic attack, resulting in overall faster synthesis of the DG library. In practice, a telescoped dialkylation-Appel procedure to access alky bromide **263** had previously been developed by Williams and Rapoport, allowing facile access to large amounts of the desired compound **263** in good yield (**Scheme 60**).[205]



*Scheme 60: The telescoped dialkylation-Appel reaction procedure developed by Williams and Rapoport which enabled access to alkyl bromide **263**. Addition of Et_2O at low temperature allowed the simple removal of $OPPh_3$ via filtration.[205]*

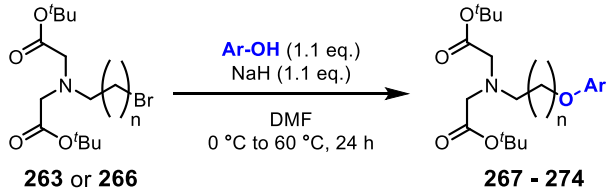
The telescoped procedure was also used to prepare the propylene linked bromide **266** beginning with 3-aminopropanol **264** (**Scheme 61**).

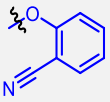
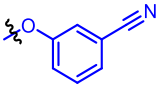
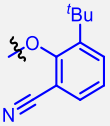
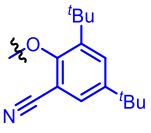


*Scheme 61: Synthesis of propylene linked alkyl bromide **266** was accessed via telescoped procedure.*

The homologated variant was obtained in comparable yield, allowing investigation of the effect of linker length on the DG.

With routes to the alkyl bromides **263** and **266** in hand, attention turned to the phenol alkylation reaction. Employing 2-cyanophenol **259** in conjunction with the ethylene linked bromide **263** as a model system, the alkylation proved simple. Deprotonation of the phenol using NaH at 0 °C in DMF, addition to a solution of the alkyl bromide **263** and gentle heating overnight resulted in excellent yield of the product **267** after a simple chromatographic purification (**Table 1**, entry 1). These conditions were then employed with a number of substituted cyanophenols and other DG motifs (**267** to **274**). The yields are displayed in **Table 1**.



Entry	Product	n	Ar-O-R	Yield	DG Effects Investigated
1	**267**	1		86%	-
2	**268**	1		69%	Directional
3	**269**	1		82%	Steric
4	**270**	1		90%	Steric

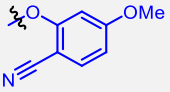
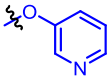
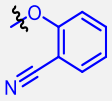
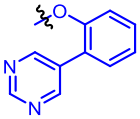
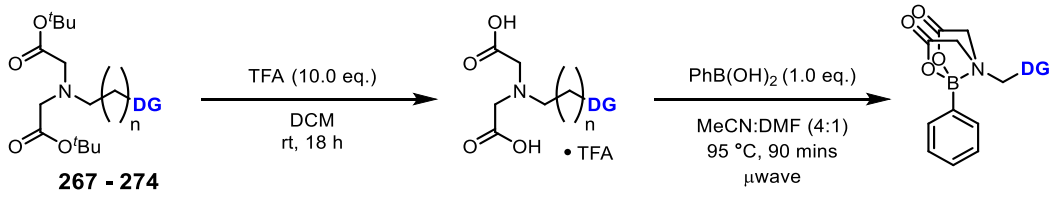
5	**271**	1		89%	Electronic
6	**272**	1		74%	Lewis base
7	**273**	2		84%	Linker length
8	**274**	2		86%	Linker length, Lewis base

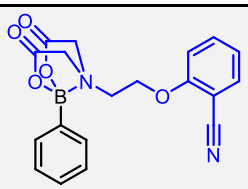
*Table 7: Alkylation reactions of various phenols using alkyl bromide **263** and **266**. Reaction scales varied (see experimental section).*

Gratifyingly, all the desired DG motifs were accessed in high yields using the developed alkylation conditions.

It was decided to telescope the subsequent deprotection and condensation steps, as the purification of the product MIDA boronates could easily be achieved using 'catch and release' conditions. Deprotection of the *tert*-butyl esters proved facile using trifluoracetic acid (TFA) in dichloromethane (CH_2Cl_2), with gaseous isobutylene the only by-product. Removal of the excess acid and solvent under vacuum revealed the diacid without need for further purification. The condensation could then quickly be performed using a modification to the microwave conditions developed by Spencer.[201] 'Catch and release' purification with Et_2O and Et_2O:MeCN revealed the desired PhB(MIDA-DG)s **275** to **282** in varying yields (**Table 8**).



267 - 274

Entry	Product	Structure	Yield	DG Effects Investigated
1	**236**		73%	-

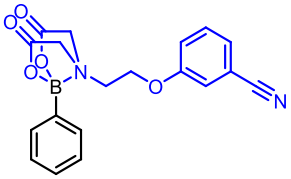
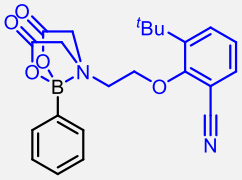
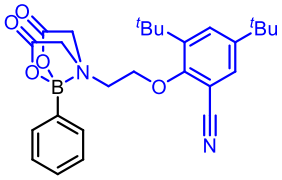
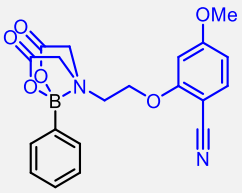
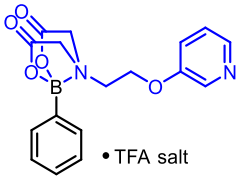
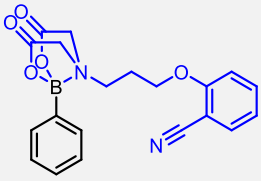
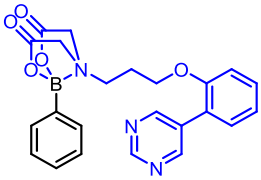
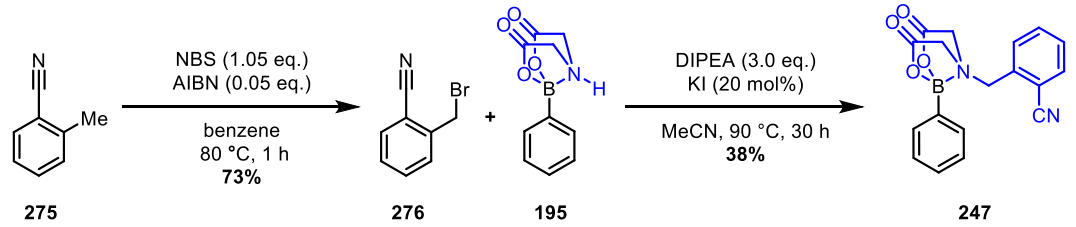
2	**242**		68%	Directional
3	**241**		50%	Steric
4	**240**		46%	Steric
5	**243**		72%	Electronic
6	**244**		66%	Lewis base
7	**245**		57%	Linker length
8	**246**		26%	Linker length and Lewis base

*Table 8: Telescoped deprotection-condensation reactions of derivatives **267-274** to obtain PhB(MIDA-DG)s. Reaction scales varied (see experimental section).*

All scaffolds were amenable to the 'catch and release' purification, except **240**, with the di-*tert*-butyl groups proving too lipophilic to 'catch' to the silica. The cause for the low yield with the pyrimidyl based system **246** was unknown and, as enough material was synthesised, not further investigated.

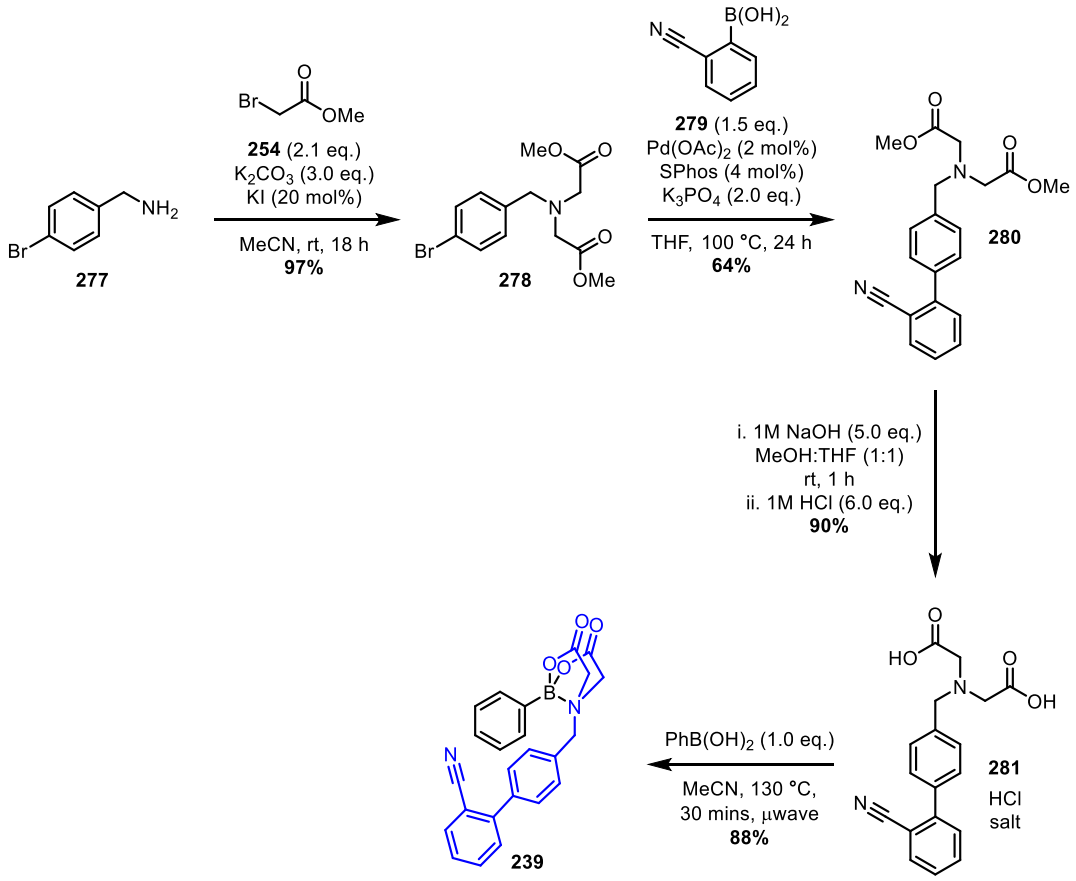


*Scheme 62: Synthesis of the benzyl linked directing group **247** in 2 steps from 2-cyanotoluene **275** and PhB(IDA) **195**.*

The last *meta* DG left to synthesise was the benzyl linked scaffold **247**. Radical bromination of 2-cyanotoluene **275** and alkylation of PhB(IDA) **195** using the previously optimised conditions (*see* **Table 3**) allowed expedient access to compound **247** for the DG screen.

3.2.2 *Para*-Selective DG

The *para*-selective design **239** was based on the scaffolds developed by Maiti[123,137] and was synthesised using a route similar to those used for the *meta*-selective DGs (**Scheme 63**).



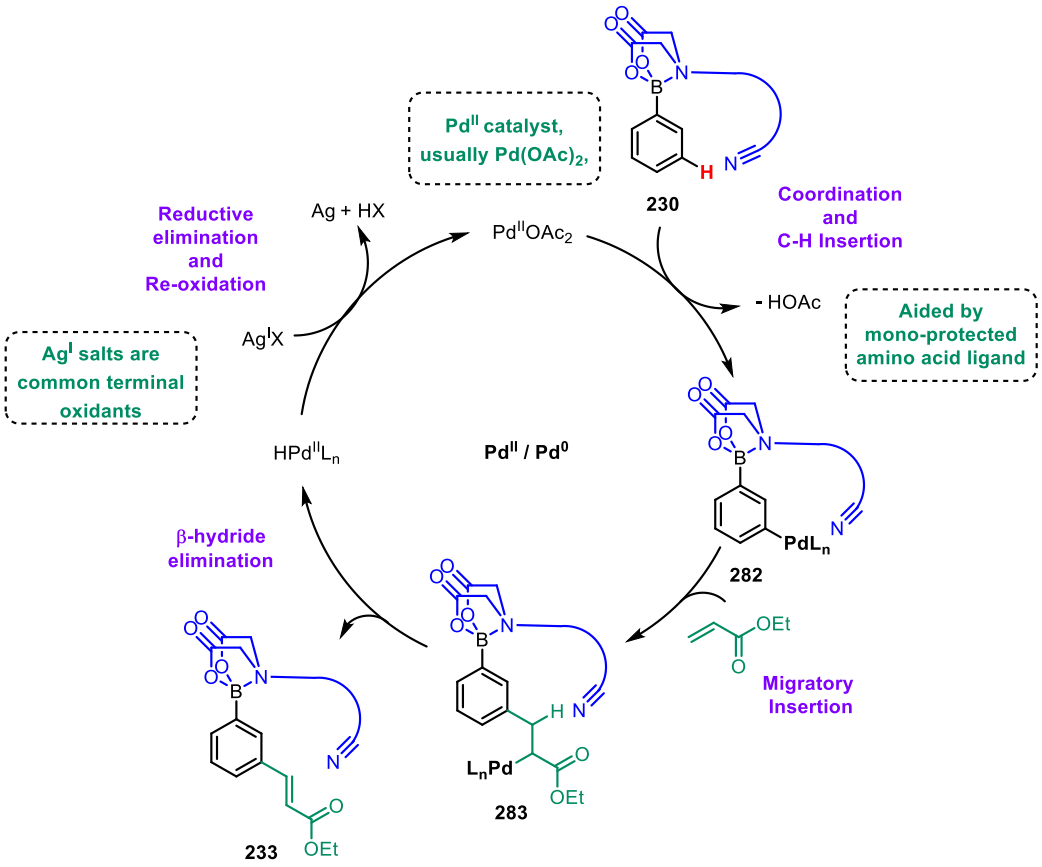
Scheme 63: The synthetic route applied to access the potentially para *directing PhB(MIDA-DG) **239**.*

Dialkylation proceeded smoothly using methyl bromoacetate **254** in acetonitrile; the absence of an alcohol FG on the amine alkylating agent removed the need for *tert*-butyl esters to prevent competing transesterification. Subsequent Suzuki-Miyaura coupling installed the nitrile directing motif, before a telescoped saponification and condensation with phenylboronic acid **108** yielded the DG **239**. The route would also be suitable for the introduction of different 2-cyanophenol substitution patterns or DG motifs via variation of the boronic acid **279** during future investigations. Consequently, PhB(MIDA-DG) **239** was accessed in just 4 steps and 49% overall yield.

3.3 Screening of the Second Generation DGs

With the PhB(MIDA-DG) scaffolds successfully synthesised, their screening against a standard set of C–H functionalisation conditions could be performed with subsequent analysis anticipated to reveal the most effective scaffold.

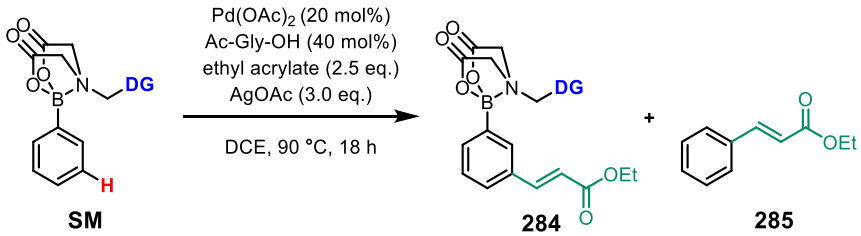
Palladium catalysed C–H alkenylations were first chosen to be investigated. This was due to the large body of literature relating to these transformations; C–H alkenylations are by far the most commonly performed C–H functionalisations when using this class of nitrile based DGs.[99,113] A set of standard conditions, that would be compatible with the PhB(MIDA-DG) scaffolds, while still allowing C–H functionalisation, were required. By considering the potential mechanism, based on a Pd^{II}/Pd^{0} cycle, it was clear a Pd^{II} catalyst, a mono-protected amino acid ligand, an acrylate ester coupling partner and a terminal oxidant would be needed (**Scheme 64**).

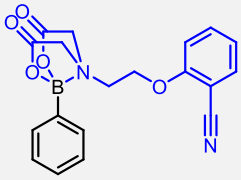
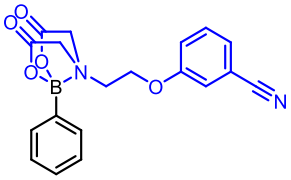
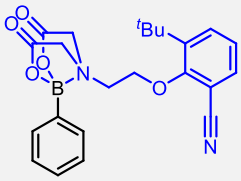
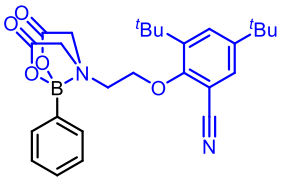
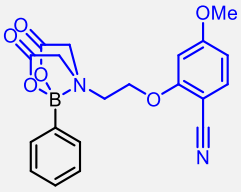
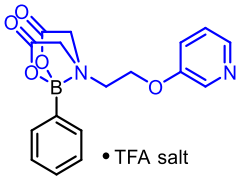
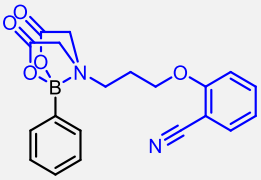


Scheme 64: The postulated mechanism for C–H alkenylations using a MIDA tethered DG, via a Pd^{II}/Pd^{0} cycle.

Bench stable, readily available $Pd(OAc)_2$ and *N*-acetyl glycine were chosen as the catalyst-ligand pair, in 20 mol% and 40 mol% respectively. The high catalyst loading was chosen to maximise the chance of success, with little effect on DG degradation from these components anticipated (based on studies with PhB(IDA-PA) **188**, *see* **Table 5**). Silver acetate was chosen as the terminal oxidant, simply due to its prevalence within the literature.[99,113] Ethyl acrylate was chosen as the initial coupling partner. Importantly, the non-nucleophilic solvent DCE was chosen, with a temperature of 90 °C, over the weakly nucleophilic HFIP. This choice was based upon previous studies with first generation designs, where rapid loss of the DGs occurred when using Ag salts in combination with HFIP (*see* **Table 6**). The highly polar PhB(MIDA-DG)s were only sparingly soluble in DCE, and so a concentration of just 0.05 M was initially chosen. However, even at this dilution and at 90 °C, the MIDA-DG boronates were observed to be only partially soluble.

Gratifyingly, with the 2-cyanophenol based scaffolds **236** and **245** peaks corresponding to the desired alkenylated products were observed to form, in 4% and 8% yield respectively (**Table 9**, entries 1 and 7).



Entry	Compound	DG	Yield 284	Yield 285	Conversion of SM
1	**236**		**4%**	39%	43%
2	**242**		0%	43%	50%
3	**241**		0%	46%	65%
4	**240**		0%	42%	58%
5	**243**		0%	40%	50%
6	**244**	 • TFA salt	0%	35%	83%
7	**245**		**8%**	32%	40%

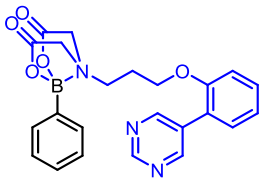
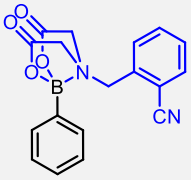
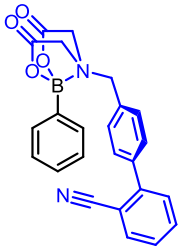
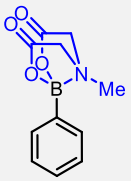
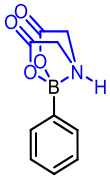
8	**246**		0%	52%	64%
9	**247**		0%	46%	ND
10	**239**		0%	22%	ND
11	**127**		0%	2%	2%
12	**195**		0%	10%	ND

Table 9: Screening of PhB(MIDA-DG)s using general C–H alkenylation conditions. All yields are measured using reaction mixture ^{1}H NMR against a CH_2Br_2 internal standard. Reactions were performed on a 0.05 mmol scale. Confirmation of product yields was performed retrospectively against authentic meta*-alkenylated products obtained via classical Heck couplings of the 3-bromophenylboronic acid analogues of MIDA-DG boronates **236** and **245**.*

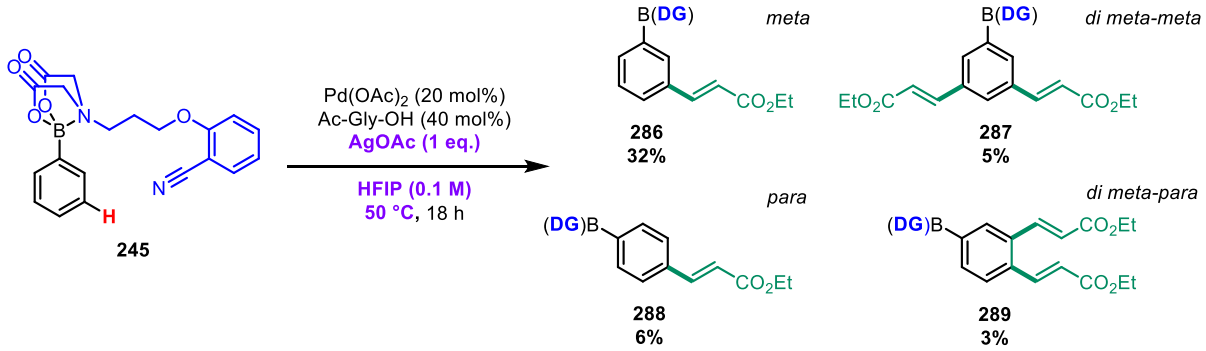
In all cases, ethyl cinnamate **285** was observed as a major by-product. Formation may have occurred either via deprotection and an oxidative Heck coupling, or a C–H alkenylation, deprotection-protodeboronation pathway. However, as the goal was retention of the B(MIDA-DG) functionality, the precise pathway by which this by-product was formed was not of primary interest — in both cases deprotection was occurring. The yield of ethyl cinnamate (**285**) did however provide a crude relative measure of the PhB(MIDA-DG) stabilities. In this regard, a drop in the yield of by-product **285** was observed on increasing the linker length by one methylene unit (**Table 9**, entry 7, compound **245**), which is perhaps consistent with what would be expected with an attenuated inductive electron withdrawing effect on the B–N bond.

Attempts to bias the steric environment (**Table 9**, entries 3 and 4) or increase the Lewis basicity of the DGs (**Table 9**, entries 5, 6 and 8) were unsuccessful. The *para*-directing functionality **239**

was also unsuccessful, however a drop in ethyl cinnamate (**285**) by-product yield was observed with the benzyl linker. The PhB(MIDA) **127** and PhB(IDA) **195** control substrates (**Table 9**, entries 11 and 12) also resulted in no product, indicating that the nitrile DGs were key to achieving reactivity. The trace amounts of ethyl cinnamate **285** observed using the PhB(MIDA) **127** also highlighted the stability of the scaffold in comparison to the MIDA-DGs.

The product formation observed with the propylene linked DG **245** indicated that the design was able to successfully direct *meta* C–H insertion of palladium. It was hypothesised that the low yield was a result of the unoptimised reaction conditions used. In particular, it was hypothesised that the increased relative stability (measured by the reduction in amount of ethyl cinnamate **285** by-product formed) compared to the ethylene linked DGs made the use of HFIP as solvent a possibility with PhB(MIDA-DG) **245**.

Consequently, the PhB(MIDA-DG) **245** was subjected to modified C–H alkenylation conditions (**Scheme 65**).



*Scheme 65: Modified C–H alkenylation conditions as applied to substrate **245** which resulted in a 6-fold increase in yield and the formation of regio and di-functionalised isomers.*

DCE was replaced with HFIP as solvent, the concentration was increased to 0.1 M and, in an effort to minimise DG loss, the temperature was lowered to 50 °C and only one equivalent of AgOAc was used. Pleasingly, a large increase in yield was observed from 8% (**Table 9**, entry 7) to 32% (**Scheme 65**) with formation of the mono alkenylated *para* isomer (**288**, 6%) and di-alkenylated *meta-meta* (**287**, 5%) and *meta-para* (**288**, 3%) isomers also observed, giving a total yield of 46%. As well as this, no ethyl cinnamate **285** by-product was observed.

A single crystal X-ray structure determination was performed on PhB(MIDA-DG) **245** (**Figure 20**).

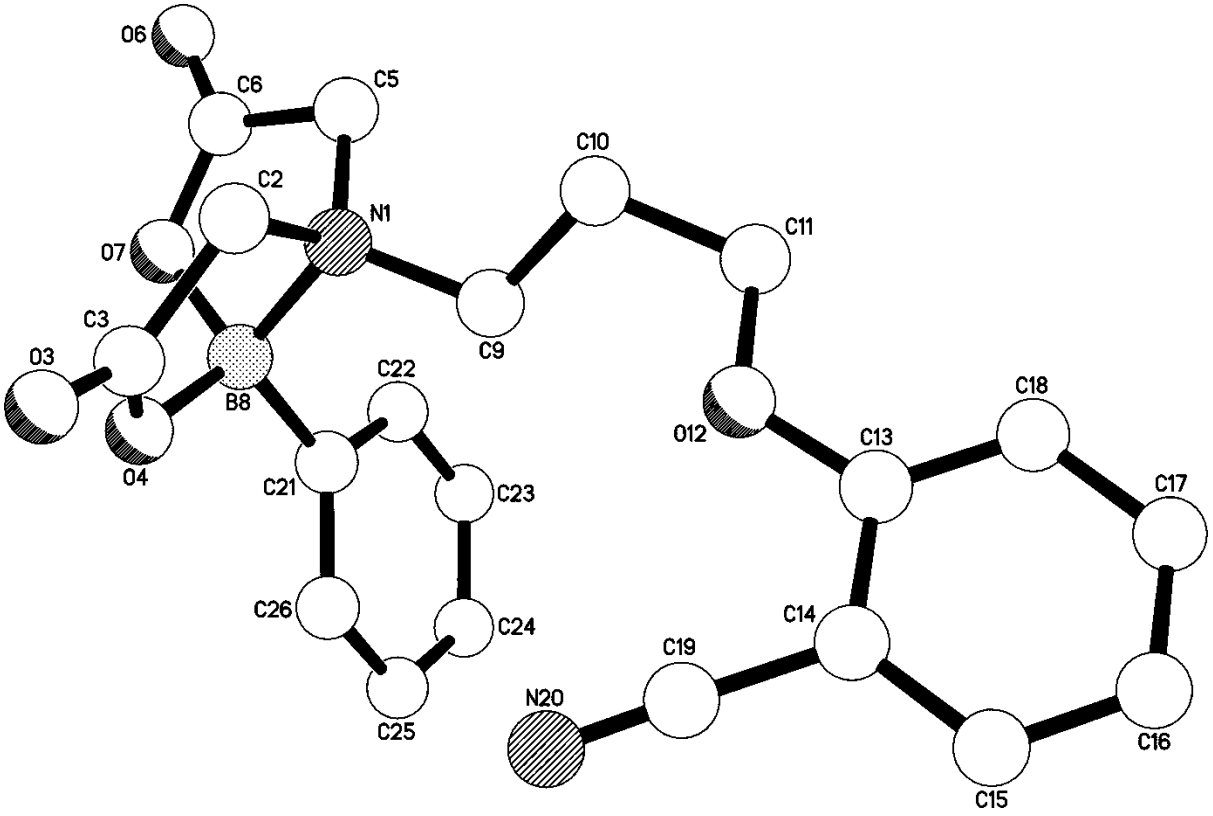


*Figure 20: The molecular structure of PhB(MIDA-DG) **245**, as obtained by a single crystal X-ray structure determination.*

Once again the B–N bond length of 1.662 Å was comparable to the literature values for PhB(MIDA) **127**, 1.662 Å and 1.673 Å.[202] The crystal structure also provided information about the directionality of the coordinating nitrile in the solid state. Pleasingly, the nitrile was observed to point inwards, towards the desired aryl ring.

4. C–H Alkenylations Using the MIDA-DG Boronate Ester

4.1 Optimisations

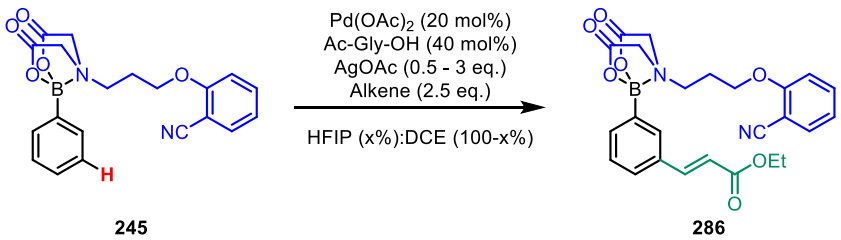
4.1.1 Design of Experiment (DOE) Optimisation of Reaction Conditions

With a successful PhB(MIDA-DG) design **245** and starting conditions for C–H alkenylations found, efforts turned to the optimisation of the reaction. In method development, 'one-factor' based optimisation is often used to interrogate the optimal reagents and conditions. This involves changing of one variable at a time. The method is particularly useful when looking at discrete variables such as different reagents or solvents. However, it does not consider the interactions between the variables.

By comparison, a design of experiment (DOE) approach allows for consideration of the interactions between the different variables being investigated.[206] The technique involves the identification of key reaction variables for investigation and a range of values for each, within which the optimum value is believed to lie. A number of experiments are then designed, incorporating the minimum, maximum and midpoint values of the variable ranges. These experiments are designed in a manner that allows a statistical model to be built. This model can subsequently be used to predict the optimum values of each variable investigated to achieve the desired output – normally the highest yield. DOE is most effective when investigating continuous variables.

A DOE approach to optimisation of the C–H alkenylations was chosen for two distinct reasons. Firstly, the observed behaviour of aryl MIDA-DG boronates, namely degradation of the PhB(MIDA-DG)s over time. It was believed a balance would be required between temperature, time, oxidant equivalents and a HFIP to DCE solvent ratio, to maximise the yield obtained while minimising the amount of degradation. Secondly, as mentioned, the reagents used for C–H alkenylations are remarkably general.[99] This would allow discrete conditions such as the oxidant, catalyst and ligand to be kept constant, reducing the number of experiments required during a DOE study.

The software used for the DOE optimisation was JMP Pro 14, with the included definitive screening design tool used to generate the experiment designs. The initial DOE study focused on reaction time, temperature, the solvent ratio (HFIP to DCE) and the amount of silver oxidant. These four continuous variables were chosen as it was expected that they would all have a positive correlation with yield and also a positive correlation with rate of degradation, requiring a balance to be struck. The ranges investigated are shown in **Table 10**.



Entry	Variable	Minimum Value	Maximum Value
1	Time (h)	10	48
2	Temperature (°C)	30	70
3	HFIP (%)[a]	0	100
4	Oxidant (eq.)	0.5	3

Table 10: The variables investigated during the initial DOE study. [a]HFIP (%) corresponds to the HFIP:DCE ratio, e.g. 50% HFIP is equivalent to 1:1 DCE:HFIP.

Percentage yield was chosen as the response, with the *meta*:*para* selectivity also measured, but not included in the model initially. The experiments generated by the definitive screening model and the obtained yields are shown in **Table 11**.

Entry	Time (hours)	Temperature (°C)	% HFIP	Oxidant equivalents	% Yield[a]	*Meta:Para*
1	48	30	100	3	36	6.5:1.0
2	48	70	0	1.75	18	7.5:1.0
3	10	70	0	0.5	4	n.d.
4	29	70	100	3	45	2.3:1.0
5	48	50	0	3	8	n.d.
6	29	50	50	1.75	58	3.9:1.0
7	10	50	100	0.5	35	5.7:1.0
8	48	70	100	0.5	29	4.1:1.0
9	10	70	50	3	40	1.3:1.0
10	10	30	0	3	0	n.d.
11	48	30	50	0.5	44	4.0:1.0
12	29	30	0	0.5	0	n.d.
13	10	30	100	1.75	72	6.7:1.0

Legend:	Minima	Midpoint	Maxima	Yield:	>45%	>5.3:1.0

Table 11: The experiments designed using the definitive screening method, with the resulting yields. Whether the values for each variable are a minimum, maximum or midpoint is highlighted using the colours shown. Yields above 45% and selectivites >5.3:1.0 (the unoptimised yields and meta:para *selectivities) are also highlighted. [a]Yields were calculated by ^1H NMR using a CH_2Br_2 internal standard.*

Once the experiments had been performed, the model was fit using the fit definitive screening tool with personality set to 'Standard Least Squares' and emphasis on 'Effect Screening'. The model indicated that by far the most important continuous variable analysed was the percentage of HFIP used, with minimal effect from the other continuous variables. This was clear from the main effect residual plot graphs generated (**Figure 21**).

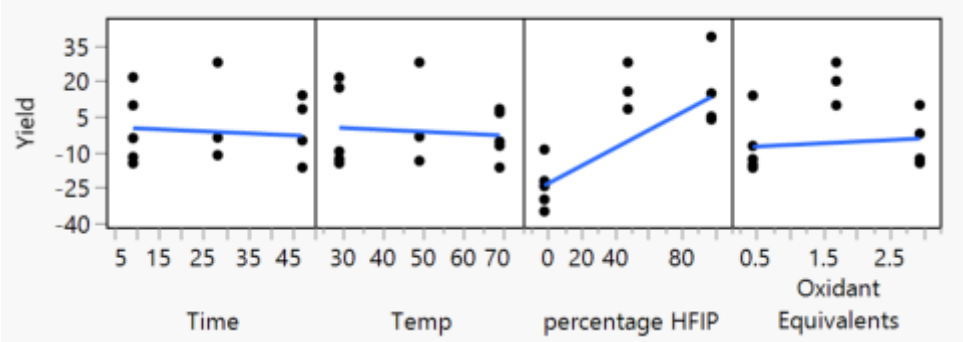


Figure 21: The main effect residual plot graphs generated from the results of the definitive screening experiments showing the general effect on yield of each variable.

Fitting the model solely on percentage HFIP and (percentage HFIP)*(percentage HFIP) gave a positive correlation between predicted and actual yield, a root mean squared error (RMSE) of 12.5 and an R^2 (RSq) value of 0.75 (**Figure 22**).

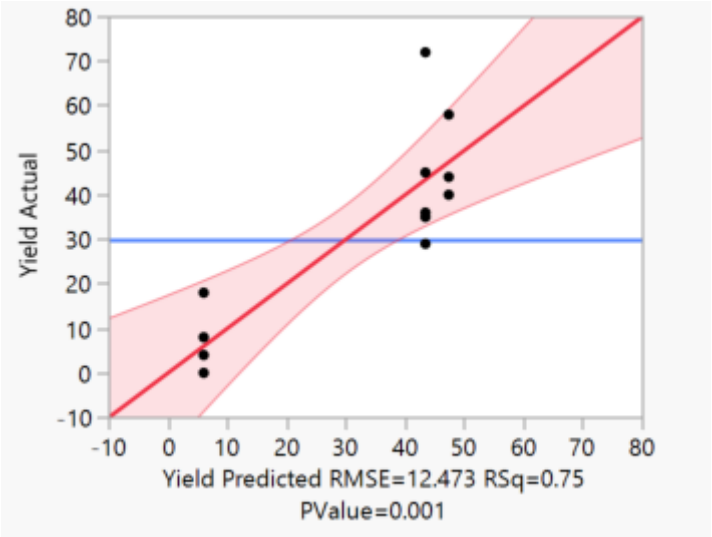


Figure 22: Plot of actual vs predicted yield, which gives an indication of the validity of the model. A RSq value closer to 1 is indicative of increased accuracy, as is a smaller RMSE value.

Unfortunately, due to the overwhelming influence of the percentage HFIP on the model, it was only useful for predicting the highest yielding value for this variable. This was predicted to be 70%, resulting in a yield of 51% (**Figure 23**).

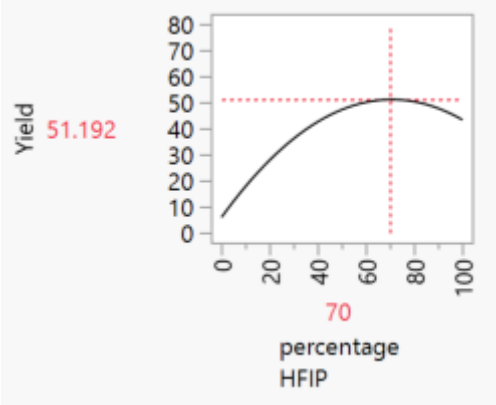
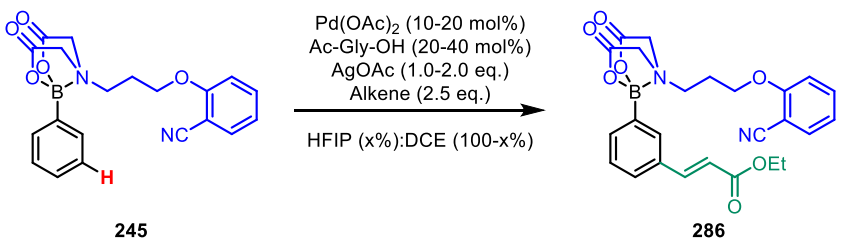


Figure 23: Plot of predicted yield vs. percentage HFIP which suggested that 70% HFIP would result in a maximum yield of 51%, based on the model.

It was expected that the reaction time, temperature and oxidant equivalents did have important effects on the reaction, however these were not being evidenced due to the overwhelming effect from changing the percentage of HFIP. By narrowing the range used for the percentage HFIP from 0-100% to 50-100% (which includes the predicted ideal value of 70%) it was anticipated that a more accurate model could be built.

The model also suggested that temperature had very little baring on the yield of the reaction, with the yield actually slightly dropping at higher temperatures (as would be expected due to degradation of the PhB(MIDA-DG) **245** at higher temperatures). Consequently, room temperature (23 °C) was chosen for further DOE studies.

A second DOE study was subsequently performed. The factors investigated were catalyst loading, time, percentage of HFIP and oxidant equivalents. In response to the results from the last study, the temperature was kept constant at 23 °C and the percentage of HFIP, time and oxidant equivalents ranges narrowed. The ratio of catalyst to ligand was kept constant during the study (catalyst:ligand, 1:2) (**Table 12**).



Entry	Variable	Minimum Value	Maximum Value
1	Catalyst loading (mol%)	10	20
2	Time (h)	1	18
3	HFIP (%)[a]	50	100
4	Oxidant (eq.)	1	2

Table 12: The variables investigated during the second DOE study. [a]HFIP (%) corresponds to the HFIP:DCE ratio, for instance 50% HFIP is equivalent to 1:1 DCE:HFIP.

Percentage yield was again chosen as the response. The experiments generated by the definitive screening model and the obtained yields are shown in **Table 13**.

Entry	Catalyst Loading (mol%)	Time (hours)	% HFIP	Oxidant equivalents	% Yield[a]	*Meta*:*para*
1	20	18	50	1.5	51	4.5:1.0
2	15	1	50	1	4	n.d.
3	10	1	50	2	3	n.d.
4	10	1	100	1.5	7	n.d.
5	20	9.5	50	2	39	3.2:1.0
6	10	18	50	1	36	5.7:1.0
7	10	9.5	100	1	28	2.3:1.0
8	20	18	100	1	50	6.1:1.0
9	20	1	100	2	13	3.0:1.0
10	15	9.5	75	1.5	32	1.9:1.0
11	10	18	75	2	42	4.5:1.0
12	15	18	100	2	60	5.6:1.0
13	20	1	75	1	8	4.0:1.0

Legend:	Minima	Midpoint	Maxima	Yield:	>45%	>5.3:1.0

Table 13: The experiments designed using the definitive screening method, with the resulting yields. Whether the values for each variable are a minimum, maximum or midpoint is highlighted using the colours shown. Yields above 45% and selectivites >5.3:1.0 (the unoptimised yields and meta:para *selectivities) are also highlighted. [a]Yields were calculated by ^{1}H NMR using a CH_2Br_2 internal standard.*

The model was again fit using the fit definitive screening tool, with personality set to 'Standard Least Squares' and emphasis on 'Effect Screening'. A positive correlation between predicted and

actual yield was found, with the RMSE and Rsq values of 4.64 and 0.96 respectively indicating a much more accurate model than in the previous study (**Figure 24**).

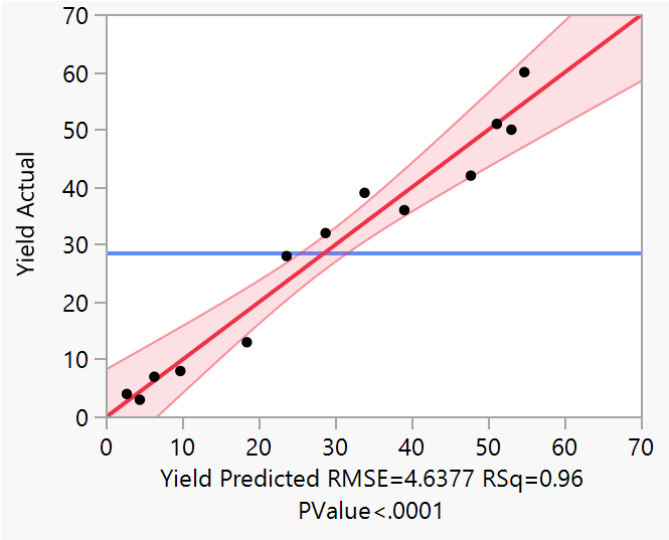


Figure 24: Plot of actual vs predicted yield for the second DOE study.

The model was subsequently used to predict the highest yielding reaction conditions (**Figure 25**).

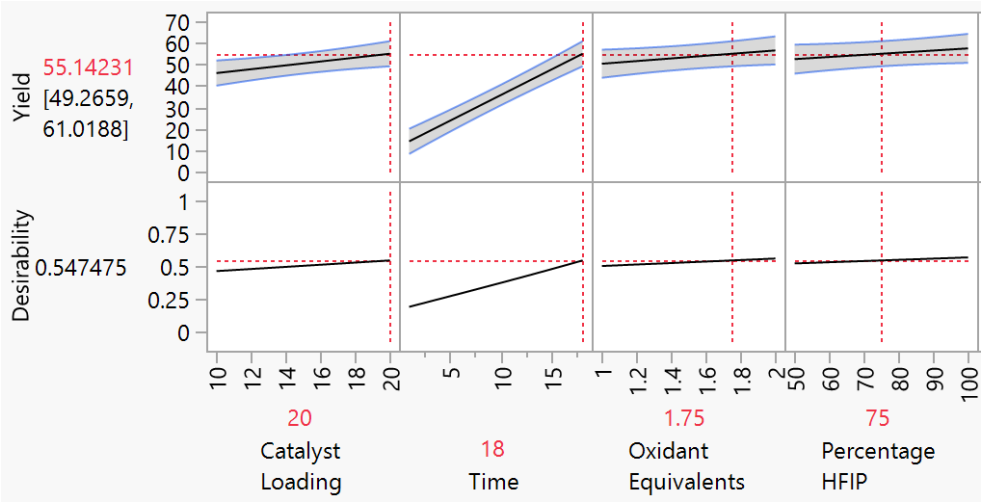
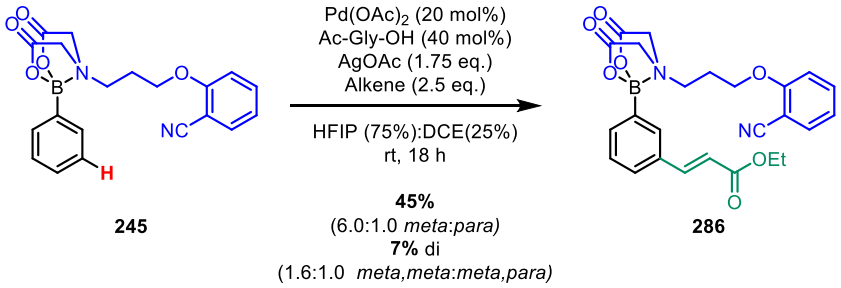


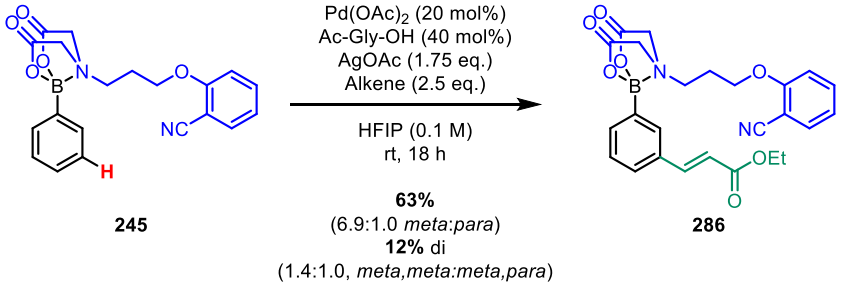
Figure 25: Prediction profiles generated using the definitive screening model which are designed to allow accurate prediction of the optimal reaction conditions to maximise yield.

Catalyst loading and time were maximised, while oxidant equivalents and % HFIP values were chosen to maximise yield while reducing the amounts required. Using the JMP 14 prediction profiler the optimum conditions were generated and then tested experimentally (**Scheme 66**).



*Scheme 66: An alkenylation reaction of substrate **245** under the conditions predicted to be highest yielding following the DOE studies.*

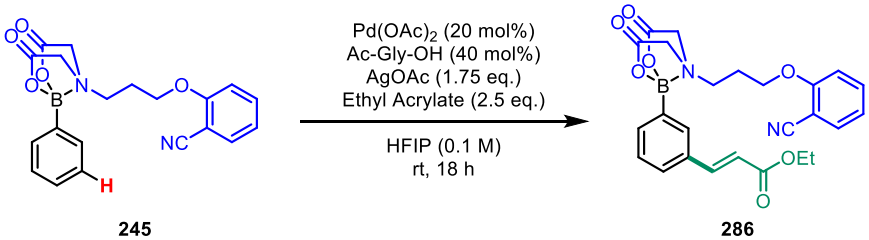
Pleasingly, the 52% yield obtained was within the range predicted by the model (55 ± 6%) and the selectivity (6.0:1.0 *meta:para*) was in line with the highest values obtained during DOE optimisation. However, it was noticed that during the initial DOE study, conditions very similar to these achieved a much higher yield (**Table 11**, entry 13). The key difference being the percentage of HFIP used. On repeating the reaction with 100% HFIP, a significant increase in yield was observed, along with a concurrent increase in *meta:para* selectivity (**Scheme 67**).



*Scheme 67: An alkenylation reaction of substrate **245** under conditions in which the % HFIP was increased to 100% (from 75%). This resulted in a >20% increase in yield and a drop in* meta *selectivity.*

Consequently, the conditions shown in **Scheme 67** were selected to carry forward into further investigations.

A number of control reactions were performed to investigate the mechanism of the C–H alkenylations and confirm that the conditions found were optimal. The results are shown in **Table 14**.



Entry	Variation from Standard Conditions	Yields[a]				Total
		Meta **286**	*Para* **288**	*m, m* **287**	*m, p* **289**	
1	No variation	55%	8%	7%	5%	75%
2	No $Pd(OAc)_2$	-	-	-	-	-
3	No AgOAc	13%	4%	-	-	17%
4	No Ac-Gly-OH	9%	4%	-	-	13%
5	PhenylB(MIDA) **127** (no DG)	-	-	-	-	-
6	Inert (N_2) atmosphere used	56%	8%	5%	2%	71%
7	Ag_2SO_4 (1.75 eq.) as oxidant	13%	-	-	-	13%
8	Ag_2CO_3 (1.75 eq.) as oxidant	13%	2%	-	-	15%
9	Boc-Gly-OH (40 mol%) as ligand	4%	-	-	-	4%
10	Z-Gly-OH (40 mol%) as ligand	7%	-	-	-	7%
11	Ac-Ile-OH (40 mol%) as ligand	28%	5%	-	-	33%
12	Ac-Val-OH (40 mol%) as ligand	31%	6%	-	-	37%
13	2.0 eq. ethyl acrylate	42%	8%	6%	2%	58%
14	1.5 eq. ethyl acrylate	38%	6%	4%	1%	49%

Table 14: Control reactions performed to investigate the mechanism of the C–H alkenylation reactions. [a]Yields were calculated by ^1H NMR using a CH_2Br_2 internal standard.

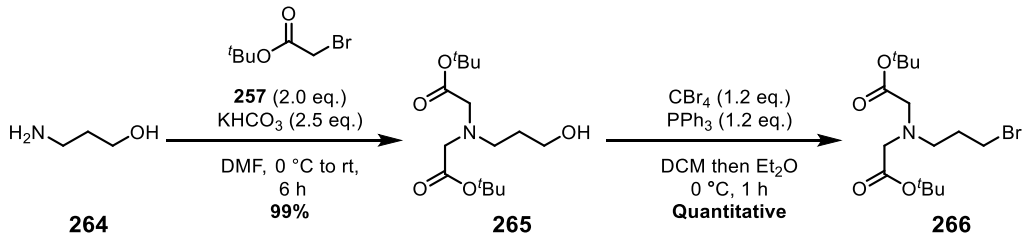
The results are in agreement with the previously proposed mechanism (**Scheme 64**). With no palladium catalyst present (**Table 14**, entry 2) and no DG (**Table 14**, entry 5), 0% yield is obtained indicating the necessity of both components. The role of the silver salt as oxidant is clearly displayed by loss of catalyst turnover in its absence (**Table 14**, entry 3). However, other roles for the Ag^I salt, such as in aiding C–H insertion, are also possible.[30] Indeed, the drop in the *meta*:*para* selectivity observed could be indicative of a heterodimeric Ag–Pd species driving selectivity, as identified by Houk and Yu in similar systems.[128,129] The removal of the mono protected amino acid (MPAA) Ac-Gly-OH (**Table 14**, entry 3) resulted in a large drop in yield, consistent with the ligand lowering the barrier to C–H insertion. [118,128,129] The drop in selectivity (6.9:1.0 *meta*:*para* to 2.3:1.0 *meta*:*para*) could also be attributed to a secondary role of the MPAA in aiding the formation of the Ag–Pd heterodimer (*see* **Figure 3**).

In additional experimental investigations, changes to the oxidant and ligand resulted only in lowered yields (**Table 14**, entries 7 to 12), as did varying the equivalents of alkene coupling partner (**Table 14**, entries 13 and 14). Lastly, using an inert nitrogen atmosphere (**Table 14**,

entry 6) saw negligible change in yield, indicating that the role of AgOAc was indeed as terminal oxidant, not atmospheric oxygen.

4.1.2 Optimisation of the MIDA-DG Synthesis

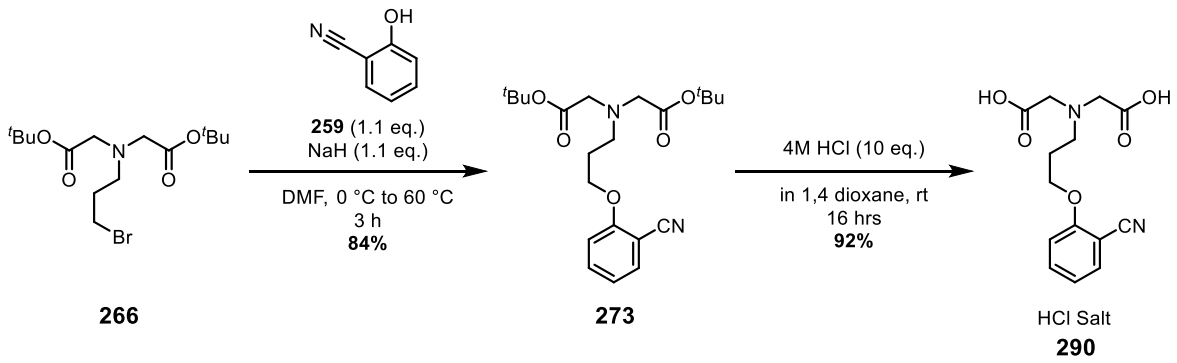
With optimised conditions for the C–H alkenylations in hand, attention turned to investigating the scope of the reaction. However, a large amount of the PhB(MIDA-DG) **245** was required for the investigations. The synthesis used previously (*see* Chapter 3.2.1) was low yielding, and involved two chromatographic purifications, making it undesirable for scale up. As such, optimisation of the synthetic route was undertaken. The initial bis-alkylation of 3-aminopropanol **264** proceeded smoothly with only two equivalents of *tert*-butyl bromoacetate **257**, giving 99% yield of **265** after aqueous work-up (**Scheme 68**).



*Scheme 68: The optimised conditions for accessing the alkyl bromide **266** on scale and with no chromatographic purification.*

A small screen of brominating reagents revealed CBr_4 as the optimal reagent, achieving quantitative yield in just 1 hour at 0 °C. The excess reagents and by-products could subsequently be removed by adding Et_2O to the reaction mixture at 0 °C to cause precipitation, followed by filtration through silica gel. The yield over the two steps was increased to 99% (from 51% previously) with no chromatographic purification required. The route was subsequently succesfully performed on a 100 mmol (> 35 g) scale.

The alkylation of the bromide **266** proceeded in 84% yield using the previously developed conditions of NaH in DMF (**Scheme 69**).



*Scheme 69: Optimised alkylation and deprotection conditions which were used to access hydrochloride salt **290** for use in investigating the C–H alkenylation scope.*

Although operationally simple on a gram scale, this procedure would require modification on any larger scales due to the dangers associated with NaH in DMF.[207]

Furthermore, the TFA salt of the diacid **290** resulting from previous *bis* deprotection conditions proved extremely hygroscopic, forming a gum on exposure to atmospheric conditions, complicating it's handling. In order to circumvent this issue, a simple procedure using HCl (4M in dioxane) was developed. The hydrochloride salt **290** precipitated out of solution during the reaction, allowing organic by-products from the alkylation step to be removed by an organic wash. While still slightly hygroscopic , the hydrochloride salt proved much easier to handle, remaining as a free-flowing solid over extended periods on the bench top. The alkylation and deprotection procedures were performed on 40 mmol scales, providing access to >14 g of the desired diacid **290** for use in investigations into the scope of the directed alkenylation method. After the optimisation, the overall yield was increased from 29% to 77% over the 4 steps, allowing multigram-scale access to the MIDA-DG salt **290**, with a reduction in the number of chromatographic purifications.

4.2 Investigating the Scope of the C–H Alkenylation Reaction

4.2.1 Varying Aryl Boronic Acids

The scope with regards to the aryl boronic acid reaction partners was investigated first. A systematic approach was taken, investigating electron-withdrawing to electron donating substituents in the *ortho*, *meta*, and *para* positions on the phenyl ring. Thus a three by three grid was devised and the required aryl MIDA boronate esters (**291** to **299**) synthesised (**Table 15**).

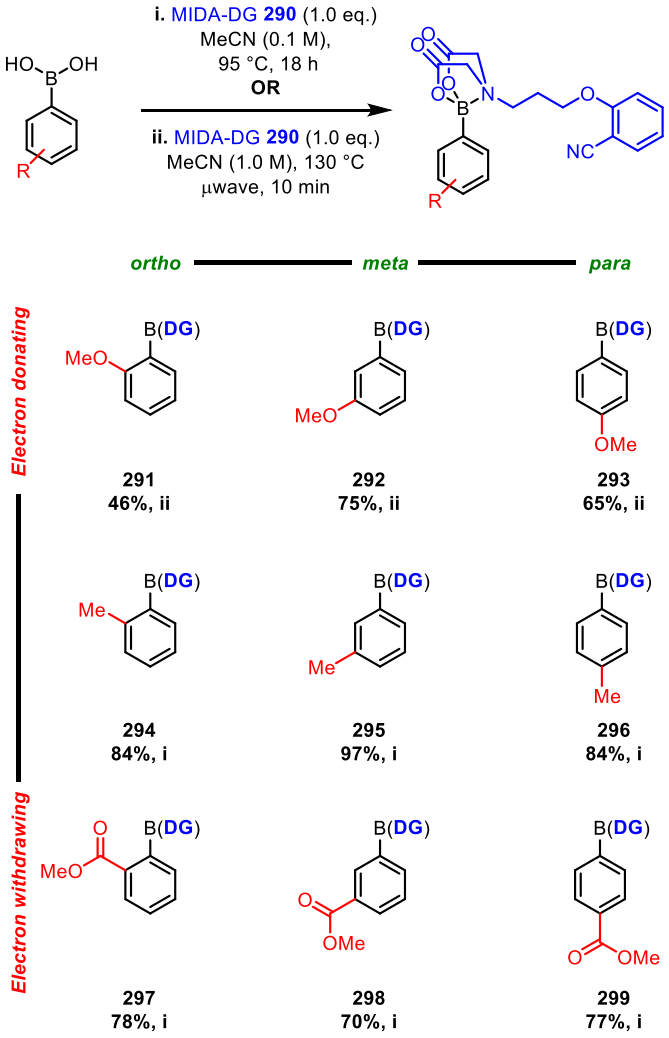


Table 15: Synthesis of aryl MIDA-DG boronate esters for investigation of substituent and electronic effects.

Two methods were used for their synthesis, using either thermal heating overnight, or a more rapid microwave heating method which provided access to the desired aryl MIDA-DG boronates in just 10 minutes.

Several other interesting aryl boronic acids were also chosen, in order to investigate the effect of halide substituents (**300** to **302**), the regioselectivity of functionalisation on napthyl rings (**303** and **304**) and the effect of blocking both *meta* positions (**305**) (**Table 16**).

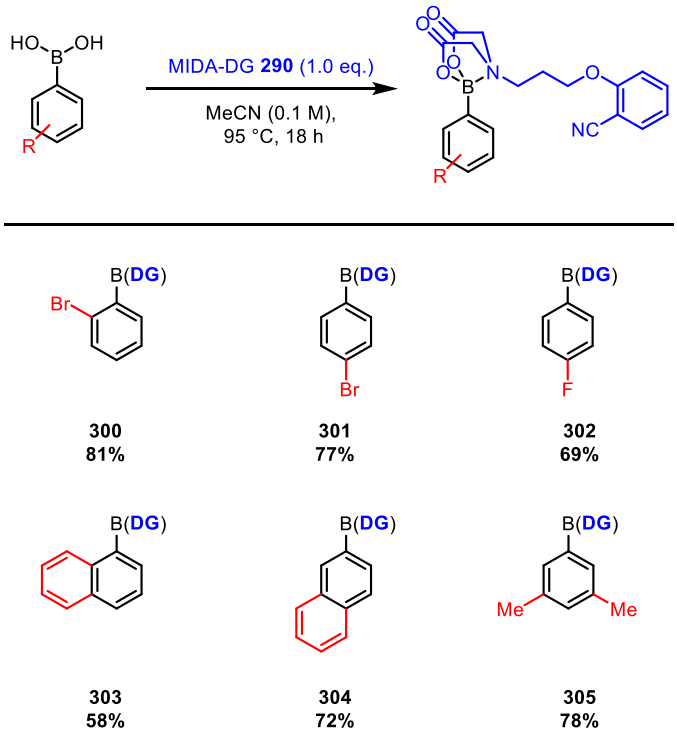


Table 16: Additional aryl MIDA-DG boronates synthesised for investigation of the C–H alkenylation scope.

The aryl MIDA-DG boronate esters (**291** to **305**) were next subjected to the optimised C–H alkenylation conditions (**Table 17**).

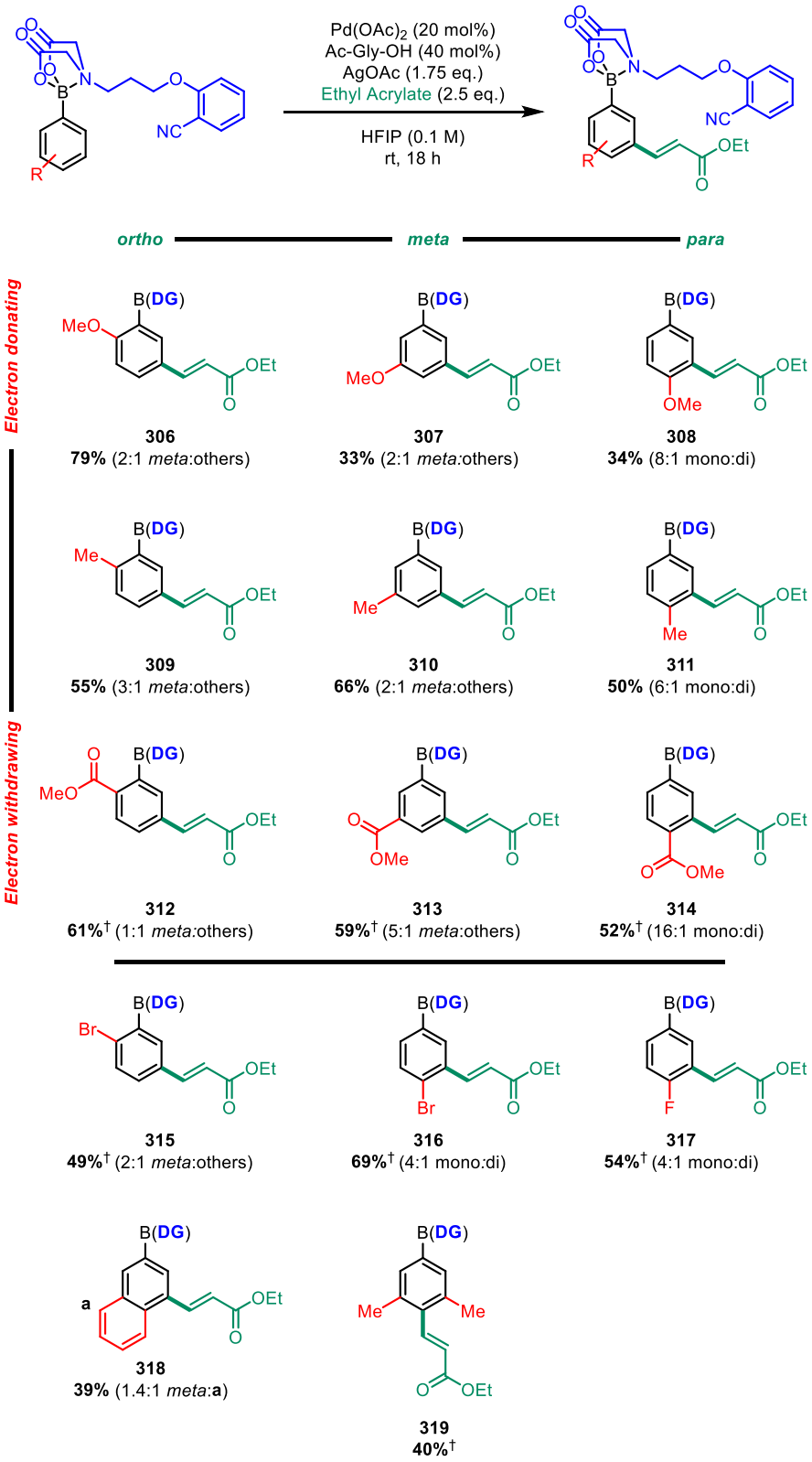
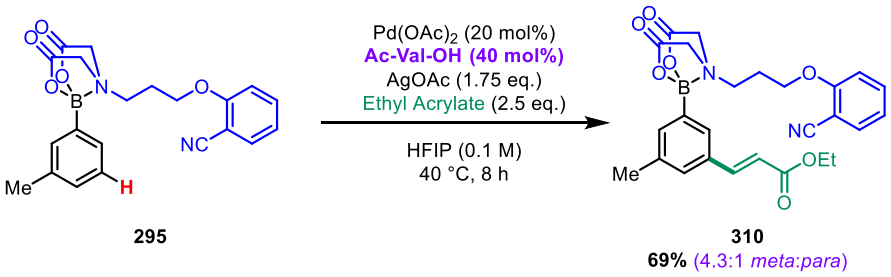


Table 17: The scope of the C–H alkenylation reaction with regard to aryl boronic acid substituents. †Reaction time was 48 h. Others *corresponds to para and di-functionalised isomers formed during the C–H functionalisations. Yields correspond to isolated material, with product ratios determined using ^{1}H NMR after 'catch and release' purification.*

Within the three by three grid (**306** to **314**), yields varied from 33% to 79%, with electron-withdrawing ester groups (**312** to **314**) requiring increased reaction times. *Ortho* substituents gave a more complex mixture of regioisomers, as the *meta* positions are no longer equivalent or blocked. Electron-withdrawing groups (**312** to **314**) appeared to strengthen the protecting group ability of the MIDA-DG and less degradation was observed, especially when compared to the *para*-methoxy analogue **308**, where a large amount of degradation was observed. This can be rationalised by the donation of electron density into the aryl ring weakening the B–N dative bond.

Fluoro (**317**) and bromo (**315** and **316**) substituted aromatics were tolerated under the conditions, with selective C–H functionalisation occurring in preference to oxidative insertion. The alkenylated products also provide handles for further S_NAr or cross-coupling reactions. The 3,5-dimethyl analogue (**319**) resulted in selective formation of the *para* product in good yield after 48 hours. 2-Napthylboronic acid derived substrate **318** gave two regio isomers at the 4- and 8-positions, with the 4-position the major product. 1-Napthylboronic acid derived substrate **303** was also subjected to the reaction conditions, however characterisation of the complex mixture of three regioisomeric products (believed to arise from reaction at the 3, 4 and either 5 or 8 positions) proved challenging.

Interestingly, by varying the ligand from Ac-Gly-OH to an acetylated valine ligand (Ac-Val-OH) and gently heating, the selectivity of the C–H alkenylation could be improved (**Scheme 70**).



*Scheme 70: Alkenylation of 3-tolylboronic acid MIDA-DG ester **295** using the sterically encumbered acetylated valine ligand, leading to an improvement in selectivity.*

Utilising the 3-tolylboronic acid MIDA-DG ester **295**, the *meta*:*para* ratio improved from 2:1 to 4:1 using the bulkier ligand, with none of the di-functionalised product formed. The result is indicative of the involvement of the MPAA ligand in the regio-selectivity defining C–H insertion step, supporting the hypothesis that the ligand assists in CMD.

4.2.2 Varying the Alkene Coupling Partner

Variations to the alkene coupling partners were also investigated, using PhB(MIDA-DG) **245** as the model substrate (**Table 18**).

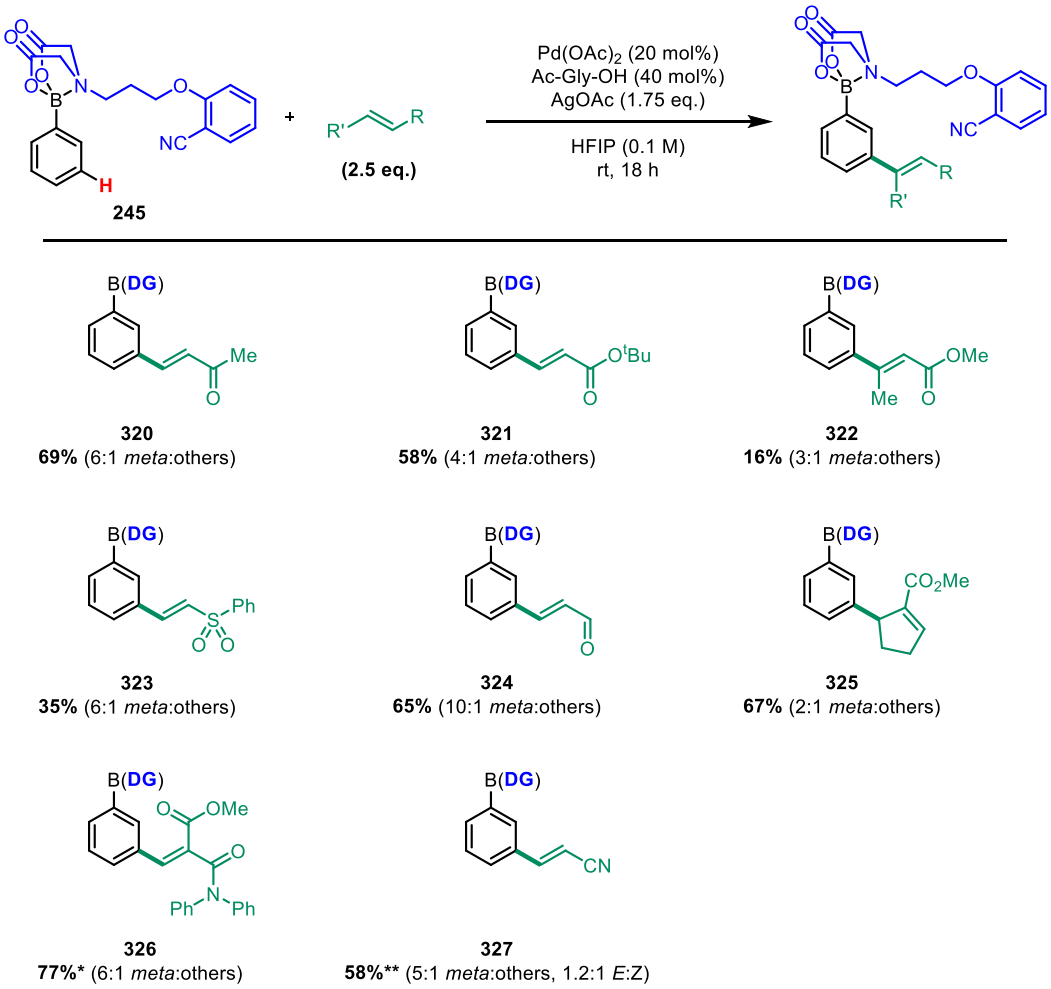


*Table 18: The scope of the C–H alkenylation with regards to the alkene coupling partner. *1.2 equivalent of alkene used. **2.0 equivalents of alkene used, with a reaction time of 48 h.*

Ketone (**320**), aldehyde (**324**), sulfone (**323**) and nitrile (**327**) electron-withdrawing groups were all suitable alkene activating groups. Competition between the acrylonitrile and the MIDA-DG for co-ordination to the catalyst required extended reaction times to furnish product **327**. As well as this, the linear nitrile exerted little effect on the stereo-defining β-hydride elimination step, resulting in a 1.2:1 *E*:*Z* mixture of isomers. A cyclic alkene was also tolerated, yielding only one alkene regioisomer (**325**). A 1,1-heterodisubstituted alkene featuring a diphenylamide was successfully coupled (compound **326**) using only 1.2 equivalents of the alkene, demonstrating that a secondary amide functional group was tolerated and that lower equivalents of alkene can be utilised if so required (the geometry of the alkene in the product **326** was not determined, but is expected to be *cis* due to the steric bulk of the diphenylamide substituent). Lastly, a crotonate was successfully coupled (compound **322**) albeit in low yield.

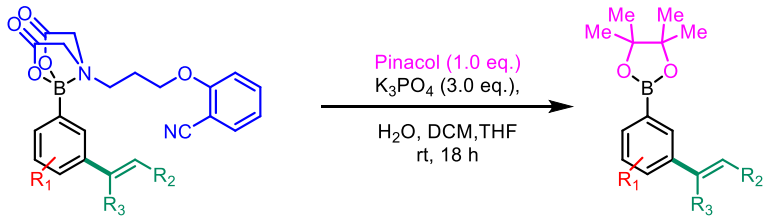
Not all alkene coupling partners were successful however. *N,N*-Dimethylacrylamide, styrene and diethyl vinylphosphonate were inactive under the standard conditions. This is probably to be due to insufficient activation of the alkene by the weakly electron-withdrawing substituents, at room temperature.

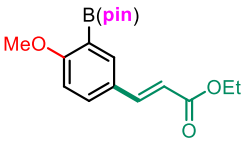
4.2.3 Protecting Group Conversion of the Alkenylated Products

The high polarities of aryl MIDA-DG esters, while useful for their purification using 'catch and release' conditions, made separation of the regio- and mono- or di-isomers impossible using normal phase chromatography. To separate the products and unambiguously characterise the alkenylated products, the MIDA-DG boronate esters were converted to their pinacol boronate ester congeners (**Table 19**).

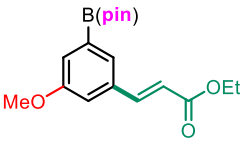
A one-pot, MIDA-DG deprotection / pinacol ester formation procedure was developed for the expedient synthesis of the alkenylated boronate pinacol esters. While not as high yielding as performing the procedure over two-steps, a biphasic mixture of aqueous K_3PO_4 and pinacol in THF and DCM allowed for the efficient synthesis of the 23 alkenylated boronate esters (**328** to **350**) in an operationally simple manner.

Interestingly, the *ortho*-methoxycarbonyl substituted pinacol ester **336** required extremely forcing conditions to remove the MIDA-DG ester. This is likely to be due to the interplay of steric blocking of nucleophilic attack at the boron, combined with increased strength of the B–N dative covalent bond due to the electron-withdrawing substituent. Mechanistic work by Lloyd-Jones *et al.* has shown that under conditions such as those used here, hydrolysis of the MIDA scaffold occurs *via* initial nucleophilic attack at the boron centre.[173] More basic conditions were avoided in order to ensure retention of the ethyl ester functional group.

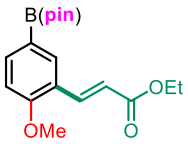




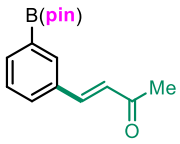
328
25% (4:1 *meta*:*para*)



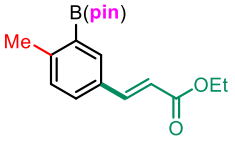
329
50% (2:1 *meta*:*para*)



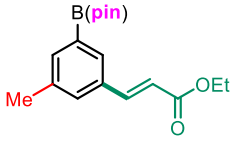
330
50%



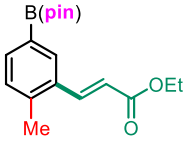
331
50% (6:1 *meta*:*para*)



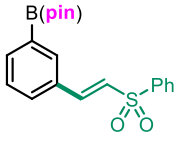
332
100% (8:4:1 *meta*:*para*:*meta'*)



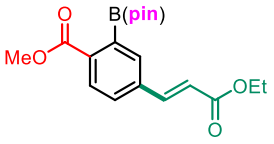
333
58% (4:1 *meta*:*para*)



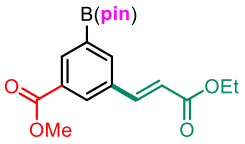
334
69%



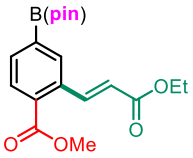
335
36% (6:1 *meta*:*para*)



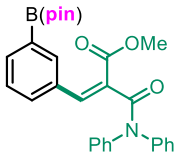
336
10%*



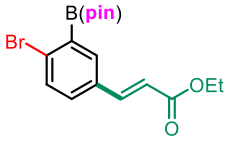
337
44% (8:2 *meta*:*para*)



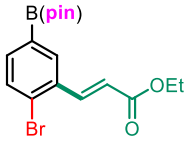
338
51%



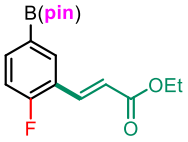
339
36% (6:1 *meta*:*para*)



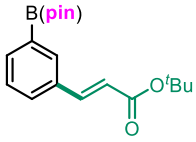
340
12% (2:1 *meta*:*para*)



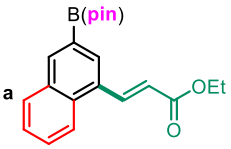
341
29%



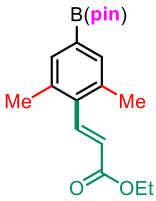
342
54%



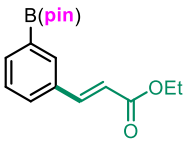
343
65% (8:1 *meta*:*para*)



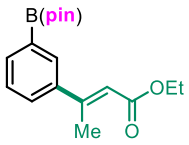
344
21% (2:1 *meta*:**a**)



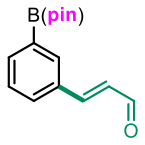
345, 50%



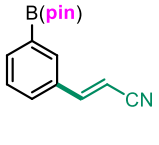
346
67% (7:1 *meta*:*para*)



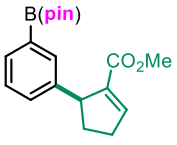
347
20% (5:1 *meta*:*para*)



348
47% (8:1 *meta*:*para*)



349
69% (*meta only*, 1:1 *E*:*Z*)



350
45% (6:1 *meta*:*para*)

*Table 19: Yields obtained when converting the aryl B(MIDA-DG)s to the corresponding aryl B(pin)s. *Pinacol (1.0 eq.), K_3PO_4 (3.0 eq.), THF (0.1 M), 90 °C, 1 h.*

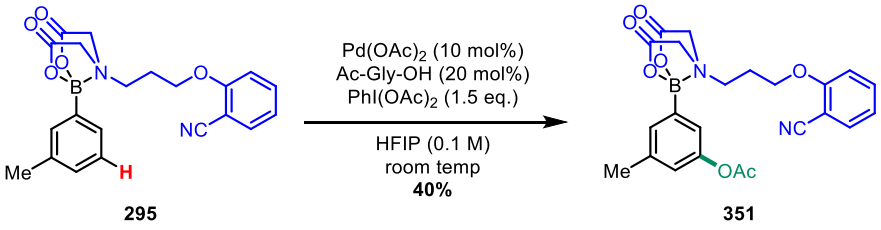
5. C–H Acetoxylations and C–H Arylations Using the MIDA-DG Boronate Ester

5.1 Development of C–H Acetoxylations

5.1.1 Reaction Discovery and Optimisation

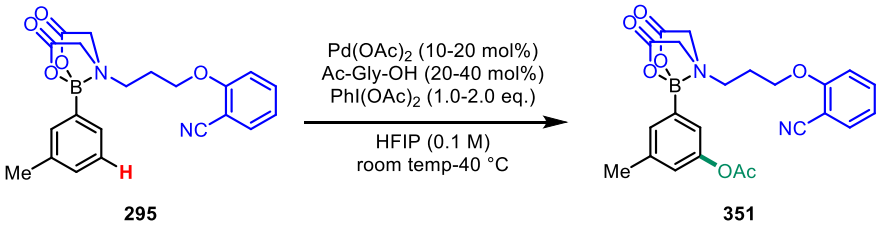
With a successful MIDA-DG scaffold **290** and conditions for C–H alkenylations in hand, attention turned to other possible transformations that might be directed by this scaffold. In contrast to the Pd^{II}/Pd^{0} mechanism invoked for the C–H alkenylations (*see* **Scheme 64**), a Pd^{II}/Pd^{IV} catalytic cycle could also be envisioned, using a suitable reagent to perform an oxidative insertion at the Pd^{II} centre formed after C–H insertion. Yu and Maiti have previously used $PhI(OAc)_2$ as a suitable oxidant to achieve this, allowing direct $C(sp^2)$–H acetoxylation of several aromatic systems.[125,126,141,145]

Gratifyingly, applying conditions based upon these, with 3-methylphenylboronic acid MIDA-DG ester **295** (chosen to simplify analysis), a yield of 40% of only the *meta*-acetoxylated isomer **351** was obtained (**Scheme 71**).



*Scheme 71: Initial conditions used to assess the reactivity of substrate **295** towards acetoxylation, which yielded the* meta *regioisomer selectively in 40% yield.*

Once again, a DOE approach was taken to optimising the reaction conditions. The software used for the DOE optimisation was again JMP Pro 14, with the included definitive screening design tool used to generate the experiment designs. Four extra runs were included in the design relative to that applied previously, in an attempt to improve the accuracy of the model. The initial DOE study focused on reaction time, temperature, the catalyst loading and the amount of $PhI(OAc)_2$ oxidant used. The ranges investigated are shown in **Table 20**.



Entry	Variable	Minimum Value	Maximum Value
1	Catalyst Loading (mol%)	10	20
2	Oxidant (eq.)	23	40
3	Temperature (°C)	25	40
4	Time (h)	6	24

Table 20: The variables investigated during the C–H acetoxylation DOE optimisation study.

Percentage yield was chosen as the response. The experiments generated by the definitive screening model and the obtained yields are shown in **Table 21**.

Entry	Catalyst Loading (mol%)	Oxidant (equivalents)	Temperature (°C)	Time (hours)	% Yield[a]
1	10	2	33	6	33
2	10	1.5	25	6	37
3	20	1	40	6	43
4	20	2	25	24	42
5	10	1	25	24	45
6	10	1	40	6	46
7	20	1	33	24	43
8	20	2	40	6	43
9	15	1	25	6	43
10	10	2	25	24	38
11	15	1.5	33	15	33
12	20	1.5	40	24	56
13	15	2	40	24	45
14	10	1	40	24	48
15	20	2	25	6	42
16	10	2	40	15	33
17	20	1	25	15	37

Legend:	Minima	Midpoint	Maxima	Yield:	>40%

Table 21: The experiments designed using the definitive screening method, with the resulting yields. Whether the values for each variable are a minimum, maximum or midpoint is highlighted using the colours shown. Yields above 40% (the unoptimised yield) are also highlighted. [a]Yields were calculated by ^{1}H NMR using a CH_2Br_2 internal standard.

With the experiments performed, the model was fit with personality set to 'Standard Least Squares' and emphasis on 'Effect Screening'. Unfortunately, the accuracy of the model was lower than those fit in previous studies, despite the inclusion of extra experiments. This can be seen from the predicted against actual yield plot (**Figure 26**) which has a number of outliers, a RMSE of 5.311 and a RSq value of just 0.41.

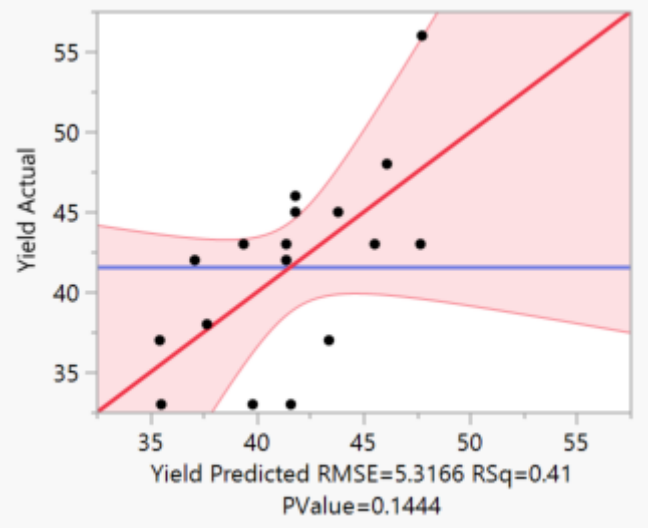


Figure 26: Plot of the predicted vs. actual yield generated from the DOE study, which highlighted the relatively low accuracy of the model.

Despite this, the prediction profiles generated by the model could be used to gain information about the reaction (**Figure 27**).

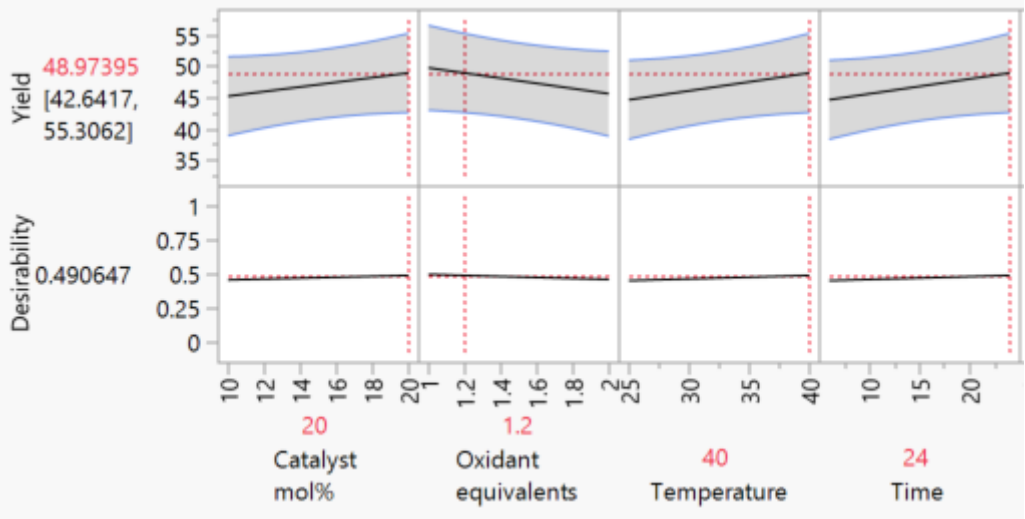


Figure 27: Prediction profiles generated using the definitive screening model when 20 mol% catalyst is employed. These are designed to allow accurate prediction of the optimal reaction conditions to maximise yield.

A positive correlation was observed between all the variables and yield, except for the $PhI(OAc)_2$, suggestive of a degradation pathway involving the oxidant. It was also observed that the model predicted a drop in just 3% yield on reducing the catalyst loading by 10% (**Figure 28**).

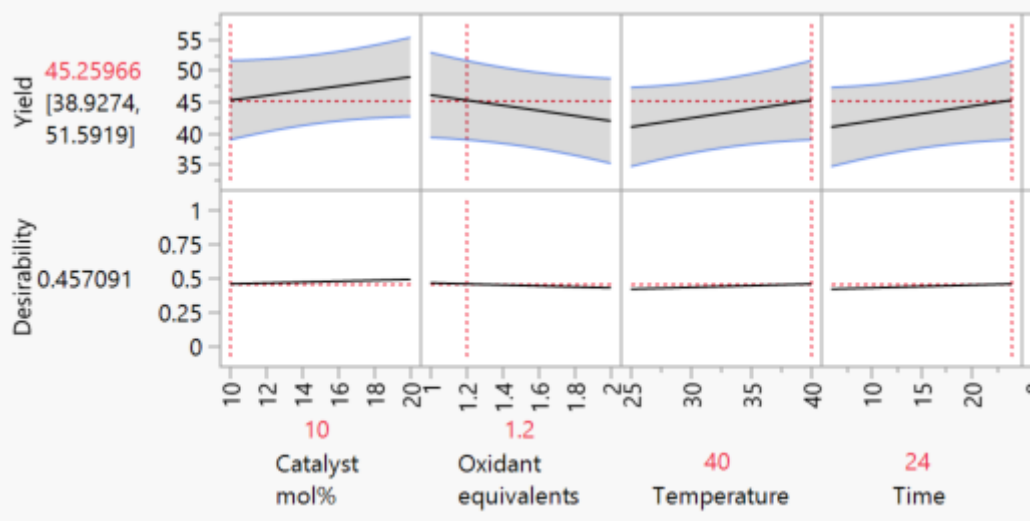
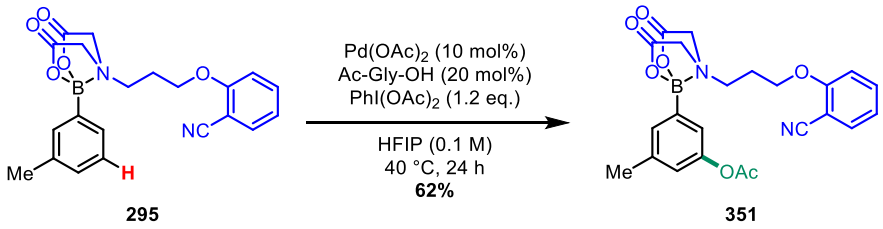


*Figure 28: Prediction profiles generated using the definitive screening model when 10 mol% catalyst is employed. These indicate that this lower catalyst loading would result in only a small drop in yield (45% cf. 49%, see **Figure 27**).*

Clearly, such diminishing returns with respect to the yield were unable to justify the application of higher catalyst loadings. Based on the above observations, the conditions expected to be optimal for the C–H acetoxylation were generated and tested experimentally (**Scheme 72**).



*Scheme 72: Acetoxylation of substrate **295** using the predicted optimum conditions, which gave an isolated yield of 62%, higher than predicted.*

Interestingly an isolated yield of 62% of only the desired *meta* isomer **351** was achieved, an improvement of 22% over the original unoptimized yield. While the optimisation was successful, it highlighted the inaccuracy of the model, with the yield obtained 17% higher than that predicted (**Figure 28**). A second DOE study with modified variables and values may have allowed for more accurate predictions, however the yield obtained was deemed sufficient to move on to investigations of the reaction scope.

5.1.2 Scope of the C–H Acetoxylation Reaction

The same three by three grid including *ortho, meta* and *para,* electron donating, neutral and electron withdrawing substituents was again employed to investigate the scope of the C–H acetoxylation reaction (**Table 22**).

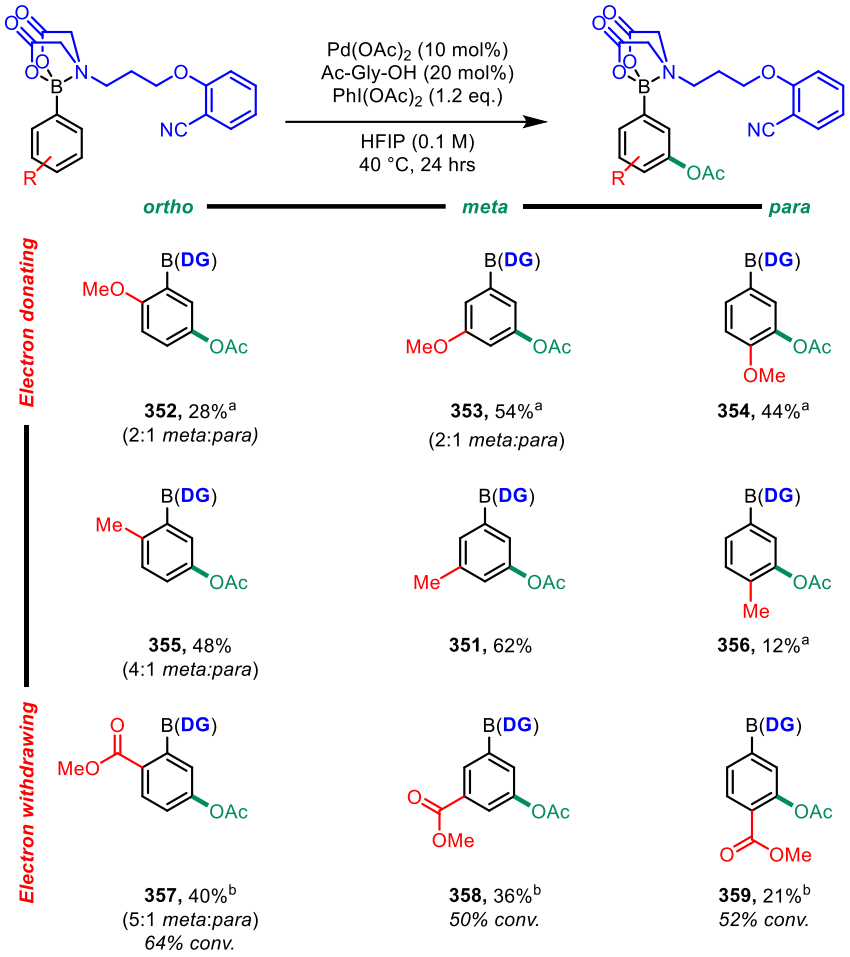


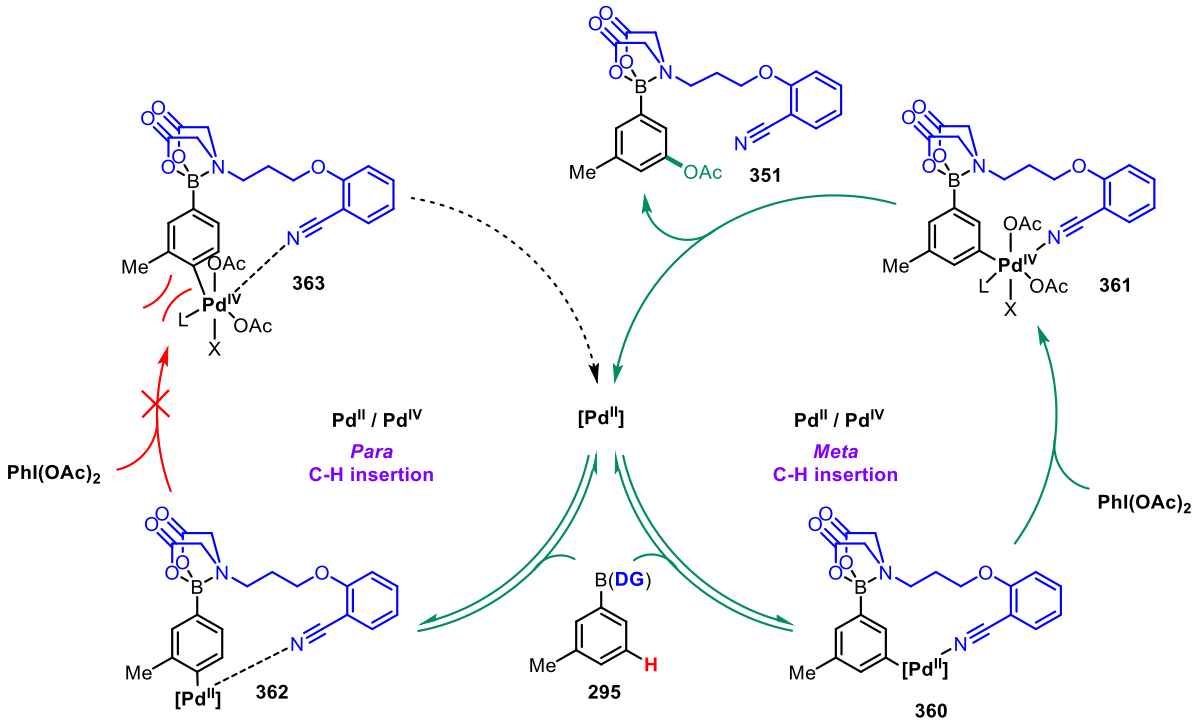
Table 22: The three by three grid used to investigate the scope of the acetoxylation reaction with respect to electronic and substituent effects. [a]Reactions performed at room temperature. [b]Reactions time increased to 48 h. Yields correspond to isolated material, with product ratios determined using ^{1}H NMR after 'catch and release' purification.

Similar trends were observed for the C–H acetoxylations when varying substrates as had been noted for the alkenylation reactions. Electron-donating groups (**352** to **354**) again saw increased degradation; lowering the temperature of the reactions from 40 °C to room temperature increased the isolated yields. The rate was again slower when using electron-withdrawing groups (**357** to **359**) and full conversions were not achieved, even after 48 hours. Changes to reaction time, oxidant equivalents and catalyst loading were unable to drive the reactions to completion.

In contrast to the C–H alkenylations, an increased sensitivity to steric effects was observed, particularly with methyl substituents (**355**, **351** and **356**). Acetoxylation *ortho* to methyl or methyl ester substituents was highly disfavoured, resulting in an increase in regioselectivities

with the *ortho* and *meta* substituted systems **351, 355, 357** and **358**. Conversely, yields suffered when *para* substituents were present (**356** and **359**).

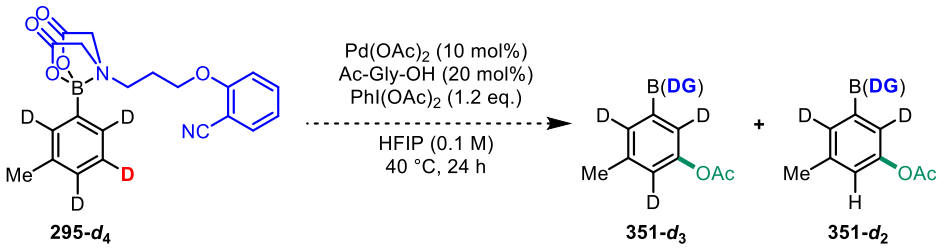
The increased regioselectivity of the acetoxylation over the alkenylation, despite the same MIDA-DG being used, is postulated to be a result of the selectivity determining step involving an octahedral Pd^{IV} intermediate **361** (**Scheme 73**).



*Scheme 73: One possible mechanistic explanation for the origin of the equisite selectivity when using substrate **351**.*

As the DG, substrate and ligands remain identical between the alkenylation and acetoxylation, it can be presumed that the selectivity of the C–H insertion into substrate **295** does not change between the reactions (a ratio of around 2:1, *meta*:*para,* based upon the regioselectivity obtained during the alkenylation reaction). If this is the case, it follows that the acetoxylation pathway resulting from *para* C–H insertion must be unproductive. It is hypothesised that oxidation of the Pd^{II} species **362** by $PhI(OAc)_2$ to give intermediate **363** is energetically unfavourable due to steric clash between ligands coordinated to the Pd^{IV} centre and the adjacent *meta* substituent. The reverse protodepalladation event is therefore favoured, resulting in regeneration of the starting material **295**. As the competing, *meta* insertion pathway (via intermediate **360**) is productive, only the *meta* acetoxylated product is obtained. The observed loss in *meta* selectivity when methoxy substituents are present (substrates **352** and **353**) may be a result of less steric bulk, or an ability to act as a co-ordinating ligand to the putative octahedral complex.

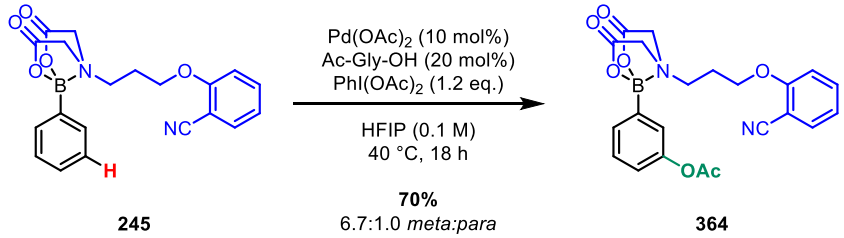
An experiment that might provide evidence for the postulated mechanism would involve the use of a deuterated 3-methylphenylboronic acid based substrate **295-*d*$_4$** (**Scheme 74**).



*Scheme 74: Proposed isotope exchange experiment using deuterated substrate **295**-d_4, designed to provide evidence for the mechanism postulated in **Scheme 73**.*

If selectivity was arising from the mechanism described above, partial protonation of the product in the *para* position would be expected, yielding a mixture of **351-*d*$_3$** and **351-*d*$_2$**, arising from the protodepalladation step (with the protons supplied by exchange with the HFIP solvent). An absence of deuteron/proton exchange at the *para* position would indicate that the selectivity arises *via* a different mechanism, prior to the C–H insertion step. Unfortunately, due to material and time constraints, the postulated experiment has not yet been performed.

A simple phenyl boronic acid based system **245** was also investigated to provide evidence for the presumption that the selectivity of the C–H insertion step does not change between the alkenylation and acetoxylation reactions (**Scheme 75**).



*Scheme 75: C–H acetoxylation of phenylboronic acid MIDA-DG ester **245**.*

The *meta* acetoxylated product **364** was obtained in 70% total yield, with a *meta:para* selectivity similar to that obtained when performing C–H alkenylations on the same substrate (6.7:1.0 compared to 6.9:1.0 obtained when performing the alkenylation reaction). This is indicative of no changes in selectivity during the alkenylation or acetoxylation C–H insertion steps and that the increase in selectivity is derived from interaction with substituents on the aryl ring.

5.1.3 Oxidation of the C–H Acetoxylated Products

To separate regioisomers and/or product/starting material mixtures, the MIDA-DG boronate products were deprotected and the resulting boronic acids oxidised to the corresponding phenols. The deprotection could be performed using K_3PO_4 as base to retain the acetate group, or using NaOH to achieve global hydrolysis of the MIDA-DG boronate and the acetoxylate. Aqueous

hydrogen peroxide was used as the oxidant in all cases. With substrates **371** and **372**, the acetate group proved labile enough to be hydrolysed under the K_3PO_4 conditions, retaining only the methyl esters. The results of the oxidations under the various reaction conditions used are displayed in **Table 23**.

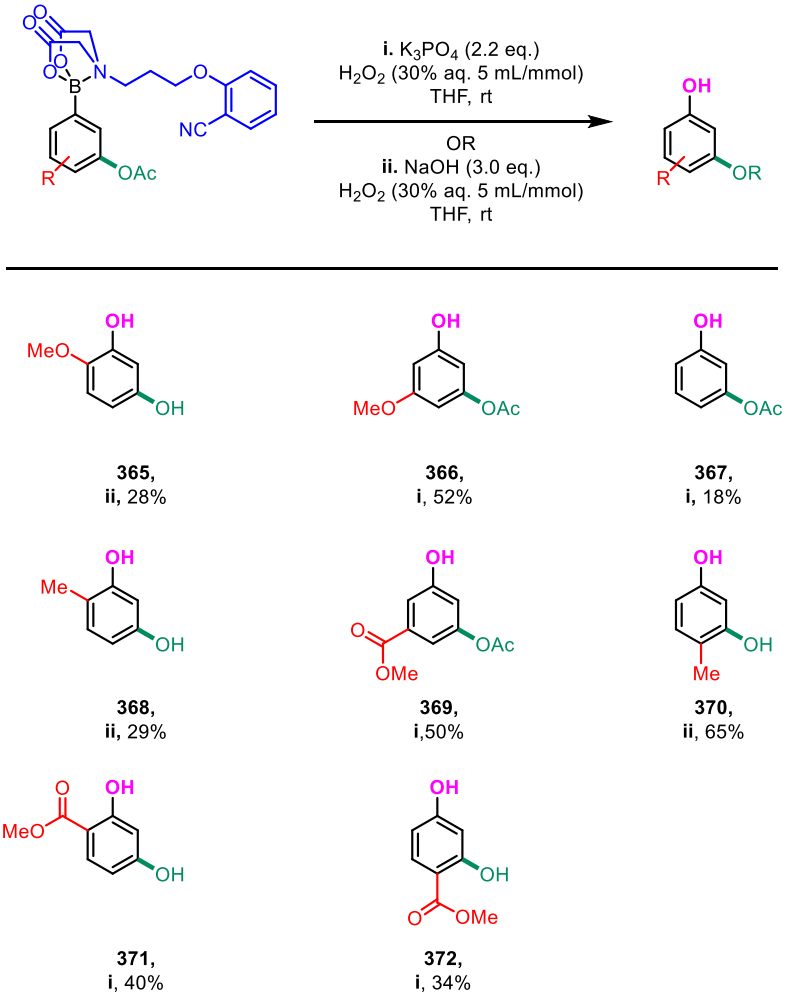


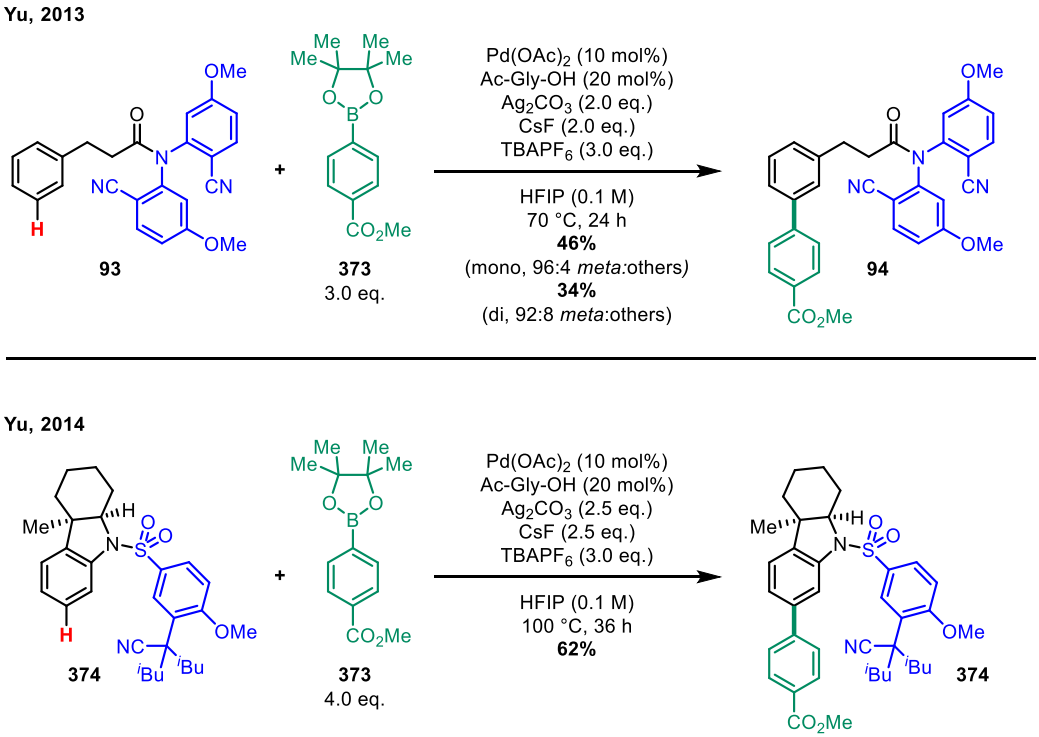
*Table 23: Deprotection/oxidation of acetoxy-MIDA-DG derivatives to yield phenolic products **365-372**. Acetoxylated MIDA boronate products that were themselves succesfully isolated were not subjected to the deprotection-oxidation sequence.*

5.2 Development of C–H Arylations

With conditions for C–H alkenylations and acetoxylations in hand, attention turned to whether *meta*-C–H arylations of boronic acids were possible using the MIDA-DG **290**. Previously, arylations were attempted using the first generation IDA-PA and IDA-AQ DGs **188** and **187** in combination with aryl iodides and diaryl iodonium salts (*see* **2.3**). It was anticipated that the same issues which were encountered using the first generation DGs, in combination with iodide or iodonium coupling partners, would likely also apply when using the PhB(MIDA-DG) **245**. The high

temperatures and alkali bases required would result in rapid loss of the DG. In light of this expectation, a different approach was required.

Yu *et al.* have previously used arylboronic acid pinacol esters as *meta*-arylating reagents in conjunction with nitrile based DGs (**Scheme 76**).[126,127]

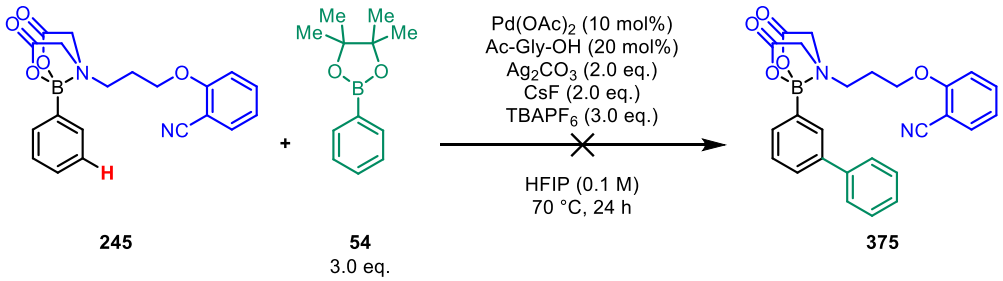


Scheme 76: Conditions developed by Yu et al. for the meta*-C–H arylation of hydrocinnamic acid **93** and indoline **374** using pinacol boronate ester **373** as coupling partner.*[126,127]

Using an arylboronic acid as the coupling partner was appealing for a number of reasons:

- Transmetalation of boronic acids can occur at room-temperatures, leading to the possibility of developing a low temperature process.[208]
- Boronic acids have low-toxicity and routes for their synthesis are well established.[156]
- The C–H arylation would represent the selective coupling of one organoboron species in the presence of another – reminiscent of Burke's iterative processes.[182–187]
- The C–H functionalised MIDA-DG boronates could subsequently be used as coupling partners themselves, after DG removal.

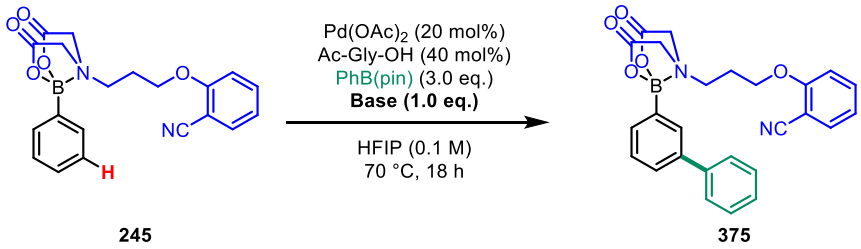
Directly applying the conditions developed by Yu with phenylboronic acid MIDA-DG ester **245** and phenylboronic acid pinacol ester **54** were initially unsuccessful however (**Scheme 77**).



*Scheme 77: Attempted arylation of phenylboronic acid MIDA-DG ester **245** using Yu's conditions.*

In light of this, consideration was given to each of the reaction components and their role. As with the acetoxylation, it was known that the combination of $Pd(OAc)_2$, Ac-Gly-OH and HFIP was required to achieve C–H insertion, with the Ag^{I} oxidant present to regenerate the Pd^{II} catalyst. The CsF base was believed to be required for activation of the boronate species, allowing transmetalation, analogous to the role of the base in a Suzuki-Miyaura coupling reaction. The $TBAPF_6$ additive was introduced by Yu to 'increase catalytic performance by preventing undesired agglomeration of Pd^0 and provide a stabilizing effect to any cationic palladium intermediates'.[209] Although key to increasing yield in Yu's system, with no yield obtained using the MIDA boronate **245**, it was deemed superfluous for our method and not included in subsequent screens.

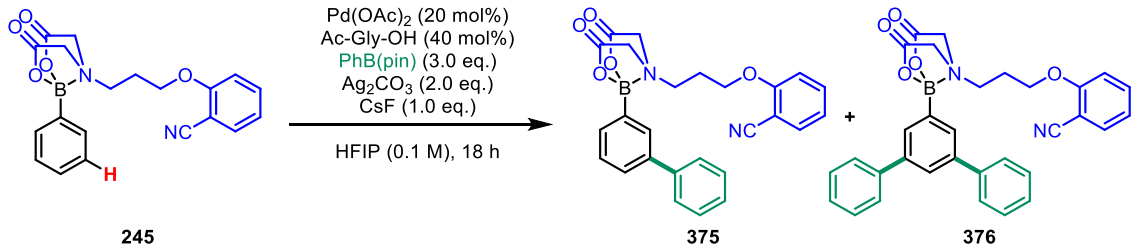
Consequently, the conditions were simplified and a small screen of bases undertaken (**Table 24**).



Entry	Base	Starting Material 245 Remaining	Yield of 375
1	CsF	34%	9%
2	KF	26%	5%
3	Cs_2CO_3	21%	-
4	K_2CO_3	13%	-

*Table 24: Screen of bases for C–H arylation of phenylboronic acid MIDA-DG ester **245** using simplified conditions. Yields are calculated using ^1H NMR against an internal standard.*

Gratifyingly, arylated product was observed to form when using either CsF or KF. With these bases identified, Ag_2CO_3 was introduced as oxidant and a screen of reaction temperatures performed (**Table 25**).

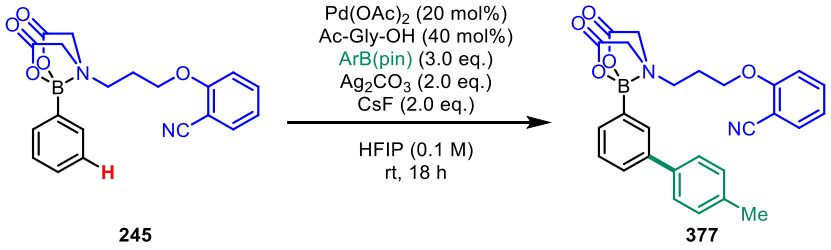


Entry	Temperature	SM 245 Remaining	Yield of 375	Yield of 376
1	70 °C	32%	20%	5%
2	50 °C	25%	27%	10%
3	**25 °C**	**70%**	**28%**	**-**

*Table 25: Investigation of the effect of lowering the reaction temperature on arylation of phenylboronic acid MIDA-DG ester **245**. Yields are calculated using ^1H NMR against an internal standard.*

Gratifyingly, as with the C–H alkenylations and acetoxylations, the arylation proceeded at room temperature to give 30% of the desired product **375**. The introduction of Ag_2CO_3 also saw an increase in yield at 70 °C, with concomitant formation of the di-funcitonalised isomer **376**, indicating that the $TBAPF_6$ additive initially included had likely been suppressing reactivity.

With the knowledge that the reaction proceeded at room temperature, a second screen of bases and oxidants was performed at the lower temperature (**Table 26**).

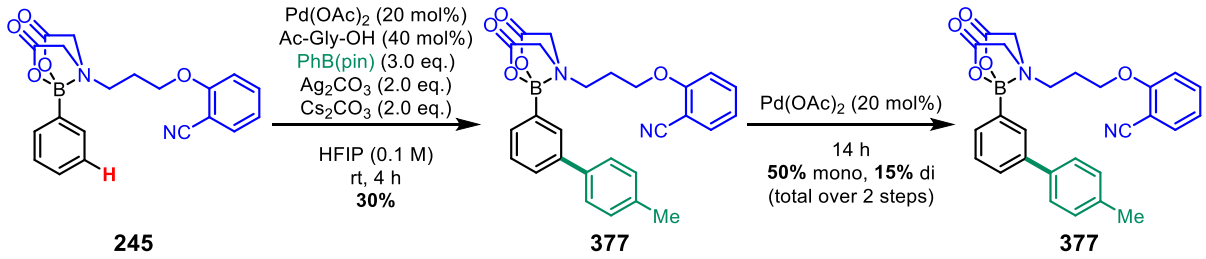


Entry	Change from Standard Conditions	Starting Material	Product
1	None	72%	22%
2	AgOAc (2.0 eq.) as oxidant	68%	18%
3	Ag_2SO_4 (2.0 eq.) as oxidant	80%	10%

4	No base	63%	19%
5	**Cs_2CO_3 (2.0 eq.) as base**	**60%**	**30%**
6	K_3PO_4 (2.0 eq.) as base	70%	3%
7	AgF (2.0 eq.) as base	69%	16%
8	4-methylphenylboronic acid (3.0 eq.)	93%	-

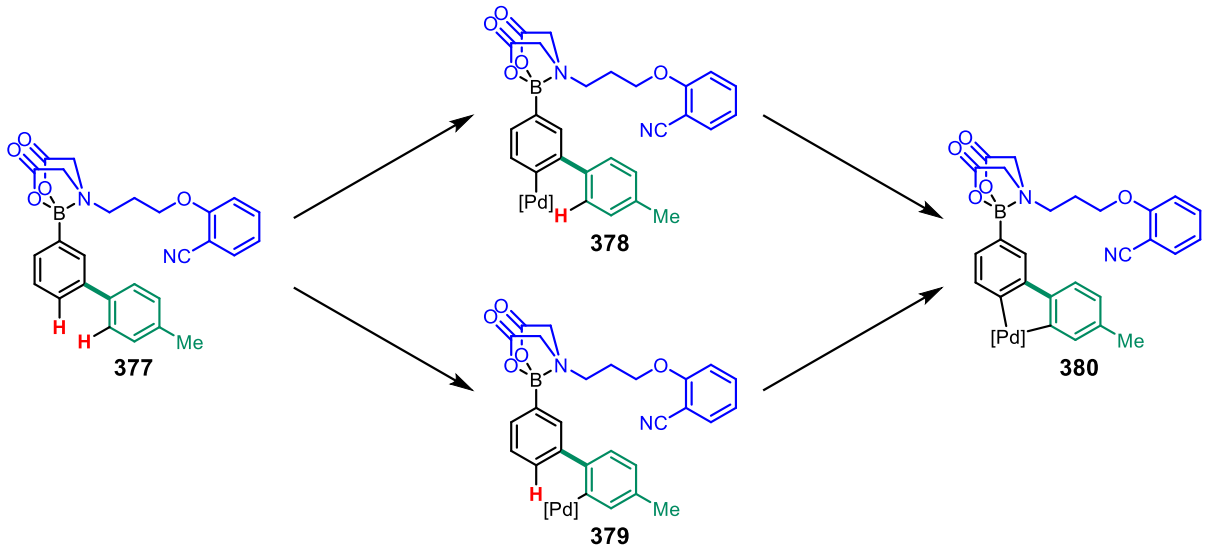
*Table 26: Investigation of the effect of various oxidants, bases and coupling partners on the arylation of phenylboronic acid MIDA-DG ester **245** at room temperature. Yields are calculated using ^{1}H NMR against an internal standard.*

4-Methylphenylboronic acid pinacol ester was used as coupling partner to investigate whether it would be possible to effect MIDA-DG boronate **245** deprotection, followed by coupling of the resulting phenylboronic acid. Free 4-methylphenylboronic acid was also investigated as coupling partner. The screen elucidated that at lower temperatures Cs_2CO_3 and Ag_2CO_3 were the optimal base and oxidant respectively. At this stage, it was noted that no yield above 30% had been achieved. It was hypothesised that the cause of this was catalyst poisoning. To investigate this, a reaction was performed with addition of a second batch of the catalyst after 4 hours (after which time the reaction rate had plateaued) (**Scheme 78**).



*Scheme 78: Arylation of phenylboronic acid MIDA-DG ester **245** using sequential addition of the catalyst, which allowed the reaction to 'restart' after the rate had plateaued. Yields are calculated using ^{1}H NMR against an internal standard and are not isolated.*

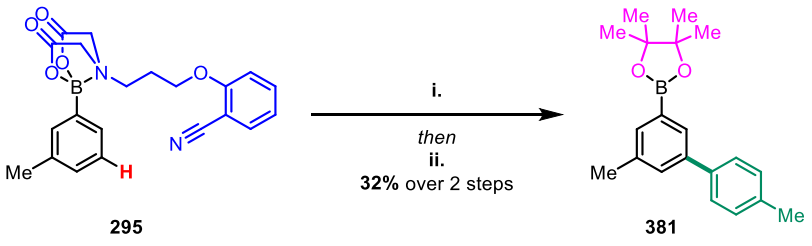
Interestingly, the addition of the second batch of $Pd(OAc)_2$ resulted in the reaction restarting, the progress of the reaction having previously plateaued, with the overall yield approximately double the value obtained before the second addition (with formation of di-arylated product observed). This result was interpreted as indicating that the catalyst was experiencing product inhibition. C–H insertion into a product *para* C–H bond (**378**) or *ortho* C–H on the newly introduced aryl ring (**379**), would leave the Pd catalyst primed for a second C–H insertion to form the biaryl palladium species **380** (**Scheme 79**).



*Scheme 79: Postulated pathways by which product **377** could inhibit catalyst turnover.*

It is hypothesised that the proposed 5-membered palladacyclic species **380** would be stable and unreactive, causing the reaction to stall. Due to time constraints, further investigations into the C–H arylation, such as experiments to provide conclusive evidence of the product inhibition and methods to circumvent this, were not undertaken. Evidence of the inhibition could be provided by synthesising and isolating the product **377**. Reaction of this compound with stoichiometric amounts of catalyst may allow for an X-ray crystal structure of the biaryl Pd complex **380** to be obtained. As well as this, subjecting 4-biphenylboronic acid MIDA-DG ester to the reaction conditions, or doping a standard reaction with this substrate, would be expected to suppress the reaction.

Although not fully optimised, this work demonstrates that C–H arylations are possible using the MIDA-DG scaffold, with the biphenylboronic acid pinacol ester **381** accessed in 32% yield over 2 steps from the simple 3-methylphenylboronic acid MIDA-DG ester **295** (**Scheme 80**).



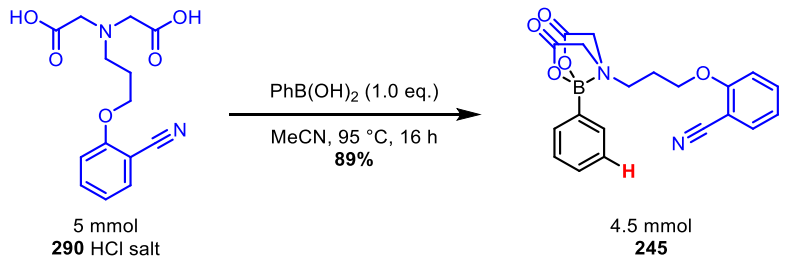
*Scheme 80: An example of C–H arylation using 3-methylphenylboronic acid MIDA-DG ester **295** to access the biphenyl product **381** in just two steps. **i.** $Pd(OAc)_2$ (40 mol%), Ac-Gly-OH (40 mol%), 3-methylphenylboronic acid pinacol ester (2.0 eq.), Ag_2CO_3 (2.0 eq.), Cs_2CO_3 (2.0 eq.), HFIP (0.1 M), rt, 18 h, **52% ii**. Pinacol (1.0 eq.), K_3PO_4 (3.0 eq.), H_2O, THF, DCM, rt, 18 h, **62%.***

6. Derivatisations and Applications of C–H Functionalised Boronic Acids

6.1 Derivatisation of Functionalised Boronic Acids

6.1.1 Large Scale C–H Alkenylation

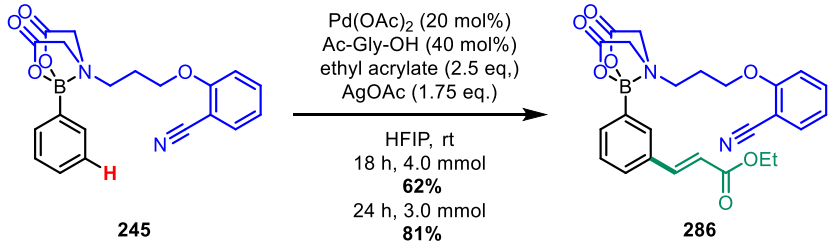
To demonstrate the synthetic versatility of the developed methods, a substantial amount of C–H functionalised product was required. Consequently, a large scale C–H alkenylation was undertaken, both to provide evidence of the scalability of the transformation and to provide material for derivatisation (**Scheme 81**).



*Scheme 81: Large scale synthesis of phenylboronic acid MIDA-DG ester **245**.*

Condensation of the MIDA-DG HCl salt **290** to phenylboronic acid **108** proceeded well on scale (5 mmol, > 1.5 g), achieving comparable yield to that previously obtained (90%, 3 mmol).

The MIDA boronate **245** was subsequently employed in a C–H alkenylation on a 4.0 mmol (1.5 g) scale (**Scheme 82**).



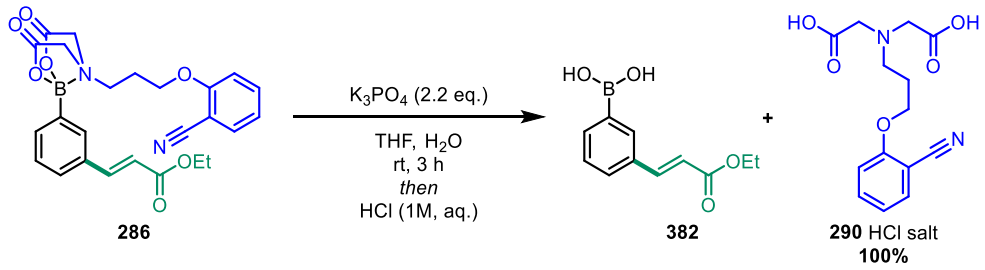
Scheme 82: The C–H alkenylation performed at 4.0 and 3.0 mmol scales (both > 1.0 g). The average yield in agreement matched those obtained on smaller scales.

The reaction was left for the standard duration of 18 hours resulting in a 62% total yield of product **286** (1.45 g, *meta*: 43%, *para*: 7%, *meta-meta*: 7%, *meta-para*: 5%). Full conversion was not achieved however, accounting for the drop in yield relative to the previous analytical scale reaction (15% starting material **245** remaining). A second, 3.0 mmol scale reaction was subsequently performed with the reaction time extended to 24 hours, after which full conversion was achieved, with a total yield of 81% (1.25 g, *meta*: 56%, *para*: 8%, *meta-meta*: 10%, *meta-para*:

7%). The average of the two yields (72%) was comparable to that achieved on small scale, indicating the feasibility of the reaction at > 1.0 g scales.

6.1.2 Deprotection and Recovery of the MIDA-DG

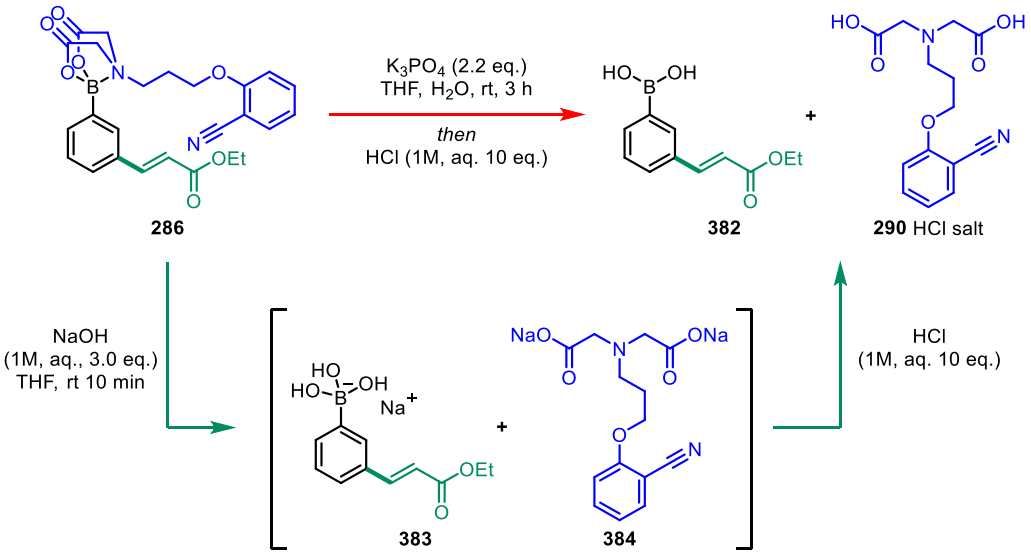
With the C–H alkenylated material **286** in hand, a method for accessing the free boronic acid **382** and recovering the MIDA-DG salt **290** was developed (**Scheme 83**).



*Scheme 83: Deprotection of MIDA-DG boronate ester **286** with quantitative recovery of the MIDA-DG HCl salt **290** after work-up.*

Tribasic potassium phosphate was initially chosen as base, in order to conserve the ethyl ester functionality. The MIDA boronate starting material **286** was used as a mixture of isomers from the C–H functionalisation step, due to the difficulties in separating the highly polar MIDA boronates. After completion of the reaction at *ca.* 3 hours, the reaction mixture was acidified using HCl (1M, aq.) allowing the facile separation of the MIDA-DG HCl salt **290** from the boronic acid **382** product. The salt **290** was isolated from the aqueous phase in quantitative yield after evaporation of the water and removal of residual NaCl by dissolution of the DG **290** in dry MeCN and filtration. The crude boronic acid **382** was not separated from other boronic acid isomers formed and yields were not calculated in anticipation of direct use of this mixture in subsequent reactions, after which purification would be performed.

As well as K_3PO_4, NaOH can be used to cleave MIDA boronate esters in a shorter time-frame.[173] While this method had previously been discounted due to the presence of the ethyl ester, it was realised that the rate of ArB(MIDA) hydrolysis using NaOH was such that it could occur selectively before competing saponification of the ethyl ester. Consequently, by using 3.0 eq. of NaOH (1M, aq.), the MIDA-DG disodium salt **384** and sodium trihydroxyarylborate **383** were accessed in just 10 minutes (**Scheme 84**).

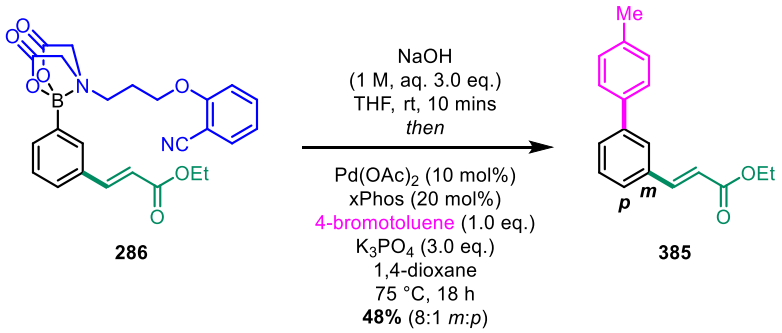


*Scheme 84: Two methods for the deprotection of MIDA-DG **286**. The conditions using NaOH allow deprotection on a shorter timeframe (via the sodium salts **383** and **384**) relative to the conditions using K_3PO_4.*

Employing the same acidification, boronic acid extraction work-up used previously, the MIDA-DG HCl salt **290** was recovered in quantitative yield and the crude boronic acid **382** obtained for subsequent functionalisation. Gratifyingly, no cleavage of the ethyl ester was detected, as evidenced by analysis of the crude reaction product by ^{1}H NMR, provided that the number of equivalents of NaOH was carefully controlled.

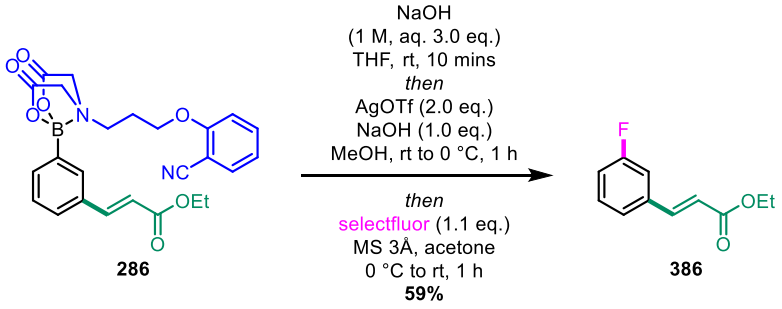
6.1.3 Derivatisation of the Deprotected Boronic Acids

With conditions for accessing the boronic acid established, attention turned to derivatisation of the products. Boronic acids are routinely employed in Suzuki-Miyaura couplings in industrial applications. The utility of the reaction is such that it appears in the top ten reactions used in medicinal chemistry applications (in 2014) and is the only reaction discovered after 1984 to feature in the list.[159] Pleasingly, telescoping the MIDA-DG deprotection of compound **286** into a Suzuki-Miyaura coupling with 4-bromotoluene using standard reagents — $Pd(OAc)_2$, Xphos and K_3PO_4 — yielded the desired biaryl product **385** in 48% yield over the two steps, with an 8:1 ratio of the *meta* alkenylated to *para* alkenylated products (**Scheme 85**).



*Scheme 85: Two-step deprotection-Suzuki-Miyaura cross-coupling of the alkenylated derivative **286**.*

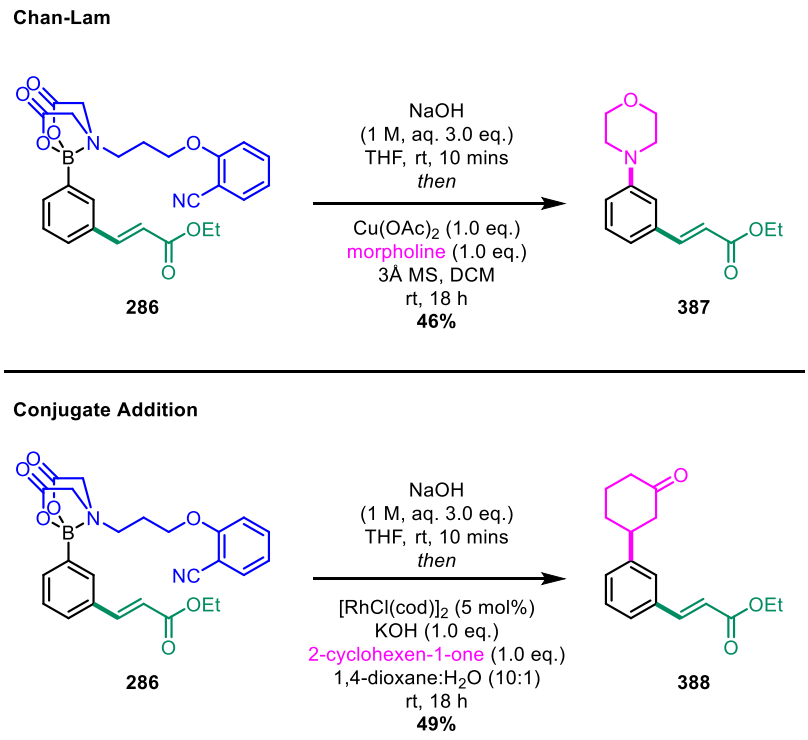
Aryl fluorides have found broad applications in materials, pharmaceuticals, and agrochemicals.[210] In 2009, Ritter and Furuya developed methodology for the fluorination of aryl boronic acids using a transmetalation-fluorination sequence.[211] This complex reaction requires the stoichiometric transmetalation of an aryl boronic acid to silver triflate, followed by a low temperature solvent exchange, before electrophilic fluorination using selectfluor. Despite the potential difficulties involved with the solvent exchange and using a crude isomeric aryl boronic acid mixture, the now three-step deprotection-transmetalation-fluorination sequence proceeded in good yield (**Scheme 86**).



*Scheme 86: Three step deprotection-transmetalation-fluorination of the alkenylated derivative **286** to access fluorinated product **386**.*

Only one regioisomer **386** was isolated, however the product did contain a small amount of ethyl cinnamate **285** by-product due to protodeboronation or protodeargentination during the reaction sequence.

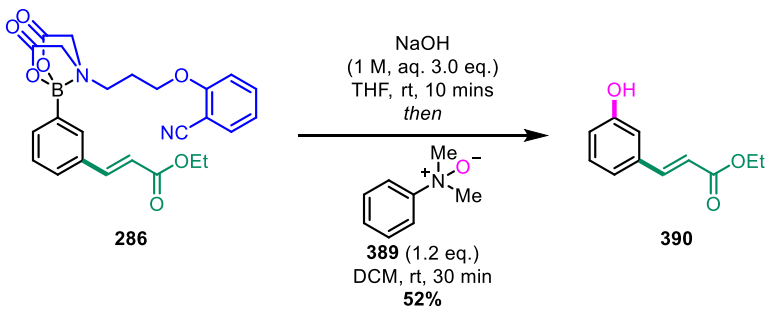
Other transition metal catalysed processes, namely a Chan-Lam coupling with morpholine and a rhodium catalysed conjugate addition to 2-cylohexen-1-one also proceeded in good yield, using standard conditions based upon those commonly employed within the literature (**Scheme 87**).



*Scheme 87: Chan-Lam and Rh-catalysed conjugate addition reactions of the alkenylated derivative **286**.*

In both cases, the products **387** and **388** were isolated as single regioisomers.

Lastly, oxidation of the boronic acid **382** to the corresponding phenol **390** was investigated. Though simple to perform using hydrogen peroxide, as shown with the hydroxylation of the acetoxylated products (*see chapter 5.1.3*), the presence of the activated alkene could potentially have caused selectivity issues. Falck *et al.* developed a rapid and simple oxidation of aryl boronic acids using *N,N*-dimethyl-4-methylaniline-*N*-oxide, which was anticipated to be completely selective for oxidation of the boronic acid.[212] Utilising a *N,N*-dimethyl-aniline-*N*-oxide **389** analogue, the selective hydroxylation was completed in just 30 minutes at room temperature to yield phenol **390** (**Scheme 88**).



*Scheme 88: Deprotection-oxidation reaction sequence on alkenylated derivative **286** in which the N-oxide **389** selectively oxidises the boronic acid over the alkene.*

Interestingly, this reactivity profile has also been employed as a method of accessing tertiary amines from their corresponding *N*-oxides using phenylboronic acid.[213]

The reactions described above constitute only a small selection of the transformations possible with aryl boronic acids. Crucially, none of the reactions required optimisation, using standard conditions directly taken from the literature or based loosely on examples found within literature. These derivatisation therefore exemplify the benefits of using a boronic acid tethered DG, as it makes innumerable C–H functionalised aryl systems accessible from a single directing motif using well established and robust protocols.

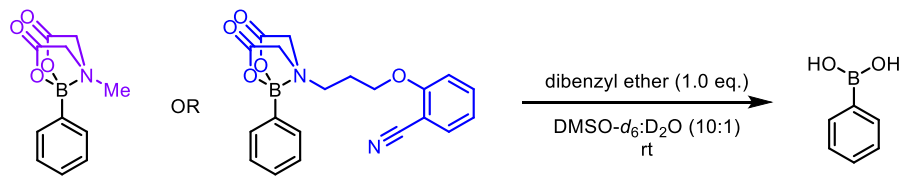
The aqueous phases containing the MIDA-DG HCl salt **290** were all collected during the derivatisations, combined, and the DG recovered in quantitative yield for reuse (*see chapter 6.2.2*).

6.2 Applications of MIDA-DG Boronate Esters

6.2.1 MIDA-DG as a Protecting Group For Boronic Acids

A key design principle considered when developing the MIDA-DG **290** was retention of the ability to act as a protecting group for boronic acids, observed with traditional MIDA boronates.[171,175] While key to preventing competing boronic acid transmetalation during C–H functionalisation, retention of the protecting group ability would also increase the likelihood of widespread adoption of MIDA-DG boronates as protecting-DGs.

The stability of phenylboronic acid MIDA-DG ester **245** to hydrolysis compared to phenylboronic acid MIDA ester **127** and other boronate esters (**54**, **104**, **120** and **128**, **Figure 5**) was evaluated using the same method as Suginome *et al.* to allow for comparison of our results with his.[164] The percentage of hydrolysis in DMSO-d_6:D_2O (10:1) at room temperature was measured every 24 hours using ^{1}H NMR with dibenzyl ether as an internal standard (**Table 27**).



127 **245** **108**

Entry	Time	MIDA 127 (mmol)	MIDA-DG 245 (mmol)	MIDA 127 (%)	MIDA-DG 245 (%)
1	0	0.024	0.021	100	100
2	24	0.023	0.016	95	74

3	48	0.021	0.011	87	50
4	72	0.019	0.008	80	35

*Table 27: A comparison between the rates of hydrolysis of phenylB(MIDA) **127** and phenylB(MIDA-DG) **245**.*

The data was plotted to allow the calculation of the half-lives of the boronate esters **127** and **245** under the experiment conditions (**Figure 29**).

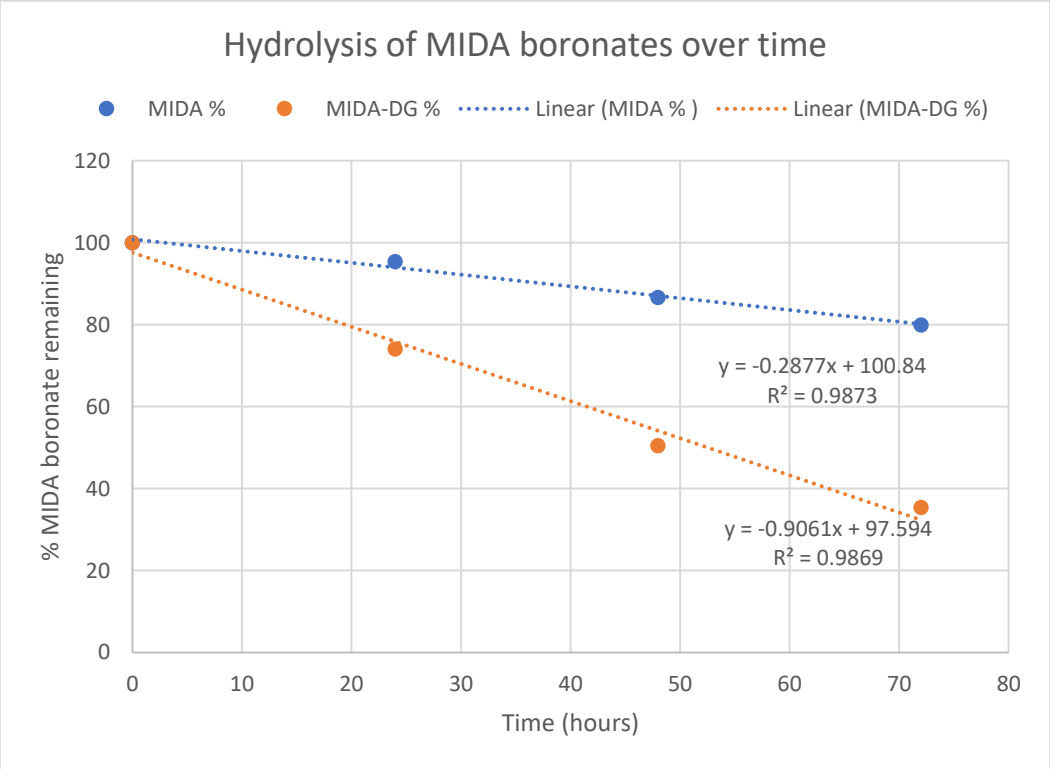
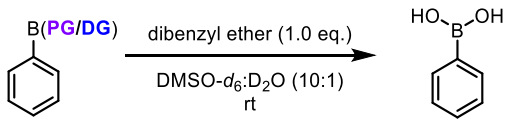


*Figure 29: Plot of percent remaining boronate vs. time during hydrolysis, to allow elucidation of the hydrolysis half-lives of the MIDA esters **127** and **245**.*

The half-lives calculated from plotting the experimental data were 177 hours for phenylboronic acid MIDA ester **127** and 53 hours for the phenylboronic acid MIDA-DG ester **245** under the hydrolysis conditions.

By using the same conditions to test the stability of the MIDA-DG boronate esters as used by Suginome *et al.* it is also possible to correlate with their experimental data for other boronic acid protecting groups (**Table 28**).



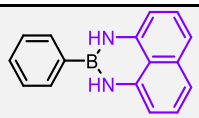
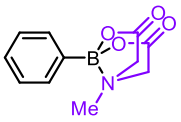
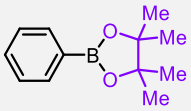
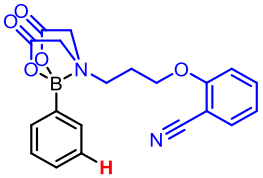
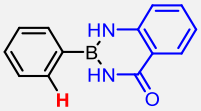
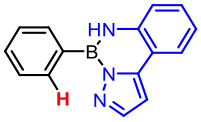
Entry	Boronic acid protecting group	Structure	Half-life (h)
1	PhB(dan) **128**		> 1440[a]
2	PhB(MIDA) **127**		159[b]
3	PhB(pin) **54**		78[a]
4	PhB(MIDA-DG) **245**		53
5	PhB(aam) **120**		10[a]
6	PhB(pza) **104**		0.07[a]

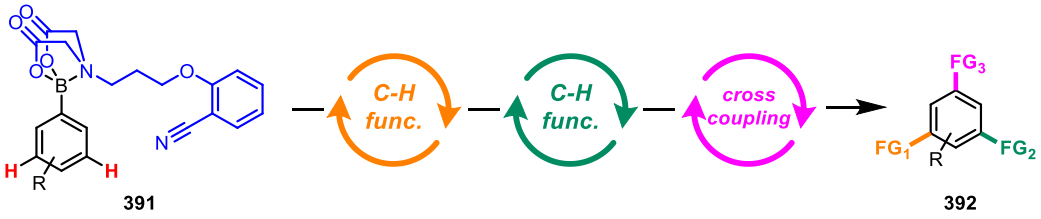
Table 28: Comparison of boronic acid protecting group (PG) and DG stabilities [a]Values taken from Suginome et al.[164] [b]Value averaged from Suginome et al. and the experimental data obtained above.

Although the phenyl MIDA-DG boronate **245** is hydrolysed at approximately three times the rate of the MIDA boronate **127**, the comparison highlights its comparative stability compared to other boronic acid tethered DGs **104** and **120**. Utilising the MIDA scaffold as the basis for the DG leads to a 5-fold increase in half-life compared to the PhB(aam) design **120**. The comparison also highlights the complementarity between the previously available *ortho*-directing motifs **104** and **120** and the *meta*-directing MIDA-DG **245**.

In practical terms, it is difficult to use the measured rate of hydrolysis of the MIDA-DG boronate **245** to infer stability under various reaction conditions, such as those performed on MIDA boronates by Burke *et al.* (*see Chapter 1.3.1,* **Scheme 35**). Unfortunately, time did not permit the subjection of a MIDA-DG protected boronic acid to various reactions to test the stability empirically.

6.2.2 Iterative Synthetic Pathways Using MIDA-DG Boronate Esters

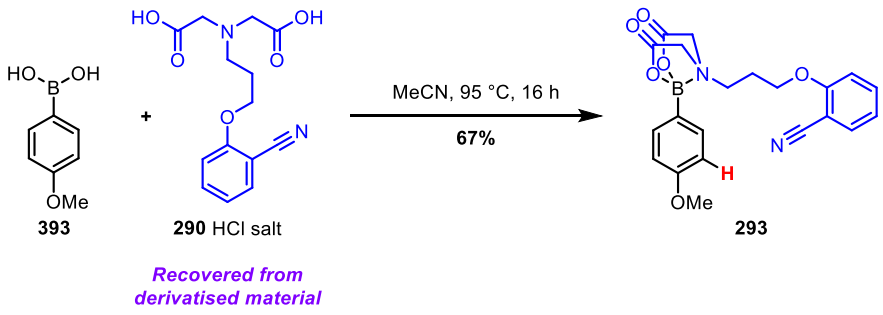
A key application of boronic acid MIDA esters is their use in iterative Suzuki-Miyaura coupling pathways which have for example been demonstrated and automated by Burke *et al.*.[175,194] It was realised that boronic acid MIDA-DG esters could be employed in iterative pathways in a similar manner, with multiple *meta*-C–H functionalisations followed by deprotection and conventional cross-coupling (**Scheme 89**).



Scheme 89: Outline of a potential iterative C–H functionalisation/cross-coupling pathway that would allow expedient access to 1,3,5-trisubstituted aromatic systems.

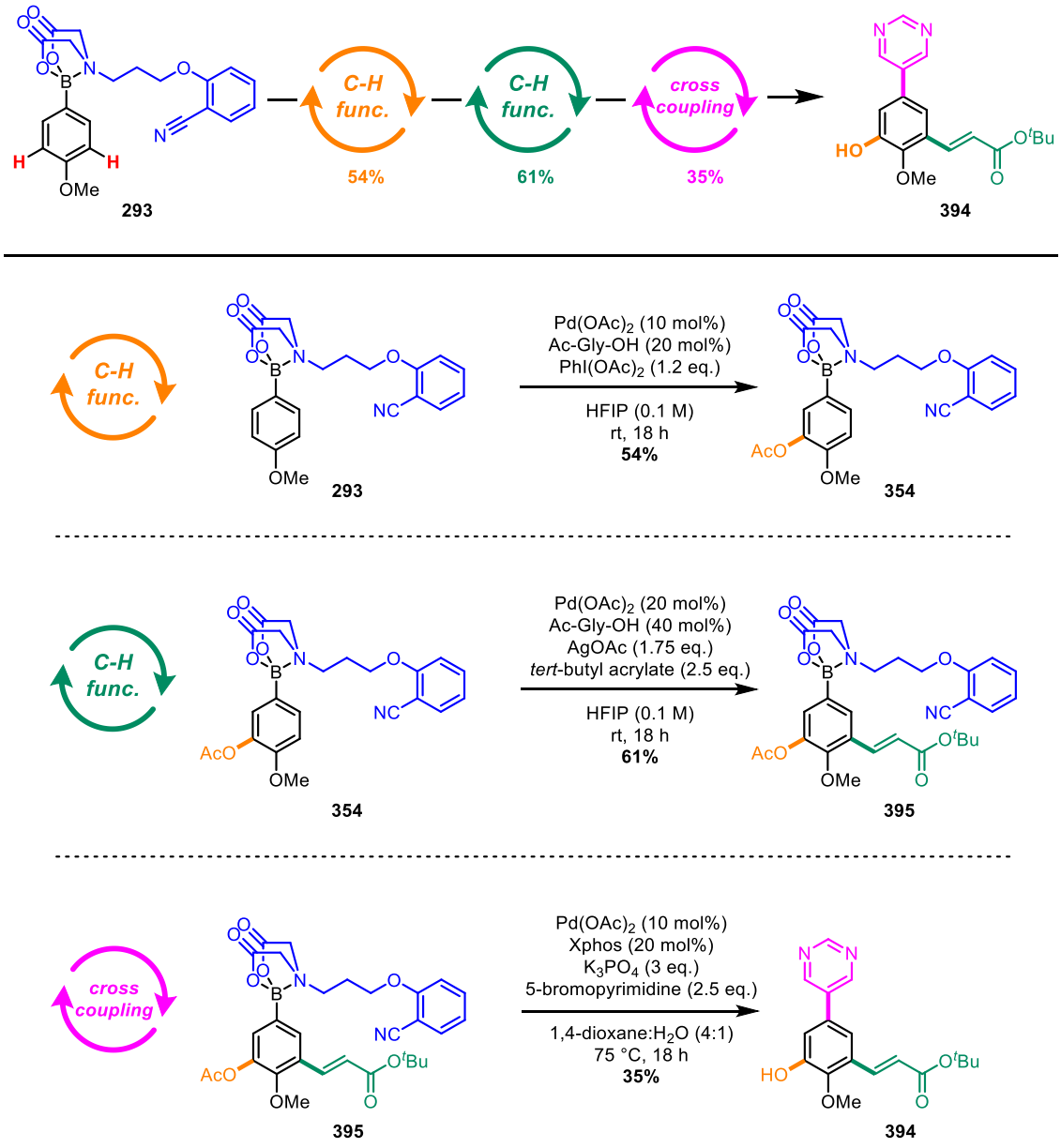
The multistep procedure could be expedited by using the rapid 'catch and release' purifications as exploited by Burke in his automated process.[194] Indeed, the iterative C–H functionalisation/cross-coupling procedure envisaged would potentially be suitable for automation using the same system. In total, the 4-step route to 1,3,5-heterotrisubstituted aromatics would involve three catalytic steps, of which two were C–H functionalisations, and only one conventional chromatographic purification.

4-Methoxyphenylboronic acid **393** was chosen as substrate to demonstrate the feasibility of the process. The *para*-substituted system was chosen to simplify the first implementation by preventing regio-isomer formation. The 4-methoxyphenylboronic acid MIDA-DG ester **293** was synthesised using MIDA-DG HCl salt **290** recovered from the product derivatisation studies (*see chapter 6.1.3*) with no drop in yield on reusing the DG (**Scheme 90**).



*Scheme 90: Synthesis of 4-methoxyphenylboronic acid MIDA-DG ester **293** using recycled MIDA-DG salt **290**.*

A C–H acetoxylation, C–H alkenylation and Suzuki-Miyaura cross-coupling sequence was then applied to **293**, with *in situ* deprotection of the MIDA-DG **290** during the Suzuki-Miyaura cross-coupling (**Scheme 91**).



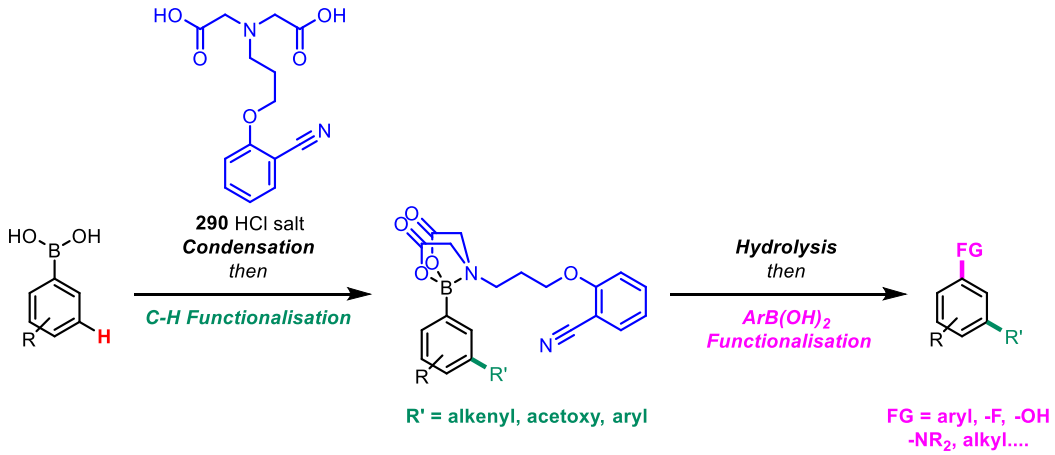
*Scheme 91: The iterative synthesis of tetrasubstituted benzene derivative **394** in just 3 catalytic steps and one chromatographic purification.*

The iterative C–H functionalisation/cross-coupling pathway was successful, providing expedient access to **394** in 3 steps and 12% total yield, with just one chromatographic purification. After each C–H functionalisation, a 'catch and release' purification was performed and the resulting product used directly in the next step, indicating that the process may be amenable to automation.

The deprotection-Suzuki-Miyaura coupling reaction was not optimised and resulted in unintended cleavage of the acetate group – lowering the reaction temperature may avoid this in future.

7. Conclusions

A modified MIDA ligand, termed MIDA-DG **290**, has been developed that can act as a protecting group and also a *meta*-DG for aryl boronic acids. The MIDA-DG **290** is simple to introduce and allows *meta*-selective C–H alkenylations, acetoxylations and arylations. Removal of the MIDA-DG **290** is facile, allows full recovery and recycling of the DG, and reveals complex, functionalised boronic acids for use in further transformations (**Scheme 92**).



*Scheme 92: An overview of the use of the MIDA-DG **290**, as a protecting-DG for the C–H functionalisation of aryl boronic acids.*

Twelve novel *N*-tethered iminodiacetic acid scaffolds were investigated as directing motifs, beginning with bidentate systems focusing on *ortho*-C–H functionalisations. Design considerations elucidated during the initial, unsuccessful, investigations were then applied in second generation designs, ultimately leading to the successful *meta*-directing design **245** (**Figure 30**).

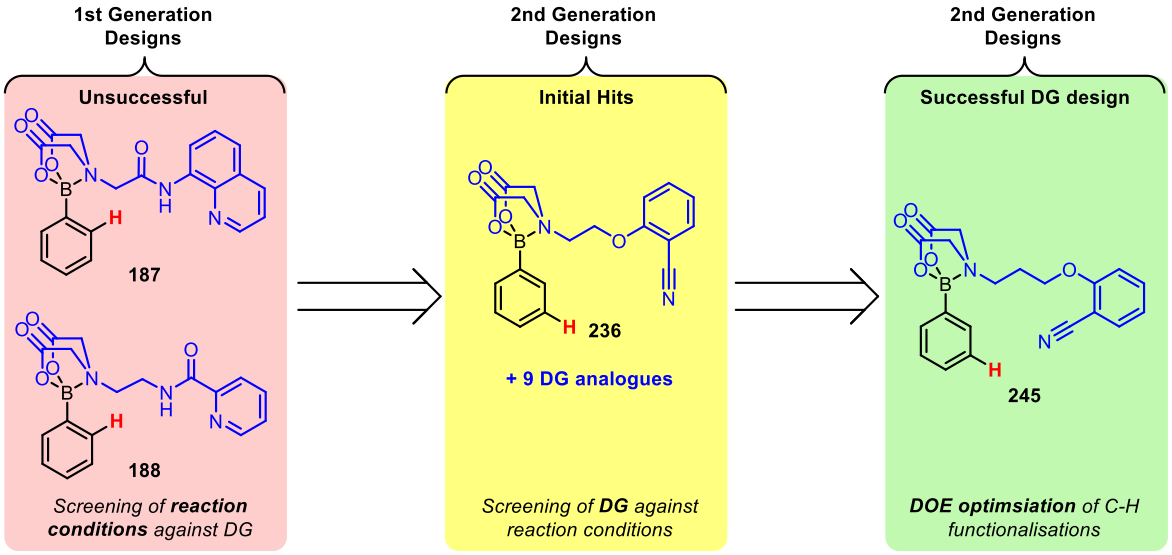
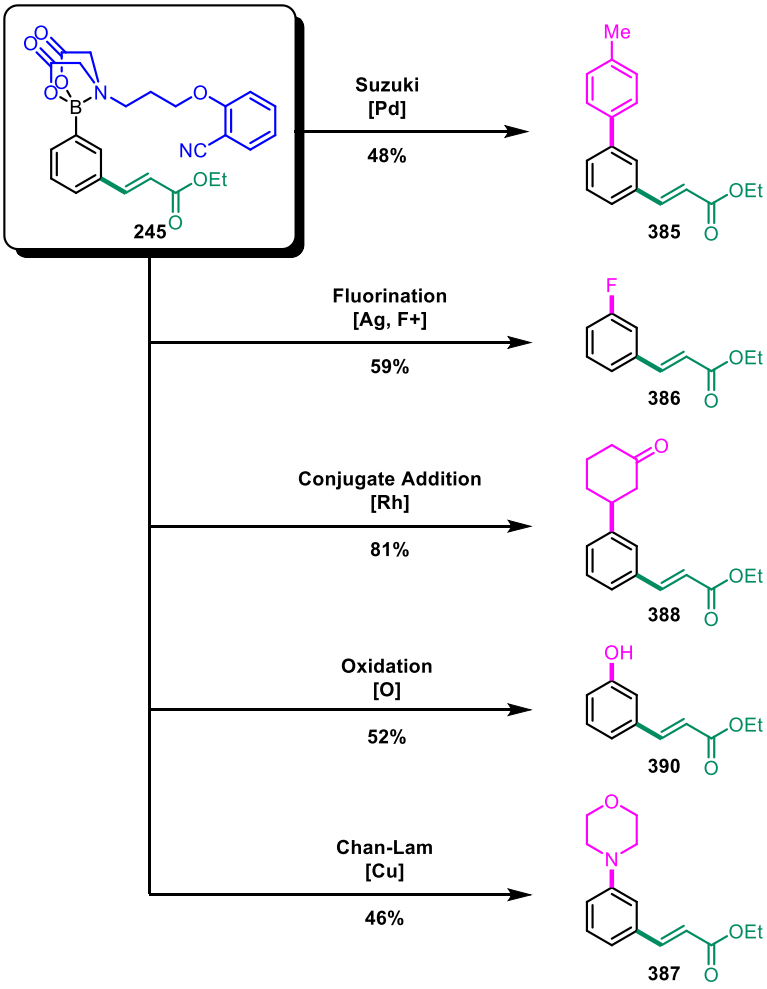


*Figure 30: An overview of the design process used to ultimately arrive at the succesful DG containing derivative **245**.*

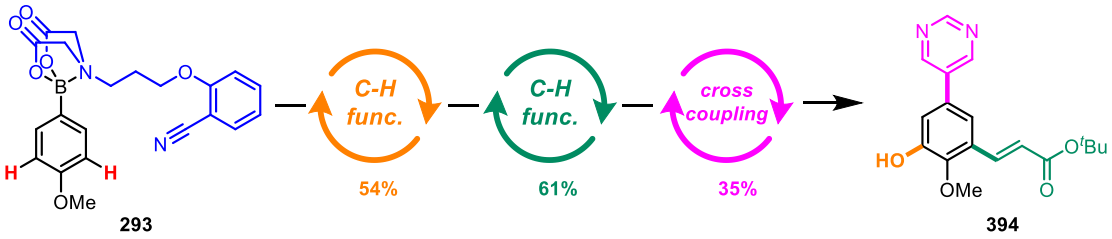
A design of experiment (DOE) approach was next applied to optimise C–H alkenylation reactions using this DG; this allowed the reaction temperature to be reduced to room temperature. With the knowledge that C–H insertion could be achieved using a combination of $Pd(OAc)_2$, Ac-Gly-OH and HFIP as solvent, the repertoire of functionalisations was subsequently expanded to include acetoxylations and select, preliminary examples of arylations. A diverse range of substrates and coupling partners were subjected to the transformations, demonstrating the broad scope of the developed methods.

The utility of the MIDA-DG **290** was exemplified by the derivatisation of C–H alkenylated material into diverse aryl systems, including those not possible to access using current DGs or that would previously require different, bespoke DGs to access (**Scheme 93**).



*Scheme 93: A selection of derivatisation reactions of the alkenylated boronate ester **245**.*

Lastly, an iterative C–H functionalisation/cross-coupling pathway, potentially amenable to automation, allowed expedient access to the diversely substituted 1,3,4,5-tetrasubstitued aromatic system **394**, in just 3 catalytic steps and one chromatographic purification (**Scheme 94**).

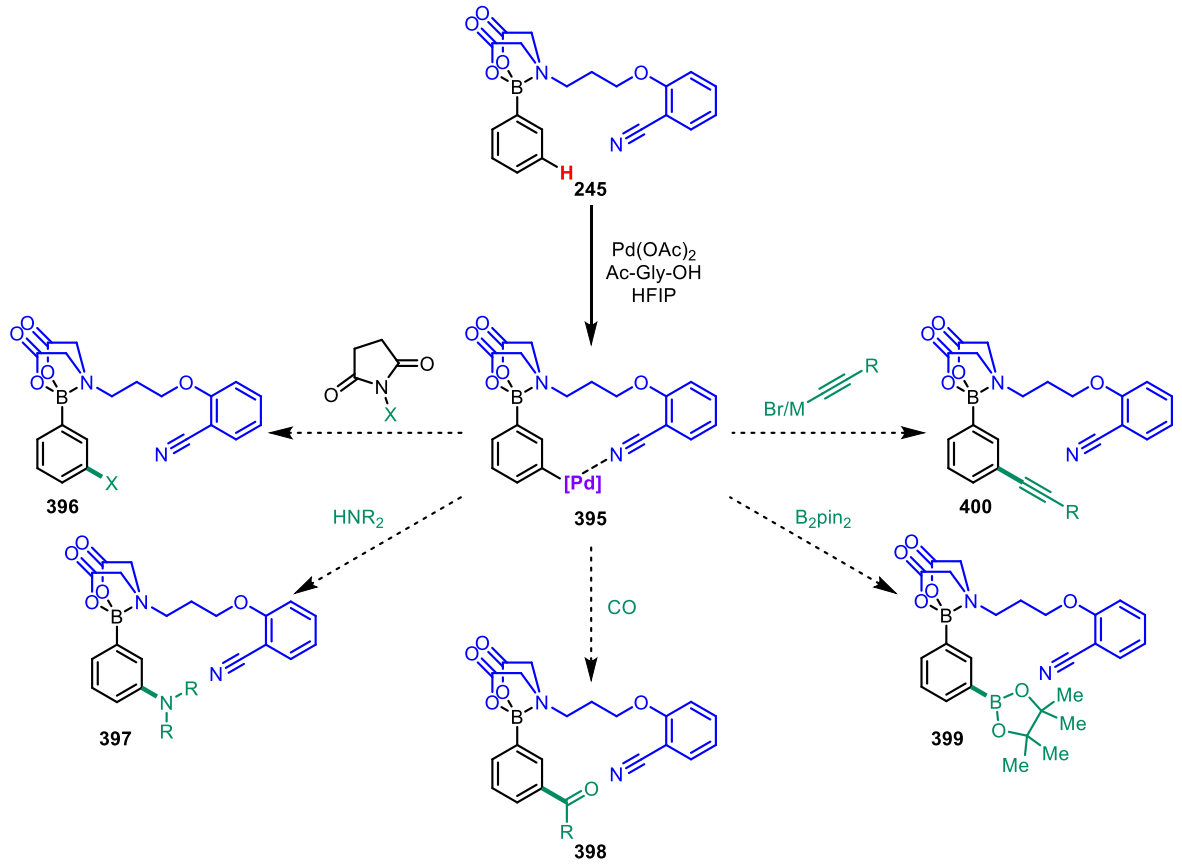


*Scheme 94: An overview of the iterative C–H functionalisation/cross-coupling reaction pathway used to access molecule **394** in just 3 catalytic steps and one chromatographic purification.*

The work contained within this thesis is believed to constitute proof of concept with regard to the uses of the MIDA-DG **290** and the concept of MIDA-tethered DGs in general. The initial success achieved in *meta*-selective functionalisations opens the door to numerous possibilities, such as:

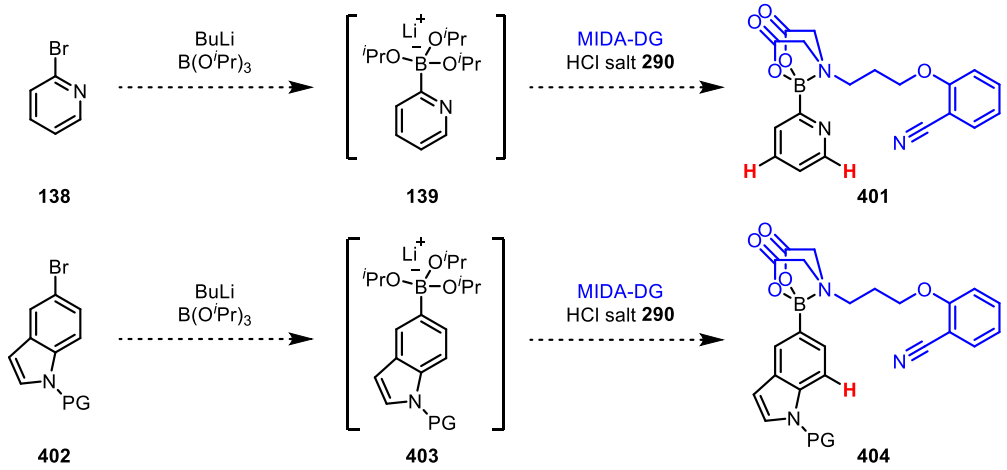
- The development of a broad library of *meta*-selective C–H functionalisation reactions to access diverse functional groups.
- The introduction of hetero-aromatics as potential substrates, and methods to access them directly via metalation-borylation synthetic routes.
- The development of a complementary *para*-selective MIDA-DG scaffold.
- The automation of the iterative C–H functionalisation/cross-coupling reaction sequence.

It is known that *meta*-selective C–H insertion of Pd^{II} into phenylboronic acids is achievable using a combination of the MIDA-DG **290**, $Pd(OAc)_2$, Ac-Gly-OH and HFIP as solvent. As with the acetoxylation and arylation reactions, it follows that the development of novel transformations becomes a question of finding suitable coupling partners and conditions. A wealth of literature on palladium catalysed directed C–H functionalisations provides a foundation to build upon, with regard to choice of reagents and possible transformations (**Scheme 95**).[5,97,214]



*Scheme 95: Potential transformations of compound **245**, which are anticipated to be feasible given that conditions for Pd C–H insertion have been established in the work in this thesis.*

Heterocyclic boronic acids, particularly 2-heterocyclicboronic acids are notoriously prone to protodeboronation, making their handling and use difficult.[172,174] Burke *et al.* were able to avert these degradation pathways by employing MIDA boronate esters, preventing protodeboronation and improving yields during cross-couplings.[195,196] Investigations into the ability of the MIDA-DG **290** to stabilise heterocyclic boronic acids, as well as direct their C–H functionalisation would greatly expand the MIDA-DG **290**'s synthetic utility. The modification of the metalation-boronation pathway used by Burke, would also allow direct access to heterocyclicboronic acid MIDA-DG esters from halide precursors (**Scheme 96**).



Scheme 96: Potential metalation-boronation reactions that would allow direct access to heterocyclic boronic acid MIDA-DG esters for C–H functionalisation and circumvent protodeboronation of unstable boronic acids.

The same design principles employed in developing the *meta*-selective MIDA-DG **290** could in turn be employed to design a *para*-directing MIDA scaffold. Indeed, one potential *para*-DG **239**, based on a design by Maiti *et al.,* was described in this thesis.[123,137] Once again, a library of analogues could be synthesised and subjected to standard C–H alkenylation conditions, until a hit is achieved, after which DOE optimisation could yield a synthetically valuable transformation (**Figure 31**).

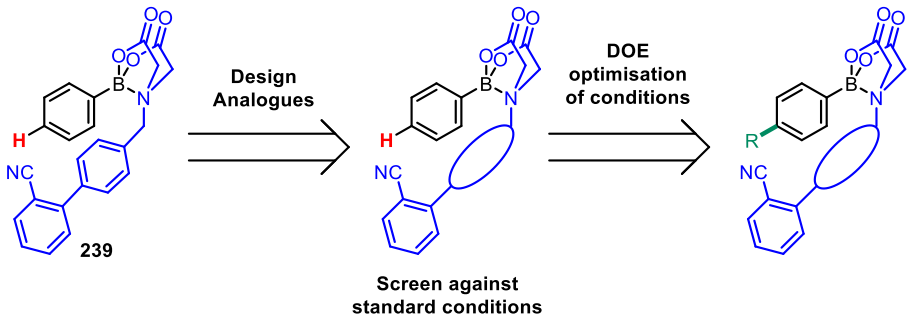
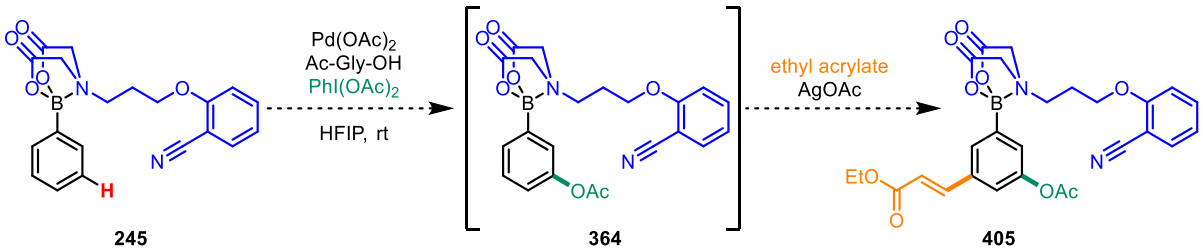


Figure 31: Potential design process to access a para-selective DG.

It is anticipated that any transformations developed for the *meta*-selective MIDA-DG **290** would prove highly transferable to a *para*-selective system.

Lastly, the iterative C–H functionalisation/cross-coupling pathway demonstrated within the thesis can be expanded upon. Further investigations into the possibility of automating the procedures can be undertaken. In addition to this, streamlining the pathway by truly telescoping the procedures, without the 'catch and release' purifications could be investigated. The similarity between C–H functionalisation conditions could be levied to allow sequential, one-pot functionalisations *via* close control of reagent equivalents and additions times, which would also reduce the waste generated during the processes (**Scheme 97**).



Scheme 97: Proposed 'one-pot' C –H acetoxylation-alkenylation reaction sequence, which may circumvent the requirement for an intermediate 'catch and release' purification step.

Overall, this thesis describes the development of a novel modified MIDA ligand **290**, to which is tethered a DG for the *meta*-selective C–H functionalisation of boronic acids. C–H alkenylations, acetoxylations and preliminary work towards C–H arylations are described, with the derivatisation of the products used to exemplify the potential of the methods.

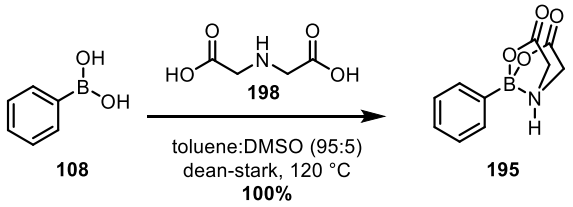
Experimental

General Experimental Details

All reactions were performed under nitrogen using oven-dried glassware unless stated otherwise. Yields refer to chromatographically and spectroscopically (^{1}H-NMR) homogenous materials, unless otherwise indicated. MeCN, CH_2Cl_2, THF, Et_2O, DMF, and toluene were dried and deoxygenated with a Grubbs PureSolv 400 solvent purification system. Hexafluorisopropanol (HFIP) was supplied by Fluorochem and used in without further purification. The moisture content of the solvents was monitored by Karl Fischer coulometric titration (Mettler-Toledo DL39). **Reagents**: used as purchased from commercial sources, unless otherwise stated, and used according to COSHH regulations. **Chromatography**: Flash column chromatography (FCC) was performed on silica gel (Merck Kieselgel 60 F254 230-400 mesh) unless otherwise stated. **Melting Points**: determined on a Stanford Research System OptiMelt. Boronic acid MIDA-DG esters were observed to degrade before melting, characterized by discolouration. **Thin Layer Chromatography (TLC)**: performed on Merck aluminium-backed plates pre-coated with silica (0.2 mm, 60 F254) which were visualized either by quenching of ultraviolet fluorescence (λmax = 254 and 366 nm) or staining with potassium permanganate/Δ, TLC dips prepared according to general procedures. **^{1}H NMR spectra**: recorded on a 400 or 500 MHz Bruker AMX-400/500 instrument. Chemical shifts (δH) are quoted in parts per million (ppm), referenced to the appropriate residual solvent peak. **^{13}C NMR spectra**: recorded at 101 MHz or 125 MHz on a Bruker AMX-400/500 instrument Chemical shifts (δC) are quoted in parts per million (ppm), referenced to the appropriate residual solvent peak. **^{11}B NMR spectra**: recorded at 128 MHz on a Bruker AMX-400 instrument. Chemical shifts (δB) are quoted in parts per million (ppm), referenced to $BF_3.Et_2O$ in $CHCl_3$. **^{19}F NMR spectra:** recorded at 377 MHz on a Bruker AMX-400 instrument. Chemical shifts (δF) are quoted in parts per million (ppm), indirectly referenced to $CFCl_3$ via measurement of the frequency of the deuterium lock signal. Product mixtures that are fully characterized were analyzed and characterized using 2D COSY, HSQC and HMBC techniques (mostly pinacol boronate ester products). **High Resolution Mass Spectra**: recorded on either a VG platform II or VG AutoSpec spectrometer, with only molecular ions ($[M+H]^+$, $[M+Na]^+$, $[M+K]^+$, $[M+H_2O]^+$, $[M-H]^-$) and major peaks being reported. ES TOF (Electro-spray ionization, time-of-flight) and APCI (atmospheric pressure chemical ionization) ionization methods were used.

Chapter 2

Phenylboronic acid IDA ester (195)



A 50 mL round-bottomed flask was charged with phenylboronic acid (1.22 g, 10 mmol) and iminodiacetic acid (1.33 g, 10 mmol). The solids were suspended in toluene (10 mL + 5% v/v DMSO), the flask fitted with Dean-Stark apparatus and the resulting suspension refluxed at 120 °C for 16 hours. The reaction mixture was cooled to room temperature giving a tan solid within a clear suspension. The solvent was removed *in vacuo* and acetone (4 mL) added, forming a white precipitate. Et_2O was then added in 1 mL portions until precipitation ceased. The solid was collected *via* vacuum filtration, washed with further Et_2O and dried to give the product **195** as a white solid (1.66 g, 76%).

ν_{max}/cm^{-1} 3112, 1731, 1433, 1309, 1233, 1011, 756, 707.

HRMS (ESI) Calcd. for $C_{10}H_9BNO_4$ ([M-H]$^-$): 218.0625. Found: 218.0634

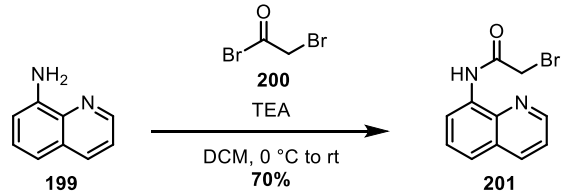
^{1}H NMR (400 MHz, CD_3CN) δ 7.56 – 7.45 (m, 2H), 7.44 – 7.33 (m, 3H), 6.58 (s, 1H), 4.15 (dd, *J* = 17.4, 8.4 Hz, 2H), 3.67 (dd, *J* = 17.4, 3.3 Hz, 2H).

^{13}C NMR (101 MHz, CD_3CN) δ 169.9, 131.8, 128.7, 127.7, 53.0.

^{11}B NMR (128 MHz, CD_3CN) δ 10.4.

*The spectroscopic properties of the compound were consistent with the data pertaining to it in the literature (*T. Mancilla *et al. J. Organomet. Chem.* 1986, **307**, 1*).*

2-Bromo-N-(quinolin-8-yl)acetamide (201)



8-Aminoquinoline (2.88 g, 20 mmol) was suspended in anhydrous CH_2Cl_2 (100 mL), triethylamine (2.78 mL, 20 mmol) under a nitrogen atmosphere and the mixture cooled to 0 °C. Bromoacetyl bromide (1.92 mL, 22 mmol) was dissolved in anhydrous CH_2Cl_2 (40 mL) before being added to the cooled solution dropwise over 15 minutes. The reaction was allowed to warm to room temperature and stirred for 21 hours. 0.3 M HCl (100 mL, 30 mmol) was added to quench the reaction. The resulting layers were separated, the organic layer dried over $MgSO_4$, filtered and

concentrated under vacuum. The residue was purified *via* FCC (2:1 hexane:EtOAc) to yield the title compound **201** as a yellow solid (3.68 g, 70%).

ν_{max}/cm^{-1} 3305, 3041, 1694, 1660, 1520, 1205, 824, 789, 769.

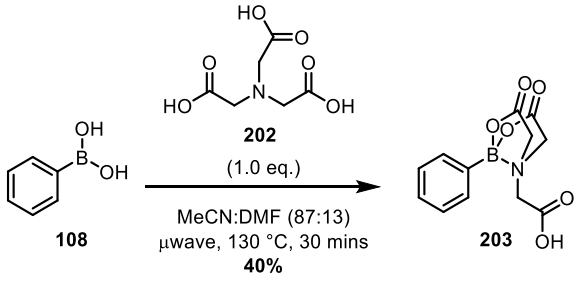
HRMS (ESI) Calcd. for $C_{11}H_{10}BrN_3O_5^+$ ([M+H]$^+$): 264.9971. Found: 264.9970.

^{1}H NMR (400 MHz, $CDCl_3$) δ 10.77 (br. s, 1H), 8.89 (dd, J = 4.3, 1.7 Hz, 1H), 8.77 (dd, J = 5.8, 3.2 Hz, 1H), 8.21 (dd, J = 8.3, 1.7 Hz, 1H), 7.62 – 7.56 (m, 2H), 7.51 (dd, J = 8.3, 4.2 Hz, 1H), 4.18 (s, 2H).

^{13}C NMR (101 MHz, $CDCl_3$) δ 164.0, 148.6, 138.7, 136.3, 133.8, 127.9, 127.2, 122.5, 121.8, 116.6, 29.7.

*The spectroscopic properties of the compound were consistent with the data pertaining to it in the literature (*Q. Yan *et al. New J. Chem.* 2017, **41**, 2372*).*

2-Phenyl-6-(prop-2-yn-1-yl)-1,3,6,2-dioxazaborocane-4,8-dione (203)



A 20 mL microwave vial was charged with nitrilotriacetic acid (1.91 g, 10 mmol), phenylboronic acid (1.22 g, 10 mmol) and anhydrous MeCN (10 mL + 12.5% v/v anhydrous DMF) and sealed. The reaction mixture was then heated to 130 °C for 30 mins using microwave irradiation at 90 W. The resulting suspension was dry loaded onto silica using MeCN. The loaded silica column was washed with copious Et_2O then eluted using copious MeCN: Et_2O (1:1). The desired fractions were concentrated *in vacuo* to yield a brown oil. CH_2Cl_2 (~ 15 mL) was added in 1 mL portions to induce precipitation of a white solid, which was collected *via* vaccum filtration, washed with further CH_2Cl_2 and dried to yield the product **203** as a white solid (1.10 g, 40%). The compound decomposed at high temperature before a melting point could be recorded.

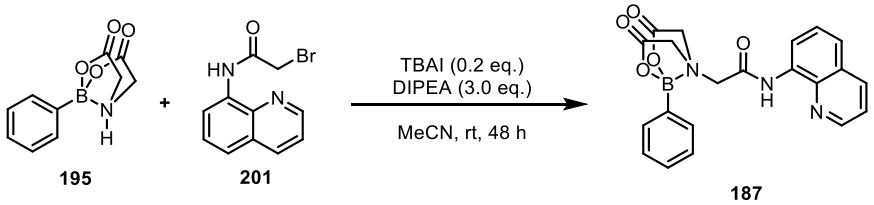
ν_{max}/cm^{-1} 3020, 1758, 1711, 1311, 1225,1187, 999, 843, 756, 701.

HRMS (ESI) Calcd. for $C_{12}H_{13}BNO_6^+$ ([M+H]$^+$): 278.0830. Found: 278.0829.

^{1}H NMR (400 MHz, CD_3CN) δ 7.57 – 7.37 (m, 5H), 4.26 (d, J = 17.6 Hz, 2H), 4.10 (d, J = 17.5 Hz, 2H), 3.47 (s, 2H).

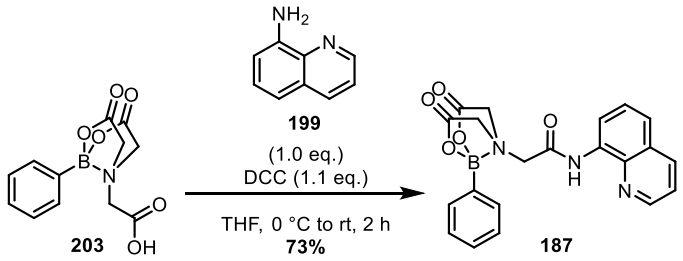
^{13}C NMR (101 MHz, CD_3CN) δ 159.4, 144.6, 142.8, 132.0, 120.8, 116.9, 37.1, 36.4. ^{11}B NMR (128 MHz, CD_3CN) δ 11.9.

Phenylboronic acid IDA-AQ ester (187)



195 201 187

Phenylboronic acid IDA ester **195** (3.04 g, 14 mmol), 2-Bromo-N-(quinolin-8-yl)acetamide **201** (3.67 g, 14 mmol) and TBAI (1.03 g, 3 mmol) were placed under a N_2 atmosphere and anhydrous MeCN (150 mL) added. Anhydrous DIPEA (7.25 mL, 42 mmol) was subsequently added and the reaction mixture stirred at room temperature for 48 hours. The solvent was removed under vacuum and the resulting residue purified *via* FCC (1:1EtOAc:petroleum ether), the appropriate fractions collected and concentrated under reduced pressure to yield the title compound **187** as a white solid (1.02 g, 18 %).



203 187

Carboxylic acid **203** (139 mg, 0.5 mmol) was dissolved in THF (2.5 mL), cooled to 0 °C and DCC (113 mg, 0.55 mL) added. The resulting suspension was stirred for 45 minutes at 0 °C before 8-aminoquinoline (72 mg, 0.5 mmol) was added, the mixture allowed to warm to room temperature and stirred for 2 hours. The reaction mixture was dry loaded onto silica, washed with copious Et_2O and eluted using Et_2O:MeCN (1:1). The Et2O:MeCN fraction was concentrated *in vacuo* to yield the title compound **187** as a pale yellow solid (150 mg, 73 %).

The compound decomposed at high temperature before a melting point could be recorded.

ν_{max}/cm^{-1} 3261, 1743, 1683, 1532, 1224, 1028, 755, 703.

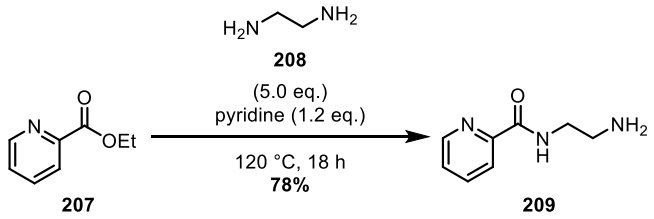
HRMS (ESI) Calcd. for $C_{21}H_{19}BN_3O_5^+$ ([M+H]$^+$): 404.1418. Found: 404.1425.

^{1}H NMR (400 MHz, Acetonitrile-d3) δ 9.78 (s, 1H), 8.81 (dd, *J* = 4.2, 1.7 Hz, 1H), 8.65 – 8.59 (m, 1H), 8.31 (dd, *J* = 8.3, 1.7 Hz, 1H), 7.68 (dd, *J* = 8.3, 1.4 Hz, 1H), 7.62 – 7.53 (m, 4H), 7.49 – 7.44 (m, 3H), 4.41 (d, *J* = 17.6 Hz, 2H), 4.26 (d, *J* = 17.5 Hz, 2H), 3.83 (s, 2H).

^{13}C NMR (101 MHz, CD_3CN) δ 168.9, 164.1, 148.9, 138.1, 136.5, 133.7, 132.7, 129.4, 128.1, 127.0, 122.8, 122.2, 116.8, 67.3, 61.5, 61.2, 25.3.

^{11}B NMR (128 MHz, CD_3CN) δ 11.9

N-(2-Picolinoyl)-1,2-diaminoethane (209)



To ethylenediamine **208** (19.35 mL, 290 mmol) was added ethyl 2-picolinate **207** (6.75 mL, 50 mmol) and pyridine (5.75 mL, 71 mmol) and the resulting solution stirred at 120 °C for 18 hours. The reaction mixture was allowed to cool to room temperature and the excess ethylenediamine removed *in vacuo*. The solution was diluted with H_2O (100 mL), acidified to pH 5 with 6M HCl and extracted with $CHCl_3$ (3 × 100 mL). The pH of the aqueous layer was then adjusted to 14 using saturated aq. NaOH before being extracted a second time with $CHCl_3$ (3 × 100 mL). The organic layers from the second extraction were combined, dried over $MgSO_4$, filtered and concentrated under vacuum to yield the title compound **209** as a pale yellow oil (6.47 g, 78%).

ν_{max}/cm^{-1} 3364, 2931, 1656. 1521, 1433, 1288, 997, 820, 748, 690.

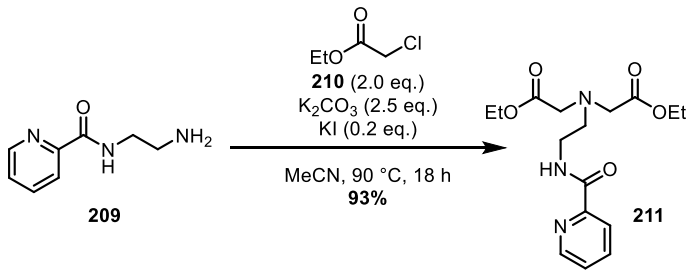
HRMS (EI+) Calcd. for $C_9H_{10}NO$ ($[M]^+$):148.0762. Found: 148.0770.

^1H NMR (400 MHz, $CDCl_3$) δ 8.57 (d, J = 4.6 Hz, 1H), 8.34 (br. s, 1H), 8.22 (d, J = 7.5 Hz, 1H), 7.86 (t, J = 7.8 Hz, 1H), 7.44 (dd, J = 7.2, 5.0 Hz, 1H), 3.56 (q, J = 6.0 Hz, 2H), 2.97 (t, J = 6.1 Hz, 2H), 1.61 – 0.83 (br. s, 2H).

^{13}C NMR (101 MHz, $CDCl_3$) δ 164.7, 150.0, 148.1, 137.3, 126.1, 122.2, 42.4, 41.7.

*The spectroscopic properties of the compound were consistent with the data pertaining to it in the literature (*M. Bukowski *et al. J. Biol. Inorg. Chem.* 2004, **9**, 39*).*

Diethyl 2,2'-((2-(picolinamido)ethyl)azanediyl)diacetate (211)



N-(2-picolinoyl)-1,2-diaminoethane (5.78 g, 35 mmol) was added to a suspension of K_2CO_3 (12.08. g, 88 mmol) and KI (1.16 g, 7.0 mmol) in anhydrous MeCN (35 mL) under a nitrogen atmosphere. Ethyl chloroacetate (7.9 mL 74 mmol) was then added dropwise over 15 minutes and the reaction mixture heated to reflux (90 °C) for 18 hours. After being allowed to cool to room temperature, the suspension was diluted with H_2O (450 mL) and extracted with $CHCl_3$ (3 × 250 mL). The organic layers were combined, dried over $MgSO_4$, filtered and concentrated *in vacuo*. The

resulting residue was purified *via* FCC (1:1 EtOAc:hexane) to yield the title compound **211** as a yellow oil (11.00 g, 93 %).

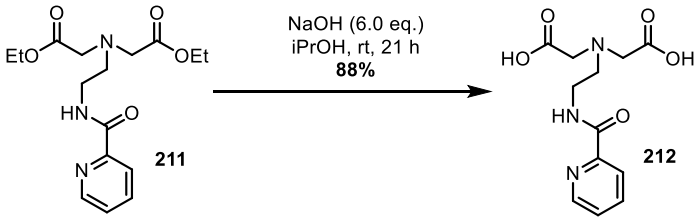
ν_{max}/cm^{-1} 3020, 1758, 1711, 1311, 1225, 1187, 1027, 843, 756, 701.

HRMS (ESI) Calcd. for $C_{16}H_{24}N_3O_5^+$ ([M+H]$^+$): 338.1716. Found: 338.1720.

^{1}H NMR (400 MHz, $CDCl_3$) δ 8.70 – 8.54 (m, 2H), 8.20 (dt, *J* = 7.9, 1.2 Hz, 1H), 7.84 (td, *J* = 7.8, 1.8 Hz, 1H), 7.42 (ddd, *J* = 7.6, 4.8, 1.2 Hz, 1H), 4.19 (q, *J* = 7.2 Hz, 4H), 3.62 (s, 4H), 3.57 (q, *J* = 5.8 Hz, 2H), 3.04 (t, *J* = 6.0 Hz, 2H), 1.27 (t, *J* = 7.2 Hz, 6H).

^{13}C NMR (101 MHz, $CDCl_3$) δ 171.4, 164.6, 150.2, 148.2, 137.1, 125.9, 122.2, 60.6, 55.4, 53.3, 37.6, 14.2.

2,2'-((2-(Picolinamido)ethyl)azanediyl)diacetic acid (212)



Diethyl ester **211** (11.0 g, 33 mmol) was dissolved in 2-propanol (32.6 mL) and 2M NaOH (98 mL, 196 mmol) added. The reaction was stirred at room temperature for 21 hours. $BaCl_2.H_2O$ (8.35 g, 34 mmol) was dissolved in H_2O (32.6 mL) at 95 °C. The reaction mixture was heated to 95 °C and the $BaCl_2$ solution added dropwise, forming an off-white precipitate. The suspension was allowed to cool to room temperature over 15 minutes, before the precipitate was collected *via* vacuum filtration. The resulting solid was dried under high-vacuum at 80 °C overnight, weighed, suspended in H_2O (75 mL) and heated to 110 °C. 5M H_2SO_4 (1.95 eq. with respect to the vacuum-dried barium chelate) was then added dropwise, causing the solution to effervesce. The suspension was kept at 110 °C for 15 minutes, allowed to cool for 5 minutes then filtered through celite. The aqueous filtrate was concentrated under vacuum to yield the crude title compound **212** as a pale yellow solid (8.02 g, 88%).

The compound decomposed at high temperature before a melting point could be recorded.

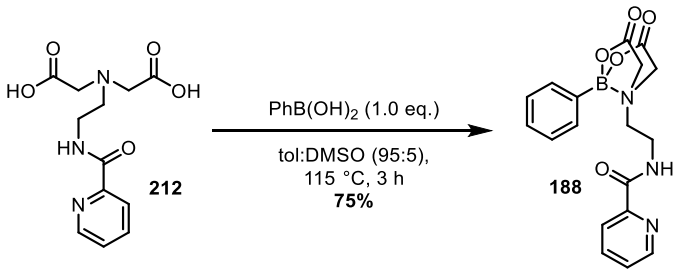
ν_{max}/cm^{-1} 3400, 1740, 1619, 1530, 1082, 1048, 977, 669.

HRMS (ESI) Calcd. for $C_{12}H_{16}N_3O_5^+$ ([M+H]$^+$): 282.1090. Found: 282.1081.

^{1}H NMR (400 MHz, D_2O) δ 8.58 (d, *J* = 4.8 Hz, 1H), 7.99 (d, *J* = 7.3 Hz, 2H), 7.66 – 7.53 (m, 1H), 3.84 (s, 4H), 3.78 (t, *J* = 5.6 Hz, 2H), 3.47 (t, *J* = 5.6 Hz, 2H).

^{13}C NMR (101 MHz, D_2O) δ 170.2, 168.1, 148.7, 148.2, 138.8, 127.6, 122.8, 57.3, 55.7, 35.0.

Phenylboronic acid IDA-PA ester (188)



Dicarboxylic acid **212** (1.36 g, 4.80 mmol) and phenylboronic acid (0.59 g, 4.80 mmol) were suspended in toluene (20 mL + 5% v/v DMSO) and heated to 116 °C with Dean-Stark apparatus for 3 hours. The reaction mixture was concentrated *in vacuo*, MeCN (10 mL) added and the mixture dry loaded onto silica. The column was flushed with copious Et_2O before being eluted with Et_2O:MeCN (1:1). The Et_2O:MeCN fraction was collected and concentrated under vacuum to give the title compound **188** as a white solid (1.33 g, 75 %).

The compound decomposed at high temperature before a melting point could be recorded. ν_{max}/cm^{-1} 3345, 1741, 1673, 1530, 1292, 1224, 1047, 986, 850, 752, 704.

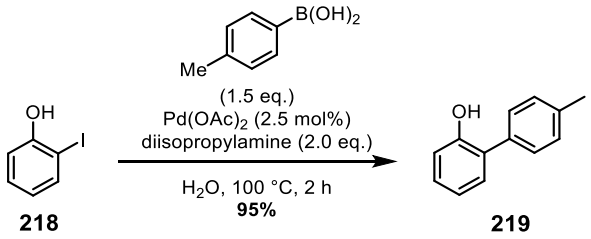
HRMS (ESI) Calcd. for $C_{18}H_{19}BN_3O_5^+$ ([M+H]$^+$): 368.1412. Found: 368.1413.

^{1}H NMR (400 MHz, CD_3CN) δ 8.59 (dt, *J* = 4.8, 1.2 Hz, 1H), 8.32 (br. d, *J* = 6.7 Hz, 1H), 8.08 (dt, *J* = 7.8, 1.1 Hz, 1H), 7.95 (td, *J* = 7.7, 1.7 Hz, 1H), 7.59 – 7.48 (m, 3H), 7.46 – 7.35 (m, 3H), 4.22 (d, *J* = 17.1 Hz, 2H), 4.07 (d, *J* = 17.1 Hz, 2H), 3.65 (q, *J* = 6.5 Hz, 2H), 2.80 (t, *J* = 6.6 Hz, 2H).

^{13}C NMR (101 MHz, CD_3CN) δ 168.6, 164.8, 149.3, 148.6, 137.7, 132.6, 129.4, 1278.0, 126.8, 121.9, 58.7, 57.5, 34.5.

^{11}B NMR (128 MHz, CD_3CN) δ 12.1.

4'-Methyl-[1,1'-biphenyl]-2-ol (219)



A one dram vial was charged with 2-iodophenol (220 mg, 1.0 mmol), *p*-tolylboronic acid (204 mg, 1.5 mmol), $Pd(OAc)_2$ (0.6 mg, 0.0025 mmol), diisopropylamine (0.280 mL, 2 mmol) and H_2O (2 mL). The resulting suspension was refluxed at 100 °C for 2 hours before being allowed to cool to room temperature. The reaction mixture was diluted with brine (2 mL) and further H_2O (6 mL) before being extracted with CH_2CL_2 (3 × 10 mL). The combined organic layers were dried over $MgSO_4$, filtered and concentrated *in vacuo*. The residue was purified *via* FCC (20:1 petroleum ether:EtOAc) to afford the title compound **219** as a clear oil (174 mg, 95%).

ν_{max}/cm^{-1} 3532, 1481, 1448, 1176, 818, 751.

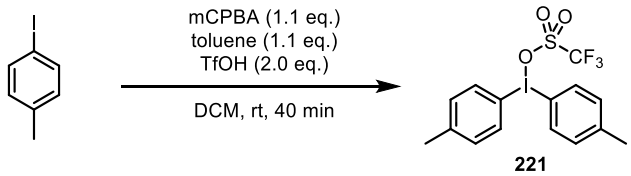
HRMS (ESI) Calcd. for $C_{13}H_{13}O^+$ ([M+H]$^+$): 185.0961. Found: 185.0961.

^{1}H NMR (400 MHz, $CDCl_3$) δ 7.41 – 7.37 (m, 2H), 7.33 (d, J = 8.1 Hz, 2H), 7.31 – 7.24 (m, 2H), 7.07 – 6.96 (m, 2H), 5.24 (s, 1H), 2.45 (s, 3H).

^{13}C NMR (101 MHz, $CDCl_3$) δ 152.6, 137.7, 134.2, 130.3, 130.0, 129.0, 129.0, 128.2, 120.9, 115.8, 21.3.

*The spectroscopic properties of the compound were consistent with the data pertaining to it in the literature (*S. Duan *et al. Chem. Commun.* 2016, **52**, 10529*).*

Bis(4-methylphenyl)iodonium trifluoromethanesulfonate (221)



221

A 100 mL round-bottom flask was charged with 4-iodotoluene (981 mg, 4.5 mmol) and *m*CPBA (855 mg, 4.95 mmol) under a nitrogen atmosphere. Anhydrous CH_2Cl_2 (21 mL) and anhydrous toluene (528 µL, 4.95 mmol) were added, then trifluromethanesulfonic acid (795 µL, 9.0 mmol) added dropwise over 5 minutes. The resulting dark brown solution was stirred at room temperature for 35 minutes before being concentrated under vacuum. Et_2O (70 mL) was added to the residue, with vigorous stirring, to induce precipitation. The suspension was then cooled to -20 °C to induce further precipitation. The solid formed was collected *via* vacuum filtration, washed with ice cold Et_2O and dried to yield the product **221** as a fine silver solid (1.03 g, 50 %).

ν_{max}/cm^{-1} 1241, 1224, 1149, 1021, 799.

HRMS (ESI) Calcd. for $C_{14}H_{14}I$ ([M]$^+$): 309.0140. Found: 309.0147.

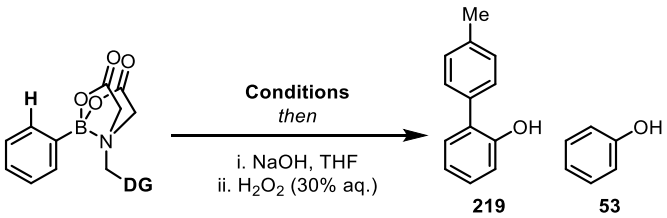
^{1}H NMR (400 MHz, DMSO-d_6) δ 8.25 (d, J = 8.3 Hz, 4H), 7.49 (d, J = 8.0 Hz, 4H), 2.50 (s, 6H).

^{13}C NMR (101 MHz, DMSO-d_6) δ 142.9, 135.5, 132.8, 113.4, 21.3.

^{19}F NMR (377 MHz, DMSO-d_6) δ -77.76.

*The spectroscopic properties of the compound were consistent with the data pertaining to it in the literature (*J. Perez *et al. RSC Adv.* 2016, **6**, 36932*).*

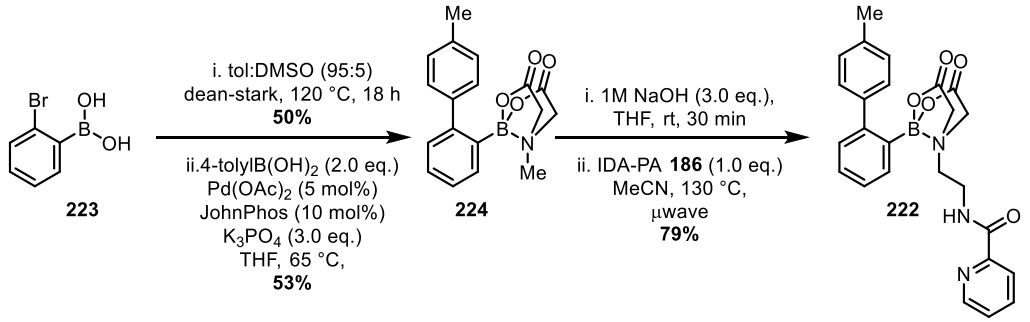
General C–H functionalization and deprotection-oxidation procedure



219 **53**

The boronic acid (IDA-DG) ester (0.1 mmol), $Pd(OAc)_2$ (10 mol%), base (250 mol%), oxidant (150 mol%) and additive (20 mol%) were added to a one-dram vial, sealed and placed under an atmosphere of N_2. Anhydrous solvent (0.1 M) and dodecane (100 mol%) were then added before the vial was placed in a pre-heated dry-syn and stirred for the allotted time. The reaction mixture was allowed to cool before being diluted with THF (1 mL) and filtered through a cotton-wool plug. The vial was washed with THF (2 × 1 mL), the washes filtered through cotton-wool and the plug washed with further THF (2 × 2 mL). The combined fractions were diluted with THF (8 mL) before aq. NaOH (2M, 500 mol%) was added and the resulting solution stirred at room temperature for 1 hour. H_2O_2 (30 % aq., 2000 mol%) was subsequently added, the mixture stirred for 1 hour and a 0.5 mL sample taken and diluted with THF to a volume of 1 mL for GC.

N-(2-(8-(4'-methyl-[1,1'-biphenyl]-2-yl)-2,6-dioxotetrahydro-8H-4l4,8l4-[1,3,2]oxazaborolo[2,3-b][1,3,2]oxazaborol-4-yl)ethyl)picolinamide (222)



Compound **224** was synthesised according to the procedure outlined in *J. Am. Chem. Soc.* 2007, **129**, 6716. 2-Bromophenylboronic acid **223** (201 mg, 1.0 mmol) was employed to yield the corresponding 2-bromophenylboronic acid MIDA ester (157 mg, 0.50 mmol, 50%) as an off-white solid. This compound (64 mg, 0.2 mmol) was then employed to yield the biaryl compound **224** (34.5 mg, 0.11 mmol, 53%) as a white solid.

^{1}H NMR (400 MHz, Acetonitrile-d_3) δ 7.73 (dd, J = 7.2, 1.9 Hz, 1H), 7.44 – 7.34 (m, 2H), 7.16 (s, 4H), 7.14 – 7.10 (m, 1H), 3.74 (d, J = 16.9 Hz, 2H), 3.28 (d, J = 16.9 Hz, 2H), 2.43 (s, 3H), 2.35 (s, 3H).

^{13}C NMR (101 MHz, Acetonitrile-d_3) δ 168.8, 148.8, 141.8, 137.4, 135.2, 132.0, 130.5, 129.9, 129.4, 127.6, 63.5, 48.5, 21.2.

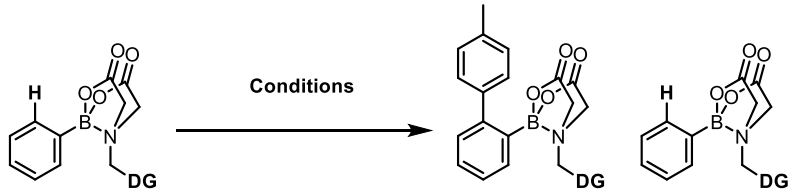
^{11}B NMR (128 MHz, Acetonitrile-d_3) δ 12.1.

*The characterisation data for **224** was in agreement with that pertaining to it within the literature*.

The biaryl compound **224** (27.4 mg, 0.09 mmol) was dissolved in THF (10 mL), NaOH (1 M, aq. 0.26 mL) added and the resulting mixture was stirred for 30 minutes at room temperature. After this time, the reaction was acidified with HCl (1 M, aq. 10 mL) and extracted with Et2O (3 × 10 mL). The combined organic phases were dried over MgSO4, filtered and concentrated to give an

off-white solid (20 mg). A microwave vial was charged with the crude material, deuterated MeCN-d_3 (1 mL) and IDA-PA **212** (28.1 mg, 0.1 mmol). The vial was sealed and irradiated to 130 °C for 15 minutes. After cooling, an NMR was taken of the reaction mixture to elucidate the 1H peaks of the diasterotopic protons alpha to the MIDA carboxylic acid functional groups. These were identified as appearing at 4.08 ppm and 3.45 ppm, with *J* values both of 17 Hz. The product **222** was not isolated.

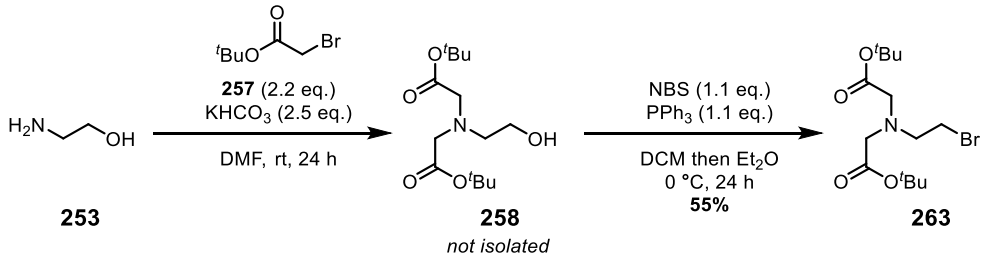
General C–H functionalization and 'catch and release' procedure



The boronic acid (IDA-DG) ester (0.1 mmol), $Pd(OAc)_2$ (10 mol%), base (250 mol%), oxidant (150 mol%) and additive (20 mol%) were added to a one-dram vial, sealed and placed under an atmosphere of N_2. Anhydrous solvent (0.1 M) was then added before the vial was placed in a pre-heated dry-syn and stirred for the allotted time. The reaction mixture was allowed to cool before being diluted with MeCN (1 mL) and filtered through celite. The vial was washed with MeCN (3 × 1 mL), the washes filtered through celite and the filter pad washed with further MeCN (3 mL). To the combined filtrates was added silica and the solvent removed under vacuum. The dry-loaded compound was added to a small silica column, washed with copious Et_2O and eluted using MeCN:Et_2O (1:1). The MeCN:Et_2O fraction was concentrated *in vacuo*, redissolved in MeCN-d_3 and an NMR taken.

Chapter 3

Di-*tert*-butyl 2,2'-((2-bromoethyl)azanediyl)diacetate (263)



$NaHCO_3$ (7.68 g, 76.8 mmol) was placed under an atmosphere of N_2, anhydrous DMF (50 mL) and *tert*-butyl bromoacetate **257** (10.2 mL, 69.2 mmol) added and the resulting suspension cooled to 0 °C. Ethanolamine (1.85 mL, 30.7 mmol) was added dropwise over a 5 minute period and the mixture stirred for 30 minutes at 0 °C before warming to room temperature and stirring for 18 hours. The reaction mixture was partitioned between Et_2O (150 mL) and sat. aq. $NaHCO_3$ (100

mL) and the layers separated. The organic fraction was further washed with sat. aq. $NaHCO_3$ (100 mL), before the combined aqueous phases were extracted with Et_2O (100 mL). The combined organic phases were washed with brine (100 mL), dried over $MgSO_4$, filtered and concentrated *in vacuo* to yield the crude product as a yellow oil.

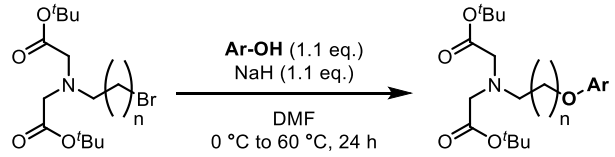
The crude product was dissolved in DCM (100 mL), PPh_3 (8.87 g, 33.8 mmol) added and the solution cooled to 0 °C. NBS (6.00 g, 33.8 mmol) was then added in portions over 10 minutes and the reaction mixture stirred at 0 °C for 1.5 hours. The solution was concentrated to an oil under vacuum, triturated with Et_2O and the precipitated $OPPh_3$ removed via filtration through silica. The filtrate was concentrated and purified *via* FCC (10% Et_2O in hexane) to yield the desired product **263** as a clear oil (5.91 g, 16.8 mmol, 55%).

^{1}H NMR (400 MHz, Chloroform-*d*) δ 3.47 (s, 4H), 3.42 (t, *J* z= 7.4 Hz, 2H), 3.12 (t, *J* = 7.4 Hz, 2H), 1.46 (s, 18H).

^{13}C NMR (101 MHz, Chloroform-*d*) δ 170.4, 81.2, 56.7, 56.5, 30.2, 28.1.

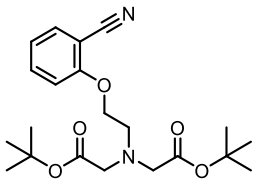
The spectroscopic properties of the compound were consistent with the data pertaining to it in the literature (*J. Org. Chem.* 1993, 58, 1151-1158).

General Procedure A for Alkylation with Phenolic Compounds



The appropriate phenol (1.1 eq.) was placed under an inert atmosphere, dissolved in anhydrous DMF (6.6 M) and cooled to 0 °C. Sodium hydride (60% in mineral oil, 1.2 eq.) was then added in portions over 5 minutes. The mixture was stirred for 30 minutes at 0 °C before the appropriate alkyl bromide (1 eq.) was added dropwise and the solution heated to 60 °C for 16 hours. The reaction was cooled to room temperature and slowly quenched with sat. aq. $NaHCO_3$ (1 mL). The reaction mixture was partitioned between Et_2O and sat. aq. $NaHCO_3$ and the layers separated. The organic fraction was further washed with sat. aq. $NaHCO_3$, before the combined aqueous phases were extracted with Et_2O. The combined organic phases were washed with brine, dried over $MgSO_4$, filtered and concentrated *in vacuo* to yield the desired product. Further purification *via* FCC was performed using Et_2O and hexanes if required.

Di-*tert*-butyl 2,2'-((3-(2-cyanophenoxy)propyl)azanediyl)diacetate (267)



General Procedure A: 2-cyanophenol (1.47 g, 4.00 mmol) was employed to obtain the desired product **267** which was isolated as a clear oil (1.43 g, 3.7 mmol, 92 %).

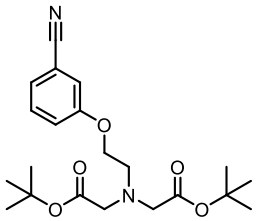
ν_{max}/cm^{-1} 2226, 1727, 1597, 1490, 1448, 1366, 1288, 1140, 752

HRMS (ES+ TOF) Calcd. for $C_{21}H_{31}N_2O_5$ ([M+H]$^+$): 391.2240. Found: 391.2228

^{1}H NMR (400 MHz, Chloroform-*d*) δ 7.60 – 7.48 (m, 2H), 7.05 – 6.95 (m, 2H), 4.27 (t, *J* = 5.8 Hz, 2H), 3.61 (s, 4H), 3.24 (t, *J* = 5.8 Hz, 2H), 1.47 (s, 18H).

^{13}C NMR (101 MHz, Chloroform-*d*) δ 170.88, 160.57, 134.28, 133.67, 120.72, 116.45, 112.21, 102.04, 81.15, 69.12, 57.35, 53.16, 28.15.

Di-*tert*-butyl 2,2'-((3-(3-cyanophenoxy)propyl)azanediyl)diacetate (268)



General procedure A: 3-Cyanophenol (578 mg, 2.00 mmol) was employed to obtain the desired product, which was isolated as a yellow oil (558 mg, 1.43 mmol, 71%).

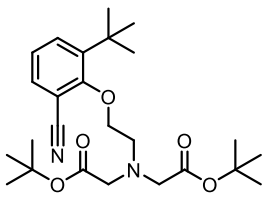
ν_{max}/cm^{-1} 2230, 1734, 1580, 1431, 1181, 1136, 793, 679

HRMS (ES+ TOF) Calcd. for $C_{21}H_{31}N_2O_5$ ([M+H]$^+$): 391.2240. Found: 391.2233

^{1}H NMR (400 MHz, Chloroform-*d*) δ 7.38 (ddd, *J* = 8.2, 7.6, 0.7 Hz, 1H), 7.25 (dt, *J* = 7.6, 1.2 Hz, 1H), 7.19 – 7.13 (m, 2H), 4.16 (t, *J* = 5.6 Hz, 2H), 3.57 (s, 4H), 3.20 (t, *J* = 5.6 Hz, 2H), 1.48 (s, 18H).

^{13}C NMR (101 MHz, Chloroform-*d*) δ 170.7, 158.9, 130.3, 124.5, 119.7, 118.7, 117.7, 113.2, 81.2, 68.1, 57.1, 52.9, 28.2.

Di-*tert*-butyl 2,2'-((3-(2-(*tert*-butyl)-6-cyanophenoxy)propyl)azanediyl)diacetate (269)



General procedure A: 2-Cyano-6-*tert*-butylphenol (530 mg, 3.03 mmol), synthesised using the literature procedure (*J. Org. Chem.* 2015, 80, 2, 1229-1234), was employed to obtain the desired product, which was isolated as a yellow oil (1.10 g, 2.47 mmol, 82%).

ν_{max}/cm^{-1} 2227, 1731, 1431, 1367, 1220, 1145, 988

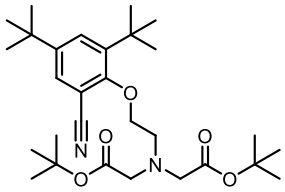
HRMS (ES+ TOF) Calcd. for $C_{25}H_{39}N_2O_5$ ([M+H]$^+$): 447.2859. Found: 447.2874

^{1}H NMR (400 MHz, Chloroform-*d*) δ 7.55 (ddd, *J* = 8.0, 1.8, 0.8 Hz, 1H), 7.46 (ddd, *J* = 7.6, 1.7, 0.8 Hz, 1H), 7.07 (td, *J* = 7.8, 0.8 Hz, 1H), 4.41 (td, *J* = 6.6, 0.8 Hz, 2H), 3.60 (d, *J* = 0.8 Hz, 4H), 3.35 (t, *J*

= 6.5 Hz, 2H), 1.48 (d, *J* = 0.9 Hz, 18H), 1.40 (d, *J* = 0.8 Hz, 9H). The NMR spectra contains THF and Et_2O impurities.

^{13}C NMR (101 MHz, Chloroform-*d*) δ 170.7, 161.1, 143.9, 132.2, 132.0, 123.3, 117.7, 106.4, 81.0, 73.5, 56.7, 54.1, 35.2, 30.4, 28.2. The NMR spectra contains THF and Et_2O impurities.

Di-*tert*-butyl 2,2'-((3-(2,4-di-*tert*-butyl-6-cyanophenoxy)propyl)azanediyl)diacetate (270)



General procedure A: 2-Cyano-3,6-di-*tert*-butylphenol (231 mg, 1.00 mmol), synthesised using literature procedure (*J. Org. Chem.* 2015, 80, 2, 1229-1234), was employed to obtain the desired product, which was isolated as a yellow oil (450 mg, 0.90 mmol, 90%).

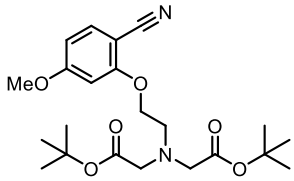
ν_{max}/cm^{-1} 2226, 1732, 1440, 1366, 1221, 1145, 988

HRMS (ES+ TOF) Calcd. for $C_{29}H_{47}N_2O_5$ ($[M+H]^+$): 503.3485. Found: 503.3498

^1H NMR (400 MHz, Chloroform-*d*) δ 7.56 (d, *J* = 2.5 Hz, 1H), 7.43 (d, *J* = 2.5 Hz, 1H), 4.38 (t, *J* = 6.5 Hz, 2H), 3.60 (s, 4H), 3.33 (t, *J* = 6.5 Hz, 2H), 1.48 (s, 18H), 1.40 (s, 9H), 1.31 (d, *J* = 1.9 Hz, 9H).

^{13}C NMR (101 MHz, Chloroform-*d*) δ 170.7, 158.7, 146.0, 129.4, 128.8, 118.2, 105.7, 81.0, 73.4, 56.6, 54.1, 35.4, 31.2, 31.2, 30.5, 29.4, 28.2.

Di-*tert*-butyl 2,2'-((3-(2-cyano-5-methoxyphenoxy)propyl)azanediyl)diacetate (271)



General procedure A: 2-Cyano-5-methoxyphenol (407 mg, 1.10 mmol), synthesised using the literature procedure (*J. Org. Chem.* 2015, 80, 2, 1229-1234), was employed to obtain the desired product, which was isolated as a yellow oil (412 mg, 0.98 mmol, 89%).

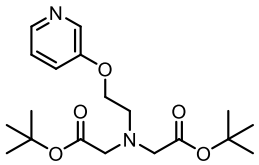
ν_{max}/cm^{-1} 2220, 1730, 1607, 1574, 1366, 1305, 1207, 1152, 1034

HRMS (ES + TOF) Calcd. for $C_{22}H_{33}N_2O_6$ ($[M+H]^+$): 421.2339. Found: 421.2339.

^1H NMR (400 MHz, Chloroform-*d*) δ 7.46 (dd, *J* = 8.4, 0.4 Hz, 1H), 6.55 – 6.50 (m, 2H), 4.24 (t, *J* = 5.9 Hz, 2H), 3.86 (s, 3H), 3.60 (s, 4H), 3.23 (t, *J* = 5.9 Hz, 2H), 1.47 (s, 18H).

^{13}C NMR (101 MHz, Chloroform-*d*) δ 170.9, 164.5, 162.3, 134.7, 116.9, 106.4, 99.0, 94.2, 81.2, 69.1, 57.3, 55.7, 53.1, 28.2.

Di-tert-butyl 2,2'-((2-(pyridin-3-yloxy)ethyl)azanediyl)diacetate (272)



General procedure A: 3-Hydroxypyridine (105 mg, 1.10 mmol) was employed to obtain the desired product, which was isolated as a yellow oil (271 mg, 0.74 mmol, 74%).

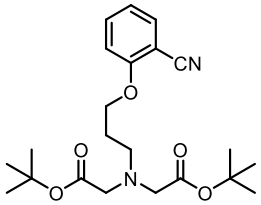
ν_{max}/cm^{-1} 2977, 1732, 1575, 1426, 1367, 1143, 1052, 1012, 707

HRMS (ES + TOF) Calcd. for $C_{19}H_{31}N_2O_5$ ([M+H]$^+$): 367.2233. Found: 367.2228.

^{1}H NMR (400 MHz, Chloroform-*d*) δ 8.33 (dd, *J* = 2.2, 1.4 Hz, 1H), 8.22 (dd, *J* = 3.4, 2.6 Hz, 1H), 7.24 – 7.20 (m, 2H), 4.19 (t, *J* = 5.7 Hz, 2H), 3.57 (s, 4H), 3.21 (t, *J* = 5.7 Hz, 2H), 1.47 (s, 18H).

^{13}C NMR (101 MHz, Chloroform-*d*) δ 170.7, 155.0, 142.1, 138.3, 123.7, 121.0, 81.1, 77.2, 57.1, 53.1, 28.2.

Di-tert-butyl 2,2'-((3-(2-cyanophenoxy)propyl)azanediyl)diacetate (273)



General procedure A: 2-Cyanophenol (131 mg, 1.10 mmol) was employed was employed to obtain the desired product, which was isolated as a yellow oil (339 mg, 0.84 mmol, 84%).

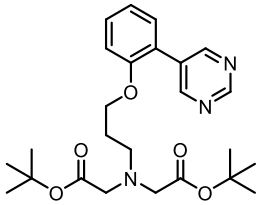
ν_{max}/cm^{-1} 2227, 1735, 1493, 1451, 1367, 1289, 1255, 1145, 755

HRMS (ES+ TOF) Calcd. for $C_{22}H_{33}N_2O_5$ ([M+H]$^+$): 405.2389. Found: 405.2392.

^{1}H NMR (400 MHz, Chloroform-*d*) δ 7.61 – 7.46 (m, 2H), 7.08 – 6.94 (m, 2H), 4.23 (t, *J* = 6.3 Hz, 2H), 3.46 (s, 4H), 2.95 (t, *J* = 6.7 Hz, 2H), 2.02 (p, *J* = 6.5 Hz, 2H), 1.47 (s, 18H).

^{13}C NMR (101 MHz, Chloroform-*d*) δ 170.7, 160.8, 134.3, 133.7, 120.5, 116.5, 112.5, 102.0, 81.1, 66.8, 56.2, 50.8, 28.2, 27.6.

Di-tert-butyl 2,2'-((3-(2-(pyrimidin-5-yl)phenoxy)propyl)azanediyl)diacetate (274)



General procedure A: 2-(pyridine-3-yl)phenol (189 mg, 1.10 mmol) (synthesised according to the literature procedure described in *Angew. Chem. Int. Ed.* 2017, 56, 3182) was employed was

employed to obtain the desired product, which was isolated as a yellow oil (394 mg, 0.86 mmol, 86%).

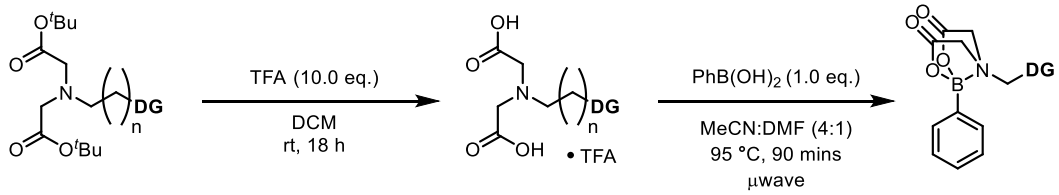
ν_{max}/cm^{-1} 2929, 1731, 1678, 1552, 1496, 1455, 1411, 1246, 1144, 752, 728

HRMS (ES+ TOF) Calcd. for $C_{25}H_{36}N_3O_5$ ([M+H]$^+$): 458.2655. Found: 458.2636.

^{1}H NMR (400 MHz, Chloroform-*d*) δ 9.16 (s, 1H), 8.93 (s, 2H), 7.41 (ddd, *J* = 8.3, 7.4, 1.7 Hz, 1H), 7.33 (dd, *J* = 7.8, 1.7 Hz, 1H), 7.09 (ddd, *J* = 8.4, 6.1, 1.1 Hz, 3H), 4.14 (t, *J* = 6.4 Hz, 2H), 3.40 (s, 4H), 2.81 (t, *J* = 6.8 Hz, 2H), 1.92 (p, *J* = 6.7 Hz, 2H), 1.45 (s, 20H).

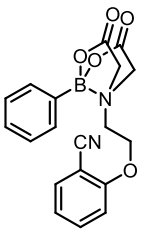
^{13}C NMR (101 MHz, Chloroform-*d*) δ 170.6, 156.8, 156.8, 156.0, 132.3, 130.5, 130.3, 130.2, 121.2, 112.6, 81.0, 77.2, 66.5, 56.1, 51.0, 28.1.

General Procedure B for *tert*-butyl deprotection and boronic acid condensation.



The appropriate di-*tert* butyl ester (1.0 eq.) was placed under an inert atmosphere and dissolved in anhydrous $CHCl_2$ (0.5 M) and trifluoroacetic acid (10 eq.) added dropwise. The resulting solution was stirred at room temperature for 18 hours. On completion, the solvent was removed under vacuum, with MeCN added to azeotrope any excess trifluoroacetic acid. The crude material was added to a microwave vial, redissolved in MeCN:DMF (4:1, 0.4 M), phenylboronic acid (1.0 eq.) added and the vial sealed. The reaction mixture was heated to 95 °C for 90 minutes using microwave irradiation on a high absorption setting. The resulting mixture was dry loaded directly onto silica and purified using FCC (EtOAc and hexanes) to yield the desired product.

2-(2-(2,6-Dioxo-8-phenyltetrahydro-8H-4l4,8l4-[1,3,2]oxazaborolo[2,3-b][1,3,2]oxazaborol-4-yl)ethoxy)benzonitrile (236)



General procedure B: Di-*tert*-butyl 2,2'-((3-(2-cyanophenoxy)propyl)azanediyl)diacetate (702 mg, 1.79 mmol) was employed to obtain the desired product, which was isolated as an off-white solid (648 mg, 1.78 mmol, 99%).

ν_{max}/cm^{-1} 2224, 1752, 1598, 1450, 1284, 1250, 1217, 1030, 998, 759.

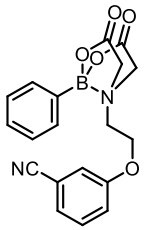
HRMS (ES+ TOF) Calcd. for $C_{19}H_{18}BN_2O_5$ ([M+H]$^+$): 365.1309. Found: 279.1029. This mass is in agreement with loss of the phenylboronic acid by fragmentation to reveal the iminodiacetic acid (Calculated mass for $C_{13}H_{15}N_2O_5$: 279.0981).

^{1}H NMR (400 MHz, Acetonitrile-d_3) δ 7.71 – 7.61 (m, 2H), 7.60 – 7.55 (m, 2H), 7.49 – 7.41 (m, 3H), 7.14 (td, *J* = 7.6, 0.9 Hz, 1H), 7.06 (dd, *J* = 8.6, 0.9 Hz, 1H), 4.38 – 4.29 (m, 4H), 4.14 (d, *J* = 17.3 Hz, 2H), 3.15 – 3.05 (m, 2H).

^{13}C NMR (101 MHz, Acetonitrile-d_3) δ 168.6, 159.5, 134.9, 133.7, 132.6, 129.5, 128.1, 121.9, 116.4, 112.4, 101.5, 63.9, 59.4, 57.0, 28.1.

^{11}B NMR (128 MHz, Acetonitrile-d_3) δ 12.3.

3-(2-(2,6-Dioxo-8-phenyltetrahydro-8H-4l4,8l4-[1,3,2]oxazaborolo[2,3-b][1,3,2]oxazaborol-4-yl)ethoxy)benzonitrile (242)



General procedure B: Di-*tert*-butyl 2,2'-((3-(3-cyanophenoxy)propyl)azanediyl)diacetate (514 mg, 1.31 mmol) was employed to obtain the desired product, which was isolated as a white solid (132 mg, 0.36 mmol, 28%).

ν_{max}/cm^{-1} 2228, 1757, 1576, 1433, 1286, 1250, 1222, 1040, 998, 703

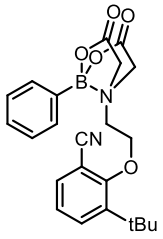
HRMS (ES- TOF) Calcd. for $C_{20}H_{18}BN_2O_7$ ([M-H]+HCO_2H): 409.1207. Found: 409.1220.

^{1}H NMR (400 MHz, Acetonitrile-d_3) δ 7.59 – 7.53 (m, 2H), 7.52 – 7.42 (m, 4H), 7.40 – 7.36 (m, 1H), 7.30 (dd, *J* = 2.6, 1.4 Hz, 1H), 7.24 (ddd, *J* = 8.4, 2.7, 1.0 Hz, 1H), 4.27 (d, *J* = 17.1 Hz, 2H), 4.25 – 4.21 (m, 2H), 4.06 (d, *J* = 17.2 Hz, 2H), 3.04 (dd, *J* = 5.4, 4.4 Hz, 2H).

^{13}C NMR (101 MHz, Acetonitrile-d_3) δ 168.6, 132.6, 130.7, 129.4, 128.1, 125.4, 119.9, 117.8, 113.3, 113.0, 63.5, 59.3, 57.2, 27.9.

^{11}B NMR (128 MHz, Acetonitrile-d_3) δ 12.1.

3-(*tert*-Butyl)-2-(2-(2,6-dioxo-8-phenyltetrahydro-8H-4l4,8l4-[1,3,2]oxazaborolo[2,3-b][1,3,2]oxazaborol-4-yl)ethoxy)benzonitrile (241)



General procedure B: Di-*tert*-butyl 2,2'-((3-(2-(*tert*-butyl)-6-cyanophenoxy)propyl)azanediyl) diacetate (334 mg, 0.75 mmol) was employed to obtain the desired product, which was isolated as a white solid (208 mg, 0.50 mmol, 66 %).

ν_{max}/cm^{-1} 2228, 1757, 1433, 1268, 1220, 1028, 995, 846, 752, 702

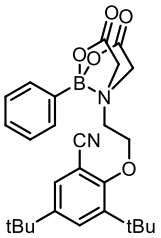
HRMS (ES- TOF) Calcd. for $C_{24}H_{26}N_2O_7B$ ([M-H]+HCO_2H): 465.1833. Found: 465.1842.

^{1}H NMR (400 MHz, Acetonitrile-d_3) δ 7.71 (d, *J* = 8.0 Hz, 1H), 7.65 – 7.56 (m, 3H), 7.45 (d, *J* = 6.1 Hz, 3H), 7.25 (t, *J* = 7.8 Hz, 1H), 4.44 – 4.34 (m, 4H), 4.25 (d, *J* = 17.2 Hz, 2H), 3.15 (t, *J* = 5.0 Hz, 2H), 1.34 (s, 9H).

^{13}C NMR (101 MHz, Acetonitrile-d_3) δ 168.5, 159.4, 150.9, 144.1, 133.2, 132.7, 132.4, 129.5, 128.1, 125.0, 117.9, 70.1, 59.6, 58.1, 34.9, 30.0.

^{11}B NMR (128 MHz, Acetonitrile-d_3) δ 12.4.

3,5-Di-*tert*-butyl-2-(2-(2,6-dioxo-8-phenyltetrahydro-8H-4l4,8l4-[1,3,2]oxazaborolo[2,3-b][1,3,2]oxazaborol-4-yl)ethoxy)benzonitrile (240)



General procedure B:

Di-*tert*-butyl 2,2'-((3-(2,4-di-*tert*-butyl-6-cyanophenoxy)propyl)azanediyl) diacetate (312 mg, 0.62 mmol) was employed to obtain the desired product, which was isolated as a white solid (174 mg, 0.37 mmol, 60 %).

ν_{max}/cm^{-1} 2227, 1761, 1435, 1223, 1030, 997, 846, 703

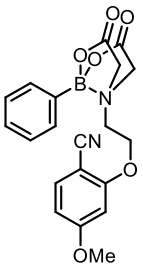
HRMS (ES- TOF) Calcd. for $C_{28}H_{34}BN_2O_7$ ([M-H]+HCO_2H): 521.2459. Found: 521.2476.

^{1}H NMR (400 MHz, Acetonitrile-d_3) δ 7.70 (d, *J* = 2.4 Hz, 1H), 7.62 (d, *J* = 2.5 Hz, 1H), 7.60 (m, 2H), 7.49 – 7.41 (m, 3H), 4.40 – 4.34 (m, 4H), 4.24 (d, *J* = 17.1 Hz, 2H), 3.13 (dd, *J* = 5.4, 4.4 Hz, 2H), 1.34 (s, 9H), 1.32 (s, 9H).

^{13}C NMR (101 MHz, Acetonitrile-d_3) δ 168.5, 157.1, 147.9, 143.2, 132.7, 130.4, 129.5, 129.1, 128.0, 118.1, 106.4, 69.9, 59.6, 58.1, 35.1, 34.5, 30.2, 30.0.

^{11}B NMR (128 MHz, Acetonitrile-d_3) δ 12.4.

2-(2-(2,6-Dioxo-8-phenyltetrahydro-8H-4l4,8l4-[1,3,2]oxazaborolo[2,3-b][1,3,2]oxazaborol-4-yl)ethoxy)-4-methoxybenzonitrile (243)



General procedure B:

Di-*tert*-butyl2,2'-((3-(2-cyano-5-methoxyphenoxy)propyl)azanediyl)diacetate (222 mg, 0.52 mmol) was employed to obtain the desired product, which was isolated as a crystalline white solid (206 mg, 0.52 mmol, 100%).

ν_{max}/cm^{-1} 2221, 1759, 1606, 1434, 1267, 1206, 1030, 999, 756, 705.

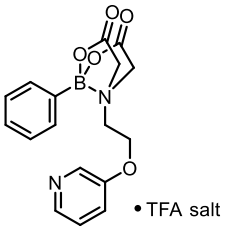
HRMS (ES- TOF) Calcd. for $C_{20}H_{18}N_2O_6B$ ([M-H]$^-$): 393.1258. Found: 393.1260.

^{1}H NMR (400 MHz, Acetonitrile-d_3) δ 7.62 – 7.54 (m, 3H), 7.48 – 7.41 (m, 3H), 6.68 (dd, *J* = 8.7, 2.2 Hz, 1H), 6.55 (d, *J* = 2.3 Hz, 1H), 4.34 – 4.27 (m, 4H), 4.13 (d, *J* = 17.3 Hz, 2H), 3.86 (s, 3H), 3.12 – 3.05 (m, 2H).

^{13}C NMR (101 MHz, Acetonitrile-d_3) δ 168.6, 164.8, 161.2, 134.9, 132.6, 129.5, 128.1, 116.7, 107.2, 99.3, 93.5, 65.3, 64.0, 59.4, 57.0, 55.8.

^{11}B NMR (128 MHz, Acetonitrile-d_3) δ 12.3.

8-Phenyl-4-(2-(pyridin-3-yloxy)ethyl)dihydro-4l4,8l4-[1,3,2]oxazaborolo[2,3-b][1,3,2]oxazaborole-2,6(3H,5H)-dione TFA salt (244)



General procedure B:

Di-tert-butyl 2,2'-((2-(pyridin-3-yloxy)ethyl)azanediyl)diacetate (256 mg, 0.70 mmol) was employed to obtain the desired product, which was isolated as a crystalline white solid (157 mg, 0.46 mmol, 66%).

ν_{max}/cm^{-1} 1761, 1669, 1599, 1250, 1224, 1180, 998, 1029, 998, 798

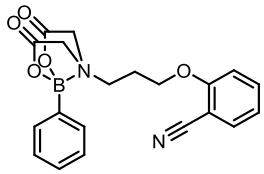
HRMS (ES+ TOF) Calcd. for $C_{17}H_{18}N_2O_5B$ ([M-H]$^-$): 341.1309. Found: 341.1319.

^{1}H NMR (400 MHz, DMSO-d_6) δ 8.36 (dd, *J* = 5.3, 2.8 Hz, 1H), 8.27 (dt, *J* = 5.5, 2.8 Hz, 1H), 7.59 – 7.29 (m, 7H), 4.61 – 4.22 (m, 6H), 3.07 (q, *J* = 5.2 Hz, 2H).

^{13}C NMR (101 MHz, DMSO-d_6) δ 169.7, 154.7, 141.8, 137.2, 134.5, 133.0, 129.5, 128.3, 125.1, 123.3, 64.1, 59.7, 57.5.

^{11}B NMR (128 MHz, DMSO-d_6) δ 12.4.

2-(3-(2,6-Dioxo-8-phenyltetrahydro-8H-4l4,8l4-[1,3,2]oxazaborolo[2,3-b][1,3,2]oxazaborol-4-yl)propoxy)benzonitrile (245)



General procedure B:

Di-tert-butyl 2,2'-((3-(2-cyanophenoxy)propyl)azanediyl)diacetate (332 mg, 0.82 mmol) was employed to obtain the desired product, which was isolated as a crystalline white solid (177 mg, 0.47 mmol, 57%).

ν_{max}/cm^{-1} 2223, 1763, 1595, 1475, 1438, 1224, 1041, 1022, 754, 704

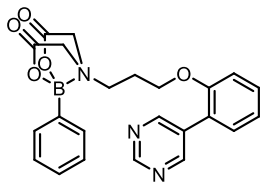
HRMS (ES+ TOF) Calcd. for $C_{20}H_{20}N_2O_5B$ ([M+H]$^+$): 379.1465. Found: 379.1481.

^{1}H NMR (400 MHz, Acetonitrile-d_3) δ 7.63 – 7.55 (m, 2H), 7.54 – 7.50 (m, 2H), 7.41 – 7.37 (m, 3H), 7.07 (td, J = 7.6, 0.9 Hz, 1H), 6.99 (dd, J = 8.6, 0.9 Hz, 1H), 4.09 (d, J = 17.1 Hz, 2H), 4.02 (d, J = 17.1 Hz, 2H), 3.97 (t, J = 6.2 Hz, 2H), 2.86 – 2.79 (m, 2H), 2.15 – 2.05 (m, 2H).

^{13}C NMR (101 MHz, Acetonitrile-d_3) δ 168.5, 159.9, 134.8, 133.7, 132.5, 129.3, 128.0, 121.3, 116.1, 112.8, 101.4, 65.8, 58.9, 55.9, 23.8.

^{11}B NMR (128 MHz, Acetonitrile-d_3) δ 11.8.

8-Phenyl-4-(3-(2-(pyrimidin-5-yl)phenoxy)propyl)dihydro-4l4,8l4-[1,3,2]oxazaborolo[2,3-b][1,3,2]oxazaborole-2,6(3H,5H)-dione (246)



General procedure B:

Di-tert-butyl 2,2'-((3-(2-(pyrimidin-5-yl)phenoxy)propyl)azanediyl)diacetate (348 mg, 0.76 mmol) was employed to obtain the desired product, which was isolated as a crystalline white solid (85 mg, 0.20 mmol, 26%). The absence of a TFA salt was confirmed using ^{19}F NMR.

ν_{max}/cm^{-1} 1762, 1499, 1411, 1282, 1224, 1044, 1021, 1002, 853, 759, 725, 701

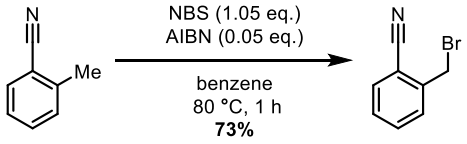
HRMS (ES+ TOF) Calcd. for $C_{23}H_{23}N_3O_5B$ ([M+H]$^+$): 432.1731. Found: 432.1728.

^{1}H NMR (400 MHz, Acetonitrile-d_3) δ 9.16 (s, 1H), 8.81 (s, 2H), 7.45 – 7.37 (m, 4H), 7.37 – 7.31 (m, 3H), 7.11 (td, *J* = 7.5, 1.0 Hz, 1H), 6.98 (dd, *J* = 8.1, 1.1 Hz, 1H), 3.97 (d, *J* = 17.1 Hz, 2H), 3.93 – 3.87 (m, 4H), 2.66 – 2.57 (m, 2H), 2.05 – 2.00 (m, 2H).

^{13}C NMR (101 MHz, Acetonitrile-d_3) δ 170.3, 168.5, 157.0, 156.6, 132.3, 130.6, 130.4, 129.2, 127.9, 123.3, 121.5, 112.4, 64.9, 58.7, 56.4, 23.7.

^{11}B NMR (128 MHz, Acetonitrile-d_3) δ 11.8.

2-(Bromomethyl)benzonitrile (276)



275 **276**

Compound **276** was synthesised using the procedure described in *Chem. Commun*., 2014, **50**, 9865-9868. A flask was charged with *N*-bromosuccinimide (934 mg, 5.25 mmol) and AIBN (41 mg, 0.25 mmol) and placed under a nitrogen atmosphere. 2-Methylbenzonitrile **275** (0.6 mL, 5 mmol) and benzene (5 mL) were added and the reaction mixture heated to 80 °C for 1 hour. The mixture was cooled to room temperature, quenched with water (10 mL) and extracted with Et_2O (3 × 10 mL). The combined organic phases were dried over $MgSO_4$, filtered and concentrated. The crude product was then purified via FCC (95:5 hexane:EtOAc) to yield the product **276** (721 mg, 3.7 mmol, 73%) as a white crystalline solid.

ν_{max}/cm^{-1} 2222, 1485, 1449, 1228, 1215, 763, 746

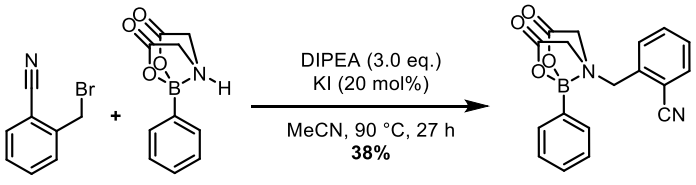
HRMS (ES- TOF) Calcd. for C_8H_5NBr ([M-H]$^-$): 193.9605. Found: 193.9610.

^{1}H NMR (400 MHz, Chloroform-*d*) δ 7.69 (dd, *J* = 7.7, 1.3 Hz, 1H), 7.65 – 7.56 (m, 2H), 7.44 (td, *J* = 7.5, 1.6 Hz, 1H), 4.66 (s, 2H).

^{13}C NMR (101 MHz, Chloroform-*d*) δ 141.2, 133.3, 133.2, 130.5, 128.9, 116.7, 112.5, 29.3.

The characterisation data was in agreement with that pertaining to it in the literature.

2-((2,6-Dioxo-8-phenyltetrahydro-8H-4l4,8l4-[1,3,2]oxazaborolo[2,3-b][1,3,2]oxazaborol-4-yl)methyl)benzonitrile (247)



276 **195** **247**

Phenylboronic acid IDA ester **195** (657 mg, 3.0 mmol), 2-(bromomethyl)benzonitrile **276** (588 mg, 3.0 mmol) and KI (99.6 mg, 0.6 mmol) were placed under a N_2 atmosphere and anhydrous

MeCN (30 mL) added. Anhydrous DIPEA (1.6 mL, 9.0 mmol) was subsequently added and the reaction mixture stirred at 90 °C for 48 hours. The solvent was removed under vacuum and the resulting residue purified *via* 'catch and release' purification. The resulting solid was recrystallised from hot MeCN to yield phenylboronic acid MIDA-DG ester **247** (377 mg, 1.1 mmol, 38%) as a white crystalline solid.

ν_{max}/cm^{-1} 2222, 1750, 1433, 1290, 1239, 1225, 1023, 1005, 984, 855, 760, 713

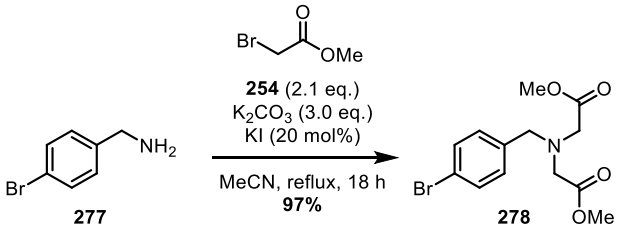
HRMS (ES- TOF) Calcd. for $C_{18}H_{14}O_4N_2B$ ([M-H]$^-$): 333.1047. Found: 333.1060.

^{1}H NMR (400 MHz, Acetonitrile-d_3) δ 7.86 (dd, *J* = 8.1, 1.4 Hz, 1H), 7.76 (td, *J* = 7.5, 1.5 Hz, 1H), 7.70 – 7.61 (m, 4H), 7.56 – 7.44 (m, 3H), 4.17 (d, *J* = 16.9 Hz, 2H), 3.94 (s, 2H), 3.86 (d, *J* = 17.0 Hz, 2H).

^{13}C NMR (101 MHz, Acetonitrile-d_3) δ 167.9, 134.1, 133.9, 133.2, 132.7, 131.8, 130.5, 129.7, 128.2, 127.9, 114.7, 59.1, 58.1.

^{11}B NMR (128 MHz, Acetonitrile-d_3) δ 12.0.

Dimethyl 2,2'-((4-bromobenzyl)azanediyl)diacetate (278)



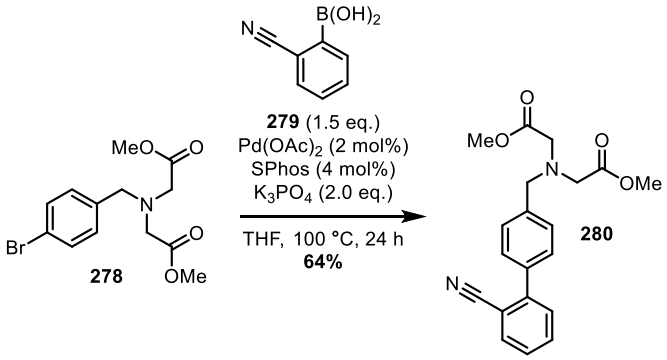
(4-bromophenyl)methanamine **277** (1.26 mL, 10 mmol) was added to a suspension of K_2CO_3 (4.14 g, 30 mmol) and KI (332 mg, 2.0 mmol) in anhydrous MeCN (10 mL) under a nitrogen atmosphere. Methyl bromoacetate (1.98 mL 21 mmol) was then added dropwise over 15 minutes and the reaction mixture heated to reflux (90 °C) for 18 hours. After being allowed to cool to room temperature, the suspension was diluted with H_2O (100 mL) and extracted with $CHCl_3$ (3 × 100 mL). The organic layers were combined, dried over $MgSO_4$, filtered and concentrated *in vacuo*. The resulting residue was purified *via* FCC (1:9 EtOAc:hexane) to yield the title compound **278** as a yellow oil (3.19 g, 9.66 mmol, 97 %).

HRMS (ES+ TOF) Calcd. for $C_{13}H_{17}O_4NBr$ ([M+H]$^+$): 330.0341. Found: 330.0340.

^{1}H NMR (400 MHz, Chloroform-*d*) δ 7.46 (d, *J* = 8.4 Hz, 2H), 7.31 – 7.27 (m, 2H), 3.88 (s, 2H), 3.72 (s, 6H), 3.56 (s, 4H).

^{13}C NMR (101 MHz, Chloroform-*d*) δ 171.48, 137.28, 131.52, 130.64, 121.26, 57.28, 53.98, 51.53.

Dimethyl 2,2'-(((2'-cyano-[1,1'-biphenyl]-4-yl)methyl)azanediyl)diacetate (280)



A microwave vial was charged with 2-cyanophenylboronic acid (992 mg, 6.75 mmol), $Pd(OAc)_2$ (20.3 mg, 0.09 mmol), sPhos (74 mg, 0.18 mmol) and K_3PO_4 (1.9 g, 9.0 mmol). The vial was placed under a nitrogen atmosphere and dimethyl 2,2'-((4-bromobenzyl)azanediyl)diacetate (1.49 g, 4.5 mmol) and anhydrous THF (9 mL) added before the vial was sealed and heated to 100 °C for 18 hours. The reaction was cooled to room temperature, dilute with water (50 mL) and extracted with DCM (3 × 50 mL). The organic phases were combined, dried over $MgSO_4$, filtered and concentrated under vacuum. The crude material was purified via FCC (7:1 EtOAc:hexane) to yield the desired compound **280** (1.01 g, 2.89 mmol, 64%) as a viscous yellow oil.

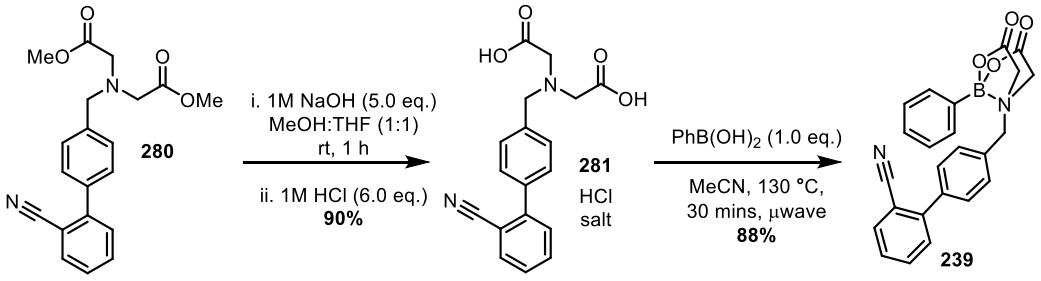
ν_{max}/cm^{-1} 2224, 1734, 1435, 1265, 1198, 1179, 1155, 1005, 732

HRMS (ES+ TOF) Calcd. for $C_{20}H_{21}O_4N_2$ ($[M+H]^+$): 353.1501. Found: 353.1511.

^1H NMR (400 MHz, Chloroform-*d*) δ 7.78 (ddd, *J* = 7.8, 1.4, 0.6 Hz, 1H), 7.66 (td, *J* = 7.7, 1.4 Hz, 1H), 7.54 (app. s, 5H), 7.46 (td, *J* = 7.6, 1.2 Hz, 1H), 4.01 (s, 2H), 3.74 (s, 6H), 3.63 (s, 4H).

^{13}C NMR (101 MHz, Chloroform-*d*) δ 171.6, 145.3, 139.0, 137.3, 133.8, 132.8, 130.1, 129.2, 128.8, 127.5, 118.7, 111.2, 57.7, 54.2, 51.6.

4'-((2,6-Dioxo-8-phenyltetrahydro-8H-4l4,8l4-[1,3,2]oxazaborolo[2,3-b][1,3,2]oxazaborol-4-yl)methyl)-[1,1'-biphenyl]-2-carbonitrile (239)



Dimethyl 2,2'-(((2'-cyano-[1,1'-biphenyl]-4-yl)methyl)azanediyl)diacetate **280** (943 mg, 2.7 mmol) was dissolved in MeOH:THF (1:1, 13.4 mL) and NaOH (1M, aq. 13.4 mL) added. The mixture was stirred for 2 hours until complete, then acidified with HCl (1M, aq. 16.0 mL). The solution was diluted with brine (50 mL) and extracted with copious EtOAc (3 × 250 mL). The

extracts were dried over $MgSO_4$, filtered and concentrated to yield the crude HCl salt **281** (781 mg, 2.41 mmol, 90%) which was directly used in the next reaction.

The diacid **281** (781 mg, 2.41 mmol) and phenylboronic acid (294 mg, 2.41 mmol) were suspended in MeCN (6 mL) in a microwave vial. The vial was sealed and irradiated at 130 °C for 30 minutes. The reaction mixture was dry loaded onto silica and purified via 'catch and release' purification, washing with copious Et_2O before eluting with Et_2O:MeCN (1:1), to yield the product **239** (869 mg, 2.12 mmol, 88%) as an off-white solid.

ν_{max}/cm^{-1} 2223, 1752, 1434, 1284, 1224, 1084, 1023, 1005, 988, 863, 846, 754, 702

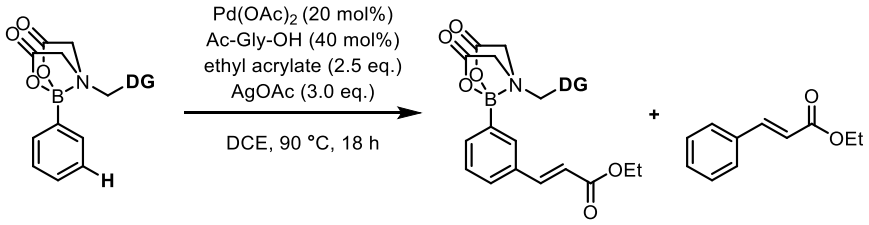
HRMS (ES+ TOF) Calcd. for $C_{24}H_{20}O_4N_2B$ ($[M+H]^+$): 411.1516. Found: 411.1529.

^1H NMR (400 MHz, Acetonitrile-d_3) δ 7.88 (dd, *J* = 8.1, 1.3 Hz, 1H), 7.76 (td, *J* = 7.8, 1.4 Hz, 1H), 7.70 – 7.64 (m, 4H), 7.60 – 7.53 (m, 4H), 7.48 (dt, *J* = 4.7, 1.6 Hz, 3H), 4.24 (d, *J* = 16.9 Hz, 2H), 3.82 (s, 2H), 3.75 (d, *J* = 16.9 Hz, 2H).

^{13}C NMR (101 MHz, Acetonitrile-d_3) δ 168.4, 143.8, 139.7, 133.9, 133.4, 132.9, 131.7, 130.6, 130.2, 129.5, 129.5, 128.4, 128.0, 118.4, 110.8, 61.0, 58.1.

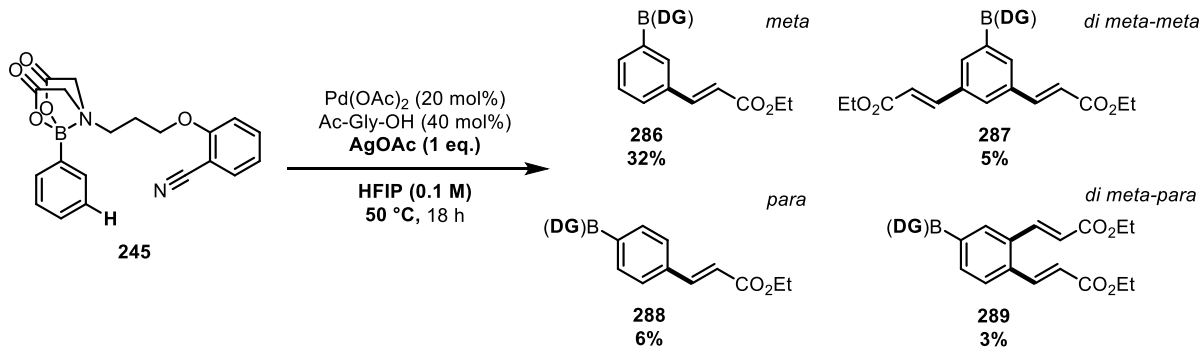
^{11}B NMR (128 MHz, Acetonitrile-d_3) δ 12.4.

General Procedure C for the Screening of Directing Groups against C–H alkenylation conditions



A 4 mL vial was charged with arylboronic acid MIDA-DG ester (0.05 mmol), AgOAc (3.0 eq.), Ac-Gly-OH (40 mol%) and $Pd(OAc)_2$ (20 mol%). The vial was then charged with anhydrous DCE (0.05 M) and the corresponding alkene coupling partner (2.5 eq.) was added. The vial was sealed and stirred at 90 °C for 18 hours. The reaction mixture was cooled to room temperature and CH_2Br_2 (1.0 eq.) added. An aliquot (approximately 0.1 mL) was taken, diluted with MeCN-d_3 (approximately 0.5 mL) and an NMR taken. The yield was determined by comparison of the alkene ^1H peak integrals with the CH_2Br_2 internal standard. NB: the internal standard was added after cooling to room temperature to prevent inaccuracies caused by loss of the internal standard during the reaction due to leakage from the vial.

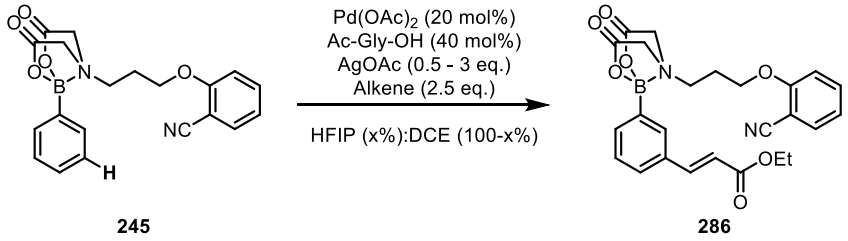
C–H Alkenylation of phenylboronic acid MIDA-DG ester 245 using HFIP as solvent



A 4 mL vial was charged with arylboronic acid MIDA-DG ester (0.1 mmol), AgOAc (1.0 eq.), Ac-Gly-OH (40 mol%) and $Pd(OAc)_2$ (20 mol%). The vial was then charged with HFIP (0.1 M) and the corresponding alkene coupling partner (2.5 eq.) was added. The vial was sealed and stirred at room temperature for 18 hours. The reaction mixture was diluted with MeCN (~5 mL) and dry loaded onto a silica column. The column was washed with copious Et_2O before the products were subsequently eluted with 1:1 MeCN:Et_2O. The eluent was concentrated under vacuum to yield the alkenylated products as an inseparable mixture of regio-isomers. The corresponding yields of each isomer were calculated using ^1H NMR analysis.

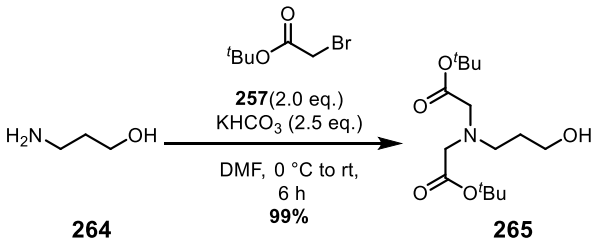
Chapter 4

General procedure D for DOE reaction screening



PhB(MIDA-DG) (0.05 mmol, 19 mg), $Pd(OAc)_2$ (X eq.), Ac-gly-OH (X eq.) and AgOAc (X eq.) were added to a one dram (4 mL) vial. Ethyl acrylate (2.5 eq., 14 µL), HFIP(:DCE) (1 mL) and CH_2Br_2 (internal standard, 1 eq., 3.5 mL) were then added and the vial sealed. The reaction mixture was added to a hot plate at the desired temperature and stirred for the desired time. On completion, a 0.1 mL aliquot was taken, diluted with MeCN-d_3, filtered and a ^1H NMR taken. The yield was calculated by comparison of integrals between the product and the CH_2Br_2 internal standard.

Di-*tert*-butyl 2,2'-((3-hydroxypropyl)azanediyl)diacetate (265)



To a suspension of $KHCO_3$ (25.0 g, 250 mmol) in anhydrous DMF (170 mL) under N_2, was added *tert*-butyl bromoacetate (29.5 mL, 200 mmol) at 0 °C. 3-Aminopropan-1-ol (8.1 mL, 100 mmol) was subsequently added dropwise, the suspension stirred for 30 minutes at 0 °C then allowed to warm to room temperature and stirred until no *tert*-butyl bromoacetate was visible *via* TLC (around 6 hours). The reaction mixture was diluted with Et_2O (500 mL) and sat. aq. $NaHCO_3$ (300 mL) and the layers separated. The organic layer was washed with further $NaHCO_3$ (300 mL), the combined aqueous layers extracted with Et_2O (300 mL) and the organic extracts combined. The combined organic layers were then washed with brine (300 mL), dried with $MgSO_4$, filtered and concentrated *in vacuo* to yield the desired product **265** as a clear oil (30.0 g, 99 mmol, 99%).

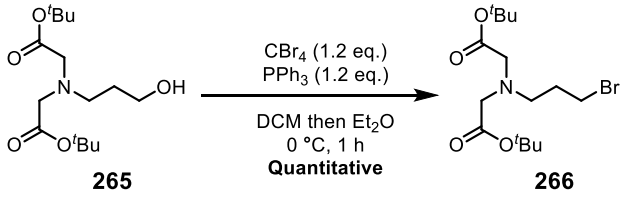
ν_{max}/cm^{-1} 3440, 2978, 2937, 1730, 1368, 1290, 1077, 1252, 1223, 1148, 1077, 846

HRMS (ES+ TOF) Calcd. for $C_{15}H_{30}NO_5$ ($[M+H]^+$): 304.2124. Found: 304.2126.

^1H NMR (400 MHz, Chloroform-*d*) δ 4.37 (s, 1H), 3.84 – 3.78 (m, 2H), 3.41 (s, 4H), 2.90 – 2.82 (m, 2H), 1.69 (dp, *J* = 10.3, 5.5 Hz, 2H), 1.49 (s, 18H).

^{13}C NMR (101 MHz, Chloroform-*d*) δ 170.5, 81.5, 62.1, 55.8, 51.9, 28.6, 28.1.

Di-*tert*-butyl 2,2'-((3-bromopropyl)azanediyl)diacetate (266)



To di-*tert*-butyl 2,2'-((3-hydroxypropyl)azanediyl)diacetate (30.0 g, 99 mmol) in anhydrous DCM (170 mL), under N_2, at 0 °C was added PPh_3 (31.3 g, 119 mmol). CBr_4 (39.5 g, 119 mmol) was then added slowly in portions over 15 minutes. The resulting solution was stirred at 0 °C for 1 hour, until TLC indicated complete conversion. Et_2O (1250 mL) was added slowly to the reaction mixture at 0 °C to induce precipitation of a white solid. The suspension was stirred at 0 °C for a further half an hour before the precipitate was removed by filtration through cotton wool and the filtrate concentrated under vacuum. The residue was redissolved in Et_2O (200 mL) and the suspension filtered through silica and concentrated. This process was then repeated again to

remove all remaining $OPPh_3$, yielding the desired product **266** as a clear oil (36.1 g, 99 mmol, 100%).

ν_{max}/cm^{-1} 2978, 2937, 1737, 1457, 1368, 1252, 1152, 842

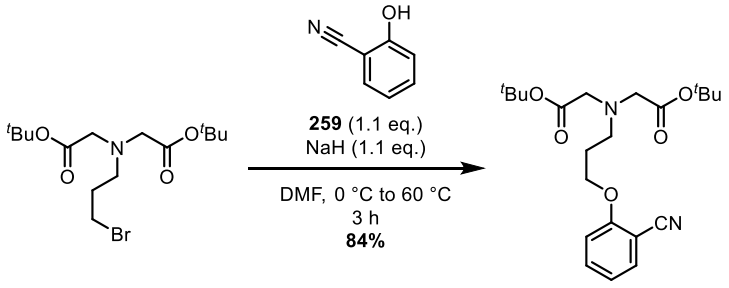
HRMS (ES+ TOF) Calcd. for $C_{15}H_{30}NO_5$ ($[M+H]^+$): 304.2124. Found: 304.2126.f

^1H NMR (400 MHz, Chloroform-*d*) δ 3.55 (t, *J* = 6.6 Hz, 2H), 3.45 (s, 4H), 2.88 (t, *J* = 6.8 Hz, 2H), 2.02 (p, *J* = 6.7 Hz, 2H), 1.49 (s, 18H).

^{13}C NMR (101 MHz, Chloroform-*d*) δ 170.7, 81.1, 56.3, 52.6, 31.8, 31.4, 28.2.

The spectroscopic properties of the compound were consistent with the data pertaining to it in the literature (*Bioorg. Med. Chem. Lett.* 2008, 18, 5233-5237).

Di-*tert*-butyl 2,2'-((3-(2-cyanophenoxy)propyl)azanediyl)diacetate (273)



266 **273**

To 2-cyanophenol (13.1 g, 110 mmol) in anhydrous DMF (500 mL) under N_2 at 0 °C was slowly added NaH (60% suspension in mineral oil) (4.4 g, 110 mmol) in small portions, causing effervescence. After addition, the reaction mixture was stirred for a further 30 minutes at 0 °C. To the suspension was added di-*tert*-butyl 2,2'-((3-bromopropyl)azanediyl)diacetate (13.1 g) as a solution in anhydrous DMF (120 mL). The reaction mixture was then heated to 60 °C and stirred for 3 hours. The reaction mixture was diluted with Et_2O (1500 mL) and sat. aq. $NaHCO_3$ (1000 mL) and the layers separated. The organic layer was washed with further $NaHCO_3$ (1000 mL), the combined aqueous layers extracted with Et_2O (1000 mL) and the organic extracts combined. The combined organic layers were then washed with brine (1500 mL), dried with $MgSO_4$, filtered and concentrated *in vacuo* to yield the desired product as a dark orange oil. The oil was dry loaded onto silica using DCM, and washed with hexanes to remove residual mineral oil. The product was then eluted using 40% EtOAc in hexane to yield the product **273** as a clear yellow oil (33.5 g, 82.8 mmol, 84%).

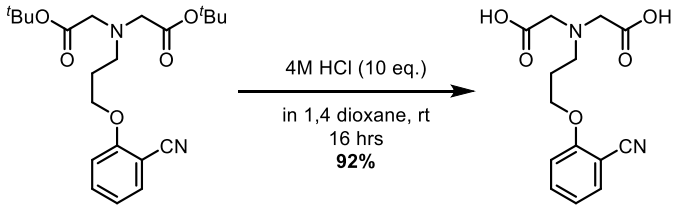
ν_{max}/cm^{-1} 2227, 1735, 1493, 1451, 1367, 1289, 1255, 1145, 755

HRMS (ES+ TOF) Calcd. for $C_{22}H_{33}N_2O_5$ ($[M+H]^+$): 405.2389. Found: 405.2392.

^1H NMR (400 MHz, Chloroform-*d*) δ 7.61 – 7.46 (m, 2H), 7.08 – 6.94 (m, 2H), 4.23 (t, *J* = 6.3 Hz, 2H), 3.46 (s, 4H), 2.95 (t, *J* = 6.7 Hz, 2H), 2.02 (p, *J* = 6.5 Hz, 2H), 1.47 (s, 18H).

^{13}C NMR (101 MHz, Chloroform-*d*) δ 170.7, 160.8, 134.3, 133.7, 120.5, 116.5, 112.5, 102.0, 81.1, 66.8, 56.2, 50.8, 28.2, 27.6.

2,2'-((3-(2-Cyanophenoxy)propyl)azanediyl)diacetic acid hydrochloride salt (290)



To di-*tert*-butyl 2,2'-((3-(2-cyanophenoxy)propyl)azanediyl)diacetate (16.0 g, 39.6 mmol) was added HCl in dioxane (3.7 – 4.3 N, 99 mL) and the reaction stirred overnight at room temperature under a nitrogen atmosphere. An off-white precipitate was observed forming after stirring for 24 hours, indicating completion of the reaction. The suspension was diluted with Et_2O (~ 500 mL) and cooled to 0 °C for 2 hours. After this time, the precipitate was collected using Buchner filtration under a stream of nitrogen, washing with copious Et_2O.

NB: The hydrochloride salt of the product is highly hygroscopic when wet. If a stream of nitrogen is not used, a brown gum will quickly form when drying under air.

The off-white solid was collected and further dried at 40 °C under high vacuum overnight, yielding the desired MIDA-DG hydrochloride salt **290** as an off white solid (11.9 g, 36.4 mmol, 92%).

ν_{max}/cm^{-1} 2229, 1733, 1599, 1495, 1450, 1416, 1379, 1290, 1200, 1118, 1081, 951, 872, 831, 757

HRMS (ES+ TOF) Calcd. for $C_{14}H_{17}N_2O_5$ ([M+H]$^+$): 293.1137. Found: 293.1142.

^{1}H NMR (400 MHz, DMSO-d_6) δ 7.75 – 7.70 (m, 1H), 7.67 (t, *J* = 7.9 Hz, 1H), 7.25 (d, *J* = 8.4 Hz, 1H), 7.10 (t, *J* = 7.4 Hz, 1H), 4.22 (t, *J* = 6.1 Hz, 2H), 4.10 (s, 4H), 3.34 (t, *J* = 7.7 Hz, 2H), 2.15 (t, *J* = 7.5 Hz, 2H).

^{13}C NMR (101 MHz, DMSO-d_6) δ 168.8, 160.3, 135.6, 134.2, 121.7, 116.7, 113.6, 101.1, 66.6, 54.6, 52.9, 24.5.

A small MeOH impurity is present in the NMR spectra.

2,2'-((3-(2-Cyanophenoxy)propyl)azanediyl)diacetic acid trifluoroacetic acid salt (290)

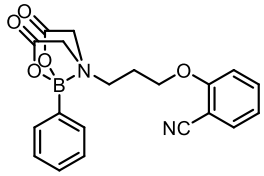
di-*tert*-butyl 2,2'-((3-(2-cyanophenoxy)propyl)azanediyl)diacetate (9.6 g, 23.8 mmol) was placed under an inert atmosphere and dissolved in anhydrous $CHCl_2$ (75 mL) and trifluoroacetic acid (13.6 mL, 10 eq.) added dropwise. The resulting solution was stirred at room temperature for 18 hours. On completion, the solvent was removed under vacuum, with MeCN added to azeotrope any excess trifluoroacetic acid, to yield the desired TFA salt **290** as a highly hygroscopic orange solid (8.9 g, 21.9 mmol, 92%).

^{1}H NMR (400 MHz, Acetonitrile-d_3) δ 7.69 – 7.62 (m, 2H), 7.18 – 7.08 (m, 2H), 4.25 (t, J = 5.7 Hz, 2H), 4.19 (s, 4H), 3.67 – 3.52 (m, 2H), 2.34 – 2.21 (m, 2H).

^{13}C NMR (101 MHz, Acetonitrile-d_3) δ 166.8, 159.9, 158.6, 134.9, 133.7, 121.5, 116.2, 114.2, 112.9, 101.5, 66.1, 55.0, 54.7, 23.7

^{19}F NMR (377 MHz, Acetonitrile-d_3) δ -76.7 (s).

Phenylboronic acid MIDA-DG ester (245)



Phenylboronic acid (363 mg, 3.00 mmol) and the MIDA-DG hydrochloric acid salt (984 mg, 3.00 mmol) were dissolved in MeCN (30 mL) and refluxed for 24 hours. The reaction mixture was cooled to room temperature, dry loaded onto silica and purified *via* FCC (75% EtOAc in hexane).The product was isolated as an off-white solid (1.06 g, 2.70 mmol, 90%).

ν_{max}/cm^{-1} 2223, 1763, 1595, 1475, 1438, 1224, 1041, 1022, 754, 704

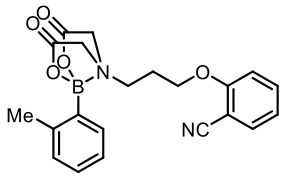
HRMS (ES+ TOF) Calcd. for $C_{20}H_{20}N_2O_5B$ ([M+H]$^+$): 379.1465. Found: 379.1481.

^{1}H NMR (400 MHz, Acetonitrile-d_3) δ 7.63 – 7.55 (m, 2H), 7.54 – 7.50 (m, 2H), 7.41 – 7.37 (m, 3H), 7.07 (td, J = 7.6, 0.9 Hz, 1H), 6.99 (dd, J = 8.6, 0.9 Hz, 1H), 4.09 (d, J = 17.1 Hz, 2H), 4.02 (d, J = 17.1 Hz, 2H), 3.97 (t, J = 6.2 Hz, 2H), 2.86 – 2.79 (m, 2H), 2.15 – 2.05 (m, 2H).

^{13}C NMR (101 MHz, Acetonitrile-d_3) δ 168.5, 159.9, 134.8, 133.7, 132.5, 129.3, 128.0, 121.3, 116.1, 112.8, 101.4, 65.8, 58.9, 55.9, 23.8.

^{11}B NMR (128 MHz, Acetonitrile-d_3) δ 11.8.

2-Methylphenylboronic acid MIDA-DG ester (294)



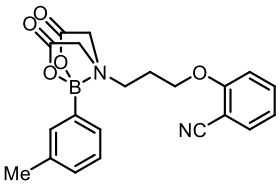
2-Methylphenylboronic acid (272 mg, 2.00 mmol) and the MIDA-DG trifluoracetic acid salt (812 mg, 2.00 mmol) were dissolved in MeCN (20 mL) and refluxed for 24 hours. The reaction mixture was cooled to room temperature, dry loaded onto silica and purified *via* FCC (75% EtOAc in hexane).The product was isolated as an off-white solid (685 mg, 1.70 mmol, 85%).

ν_{max}/cm^{-1} 2222, 1759, 1595, 1495, 1450, 1286, 1238, 1204, 1018, 857, 757.

HRMS (ES+ TOF) Calcd. For $C_{21}H_{21}BN_2O_5K$ ([M + K]$^+$): 431.1181. Found: 431.1183.

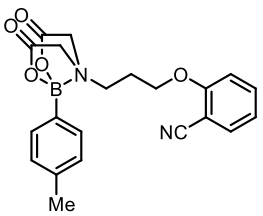
^{1}H NMR (400 MHz, Acetonitrile-d_3) δ 7.63 – 7.55 (m, 2H), 7.44 (dd, *J* = 7.5, 1.6 Hz, 1H), 7.28 (td, *J* = 7.5, 1.6 Hz, 1H), 7.23 – 7.15 (m, 2H), 7.07 (td, *J* = 7.6, 0.9 Hz, 1H), 7.02 – 6.98 (m, 1H), 4.09 (d, *J* = 17.2 Hz, 2H), 4.05 – 3.98 (m, 4H), 2.87 – 2.81 (m, 2H), 2.41 (s, 3H), 2.19 – 2.08 (m, 2H).
^{13}C NMR (101 MHz, Acetonitrile-d_3) δ 168.5, 159.9, 142.4, 134.8, 134.1, 133.7, 131.1, 129.4, 125.3, 121.3, 116.1, 112.7, 101.3, 65.7, 59.6, 55.9, 24.0, 22.2.
^{11}B NMR (128 MHz, Acetonitrile-d_3) δ 12.5.

3-Methylphenylboronic acid MIDA-DG ester (295)



3-Methylphenylboronic acid (476 mg, 3.50 mmol) and the MIDA-DG trifluoracetic acid salt (1.42 g, 3.50 mmol) were dissolved in MeCN (35 mL) and refluxed for 6 hours. The reaction mixture was cooled to room temperature, dry loaded onto silica and purified *via* FCC (washed with Et_2O then eluted with MeCN 50% in Et_2O).The product was isolated as a yellow crystalline solid (1.34 g, 3.38 mmol, 97%).
ν_{max}/cm^{-1} 2225, 1744, 1599, 1490, 1450, 1290, 1256, 1166, 1006, 864, 783, 753, 708.
HRMS (ES+ TOF) Calcd. For $C_{21}H_{21}BN_2O_5K$ ([M + K]$^+$): 431.1181. Found: 431.1178.
^{1}H NMR (400 MHz, Acetonitrile-d_3) δ 7.63 – 7.58 (m, 1H), 7.58 – 7.54 (m, 1H), 7.34 – 7.28 (m, 2H), 7.26 (td, *J* = 7.3, 0.7 Hz, 1H), 7.23 – 7.17 (m, 1H), 7.07 (td, *J* = 7.6, 0.9 Hz, 1H), 6.98 (dd, *J* = 8.6, 1.1 Hz, 1H), 4.08 (d, *J* = 17.1 Hz, 2H), 4.02 (d, *J* = 17.1 Hz, 2H), 3.97 (t, *J* = 6.2 Hz, 2H), 2.86 – 2.80 (m, 2H), 2.34 (s, *J* = 0.7 Hz, 3H), 2.15 – 2.05 (m, 2H).
^{13}C NMR (101 MHz, Acetonitrile-d_3) δ 168.6, 159.9, 137.4, 134.8, 133.7, 133.1, 130.0, 129.5, 127.9, 121.3, 116.1, 112.7, 101.4, 65.8, 58.9, 55.9.
^{11}B NMR (128 MHz, Acetonitrile-d_3) δ 11.8.

4-Methylphenylboronic acid MIDA-DG ester (296)



4-Methylphenylboronic acid (136 mg, 1.00 mmol) and the MIDA-DG trifluoracetic acid salt (406 mg, 1.00 mmol) were dissolved in MeCN (10 mL) and refluxed for 6 hours. The reaction mixture was cooled to room temperature, dry loaded onto silica and purified *via* FCC (washed with Et_2O

then eluted with MeCN 50% in Et_2O).The product was isolated as an off-white solid (329 mg, 0.84 mmol, 84%).

ν_{max}/cm^{-1} 2225, 1767, 1595, 1476, 1279, 1044, 943, 869, 813, 764.

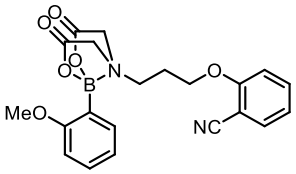
HRMS (ES+ TOF) Calcd. For $C_{21}H_{22}BN_2O_5$ ($[M+H]^+$): 393.1622. Found: 393.1639.

^1H NMR (400 MHz, Acetonitrile-d_3) δ 7.63 – 7.55 (m, 2H), 7.42 – 7.37 (m, 2H), 7.22 – 7.17 (m, 2H), 7.07 (td, *J* = 7.6, 0.9 Hz, 1H), 6.99 (d, *J* = 8.4 Hz, 1H), 4.07 (d, *J* = 17.1 Hz, 2H), 4.03 – 3.96 (m, 4H), 2.86 – 2.78 (m, 2H), 2.34 (s, 3H), 2.14 – 2.05 (m, 2H).

^{13}C NMR (101 MHz, Acetonitrile-d_3) δ 168.6, 159.7, 139.1, 134.8, 133.7, 132.5, 128.7, 121.3, 116.1, 112.8, 101.4, 65.8, 58.8, 55.9, 23.8.

^{11}B NMR (128 MHz, Acetonitrile-d_3) δ 12.0.

2-Methoxyphenylboronic acid MIDA-DG ester (291)



A microwave vial was charged with 2-methoxyphenylboronic acid (152 mg, 1.00 mmol), the MIDA-DG hydrochloric acid salt (328 mg, 1.00 mmol) and anhydrous MeCN (1 mL). The reaction mixture was irradiated in a microwave to 130 °C for 10 minutes before being allowed to cool to room temperature and concentrated *in vacuo*. To the resulting solid was added water (5 mL) and Et_2O (5 mL) and the suspension sonicated to cause trituration. After cooling to 0 °C, the resulting solid was collected, washed with ice cold water (2.5 mL) then ice cold Et_2O (2.5 mL) and air dried. The product was isolated as an off-white solid (188 mg, 0.46 mmol, 46%).

ν_{max}/cm^{-1} 2229, 1774, 1595, 1487,1453, 1316, 1230, 1029, 984, 749.

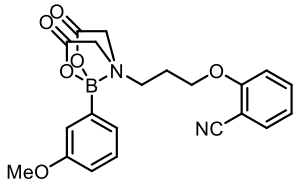
HRMS (ES+ TOF) Calcd. For $C_{21}H_{21}BN_2O_6K$ ($[M + K]^+$): 447.1130. Found: 447.1133.

^1H NMR (400 MHz, Acetonitrile-d_3) δ 7.62 – 7.53 (m, 3H), 7.40 – 7.31 (m, 1H), 7.06 (td, *J* = 7.6, 0.9 Hz, 1H), 6.98 – 6.92 (m, 3H), 4.15 (d, *J* = 16.9 Hz, 2H), 4.02 (d, *J* = 17.0 Hz, 2H), 3.98 (t, *J* = 6.1 Hz, 2H), 3.80 (s, 3H), 3.06 – 2.99 (m, 2H), 2.15 – 2.06 (m, 2H).

^{13}C NMR (101 MHz, Acetonitrile-d_3) δ 168.7, 162.3, 159.8, 134.8, 134.3, 133.7, 131.0, 121.2, 120.5, 116.1, 112.5, 110.3, 101.3, 65.8, 60.6, 55.6, 54.6, 23.8.

^{11}B NMR (128 MHz, Acetonitrile-d_3) δ 11.9.

3-Methoxyphenylboronic acid MIDA-DG ester (292)



A microwave vial was charged with 3-methoxyphenylboronic acid (152 mg, 1.00 mmol), the MIDA-DG hydrochloric acid salt (328 mg, 1.00 mmol) and anhydrous MeCN (1 mL). The reaction mixture was irradiated in a microwave to 130 °C for 10 minutes before being allowed to cool to room temperature and concentrated *in vacuo*. To the resulting solid was added water (5 mL) and Et_2O (5 mL) and the suspension sonicated to cause trituration. After cooling to 0 °C, the resulting solid was collected, washed with ice cold water (2.5 mL) then ice cold Et_2O (2.5 mL) and air dried. The product was isolated as an off-white solid (304 mg, 0.75 mmol, 75%).

ν_{max}/cm^{-1} 2229, 1748, 1599, 1494, 1454, 1416, 1293, 1264, 1021, 999, 790, 757, 708

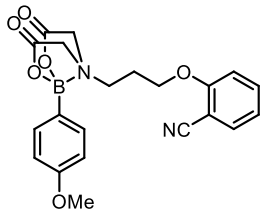
HRMS (ES+ TOF) Calcd. For $C_{21}H_{21}BN_2O_6K$ ([M + K]$^+$): 447.1130. Found: 447.1129.

^{1}H NMR (400 MHz, Acetonitrile-d_3) δ 7.63 – 7.54 (m, 2H), 7.31 (t, J = 7.7 Hz, 1H), 7.10 – 7.01 (m, 3H), 6.99 (d, J = 8.5 Hz, 1H), 6.94 (ddd, J = 8.2, 2.7, 1.0 Hz, 1H), 4.09 (d, J = 17.1 Hz, 2H), 4.05 – 3.97 (m, 4H), 3.80 (s, 3H), 2.88 – 2.81 (m, 2H), 2.17 – 2.04 (m, 2H).

^{13}C NMR (101 MHz, Acetonitrile-d_3) δ 168.5, 159.9, 159.4, 134.8, 133.7, 129.3, 124.6, 121.3, 116.1, 115.0, 112.8, 101.4, 65.8, 58.9, 55.9, 54.7, 23.8. One Ar-C peak obscured by solvent peak.

^{11}B NMR (128 MHz, Acetonitrile-d_3) δ 11.7.

4-Methoxyphenylboronic acid MIDA-DG ester (293)



A microwave vial was charged with 4-methoxyphenylboronic acid (152 mg, 1.00 mmol), the MIDA-DG hydrochloric acid salt (328 mg, 1.00 mmol) and anhydrous MeCN (1 mL). The reaction mixture was irradiated in a microwave to 130 °C for 10 minutes before being allowed to cool to room temperature and concentrated *in vacuo*. To the resulting solid was added water (5 mL) and Et_2O (5 mL) and the suspension sonicated to cause trituration. Unfortunately, trituration proved unsuccessful. The solvents were removed under a stream of nitrogen, the residue dissolved in MeCN (5 mL), dry loaded onto silica and purified by FCC (75% EtOAc in hexane). The product was isolated as a white crystalline solid (266 mg, 0.65 mmol, 65%).

ν_{max}/cm^{-1} 2225, 1748, 1602, 1513, 1450, 1290, 1219, 1179, 1018, 984, 861, 824, 757.

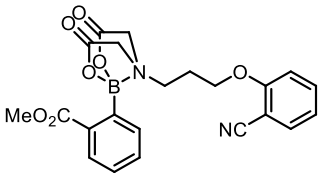
HRMS (ES+ TOF) Calcd. For $C_{21}H_{21}BN_2O_6K$ ([M + K]$^+$): 447.1130. Found: 447.1138.

^{1}H NMR (400 MHz, Acetonitrile-d_3) δ 7.63 – 7.54 (m, 2H), 7.45 – 7.40 (m, 2H), 7.07 (td, *J* = 7.6, 0.9 Hz, 1H), 7.00 (d, *J* = 8.5 Hz, 1H), 6.95 – 6.90 (m, 2H), 4.06 (d, *J* = 17.1 Hz, 2H), 4.02 – 3.96 (m, 4H), 3.79 (s, 3H), 2.86 – 2.78 (m, 2H), 2.14 – 2.04 (m, 2H).

^{13}C NMR (101 MHz, Acetonitrile-d_3) δ 168.5, 160.7, 159.9, 134.8, 133.9, 133.7, 121.3, 116.1, 113.5, 112.8, 101.4, 65.8, 58.8, 55.9, 54.7, 23.8.

^{11}B NMR (128 MHz, Acetonitrile-d_3) δ 12.0.

2-Methoxycarbonylphenylboronic acid MIDA-DG ester (297)



2-Methoxycarbonylphenylboronic acid (180 mg, 1.00 mmol) and the MIDA-DG hydrochloric acid salt (328 mg, 1.00 mmol) were dissolved in MeCN (10 mL) and refluxed for 16 hours. The reaction mixture was cooled to room temperature, dry loaded onto silica and purified *via* FCC (75% EtOAc in hexane). The product was isolated as a white crystalline solid (342 mg, 0.78 mmol, 78%).

ν_{max}/cm^{-1} 2225, 1756, 1715, 1595, 1491, 1450, 1290, 1260, 1197, 1133, 1006, 954, 865, 753

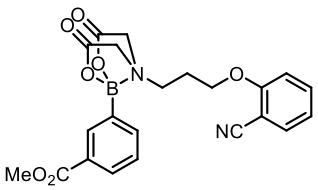
HRMS (ES+ TOF) Calcd. For $C_{22}H_{21}BN_2O_7Na$ ([M + Na]$^+$): 459.1340. Found: 459.1344.

^{1}H NMR (400 MHz, Acetonitrile-d_3) δ 7.69 (dd, *J* = 7.5, 1.4 Hz, 1H), 7.65 – 7.51 (m, 5H), 7.50 – 7.45 (m, 1H), 7.06 (tt, *J* = 7.6, 0.8 Hz, 1H), 7.00 (d, *J* = 8.5 Hz, 1H), 4.27 (d, *J* = 17.2 Hz, 2H), 4.06 – 3.99 (m, 5H), 3.82 (s, 4H), 3.19 (dd, *J* = 10.1, 6.1 Hz, 2H), 2.22 (dd, *J* = 9.9, 6.3 Hz, 2H).

^{13}C NMR (101 MHz, Acetonitrile-d_3) δ 171.40, 168.87, 159.83, 137.13, 134.75, 134.72, 133.70, 130.34, 129.14, 128.44, 121.25, 116.01, 112.73, 101.37, 65.81, 61.28, 57.89, 52.37, 24.21.

^{11}B NMR (128 MHz, Acetonitrile-d_3) δ 12.03.

3-Methoxycarbonylphenylboronic acid MIDA-DG ester (298)



3-Methoxycarbonylphenylboronic acid (180 mg, 1.00 mmol) and the MIDA-DG hydrochloric acid salt (328 mg, 1.00 mmol) were dissolved in anhydrous MeCN (10 mL) and refluxed for 16 hours. The reaction mixture was then concentrated *in vacuo*. To the resulting residue was added water (5 mL) and Et_2O (5 mL) and the suspension sonicated to cause trituration. After cooling to 0 °C,

the resulting solid was collected, washed with ice cold water (2.5 mL) then ice cold Et_2O (2.5 mL) and air dried. The product was isolated as an off-white solid (304 mg, 0.70 mmol, 70%).

ν_{max}/cm^{-1} 2229, 1767, 1707, 1599, 1495, 1446, 1290, 1215, 1006, 973, 865, 753, 705

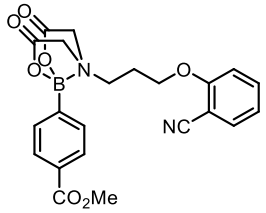
HRMS (ES+ TOF) Calcd. For $C_{22}H_{21}BN_2O_7Na$ ($[M + Na]^+$): 459.1340. Found: 459.1339.

^1H NMR (400 MHz, Acetonitrile-d_3) δ 8.13 (s, 1H), 8.01 (dt, *J* = 7.7, 1.5 Hz, 1H), 7.75 (dt, *J* = 7.5, 1.4 Hz, 1H), 7.61 – 7.47 (m, 3H), 7.06 (td, *J* = 7.6, 0.9 Hz, 1H), 6.97 (d, *J* = 8.5 Hz, 1H), 4.12 (d, *J* = 17.2 Hz, 2H), 4.05 (d, *J* = 17.2 Hz, 2H), 3.98 (t, *J* = 6.2 Hz, 2H), 3.89 (s, 3H), 2.87 – 2.78 (m, 2H), 2.15 – 2.05 (m, 2H).

^{13}C NMR (101 MHz, Acetonitrile-d_3) δ 168.4, 166.9, 159.8, 137.2, 134.7, 133.6, 133.2, 130.2, 129.8, 128.3, 121.3, 116.0, 112.7, 101.4, 65.7, 59.1, 56.2, 51.7, 23.8.

^{11}B NMR (128 MHz, Acetonitrile-d_3) δ 11.6.

4-Methoxycarbonylphenylboronic acid MIDA-DG ester (299)



4-Methoxycarbonylphenylboronic acid (180 mg, 1.00 mmol) and the MIDA-DG hydrochloric acid salt (328 mg, 1.00 mmol) were dissolved in MeCN (10 mL) and refluxed for 16 hours. The reaction mixture was cooled to room temperature, dry loaded onto silica and purified *via* FCC (washed with Et_2O then eluted with EtOAc). The product was isolated as a white crystalline solid (336 mg, 0.77 mmol, 77%).

ν_{max}/cm^{-1} 2225, 1759, 1715, 1599, 1491, 1450, 1394, 1275, 1219, 1111, 1044, 999, 842, 764, 708

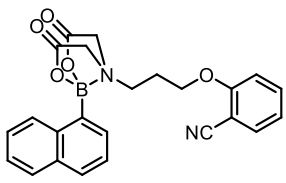
HRMS (ES+ TOF) Calcd. For $C_{22}H_{21}BN_2O_7K$ ($[M + K]^+$): 475.1079. Found: 475.1082.

^1H NMR (400 MHz, Acetonitrile-d_3) δ 7.99 – 7.94 (m, 2H), 7.66 – 7.61 (m, 2H), 7.61 – 7.53 (m, 2H), 7.05 (td, *J* = 7.6, 0.9 Hz, 1H), 7.00 – 6.94 (m, 1H), 4.11 (d, *J* = 17.1 Hz, 2H), 4.05 (d, *J* = 17.2 Hz, 2H), 3.98 (t, *J* = 6.2 Hz, 2H), 3.89 (s, 3H), 2.86 – 2.80 (m, 2H), 2.14 – 2.04 (m, 2H).

^{13}C NMR (101 MHz, Acetonitrile-d_3) δ 168.4, 166.8, 159.8, 134.7, 133.6, 132.7, 130.9, 128.6, 121.3, 116.1, 112.7, 101.4, 65.7, 59.0, 56.1, 51.7, 23.8.

^{11}B NMR (128 MHz, Acetonitrile-d_3) δ 11.5.

1-Napthylboronic acid MIDA-DG ester (303)



1-Napthylboronic acid (172 mg, 1.00 mmol) and the MIDA-DG trifluoroacetic acid salt (408 mg, 1.00 mmol) were dissolved in MeCN (13 mL) and refluxed for 16 hours. The reaction mixture was cooled to room temperature, dry loaded onto silica and purified *via* FCC (washed with Et_2O then eluted with EtOAc). The product was isolated as a white crystalline solid (249 mg, 0.58 mmol, 58%).

ν_{max}/cm^{-1} 2225, 1748, 1599, 1491, 1454, 1290, 1260, 1234, 1170, 1103, 1013, 173, 854, 753, 708.

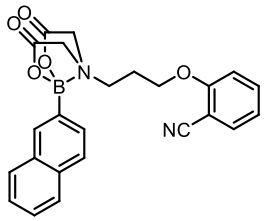
HRMS (ES- TOF) Calcd. for $C_{25}H_{22}BN_2O_7$ ([M-H]+HCO_2H): 473.1520. Found: 473.1530.

^{1}H NMR (400 MHz, Acetonitrile-d_3) δ 8.26 (dt, *J* = 8.5, 0.9 Hz, 1H), 7.97 – 7.88 (m, 2H), 7.71 (dd, *J* = 6.9, 1.3 Hz, 1H), 7.59 – 7.45 (m, 5H), 7.02 (td, *J* = 7.6, 0.8 Hz, 1H), 6.83 (d, *J* = 8.3 Hz, 1H), 4.16 (d, *J* = 17.2 Hz, 2H), 4.09 (d, *J* = 17.2 Hz, 2H), 3.81 (t, *J* = 6.3 Hz, 2H), 2.90 – 2.82 (m, 2H), 2.07 (dtd, *J* = 11.1, 8.0, 7.1, 5.4 Hz, 2H).

^{13}C NMR (101 MHz, Acetonitrile-d_3) δ 168.6, 159.8, 136.4, 134.7, 133.9, 133.6, 133.5, 130.4, 129.1, 127.2, 126.2, 125.3, 125.3, 121.2, 116.0, 112.7, 101.3, 65.6, 59.2, 55.4, 23.9.

^{11}B NMR (128 MHz, Acetonitrile-d_3) δ 12.6.

2-Napthylboronic acid MIDA-DG ester (304)



2-Napthylboronic acid (172 mg, 1.00 mmol) and the MIDA-DG trifluoroacetic acid salt (408 mg, 1.00 mmol) were dissolved in MeCN (13 mL) and refluxed for 16 hours. The reaction mixture was cooled to room temperature, dry loaded onto silica and purified *via* FCC (washed with Et_2O then eluted with EtOAc). The product was isolated as a white crystalline solid (307 mg, 0.72 mmol, 72%).

ν_{max}/cm^{-1} 2222, 1744, 1595, 1491, 1450, 1290, 1260, 1208, 1185, 1003, 951, 857, 824, 746

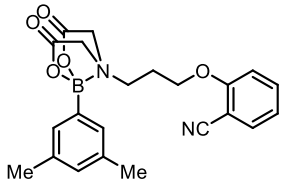
HRMS (ES- TOF) Calcd. for $C_{25}H_{22}BN_2O_7$ ([M-H]+HCO_2H): 473.1520. Found: 473.1534.

^{1}H NMR (400 MHz, Acetonitrile-d_3) δ 8.08 (d, *J* = 1.2 Hz, 1H), 7.97 – 7.91 (m, 1H), 7.91 – 7.86 (m, 2H), 7.61 (dd, *J* = 8.2, 1.4 Hz, 1H), 7.57 – 7.45 (m, 4H), 7.00 (td, *J* = 7.6, 0.9 Hz, 1H), 6.88 (dd, *J* = 8.6, 0.9 Hz, 1H), 4.15 (d, *J* = 17.1 Hz, 2H), 4.07 (d, *J* = 17.1 Hz, 2H), 3.91 (t, *J* = 6.2 Hz, 2H), 2.90 – 2.82 (m, 2H), 2.15 – 2.06 (m, 2H).

^{13}C NMR (101 MHz, Acetonitrile-d_3) δ 168.6, 159.8, 134.7, 134.0, 133.6, 133.1, 129.2, 128.4, 127.6, 127.2, 126.4, 125.9, 121.2, 116.1, 112.7, 101.3, 65.7, 59.0, 56.0, 23.9.

^{11}B NMR (128 MHz, Acetonitrile-d_3) δ 12.1.

3,5-Dimethylphenylboronic acid MIDA-DG ester (305)



3,5-Dimethylphenylboronic acid (150 mg, 1.00 mmol) and the MIDA-DG trifluoroacetic acid salt (408 mg, 1.00 mmol) were dissolved in MeCN (13 mL) and refluxed for 16 hours. The reaction mixture was cooled to room temperature, dry loaded onto silica and purified *via* FCC (washed with Et_2O then eluted with EtOAc). The product was isolated as a white crystalline solid (318 mg, 0.78 mmol, 78%).

ν_{max}/cm^{-1} 2225, 1744, 1595, 1491, 1450, 1290, 1182, 1018, 939, 876, 846, 753, 708

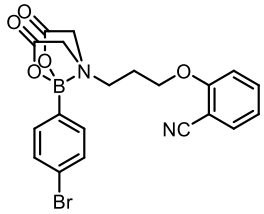
HRMS (ES- TOF) Calcd. for $C_{23}H_{24}BN_2O_7$ ([M-H]+HCO_2H): 451.1677. Found: 451.1693.

^{1}H NMR (400 MHz, Acetonitrile-d_3) δ 7.64 – 7.53 (m, 2H), 7.11 (s, 2H), 7.07 (td, *J* = 7.6, 0.9 Hz, 1H), 7.02 (s, 1H), 6.98 (d, *J* = 8.5 Hz, 1H), 4.07 (d, *J* = 17.1 Hz, 2H), 4.03 – 3.95 (m, 4H), 2.87 – 2.79 (m, 2H), 2.32 – 2.28 (m, 5H), 2.14 – 2.04 (m, 2H).

^{13}C NMR (101 MHz, Acetonitrile-d_3) δ 168.6, 159.9, 137.3, 134.8, 133.6, 130.8, 130.2, 121.3, 116.1, 112.7, 101.4, 65.8, 58.9, 55.9, 23.8, 20.5.

^{11}B NMR (128 MHz, Acetonitrile-d_3) δ 12.0.

4-Bromophenylboronic acid MIDA-DG ester (301)



4-Bromophenylboronic acid (201 mg, 1.00 mmol) and the MIDA-DG trifluoroacetic acid salt (408 mg, 1.00 mmol) were dissolved in MeCN (13 mL) and refluxed for 16 hours. The reaction mixture was cooled to room temperature, dry loaded onto silica and purified *via* FCC (washed with Et_2O then eluted with EtOAc). The product was isolated as a white crystalline solid (350 mg, 0.77 mmol, 77%).

ν_{max}/cm^{-1} 2222, 1759, 1584, 1495, 1454, 1386, 1290, 1260, 1219, 1044, 1003, 869, 813, 760

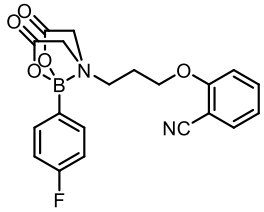
HRMS (ES- TOF) Calcd. for $C_{21}H_{19}BN_2O_7Br$ ([M-H]+HCO_2H): 501.0469. Found: 501.0466.

^{1}H NMR (400 MHz, Acetonitrile-d_3) δ 7.63 – 7.55 (m, 2H), 7.55 – 7.51 (m, 2H), 7.45 – 7.40 (m, 2H), 7.08 (td, *J* = 7.6, 0.9 Hz, 1H), 6.99 (d, *J* = 8.5 Hz, 1H), 4.09 (d, *J* = 17.1 Hz, 2H), 4.06 – 3.98 (m, 4H), 2.88 – 2.79 (m, 2H), 2.15 – 2.05 (m, 2H).

^{13}C NMR (101 MHz, Chloroform-*d*) δ 173.7, 165.2, 140.1, 139.9, 139.0, 136.3, 128.8, 126.6, 121.4, 118.0, 106.7, 71.0, 64.3, 61.4, 29.1.

^{11}B NMR (128 MHz, Acetonitrile-d_3) δ 11.6.

4-Fluorophenylboronic acid MIDA-DG ester (302)



4-Fluorophenylboronic acid (140 mg, 1.00 mmol) and the MIDA-DG trifluoroacetic acid salt (408 mg, 1.00 mmol) were dissolved in MeCN (13 mL) and refluxed for 16 hours. The reaction mixture was cooled to room temperature, dry loaded onto silica and purified *via* FCC (washed with Et_2O then eluted with EtOAc). The product was isolated as a white crystalline solid (274 mg, 0.69 mmol, 69%).

ν_{max}/cm^{-1} 225, 1767, 1595, 1476, 1402, 1256, 1215, 1044, 1001, 943, 872, 835, 764

HRMS (ES+ TOF) Calcd. For $C_{20}H_{19}BN_2O_5F$ ([M + H]$^+$): 397.1371. Found: 397.1377.

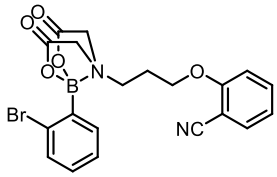
^{1}H NMR (400 MHz, Acetonitrile-d_3) δ 7.63 – 7.56 (m, 2H), 7.56 – 7.51 (m, 2H), 7.14 – 7.05 (m, 3H), 7.00 (d, *J* = 8.4 Hz, 1H), 4.08 (d, *J* = 17.1 Hz, 2H), 4.04 – 3.98 (m, 4H), 2.86 – 2.78 (m, 2H), 2.15 – 2.04 (m, 2H).

^{13}C NMR (101 MHz, Acetonitrile-d_3) δ 168.4, 162.6, 159.9, 134.8, 134.7, 133.7, 121.3, 116.1, 114.9, 114.7, 112.7, 101.4, 65.7, 58.9, 56.0, 23.8.

^{11}B NMR (128 MHz, Acetonitrile-d_3) δ 11.6.

^{19}F NMR (377 MHz, Acetonitrile-d_3) δ -76.5, -114.0 (q, *J* = 7.2 Hz). The material contained residual (15%) trifluoroacetic acid as an impurity resulting from utilising the MIDA-DG TFA salt.

2-Bromophenylboronic acid MIDA-DG ester (300)



2-Bromophenylboronic acid (201 mg, 1.00 mmol) and the MIDA-DG trifluoroacetic acid salt (408 mg, 1.00 mmol) were dissolved in MeCN (13 mL) and refluxed for 16 hours. The reaction mixture was cooled to room temperature, dry loaded onto silica and purified *via* FCC (washed with Et_2O then eluted with EtOAc). The product was isolated as a white crystalline solid (372 mg, 0.81 mmol, 81%).

ν_{max}/cm^{-1} 2222, 1767, 1491, 1424, 1293, 1200, 1125, 1059, 1018, 954, 861, 760

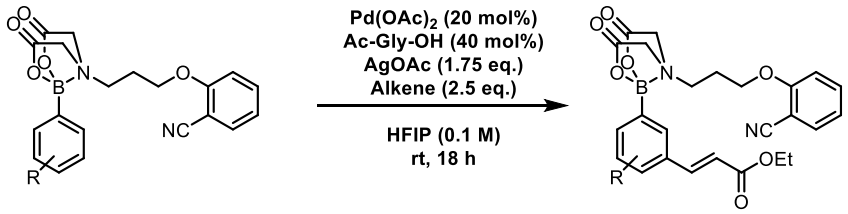
HRMS (ES- TOF) Calcd. for $C_{21}H_{19}BN_2O_7Br$ ([M-H]+HCO_2H): 501.0469. Found: 501.0479.

^{1}H NMR (400 MHz, Acetonitrile-d_3) δ 7.70 (dd, *J* = 7.5, 1.9 Hz, 1H), 7.63 – 7.54 (m, 3H), 7.38 (td, *J* = 7.4, 1.2 Hz, 1H), 7.29 (ddd, *J* = 7.9, 7.3, 1.9 Hz, 1H), 7.07 (td, *J* = 7.6, 0.9 Hz, 1H), 7.02 – 6.96 (m, 1H), 4.23 (d, *J* = 17.2 Hz, 2H), 4.09 (d, *J* = 17.2 Hz, 2H), 4.02 (t, *J* = 6.1 Hz, 2H), 3.11 – 3.03 (m, 2H), 2.23 – 2.13 (m, 2H).

^{13}C NMR (101 MHz, Acetonitrile-d_3) δ 168.5, 159.8, 136.5, 134.7, 133.7 (2Ar-C), 131.4, 127.9, 127.0, 121.3, 116.1, 112.6, 101.3, 65.6, 61.2, 56.8, 24.1.

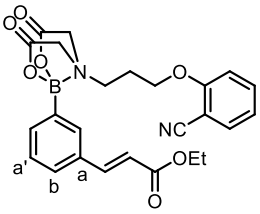
^{11}B NMR (128 MHz, Acetonitrile-d_3) δ 11.8.

General Procedure E for the C–H alkenylation of aryl boronic acid MIDA-DG esters:



A 20 mL vial was charged with arylboronic acid MIDA-DG ester (1.0 eq.), AgOAc (1.75 eq.), Ac-Gly-OH (40 mol%) and $Pd(OAc)_2$ (20 mol%). The vial was then charged with HFIP (0.1 M) and the corresponding alkene coupling partner (2.5 eq.) was added. The vial was sealed and stirred at room temperature for 18 hours. The reaction mixture was diluted with MeCN (~5 mL) and dry loaded onto a silica column. The column was washed with Et_2O (100 mL) before the products were subsequently eluted with 1:1 MeCN:Et_2O. The eluent was concentrated under vacuum to yield the alkenylated products as an inseparable mixture of regio-isomers. The corresponding yields of each isomer were calculated using ^{1}H NMR analysis.

3-(Ethyl prop-2-enoate)phenylboronic acid MIDA-DG ester (286) and Isomers



General Procedure E: Phenylboronic acid MIDA-DG ester (151 mg, 0.4 mmol) was employed to yield the products as an off-white mixture of solids (147 mg, 75% total yield: **a**: 55%, **b**: 8%, **a**+**a'**: 8%, **a**+**b**: 4% as determined by ^{1}H NMR).

Characterisation data for major isomer:

HRMS (ES+ TOF) Calcd. for $C_{25}H_{26}N_2O_7B$ ($[M + H]^+$): 477.1833. Found: 477.1841.

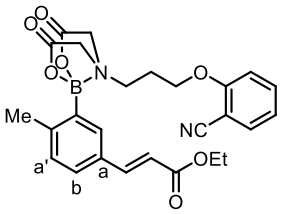
^{1}H NMR (400 MHz, Acetonitrile-d_3) δ 7.75 – 7.64 (m, 3H), 7.61 – 7.54 (m, 3H), 7.42 (t, *J* = 7.5 Hz, 1H), 7.05 (td, *J* = 7.6, 0.9 Hz, 1H), 6.97 (d, *J* = 8.4 Hz, 1H), 6.53 (d, *J* = 16.1 Hz, 1H), 4.23 (q, *J* = 7.1

Hz, 2H), 4.11 (d, *J* = 17.1 Hz, 2H), 4.04 (d, *J* = 17.1 Hz, 2H), 3.98 (t, *J* = 6.2 Hz, 2H), 2.87 – 2.81 (m, 2H), 2.14 – 2.06 (m, 2H), 1.31 (t, *J* = 7.1 Hz, 3H).

^{13}C NMR (101 MHz, Acetonitrile-d_3) δ 168.4, 166.58, 159.9, 144.5, 143.78, 134.8, 134.6, 134.0, 133.6, 133.1, 132.8, 132.5, 128.6, 128.6, 121.3, 119.2, 118.3, 116.1, 112.7, 101.4, 65.7, 60.2, 59.0, 56.1, 29.4, 23.8, 13.7. Unable to distinguish ^{13}C peaks between regioisomers.

^{11}B NMR (128 MHz, Acetonitrile-d_3) δ 11.6.

2-Methyl-5-(ethyl prop-2-enoate)phenylboronic acid MIDA-DG ester (309) and Isomers



General Procedure E: 2-Methylphenylboronic acid MIDA-DG ester (118 mg, 0.3 mmol) was employed to yield the products as an off-white mixture of solids (97 mg, 54% total yield: **a**: 43%, **b**: 3%, **a'**: 4%, **a**+**b** and **a'**+**b**: 4%, **SM**: 13% as determined by ^{1}H NMR).

Characterisation data for major isomer:

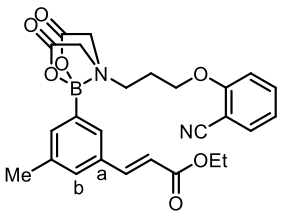
HRMS (ES+ TOF) Calcd. for $C_{26}H_{27}N_2O_7BNa$ ([M + Na]$^+$): 513.1809. Found: 513.1824.

^{1}H NMR (400 MHz, Acetonitrile-d_3) δ 7.67 (d, *J* = 16.0 Hz, 1H), 7.62 (d, *J* = 2.1 Hz, 1H), 7.61 – 7.54 (m, 3H), 7.23 (d, *J* = 7.9 Hz, 1H), 7.08 – 7.04 (m, 1H), 6.99 (d, *J* = 8.5 Hz, 1H), 6.45 (d, *J* = 16.0 Hz, 1H), 4.22 (q, *J* = 7.1 Hz, 2H), 4.12 (d, *J* = 17.2 Hz, 2H), 4.04 (d, *J* = 15.1 Hz, 2H), 4.00 (t, *J* = 5.2 Hz, 2H), 2.88 – 2.81 (m, 2H), 2.44 (s, 3H), 2.16 – 2.10 (m, 2H), 1.31 (t, *J* = 7.1 Hz, 3H).

^{13}C NMR (101 MHz, Acetonitrile-d_3) δ 168.4, 166.7, 159.9, 145.4, 144.5, 134.8, 133.6, 131.8, 131.4, 128.4, 121.3, 116.1, 112.7, 101.4, 65.7, 60.1, 59.8, 59.6, 56.1, 24.0, 22.2, 13.7. Unable to distinguish ^{13}C peaks between regioisomers.

^{11}B NMR (128 MHz, Acetonitrile-d_3) δ 12.5.

3-Methyl-5-(ethyl prop-2-enoate)phenylboronic acid MIDA-DG ester (310) and Isomers



General Procedure E: 3-Methylphenylboronic acid MIDA-DG ester (118 mg, 0.3 mmol) was employed to yield the products as an off-white mixture of solids (99 mg, 66% total yield: **a**: 42%, **b**: 21%, **a**+**b**: 3%, as determined by ^{1}H NMR).

Characterisation data for major isomer:

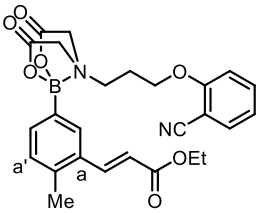
HRMS (ES+ TOF) Calcd. for $C_{26}H_{27}N_2O_7BNa$ ([M + Na]$^+$): 513.1809. Found: 513.1818.

^{1}H NMR (400 MHz, Acetonitrile-d_3) δ 7.66 (d, *J* = 16.1 Hz, 1H), 7.60 – 7.53 (m, 2H), 7.50 (s, 1H), 7.49 (s, 1H), 7.38 (s, 1H), 7.05 (td, *J* = 7.6, 0.9 Hz, 1H), 6.96 (d, *J* = 8.5 Hz, 1H), 6.50 (d, *J* = 16.0 Hz, 1H), 4.23 (q, *J* = 7.2 Hz, 2H), 4.11 (d, *J* = 17.1 Hz, 2H), 4.03 (d, *J* = 17.0 Hz, 2H), 3.98 (t, *J* = 5.5 Hz, 2H), 2.89 – 2.80 (m, 2H), 2.37 (s, 3H), 2.14 – 2.05 (m, 2H), 1.31 (t, *J* = 7.1 Hz, 3H).

^{13}C NMR (101 MHz, Acetonitrile-d_3) δ 168.4, 166.6, 166.6, 159.9, 159.8, 144.7, 141.7, 141.5, 138.3, 137.1, 135.4, 135.0, 134.7, 134.0, 133.7, 133.6, 130.4, 130.1, 129.1, 125.9, 121.3, 119.5, 118.0, 116.1, 112.7, 101.4, 65.8, 60.3, 60.2, 59.0, 56.1, 29.4, 23.8, 23.8, 20.4, 18.9, 13.7. Unable to distinguish ^{13}C peaks between regioisomers.

^{11}B NMR (128 MHz, Acetonitrile-d_3) δ 11.8.

4-Methyl-3-(ethyl prop-2-enoate)phenylboronic acid MIDA-DG ester (311) and Isomers



General Procedure E: 4-Methylphenylboronic acid MIDA-DG ester (118 mg, 0.3 mmol) was employed to yield the products as an off-white mixture of solids (95 mg, 50% total yield: **a**: 43%, **a**+**a'**: 7%, **SM**: 16%, as determined by ^{1}H NMR).

Characterisation data for major isomer:

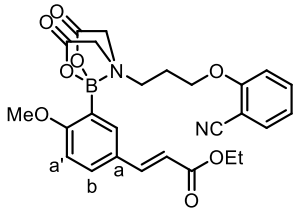
HRMS (ES+ TOF) Calcd. for $C_{26}H_{27}N_2O_7BNa$ ([M + Na]$^+$): 513.1809. Found: 513.1814.

^{1}H NMR (400 MHz, Acetonitrile-d_3) δ 7.66 (d, *J* = 16.1 Hz, 1H), 7.60 – 7.53 (m, 2H), 7.52 – 7.47 (m, 2H), 7.38 (s, 1H), 7.05 (td, *J* = 7.6, 0.9 Hz, 1H), 6.96 (d, *J* = 8.5 Hz, 1H), 6.50 (d, *J* = 16.0 Hz, 1H), 4.23 (q, *J* = 7.2 Hz, 2H), 4.11 (d, *J* = 17.1 Hz, 2H), 4.03 (d, *J* = 17.0 Hz, 2H), 3.98 (t, *J* = 6.1 Hz, 2H), 2.90 – 2.80 (m, 2H), 2.36 (s, 3H), 2.14 – 2.05 (m, 2H), 1.31 (t, *J* = 7.1 Hz, 3H).

^{13}C NMR (101 MHz, Acetonitrile-d_3) δ 168.4, 166.6, 159.9, 144.7, 141.7, 138.3, 137.1, 135.4, 135.0, 134.7, 134.0, 133.7, 133.6, 130.4, 130.1, 129.1, 125.9, 121.3, 119.5, 118.0, 116.1, 112.7, 101.4, 65.8, 60.3, 60.2, 59.0, 56.1, 29.4, 23.8, 20.4, 18.9, 13.7. Unable to distinguish ^{13}C peaks between regioisomers.

^{11}B NMR (128 MHz, Acetonitrile-d_3) δ 11.8.

2-Methoxy-5-(ethyl prop-2-enoate)phenylboronic acid MIDA-DG ester (306) and Isomers



General Procedure E: 2-Methoxyphenylboronic acid MIDA-DG ester (122 mg, 0.3 mmol) was employed to yield the products as an off-white mixture of solids (121 mg, 79% total yield: **a**: 58%, **b**: 15%, **a**+**b**: 6%, as determined by ^{1}H NMR).

Characterisation data for major isomer:

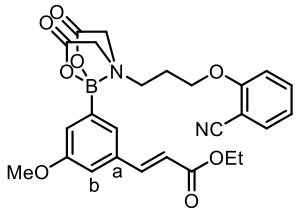
HRMS (ES+ TOF) Calcd. for $C_{26}H_{27}N_2O_8BNa$ ([M + Na]$^+$): 529.1758. Found: 529.1760.

^{1}H NMR (400 MHz, Acetonitrile-d_3) δ 7.79 (d, J = 2.3 Hz, 1H), 7.68 – 7.48 (m, 4H), 7.04 (td, J = 7.6, 0.8 Hz, 1H), 6.98 (d, J = 8.6 Hz, 1H), 6.92 (d, J = 8.5 Hz, 1H), 6.35 (d, J = 16.0 Hz, 1H), 4.22 (d, J = 7.1 Hz, 2H), 4.15 (d, J = 17.0 Hz, 2H), 4.04 (d, J = 17.0 Hz, 2H), 3.99 (t, J = 5.9 Hz, 2H), 3.85 (s, 3H), 3.08 – 2.99 (m, 2H), 2.10 (dt, J = 10.4, 5.8 Hz, 2H), 1.31 (t, J = 7.1 Hz, 3H).

^{13}C NMR (101 MHz, Acetonitrile-d_3) δ 168.6, 166.8, 164.1, 159.7, 144.3, 135.0, 134.7, 133.7, 133.7, 131.0, 126.8, 121.2, 120.9, 118.7, 116.1, 115.7, 112.5, 110.9, 109.4, 101.2, 65.7, 60.3, 60.0, 55.7, 55.6, 55.1, 54.9, 23.8, 13.7. Unable to distinguish ^{13}C peaks between regioisomers.

^{11}B NMR (128 MHz, Acetonitrile-d_3) δ 11.7.

3-Methoxy-5-(ethyl prop-2-enoate)phenylboronic acid MIDA-DG ester (307) and Isomers



General Procedure E: 3-Methoxyphenylboronic acid MIDA-DG ester (122 mg, 0.3 mmol) was employed to yield the products as an off-white mixture of solids (92 mg, 33% total yield: **a**: 23%, **b**: 10%, **SM**: 35% as determined by ^{1}H NMR).

Characterisation data for major isomer:

HRMS (ES+ TOF) Calcd. for $C_{26}H_{27}N_2O_8BNa$ ([M + Na]$^+$): 529.1758. Found: 529.1760.

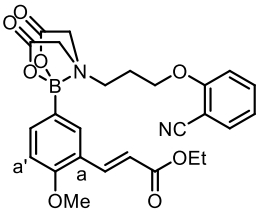
^{1}H NMR (400 MHz, Acetonitrile-d_3) δ 7.92 (d, J = 16.2 Hz, 1H), 7.63 – 7.53 (m, 2H), 7.12 (s, 1H), 7.10 – 7.04 (m, 3H), 7.03 (dt, J = 3.4, 1.1 Hz, 1H), 7.01 – 6.97 (m, 1H), 6.56 (d, J = 16.2 Hz, 1H), 4.23 (q, J = 7.1 Hz, 2H), 4.11 (d, J = 17.1 Hz, 2H), 4.04 (d, J = 13.1 Hz, 2H), 4.01 – 3.97 (m, 2H), 3.92 (s, 3H), 2.91 – 2.82 (m, 2H), 2.15 – 2.06 (m, 2H), 1.31 (t, J = 7.1 Hz, 3H).

^{13}C NMR (101 MHz, Acetonitrile-d_3) δ 168.5, 168.4, 159.9, 159.4, 144.4, 139.2, 134.7, 133.7, 129.3, 128.3, 125.4, 124.7, 124.6, 123.7, 121.3, 120.0, 118.8, 118.5, 116.1, 115.0, 113.4, 112.8, 101.4, 65.8,

60.2, 60.1, 59.1, 59.0, 58.9, 56.0, 55.9, 55.3, 55.0, 54.7, 23.8, 13.7. Unable to distinguish ^{13}C peaks between regioisomers.

^{11}B NMR (128 MHz, Acetonitrile-d_3) δ 11.7.

4-Methoxy-3-(ethyl prop-2-enoate)phenylboronic acid MIDA-DG ester (308) and Isomers



General Procedure E: 4-Methoxyphenylboronic acid MIDA-DG ester (122 mg, 0.3 mmol) was employed to yield the products as an off-white mixture of solids (53 mg, 34% total yield: **a**: 30%, **a**+**a'**: 4%, as determined by ^{1}H NMR).

Characterisation data for major isomer:

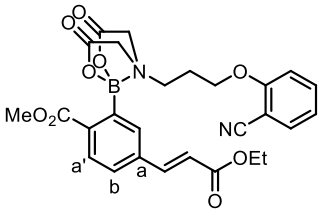
HRMS (ES+ TOF) Calcd. for $C_{26}H_{27}N_2O_8BNa$ ([M + Na]$^+$): 529.1758. Found: 529.1767.

^{1}H NMR (400 MHz, Acetonitrile-d_3) δ 7.89 (d, J = 16.2 Hz, 1H), 7.67 (d, J = 1.9 Hz, 1H), 7.61 – 7.50 (m, 3H), 7.08 – 7.00 (m, 2H), 6.96 (d, J = 8.5 Hz, 1H), 6.58 (d, J = 16.2 Hz, 1H), 4.22 (q, J = 7.1 Hz, 2H), 4.10 (d, J = 17.1 Hz, 2H), 4.04 – 3.97 (m, 4H), 3.90 (s, 3H), 2.89 – 2.81 (m, 2H), 2.10 (ddt, J = 12.1, 8.1, 5.3 Hz, 2H), 1.30 (t, J = 7.1 Hz, 3H).

^{13}C NMR (101 MHz, Acetonitrile-d_3) δ 168.5, 167.0, 166.6, 159.9, 159.3, 139.8, 138.4, 136.2, 134.7, 134.4, 133.6, 133.5, 128.7, 128.2, 122.6, 121.3, 120.4, 118.8, 116.1, 113.7, 112.7, 111.2, 101.4, 65.8, 60.3, 60.1, 59.0, 56.1, 55.3, 23.8, 13.7. Unable to distinguish ^{13}C peaks between regioisomers.

^{11}B NMR (128 MHz, Acetonitrile-d_3) δ 11.9.

2-Methoxycarbonyl-5-(ethyl prop-2-enoate)phenylboronic acid MIDA-DG ester (312) and Isomers



General Procedure E: 2-Methoxycarbonylphenylboronic acid MIDA-DG ester (131 mg, 0.3 mmol) was employed to yield the products as a white mixture of solids(139 mg, 34% total yield: **a**: 16%, **b**: 11%, **a'**: 7%, **SM**: 65%, as determined by ^{1}H NMR). The reaction was repeated using 0.2 mmol of MIDA-DG ester for an extended time of 48 hours. The products were isolated as a white mixture of solids (96 mg, 61% total yield: **a**: 32%, **b**:10%, **a'**: 13%, **di**: 6%, **SM**: 32%, as determined by ^{1}H NMR).

Characterisation data for major isomer:

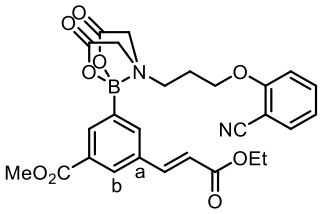
HRMS (ES+ TOF) Calcd. for $C_{27}H_{27}N_2O_9BNa$ ([M + Na]$^+$): 557.1707. Found: 557.1707.

^{1}H NMR (400 MHz, Acetonitrile-d_3) δ 7.88 (d, *J* = 1.7 Hz, 1H), 7.71 (m, 2H), 7.67 – 7.61 (m, 1H), 7.60 – 7.51 (m, 2H), 7.09 – 7.01 (m, 1H), 7.01 – 6.96 (m, 1H), 6.59 (d, *J* = 16.1 Hz, 1H), 4.28 (d, *J* = 17.1 Hz, 2H), 4.08 – 3.99 (m, 7H), 3.83 (s, 3H), 3.26 – 3.13 (m, 2H), 2.28 – 2.13 (m, 2H), 1.31 (t, *J* = 7.1 Hz, 3H).

^{13}C NMR (101 MHz, Acetonitrile-d_3) δ 170.9, 168.8, 166.3, 159.8, 143.3, 140.7, 138.4, 137.1, 135.7, 134.9, 134.7, 133.7, 130.4, 129.4, 129.1, 129.0, 128.6, 128.3, 127.9, 127.6, 121.3, 120.9, 120.1, 116.0, 112.7, 101.4, 65.8, 61.3, 60.4, 57.9, 52.5, 52.4, 24.2, 13.6. Unable to distinguish ^{13}C peaks between regioisomers.

^{11}B NMR (128 MHz, Acetonitrile-d_3) δ 12.0.

3-Methoxycarbonyl-5-(ethyl prop-2-enoate)phenylboronic acid MIDA-DG ester (313) and Isomers



General Procedure E: 3-Methoxycarbonylphenylboronic acid MIDA-DG ester (131 mg, 0.3 mmol) was employed to yield the products as a white mixture of solids (137 mg, 32% total yield: **a**: 29%, **b**: 3%, **SM**: 66% as determined by ^{1}H NMR). The reaction was repeated using 0.2 mmol of MIDA-DG ester for an extended time of 48 hours. The products were isolated as a white mixture of solids (93 mg, 59% total yield: **a**: 49%, **b**:10%, **SM**: 34%, as determined by ^{1}H NMR).

Characterisation data for major isomer:

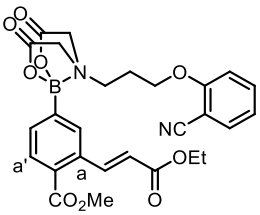
HRMS (ES+ TOF) Calcd. for $C_{27}H_{27}N_2O_9BNa$ ([M + Na]$^+$): 557.1707. Found: 557.1702.

^{1}H NMR (400 MHz, Acetonitrile-d_3) δ 8.22 (t, *J* = 1.8 Hz, 1H), 8.13 (dt, *J* = 2.6, 1.4 Hz, 1H), 7.94 (d, *J* = 1.4 Hz, 1H), 7.75 (d, *J* = 16.1 Hz, 1H), 7.61 – 7.51 (m, 2H), 7.06 – 7.02 (m, 1H), 6.95 (d, *J* = 8.1 Hz, 1H), 6.61 (d, *J* = 16.1 Hz, 1H), 4.24 (q, *J* = 7.1 Hz, 2H), 4.15 (d, *J* = 17.1 Hz, 2H), 4.06 (d, *J* = 17.1 Hz, 2H), 3.99 (t, *J* = 6.1 Hz, 2H), 3.91 (s, 3H), 2.89 – 2.80 (m, 2H), 2.10 (m, 2H), 1.32 (t, *J* = 7.1 Hz, 3H).

^{13}C NMR (101 MHz, Acetonitrile-d_3) δ 168.3, 166.4, 159.8, 143.4, 137.2, 136.7, 136.4, 134.8, 134.7, 134.6, 133.6, 133.6, 133.2, 130.6, 130.2, 129.6, 128.3, 127.4, 121.3, 119.6, 116.0, 112.7, 101.4, 65.7, 60.3, 59.2, 59.1, 59.1, 56.3, 56.2, 56.2, 51.9, 51.7, 23.8, 23.8, 13.6. Unable to distinguish ^{13}C peaks between regioisomers.

^{11}B NMR (128 MHz, Acetonitrile-d_3) δ 11.5.

4-Methoxycarbonyl-3-(ethyl prop-2-enoate)phenylboronic acid MIDA-DG ester (314) and Isomers



General Procedure E: 4-Methoxycarbonylphenylboronic acid MIDA-DG ester (131 mg, 0.3 mmol) was employed to yield the products as a white mixture of solids (138 mg, 22% total yield: **a**: 22%, **SM**: 78%, as determined by ^{1}H NMR). The reaction was repeated using 0.1 mmol of MIDA-DG ester for an extended time of 48 hours. The products were isolated as a white mixture of solids (49 mg, 52% total yield: **a**: 49%, **a+a'**: 3%, **SM**: 47%, as determined by ^{1}H NMR).

Characterisation data for major isomer:

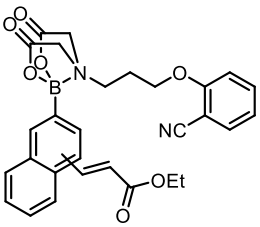
HRMS (ES+ TOF) Calcd. for $C_{27}H_{27}N_2O_9BNa$ ([M + Na]$^{+}$): 557.1707. Found: 557.1705.

^{1}H NMR (400 MHz, Acetonitrile-d_3) δ 8.34 (d, J = 16.0 Hz, 1H), 7.90 (d, J = 7.8 Hz, 1H), 7.82 – 7.78 (m, 1H), 7.63 (dq, J = 7.8, 1.5 Hz, 1H), 7.60 – 7.50 (m, 2H), 7.04 (tdd, J = 7.6, 2.2, 0.9 Hz, 1H), 6.95 (d, J = 8.5 Hz, 1H), 6.43 (d, J = 16.0 Hz, 1H), 4.24 (q, J = 7.1 Hz, 2H), 4.15 (d, J = 17.2 Hz, 2H), 4.07 (d, J = 17.1 Hz, 2H), 3.98 (dt, J = 7.3, 6.2 Hz, 2H), 3.89 (s, 3H), 2.90 – 2.79 (m, 2H), 2.17 – 2.04 (m, 2H), 1.31 (t, J = 7.1 Hz, 3H).

^{13}C NMR (101 MHz, Acetonitrile-d_3) δ 168.4, 168.4, 167.1, 166.8, 166.4, 159.9, 159.8, 143.5, 140.6, 135.2, 134.7, 133.8, 133.6, 133.6, 132.7, 132.5, 132.1, 130.9, 130.7, 129.9, 128.6, 121.3, 120.8, 116.1, 116.1, 112.7, 112.7, 101.4, 65.7, 65.6, 63.8, 60.4, 59.2, 59.1, 56.3, 56.1, 52.0, 51.7, 28.1, 23.9, 23.8, 13.7, 13.6. Unable to distinguish ^{13}C peaks between regioisomers.

^{11}B NMR (128 MHz, Acetonitrile-d_3) δ 11.4.

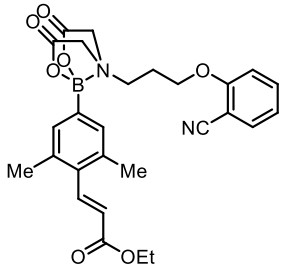
Alkenylated 2-napythphenylboronic acid MIDA-DG ester (318)



General Procedure E: 2-Napthylboronic acid MIDA-DG ester (128 mg, 0.3 mmol) was employed to yield the products as a white mixture of solids (99 mg). The product gave a complex mixture of regio and mono or di isomers. The yield calculation and characterisation were performed after

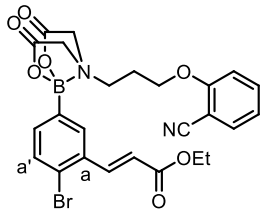
forming the pinacol boronate ester to allow separation and easier elucidation. Please see below for the relevant yield and characterisation data after synthesis of the pinacol ester.
HRMS (ES+ TOF) Calcd. for $C_{29}H_{28}N_2O_7B$ ([M + H]$^+$): 527.1990. Found: 527.1988.

3,5-Dimethyl-4-(ethyl prop-2-enoate)phenylboronic acid MIDA-DG ester (319)



General Procedure E: 3,5-Dimethylphenylboronic acid MIDA-DG ester (122 mg, 0.3 mmol) was employed to yield the products as a white mixture of solids after 48 hours (115 mg, 40% yield, **SM**: 45%, as determined by ^{1}H NMR).
Characterisation data for major isomer:
HRMS (ES+ TOF) Calcd. for $C_{27}H_{30}N_2O_7B$ ([M + H]$^+$): 505.2146. Found: 505.2144.
^{1}H NMR (400 MHz, Acetonitrile-d_3) δ 7.82 (d, J = 16.4 Hz, 1H), 7.63 – 7.54 (m, 2H), 7.22 (s, 2H), 7.06 (td, J = 7.6, 0.8 Hz, 1H), 6.99 (d, J = 8.5 Hz, 1H), 6.10 (d, J = 16.4 Hz, 1H), 4.25 (q, J = 7.1 Hz, 2H), 4.09 (d, J = 17.0 Hz, 2H), 4.04 – 3.96 (m, 4H), 2.91 – 2.78 (m, 2H), 2.33 (s, 6H), 2.15 – 2.05 (m, 2H), 1.32 (t, J = 7.1 Hz, 3H).
^{13}C NMR (101 MHz, Acetonitrile-d_3) δ 168.5, 166.3, 159.8, 142.8, 137.3, 136.1, 134.7, 133.6, 130.2, 123.9, 121.3, 116.0, 112.7, 101.4, 65.8, 60.3, 59.0, 56.0, 23.8, 20.2, 13.6.
^{11}B NMR (128 MHz, Acetonitrile-d_3) δ 11.9.

4-Bromo-3-(ethyl prop-2-enoate)phenylboronic acid MIDA-DG ester (316) and Isomers



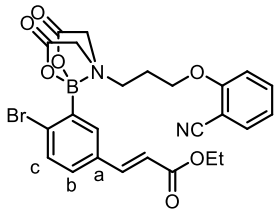
General Procedure E: 4-Bromophenylboronic acid MIDA-DG ester (137 mg, 0.3 mmol) was employed to yield the products as an off-white mixture of solids after 48 hours (136 mg, 69% total yield, **a**: 55%, **a+a'**: 14%, **SM**: 16%, as determined by ^{1}H NMR).
Characterisation data for major isomer:
HRMS (ES+ TOF) Calcd. for $C_{25}H_{24}N_2O_7BBrNa$ ([M + Na]$^+$): 577.0758. Found: 577.0760.
^{1}H NMR (400 MHz, Acetonitrile-d_3) δ 7.95 (d, J = 16.0 Hz, 1H), 7.80 (d, J = 1.8 Hz, 1H), 7.65 (d, J = 8.0 Hz, 1H), 7.61 – 7.53 (m, 2H), 7.42 (dt, J = 8.0, 2.2 Hz, 1H), 7.06 (td, J = 7.6, 1.0 Hz, 1H), 7.00 –

6.96 (m, 1H), 6.53 (d, *J* = 15.9 Hz, 1H), 4.25 (q, *J* = 7.1 Hz, 2H), 4.12 (d, *J* = 17.1 Hz, 2H), 4.09 – 3.97 (m, 4H), 2.91 – 2.83 (m, 2H), 2.16 – 2.06 (m, 2H), 1.32 (t, *J* = 7.1 Hz, 3H).

^{13}C NMR (101 MHz, Acetonitrile-d_3) δ 168.3, 166.1, 166.0, 159.9, 142.7, 142.3, 135.7, 135.4, 134.8, 134.6, 133.8, 133.7, 133.6, 133.6, 132.9, 132.3, 131.0, 126.1, 122.4, 121.5, 121.3, 116.1, 112.7, 101.4, 65.7, 60.6, 60.5, 59.3, 59.1, 59.0, 56.5, 56.3, 56.1, 23.9, 23.9, 23.8, 13.6. Unable to distinguish ^{13}C peaks between regioisomers.

^{11}B NMR (128 MHz, Acetonitrile-d_3) δ 11.5.

2-Bromo-5-(ethyl prop-2-enoate)phenylboronic acid MIDA-DG ester (315) and Isomers



General Procedure E: 2-Bromophenylboronic acid MIDA-DG ester (137 mg, 0.3 mmol) was employed to yield the products as an off-white mixture of solids after 48 hours (142 mg, 49% total yield, **a**: 32%, **b**: 13%, **c**: 3%, **di**: 1%, **SM**: 42%, as determined by ^{1}H NMR).

Characterisation data for major isomer:

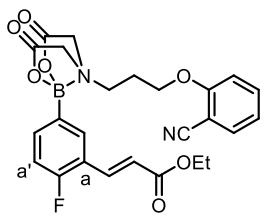
HRMS (ES+ TOF) Calcd. for $C_{25}H_{24}N_2O_7BBrNa$ ([M + Na]$^+$): 577.0758. Found: 577.0777.

^{1}H NMR (400 MHz, Acetonitrile-d_3) δ 7.86 (d, *J* = 2.4 Hz, 1H), 7.76 – 7.66 (m, 1H), 7.65 – 7.48 (m, 4H), 7.10 – 7.02 (m, 1H), 7.01 – 6.95 (m, 1H), 6.51 (d, *J* = 16.1 Hz, 1H), 4.28 – 4.18 (m, 4H), 4.14 – 4.05 (m, 2H), 4.02 (t, *J* = 6.1 Hz, 2H), 3.11 – 3.03 (m, 2H), 2.24 – 2.11 (m, 2H), 1.31 (t, *J* = 7.1 Hz, 3H).

^{13}C NMR (101 MHz, Acetonitrile-d_3) δ 168.5, 166.3, 166.1, 159.8, 143.9, 143.2, 138.1, 136.7, 136.5, 134.8, 134.3, 133.7, 133.2, 131.3, 130.0, 129.7, 127.9, 127.5, 127.0, 121.3, 119.1, 116.1, 112.6, 101.3, 65.6, 61.5, 61.2, 60.3, 56.8, 24.1, 13.6. Unable to distinguish ^{13}C peaks between regioisomers.

^{11}B NMR (128 MHz, Acetonitrile-d_3) δ 11.7.

4-Fluoro-3-(ethyl prop-2-enoate)phenylboronic acid MIDA-DG ester (317) and Isomers



General Procedure E: 4-Fluorophenylboronic acid MIDA-DG ester (119 mg, 0.3 mmol) was employed to yield the products as an off-white mixture of solids after 48 hours (101 mg, 54% total yield, **a**: 43%, **a+a'**: 11%, **SM**: 15%, as determined by ^{1}H NMR).

Characterisation data for major isomer:

HRMS (ES+ TOF) Calcd. for $C_{25}H_{25}N_2O_7BF$ ([M + Na]$^{+}$): 495.1739. Found: 495.1750.

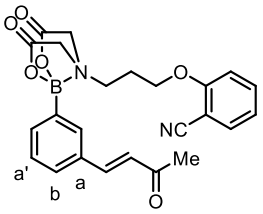
^{1}H NMR (400 MHz, Acetonitrile-d_3) δ 7.80 – 7.73 (m, 2H), 7.62 – 7.50 (m, 3H), 7.17 (dd, *J* = 11.2, 8.3 Hz, 1H), 7.05 (td, *J* = 7.6, 0.9 Hz, 1H), 6.98 (d, *J* = 8.3 Hz, 1H), 6.60 (d, *J* = 16.2 Hz, 1H), 4.24 (q, *J* = 7.1 Hz, 2H), 4.11 (d, *J* = 17.1 Hz, 2H), 4.08 – 3.96 (m, 4H), 2.88 – 2.82 (m, 4H), 2.15 – 2.05 (m, 2H), 1.31 (t, *J* = 7.1 Hz, 3H).

^{13}C NMR (101 MHz, Acetonitrile-d_3) δ 168.3, 166.4, 159.9, 136.8 (d, *J* = 2.7 Hz), 136.5, 136.4, 134.7, 134.7, 134.0, 134.0, 133.7, 133.6, 121.3, 121.1, 121.0, 116.1, 115.7, 115.5, 112.7, 101.4, 65.7, 60.4, 59.2, 59.0, 58.9, 56.2, 56.0, 23.8, 13.6.

^{11}B NMR (128 MHz, Acetonitrile-d_3) δ 11.5.

^{19}F NMR (377 MHz, Acetonitrile-d_3) δ -115.9 (dt, *J* = 12.8, 7.1 Hz).

3-(But-3-ene-2-enone)phenylboronic acid MIDA-DG ester (320) and Isomers



General Procedure E: Phenylboronic acid MIDA-DG ester (113 mg, 0.3 mmol) was employed to yield the products as a white mixture of solids (93 mg, 69% total yield: **a**: 59%, **b**: 8%, **a+a'**: 2%, as determined by ^{1}H NMR).

Characterisation data for major isomer:

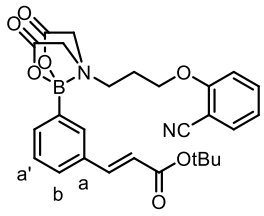
HRMS (ES- TOF) Calcd. for $C_{25}H_{24}N_2O_8B$ ([M + HCOO]$^{-}$): 491.1626. Found: 491.1632.

^{1}H NMR (400 MHz, Acetonitrile-d_3) δ 7.75 (s, 1H), 7.68 (dt, *J* = 7.8, 1.6 Hz, 1H), 7.65 – 7.55 (m, 4H), 7.43 (t, *J* = 7.6 Hz, 1H), 7.05 (tt, *J* = 7.6, 0.8 Hz, 1H), 6.97 (d, *J* = 8.5 Hz, 1H), 6.77 (d, *J* = 16.4 Hz, 1H), 4.12 (d, *J* = 17.0 Hz, 2H), 4.05 (d, *J* = 17.1 Hz, 2H), 3.98 (t, *J* = 6.1 Hz, 2H), 2.89 – 2.82 (m, 2H), 2.34 (s, 3H), 2.14 – 2.06 (m, 2H).

^{13}C NMR (101 MHz, Acetonitrile-d_3) δ 198.2, 168.4, 159.9, 143.3, 134.8, 134.6, 134.3, 133.7, 133.6, 133.0, 132.5, 128.7, 128.6, 128.0, 127.7, 127.2, 121.3, 116.1, 112.7, 101.4, 65.7, 59.0, 56.1, 26.7, 23.8. Unable to distinguish ^{13}C peaks between regioisomers.

^{11}B NMR (128 MHz, Acetonitrile-d_3) δ 11.6.

3-(*tert*-Butyl prop-2-enoate)phenylboronic acid MIDA-DG ester (321) and Isomers



General Procedure E: Phenylboronic acid MIDA-DG ester (113 mg, 0.3 mmol) was employed to yield the products as a white mixture of solids (119 mg, 58% total yield: **a**: 46%, **b**: 7%, **a+a'**: 3%, **a+b**: 2%, **SM**: 26% as determined by ^{1}H NMR).

Characterisation data for major isomer:

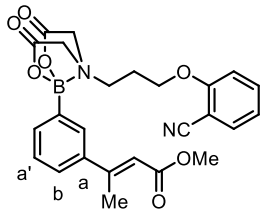
HRMS (ES- TOF) Calcd. for $C_{28}H_{30}N_2O_9B$ ([M + HCOO]$^-$): 549.2044. Found: 549.2054.

^{1}H NMR (400 MHz, Acetonitrile-d_3) δ 7.71 – 7.63 (m, 2H), 7.62 – 7.51 (m, 4H), 7.42 (d, J = 7.6 Hz, 1H), 7.10 – 7.03 (m, 1H), 6.97 (d, J = 8.3 Hz, 1H), 6.43 (d, J = 16.0 Hz, 1H), 4.11 (d, J = 17.1 Hz, 2H), 4.03 (d, J = 17.1 Hz, 2H), 3.98 (t, J = 6.2 Hz, 2H), 2.87 – 2.80 (m, 2H), 2.15 – 2.06 (m, 2H), 1.53 (s, 9H).

^{13}C NMR (101 MHz, Acetonitrile-d_3) δ 168.5, 168.4, 159.7, 143.7, 134.8, 134.3, 133.7, 133.6, 132.6, 132.5, 128.5, 128.0, 127.5, 121.3, 120.0, 116.1, 112.8, 109.8, 65.8, 59.0, 56.1, 27.4, 23.8. Unable to distinguish ^{13}C peaks between regioisomers.

^{11}B NMR (128 MHz, Acetonitrile-d_3) δ 11.7.

3-(4-Methoxy-4-oxobut-2-en-2-yl)phenylboronic acid MIDA-DG ester (322) and Isomers



General Procedure E: Phenylboronic acid MIDA-DG ester (113 mg, 0.3 mmol) was employed to yield the products as a white mixture of solids (48 mg, 16% total yield: **a**: 12%, **b**: 3%, **a+a'**: 1%, **SM**: 21%, as determined by ^{1}H NMR).

Characterisation data for major isomer:

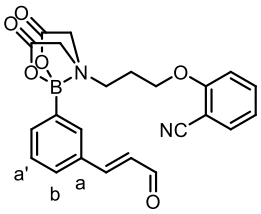
HRMS (ES+ TOF) Calcd. for $C_{25}H_{26}N_2O_7B$ ([M + H]$^+$): 477.1833. Found: 477.1849.

^{1}H NMR (400 MHz, Acetonitrile-d_3) δ 7.64 – 7.56 (m, 3H), 7.56 – 7.53 (m, 2H), 7.42 (d, J = 7.6 Hz, 1H), 7.06 (td, J = 7.6, 0.8 Hz, 1H), 6.98 (d, J = 8.5 Hz, 1H), 6.17 (q, J = 1.3 Hz, 1H), 4.11 (d, J = 17.0 Hz, 2H), 4.03 (d, J = 17.1 Hz, 2H), 3.99 – 3.96 (m, 2H), 3.72 (s, 3H), 2.88 – 2.79 (m, 2H), 2.56 (s, 3H), 2.16 – 2.06 (m, 2H).

^{13}C NMR (101 MHz, Acetonitrile-d_3) δ 170.4, 168.5, 168.5, 141.5, 134.8, 133.7, 133.6, 133.4, 132.5, 130.3, 129.3, 128.2, 128.0, 127.4, 121.3, 116.4, 112.7, 106.7, 101.4, 65.8, 65.8, 59.0, 58.9, 56.1, 55.9, 23.8, 23.8, 17.2. Unable to distinguish 13C peaks between regioisomers.

^{11}B NMR (128 MHz, Acetonitrile-d_3) δ 11.8.

3-(Prop-2-enal)phenylboronic acid MIDA-DG ester (324) and Isomers



General Procedure E: Phenylboronic acid MIDA-DG ester (113 mg, 0.3 mmol) was employed to yield the products as a white mixture of solids (111 mg, 65% total yield: **a**: 60%, **b**: 5%, **SM**: 24%, as determined by ^{1}H NMR).

Characterisation data for major isomer:

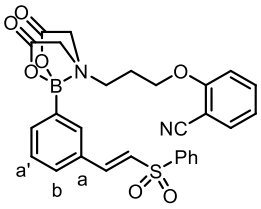
HRMS (ES+ TOF) Calcd. for $C_{23}H_{22}N_2O_6B$ ([M + H]$^+$): 433.1571. Found: 433.1581.

^{1}H NMR (400 MHz, Acetonitrile-d_3) δ 9.69 (d, J = 7.7 Hz, 1H), 7.77 (d, J = 1.6 Hz, 1H), 7.71 (dt, J = 7.9, 1.5 Hz, 1H), 7.66 (d, J = 16.0 Hz, 1H), 7.61 – 7.54 (m, 2H), 7.47 (t, J = 7.6 Hz, 1H), 7.05 (tt, J = 7.6, 0.9 Hz, 1H), 6.97 (d, J = 8.4 Hz, 1H), 6.77 (dd, J = 16.0, 7.7 Hz, 1H), 4.12 (d, J = 17.0 Hz, 2H), 4.05 (d, J = 17.0 Hz, 2H), 3.99 (t, J = 5.9 Hz, 2H), 2.89 – 2.83 (m, 2H), 2.15 – 2.06 (m, 2H).

^{13}C NMR (101 MHz, Acetonitrile-d_3) δ 194.0, 168.4, 153.2, 135.4, 134.8, 133.7, 133.6, 133.2, 132.5, 129.3, 129.0, 128.7, 128.5, 128.0, 128.0, 121.3, 116.1, 112.7, 101.4, 65.7, 59.1, 56.1, 23.8. Unable to distinguish ^{13}C peaks between regioisomers.

^{11}B NMR (128 MHz, Acetonitrile-d_3) δ 11.6.

3-(2-(Phenylsulfonyl)vinyl)phenylboronic acid MIDA-DG ester (323) and Isomers



General Procedure E: Phenylboronic acid MIDA-DG ester (113 mg, 0.3 mmol) was employed to yield the products as a white mixture of solids (113 mg, 35% total yield: **a**: 30%, **b**: 5%, **SM**: 49%, as determined by ^{1}H NMR).

Characterisation data for major isomer:

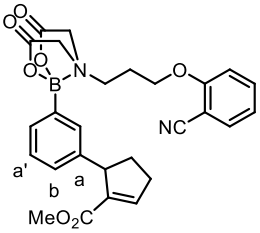
HRMS (ES+ TOF) Calcd. for $C_{28}H_{26}N_2O_7BS$ ([M + H]$^+$): 545.1554. Found: 545.1564.

^{1}H NMR (400 MHz, Acetonitrile-d_3) δ 7.98 – 7.93 (m, 2H), 7.74 – 7.68 (m, 3H), 7.67 – 7.55 (m, 6H), 7.43 (d, J = 7.6 Hz, 1H), 7.17 (d, J = 15.5 Hz, 1H), 7.04 (td, J = 7.6, 0.8 Hz, 1H), 6.94 (dt, J = 8.4, 0.8 Hz, 1H), 4.11 (d, J = 17.1 Hz, 2H), 4.03 (d, J = 17.1 Hz, 2H), 3.96 (t, J = 6.1 Hz, 2H), 2.82 (ddd, J = 11.3, 4.7, 3.1 Hz, 2H), 2.15 – 2.05 (m, 2H).

^{13}C NMR (101 MHz, Acetonitrile-d_3) δ 168.4, 159.8, 142.7, 141.1, 135.4, 133.6, 133.5, 133.2, 132.3, 129.5, 129.5, 129.4, 128.7, 127.6, 127.4, 121.2, 116.1, 101.4, 65.7, 59.1, 56.1, 23.8. Unable to distinguish ^{13}C peaks between regioisomers.

^{11}B NMR (128 MHz, Acetonitrile-d_3) δ 11.8.

3-(2-(2-(Methoxycarbonyl)cyclopent-2-en-1-yl)phenylboronic acid MIDA-DG ester (325) and Isomers



General Procedure E: Phenylboronic acid MIDA-DG ester (113 mg, 0.3 mmol) was employed to yield the products as a white mixture of solids (125 mg, 67% total yield: **a**: 46%, **b**: 21%, **SM**: 22%, as determined by ^{1}H NMR).

Characterisation data for major isomer:

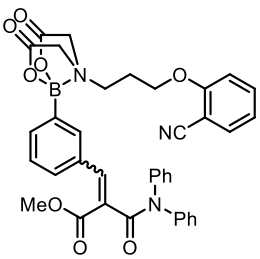
HRMS (ES- TOF) Calcd. for $C_{28}H_{28}N_2O_9B$ ([M + HCOO]$^-$): 547.1888. Found: 547.1900.

^{1}H NMR (400 MHz, Acetonitrile-d_3) δ 7.63 – 7.55 (m, 2H), 7.34-7.28 (m, 2H), 7.18 (dt, J = 7.1, 2.1 Hzj, 1H), 7.13 – 7.04 (m, 2H), 7.00 (dt, J = 8.6, 3.0 Hz, 1H), 6.95 (dp, J = 6.7, 1.9 Hz, 1H), 4.16 – 4.09 (m, 1H), 4.08 – 4.00 (m, 4H), 3.99-3.92 (m, 2H), 3.51 (s, 3H), 2.87 – 2.77 (m, 2H), 2.69 – 2.58 (m, 1H), 2.56 – 2.44 (m, 2H), 2.14 – 2.05 (m, 2H), 1.88 – 1.74 (m, 1H).

^{13}C NMR (101 MHz, Acetonitrile-d_3) δ 168.5, 164.8, 159.9, 145.1, 138.8, 134.8, 133.6, 132.5, 131.3, 130.3, 129.3, 129.1, 128.0, 126.6, 121.3, 116.1, 112.8, 101.4, 65.8, 65.8, 58.9, 56.0, 50.7, 50.0, 33.8, 31.9, 23.8. Unable to distinguish ^{13}C peaks between regioisomers.

^{11}B NMR (128 MHz, Acetonitrile-d_3) δ 11.9.

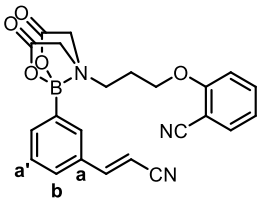
1-(Methoxycarbonyl)-1-(bisphenylamido)Ethene alkenylated phenyboronic acid MIDA-DG ester (326) and Isomers



General Procedure E: Phenylboronic acid MIDA-DG ester (113 mg, 0.3 mmol) was employed, with only 1.2 equivalents of the coupling partner (accessed using the method described in *J. Org.*

Chem. 2016, 81, 9947-9956), to yield the product as a white mixture of solids (156 mg, 0.24 mmol, 79% as a 6 : 1 ratio of *meta*:*para* isomers as determined by ^{1}H NMR). The *E:Z* ratio is unknown.
Characterisation data for major isomer:
HRMS (ES+ TOF) Calcd. for $C_{37}H_{33}N_3O_8B$ ([M + H]$^+$): 658.2361. Found: 658.2374.
^{1}H NMR (400 MHz, Acetonitrile-d_3) δ 7.75 (d, *J* = 1.5 Hz, 1H), 7.70 – 7.61 (m, 2H), 7.60 – 7.50 (m, 3H), 7.46 – 7.42 (m, 6H), 7.42 – 7.36 (m, 2H), 7.34 – 7.26 (m, 3H), 7.18 (dd, *J* = 8.3, 6.4 Hz, 2H), 7.04 (td, *J* = 7.7, 1.0 Hz, 1H), 6.93 (dd, *J* = 8.3, 1.2 Hz, 3H), 4.05 (dd, *J* = 5.2, 3.5 Hz, 4H), 3.89 (t, *J* = 6.2 Hz, 2H), 3.83 (s, 1H), 3.80 (s, 3H), 2.80 (dd, *J* = 10.2, 5.9 Hz, 2H), 2.12 – 2.01 (m, 2H). Integrals corresponding to aromatic protons are combined with the *para* isomer.
^{13}C NMR (101 MHz, Acetonitrile-d_3) δ 168.4, 168.4, 166.1, 165.3, 164.9, 159.8, 142.9, 142.2, 141.8, 141.1, 134.9, 134.7, 134.2, 133.9, 133.7, 133.4, 133.2, 133.1, 132.5, 130.5, 129.3, 129.2, 129.2, 129.1, 128.7, 128.2, 127.7, 127.6, 127.1, 126.9, 126.6, 121.3, 116.1, 112.7, 101.4, 65.7, 59.0, 58.9, 56.0, 56.0, 52.2, 51.7, 23.8. Unable to distinguish ^{13}C peaks between regioisomers.
^{11}B NMR (128 MHz, Acetonitrile-d_3) δ 11.7.

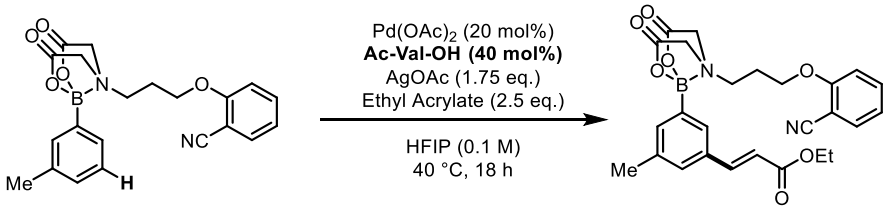
3-(2-Cyanovinyl)phenylboronic acid MIDA-DG ester (327) and Isomers



General Procedure E: Phenylboronic acid MIDA-DG ester (113 mg, 0.3 mmol) was employed, with only 2 equivalents of the vinyl cyanide, to yield the products as a white mixture of solids after 48 hours (104 mg, 58% total yield: **a**: 50%, **b**: 8%, **SM**: 26%, as determined by ^{1}H NMR). The *meta* and *para* products were a mixture of *E* and *Z* isomers both in a 1.2 :1.0 ratio respectively.
Characterisation data for major isomer:
HRMS (ES+ TOF) Calcd. for $C_{23}H_{21}N_3O_5B$ ([M + H]$^+$): 430.1574. Found: 430.1586.
Aromatic peaks that could not be assigned to a certain stereoisomer are labelled: ***E** or **Z***
Peaks that overlap for both isomers are labelled: ***E** and **Z***, and the integral corresponding to one isomer given.
^{1}H NMR (400 MHz, Acetonitrile-d_3) δ 7.88 (d, *J* = 1.4 Hz, 1H, ***E** or **Z***), 7.66 (d, *J* = 1.6 Hz, 1H, ***E** or **Z***), 7.63 – 7.55 (m, 2H, ***E** and **Z***), 7.52 – 7.49 (m, 1H, ***E** or **Z***), 7.44 (t, *J* = 7.6 Hz, 1H, ***E** or **Z***), 7.34 (d, *J* = 12.1 Hz, 1H, ***Z***), 7.07 (dddd, *J* = 8.5, 7.6, 1.9, 0.9 Hz, 1H, ***E** and **Z***), 6.97 (d, *J* = 8.5 Hz, 1H, ***E** and **Z***), 6.13 (d, *J* = 16.8 Hz, 1H, ***E***), 5.62 (d, *J* = 12.1 Hz, 1H, ***Z***), 4.11 (d, *J* = 17.1 Hz, 2H, ***E** and **Z***), 4.04 (d, *J* = 18.6 Hz, 2H, ***E** and **Z***), 4.01 – 3.96 (m, 2H, ***E** and **Z***), 2.89 – 2.79 (m, 2H, ***E** or **Z***), 2.15 – 2.05 (m, 2H, ***E** or **Z***).

^{13}C NMR (101 MHz, Acetonitrile-d_3) δ 168.5, 168.4, 159.8, 150.8, 149.2, 135.3, 134.9, 133.5, 133.3, 132.5, 132.0, 129.3, 129.2, 128.7, 128.6, 128.1, 128.0, 126.9, 121.3, 116.1, 112.7, 101.3, 96.4, 95.4, 65.8, 65.7, 59.0, 56.1, 56.0, 23.8. Unable to distinguish ^{13}C peaks between regioisomers.
^{11}B NMR (128 MHz, Acetonitrile-d_3) δ 11.8.

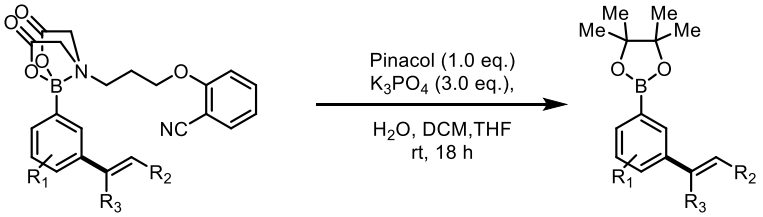
3-Methyl-5-(ethyl prop-2-enoate)phenylboronic acid MIDA-DG ester (295) and Isomers (with Ac-Val-OH as ligand)



295 **310**
66% (4:1 *meta*:others)

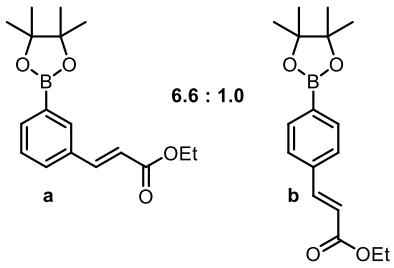
A 20 mL vial was charged with 3-Methylphenylboronic acid MIDA-DG ester (118 mg, 0.3 mmol), AgOAc (88 mg, 0.53 mmol), Ac-Val-OH (19 mg, 0.12 mmol) and $Pd(OAc)_2$ (14 mg, 0.06 mmol). The vial was then charged with HFIP (3 mL, 0.1 M) and ethyl acrylate (82 μL, 0.75 mmol) was added. The vial was sealed and stirred at 40 °C for 8 hours. The reaction mixture was diluted with MeCN (~5 mL) and dry loaded onto a silica column. The column was washed with Et_2O (100 mL) before the products were subsequently eluted with 1:1 MeCN:Et_2O. The eluent was concentrated under vacuum to yield the alkenylated products as an off-white mixture of solids (133 mg, 69% total yield: ***meta***: 56%, ***para***: 13%, **SM**: 27%, as determined by ^{1}H NMR). The characterisation data was in agreement with that reported above.

General procedure F for the synthesis of aryl boronic acid pinacol esters from the corresponding MIDA-DG ester:



To a 20 mL vial was added the alkenylated boronic acid MIDA-DG mixture (1 eq.), pinacol (1 eq.) and K_3PO_4 (3 eq.). The mixture was suspended in DCM (0.1 M), THF (1 M) and water (0.2 M), the vial sealed and stirred at 40 °C for 16 hours. The reaction mixture was then cooled to room temperature, diluted with water (1.5 mL), the organic layer separated and the aqueous layer further extracted with DCM (2 × 3 mL). The organic mixture was concentrated and purified *via* FCC (10% EtOAc in hexane) to yield the desired mono-alkenylated aryl boronic acid pinacol ester.

Ethyl (*E*)-3-(3-(4,4,5,5-tetramethyl-1,3,2-dioxaborolan-2-yl)phenyl)acrylate (346)



General procedure F: The corresponding alkenylated boronic acid MIDA-DG ester (0.26 mmol) was used as a mixture of regioisomers to yield the mono-alkenylated pinacol boronate esters as a white solid. The ratio of *meta* (**a**) : *para* (**b**) in the isolated mixture was 6.6 : 1.0 (53 mg, 0.17 mmol, 67%).

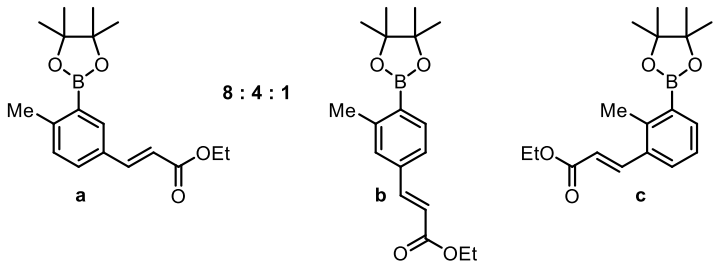
^{1}H NMR (400 MHz, Chloroform-*d*) δ 8.01 (td, *J* = 1.4, 0.7 Hz, 1H, **a**), 7.83 (dt, *J* = 7.3, 1.2 Hz, 1H, **a** and **b**), 7.73 (d, *J* = 16.0 Hz, 1H, **a** and **b**), 7.65 – 7.58 (m, 1H, **a**), 7.54 (d, *J* = 7.9 Hz, 1H, **b**), 7.41 (t, *J* = 7.6 Hz, 1H, **a**), 6.56 – 6.48 (m, 1H, **a** and **b**), 4.28 (q, *J* = 7.1 Hz, 2H, **a** and **b**), 1.40 – 1.32 (m, 18H **a** and **b**).

^{13}C NMR (101 MHz, Chloroform-*d*) δ 167.0 (**a** and **b**), 144.5 (**a**), 144.4 (**b**), 136.9 (**b**), 136.5 (**a**), 135.2 (**b**), 134.7 (**b**), 134.4 (**a**), 133.8 (**a**), 131.2, 130.8 (**a**), 128.3 (**a**), 127.2 (**b**), 119.2 (**b**), 118.4 (**a**), 84.0 (**a** and **b**), 60.5 (**b**), 60.4 (**a**), 24.9 (**a** and **b**), 14.3 (**a** and **b**).

^{11}B NMR (128 MHz, Chloroform-*d*) δ 30.9.

The characterisation data is in agreement with that reported in the literature (*Org. Lett.* 2015, 17, 5792-5795).

Ethyl (*E*)-3-(4-methyl-3-(4,4,5,5-tetramethyl-1,3,2-dioxaborolan-2-yl)phenyl)acrylate (332)



General procedure F: The corresponding alkenylated boronic acid MIDA-DG ester (0.09 mmol) was used as a mixture of regioisomers to yield the mono-alkenylated pinacol boronate esters as a clear glassy solid. The ratio of *meta* (**a**) : *para* (**b**) : *meta* (**c**) in the isolated mixture was 8 : 4 : 1 (28 mg, 0.09 mmol, 100%).

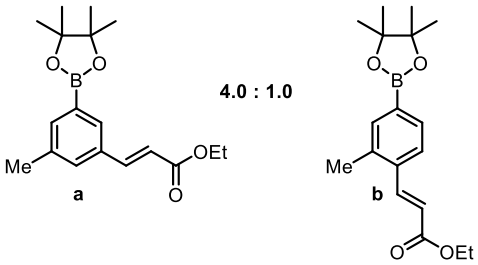
HRMS (APCI +) Calcd. for $C_{18}H_{26}O_4B$ ([M + H]$^+$): 317.1919. Found: 317.1909.

^{1}H NMR (400 MHz, Chloroform-*d*) δ 8.10 (d, *J* = 15.8 Hz, 1H, **c**), 7.96 (d, *J* = 2.0 Hz, 1H, **a**), 7.79 (d, *J* = 7.6 Hz, 1H, **b** and **c**), 7.75 – 7.66 (d, *J* = 15.8 Hz, 1H, **a**), 7.67 (d, , *J* = 15.8 Hz, 1H, **b**), 7.61 (dd, J = 7.8, 1.4 Hz, 1H, **c**), 7.49 (dd, *J* = 7.9, 2.1 Hz, 1H, **a**), 7.35 (d, *J* = 1.7 H, 1H, **b**), 7.33 (s, 1H, **a**), 7.20 (d, *J* = 7.9 Hz, 1H, **a**, **b**, and **c**), 6.49 (d, *J* = 15.8 Hz, 1H, **b**), 6.46 (d, *J* = 15.8 Hz, 1H, **a**), 6.33 (d, *J* = 15.8 Hz, 1H, **c**), 4.28 (qd, *J* = 7.1, 2.6 Hz, 2H, **a**, **b**, and **c**), 2.65 (s, 3H, **c**), 2.57 (s, 3H, **a** and **b**), 1.43 – 1.30 (m, 15H, **a**, **b**, and **c**).

^{13}C NMR (101 MHz, Chloroform-*d*) δ 167.2 (**a**), 167.0 (**b** and **c**), 147.6 (**a**), 145.4 (**b)**, 144.6 (**a**), 144.6 (**b** and **c**), 137.6 (**b**), 136.5 (**c**), 136.4 (**b**), 135.8 (**a**), 131.0 (**a**), 130.8 (**c**), 130.4 (**a**), 130.2 (**a**), 129.8 (**c** and **b**), 129.4 (**a**), 129.0 (**c**), 125.4 (**c**), 124.7 (**c**), 124.2 (**b**), 118.9 (**b**), 117.1 (**a**), 83.7 (**a**, and **c**), 83.6 (**b**), 60.5 (**b**), 60.3 (**a** and **c**), 24.9 (**a**, **b**, and **c**), 22.2 (**a** and **c**), 22.2 (**b**), 14.4 (**a**, **b**, and **c**).

^{11}B NMR (128 MHz, Chloroform-*d*) δ 31.3.

Ethyl (*E*)-3-(3-methyl-5-(4,4,5,5-tetramethyl-1,3,2-dioxaborolan-2-yl)phenyl)acrylate (333)



General procedure F: The corresponding alkenylated boronic acid MIDA-DG ester (0.26 mmol) was used as a mixture of regioisomers to yield the mono-alkenylated pinacol boronate esters as a clear glassy solid. The ratio of *meta* (**a**) : *para* (**b**) in the isolated mixture was 4.0 : 1.0 (48 mg, 0.15 mmol, 58%).

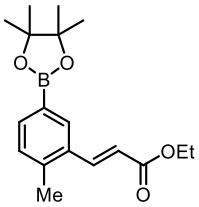
HRMS (APCI +) Calcd. for $C_{18}H_{26}O_4B$ ([M + H]$^+$): 317.1919. Found: 317.1920.

^{1}H NMR (400 MHz, Chloroform-*d*) δ 8.00 (d, *J* = 15.9 Hz, 1H, **b**), 7.84 – 7.80 (m, 1H, **a**), 7.74 – 7.63 (m, 2H, **a** and **b**), 7.57 (d, *J* = 7.8 Hz, 1H, **b**), 7.44 (td, *J* = 1.7, 0.8 Hz, 1H, **a**), 6.50 (d, *J* = 16.0 Hz, 1H, **a**), 6.42 (d, *J* = 15.9 Hz, 1H, **b**), 4.27 (q, *J* = 7.1 Hz, 2H, **a** and **b**), 2.46 (s, 4H, **b**), 2.39 (s, 3H, **a**), 1.39 – 1.32 (m, 15H, **a** and **b**).

^{13}C NMR (101 MHz, Chloroform-*d*) δ 167.1 (**a**), 167.0 (**b**), 144.7 (**a**), 142.1 (**b**), 137.8 (**b**), 137.3 (**a**), 137.1 (**a**), 136.7 (**b**), 135.3 (**b**), 133.9 (**b**), 132.6 (**a**), 131.8 (**b**), 131.7 (**a**), 131.5 (**a**), 125.6 (**b**), 120.1 (**b**), 118.2 (**a**), 84.0 (**a**), 84.0 (**b**), 60.5 (**b**), 60.4 (**a**), 24.9 (**a** and **b**), 21.1 (**a**), 19.6 (**b**), 14.3 (**a** and **b**).

^{11}B NMR (128 MHz, Chloroform-*d*) δ 31.1.

Ethyl (*E*)-3-(2-methyl-5-(4,4,5,5-tetramethyl-1,3,2-dioxaborolan-2-yl)phenyl)acrylate (334)



General procedure F: The corresponding alkenylated boronic acid MIDA-DG ester (0.13 mmol) was used as a mixture of regioisomers to yield the pinacol boronate ester as a clear glassy solid (28 mg, 0.09 mmol, 69%).

ν_{max}/cm^{-1} 2978, 1715, 1636, 1607, 1357, 1320, 1260, 1163, 965, 857, 708

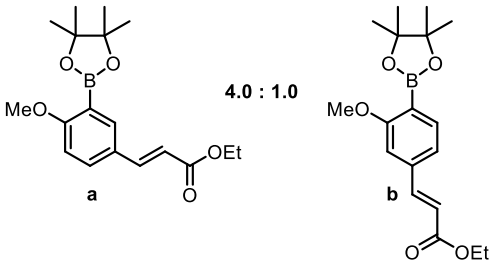
HRMS (APCI +) Calcd. for $C_{18}H_{26}O_4B$ ([M + H]$^+$): 317.1919. Found: 317.1921.

^{1}H NMR (400 MHz, Chloroform-*d*) δ 8.04 (d, *J* = 1.2 Hz, 1H), 8.00 (d, *J* = 15.9 Hz, 1H), 7.72 (dd, *J* = 7.5, 1.3 Hz, 1H), 7.23 (d, *J* = 7.6 Hz, 1H), 6.50 (d, *J* = 15.8 Hz, 1H), 4.29 (q, *J* = 7.1 Hz, 2H), 2.48 (s, 3H), 1.37 (d, *J* = 1.8 Hz, 15H).

^{13}C NMR (101 MHz, Chloroform-*d*) δ 167.1, 142.1, 140.8, 136.2, 133.0, 132.9, 130.2, 119.5, 83.9, 60.4, 24.9, 20.1, 14.4.

^{11}B NMR (128 MHz, Chloroform-*d*) δ 30.8.

Ethyl (*E*)-3-(4-methoxy-3-(4,4,5,5-tetramethyl-1,3,2-dioxaborolan-2-yl)phenyl)acrylate (328)



General procedure F: The corresponding alkenylated boronic acid MIDA-DG ester (0.21 mmol) was used as a mixture of regioisomers to yield the mono-alkenylated pinacol boronate esters as a clear glassy solid. The ratio of *meta* (**a**) : *para* (**b**) in the isolated mixture was 4.0 : 1.0 (17 mg, 0.05 mmol, 25%).

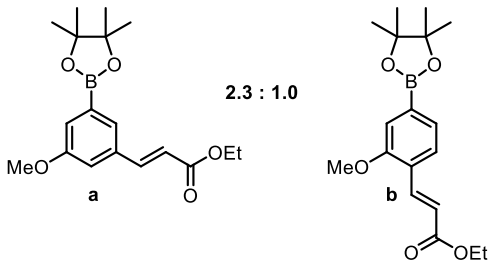
HRMS (APCI +) Calcd. for $C_{18}H_{26}O_5B$ ([M + H]$^+$): 333.1868. Found: 333.1860.

^{1}H NMR (400 MHz, Chloroform-*d*) δ 7.91 (d, *J* = 2.4 Hz, 1H, **a**), 7.73 – 7.64 (m, 1H, **a** and 2H, **b**), 7.58 (dd, *J* = 8.7, 2.4 Hz, 1H, **a**), 7.13 (dd, *J* = 7.6, 1.3 Hz, 1H, **b**), 6.99 (d, *J* = 1.3 Hz, 1H, **b**), 6.88 (d, *J* = 8.6 Hz, 1H, **a**), 6.49 (d, *J* = 16.0 Hz, 1H, **b**), 6.37 (d, *J* = 16.0 Hz, 1H, **a**), 4.32 – 4.22 (m, 2H, **a** and **b**), 3.88 (s, 3H, **a** and **b**), 1.39 – 1.32 (m, 15H, **a** and **b**).

^{13}C NMR (101 MHz, Chloroform-*d*) δ 167.4 (**a**), 166.9 (**b**), 165.8 (**a**), 164.4 (**b**), 144.5 (**b**), 144.2 (**a**), 138.4 (**b**), 137.1 (**b**), 136.8 (**a**), 132.7 (**a**), 129.8 (**b**), 126.6 (**a**), 120.2 (**b**), 119.1 (**b**), 115.7 (**a**), 110.6 (**a**), 109.4 (**b**), 83.7 (**a**), 83.7 (**b**), 60.6 (**b**), 60.3 (**a**), 55.9(**a**), 55.8 (**b**), 24.8 (**a** and **b**), 14.4 (**a**), 14.3 (**b**).

^{11}B NMR (128 MHz, Chloroform-*d*) δ 31.6.

Ethyl (*E*)-3-(3-methoxy-5-(4,4,5,5-tetramethyl-1,3,2-dioxaborolan-2-yl)phenyl)acrylate (329)



General procedure F: The corresponding alkenylated boronic acid MIDA-DG ester (0.10 mmol) was used as a mixture of regioisomers to yield the mono-alkenylated pinacol boronate esters as a clear glassy solid. The ratio of *meta* (**a**) : *para* (**b**) in the isolated mixture was 2.3 : 1.0 (18 mg, 0.05 mmol, 50%).

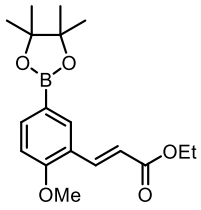
HRMS (APCI +) Calcd. for $C_{18}H_{26}O_5B$ ($[M + H]^+$): 333.1868. Found: 333.1867.

^{1}H NMR (400 MHz, Chloroform-*d*) δ 8.02 (d, *J* = 16.2 Hz, 1H, **a**), 7.69 (d, *J* = 16.0 Hz, 1H, **b**), 7.64 – 7.59 (m, 1H, **b**), 7.53 (d, *J* = 7.6 Hz, 1H, **a**), 7.42 (dd, *J* = 7.5, 1.0 Hz, 1H, **a**), 7.37 – 7.32 (m, 1H, **a** and **b**), 7.15 (dd, *J* = 2.7, 1.6 Hz, 1H, **b**), 6.59 (d, *J* = 16.2 Hz, 1H, **a**), 6.50 (d, *J* = 16.0 Hz, 1H, **b**), 4.28 (qd, *J* = 7.2, 2.0 Hz, 2H, **a** and **b**), 3.95 (s, 3H, **a**), 3.87 (d, *J* = 2.0 Hz, 3H, **b**), 1.36 (m, 15H, **a** and **b**).

^{13}C NMR (101 MHz, Chloroform-*d*) δ 167.4 (**a**), 167.0 (**b**), 159.4 (**b**), 157.6 (**a**), 144.4 (**b**), 139.9 (**a**), 135.3 (**b**), 128.1 (**a**), 127.1 (**a** and **b**), 126.1 (**a**), 120.9 (**b**), 119.7 (**a**), 118.7 (**b**), 116.7 (**b**), 116.7 (**a**), 84.1 (**b**), 84.1 (**a**), 60.5 (**b**), 60.4 (**a**), 55.6 (**a**), 55.4 (**b**), 24.9 (**a** and **b**), 14.4 (**a**), 14.3 (**b**).

^{11}B NMR (128 MHz, Chloroform-*d*) δ 30.8.

Ethyl (*E*)-3-(2-methoxy-5-(4,4,5,5-tetramethyl-1,3,2-dioxaborolan-2-yl)phenyl)acrylate (330)



General procedure F: The corresponding alkenylated boronic acid MIDA-DG ester (0.09 mmol) was used as a mixture of regioisomers to yield the pinacol boronate ester as a clear glassy solid (15 mg, 0.05 mmol, 50%).

ν_{max}/cm^{-1} 2978, 1707, 1632, 1603, 1357, 1249, 1163, 1126, 1025, 988, 854, 671

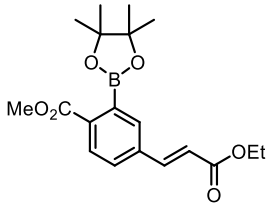
HRMS (APCI +) Calcd. for $C_{18}H_{26}O_5B$ ([M + H]$^+$): 333.1868. Found: 333.1856.

^{1}H NMR (400 MHz, Chloroform-*d*) δ 8.07 – 7.98 (m, 2H), 7.81 (dd, *J* = 8.3, 1.6 Hz, 1H), 6.93 (d, *J* = 8.3 Hz, 1H), 6.62 (d, *J* = 16.2 Hz, 1H), 4.27 (q, *J* = 7.1 Hz, 2H), 3.93 (s, 3H), 1.36 (d, *J* = 3.3 Hz, 15H).

^{13}C NMR (101 MHz, Chloroform-*d*) δ 167.5, 160.7, 139.8, 138.3, 135.8, 122.9, 118.9, 110.4, 83.8, 60.3, 55.5, 24.9, 14.4.

^{11}B NMR (128 MHz, Chloroform-*d*) δ 31.0.

Methyl (*E*)-3-(3-ethoxy-3-oxoprop-1-en-1-yl)-5-(4,4,5,5-tetramethyl-1,3,2-dioxaborolan-2-yl)benzoate (336)



The 2-methoxycarbonylphenylboronic acid MIDA-DG ester proved particularly hard to deprotect and, as such, more forcing conditions were required to access the pinacol ester.

The corresponding alkenylated boronic acid MIDA-DG ester (0.09 mmol) was used as a mixture of regioisomers . The boronic acid was dissolved in THF (1 mL) in a microwave vial, K_3PO_4 (3.0 eq.) and pinacol (1.0 eq.) added and the vial sealed. The reaction mixture was heated to 90 °C for one hour, cooled to room temperature, filtered and purified using preparative TLC to yield the mono-alkenylated pinacol boronate ester as a clear glassy solid (3 mg, 0.01 mmol, 10%). *The isolated sample contained a 10% impurity believed to be the* para *functionalised isomer.*

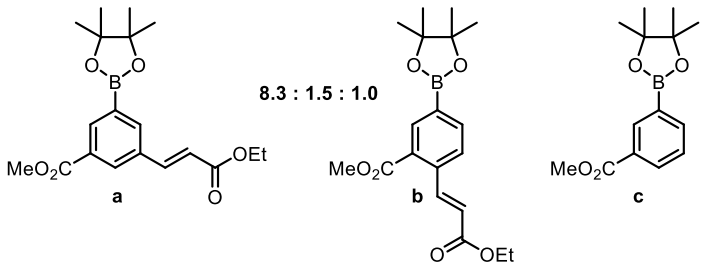
HRMS (APCI +) Calcd. for $C_{19}H_{26}O_6B$ ([M + H]$^+$): 361.1817. Found: 361.1822.

^{1}H NMR (400 MHz, Chloroform-*d*) δ 7.97 (d, *J* = 8.1 Hz, 1H), 7.71 (d, *J* = 16.1 Hz, 1H), 7.65 (d, *J* = 1.8 Hz, 1H), 7.57 (dd, *J* = 8.2, 1.9 Hz, 1H), 6.53 (d, *J* = 16.0 Hz, 1H), 4.29 (q, *J* = 7.1 Hz, 2H), 3.94 (s, 3H), 1.46 (s, 12H), 1.36 (t, *J* = 7.1 Hz, 3H).

^{13}C NMR (126 MHz, Chloroform-*d*) δ 167.9, 166.6, 143.3, 137.5, 134.6, 131.7, 129.3, 128.5, 120.5, 84.3, 60.7, 52.5, 24.9, 14.3.

^{11}B NMR (160 MHz, Chloroform-*d*) δ 31.4.

Methyl (*E*)-3-(3-ethoxy-3-oxoprop-1-en-1-yl)-5-(4,4,5,5-tetramethyl-1,3,2-dioxaborolan-2-yl)benzoate (337)



General procedure F: The corresponding alkenylated boronic acid MIDA-DG ester (0.09 mmol) was used as a mixture of regioisomers to yield the mono-alkenylated pinacol boronate esters as a clear glassy solid. The ratio of *meta* (**a**) : *para* (**b**) : starting material (**c**) in the isolated mixture was 8.3 : 1.5 : 1.0 (14 mg, 0.04 mmol, 44%).

HRMS (APCI +) Calcd. for $C_{19}H_{26}O_6B$ ([M + H]$^+$): 361.1817. Found: 361.1821.

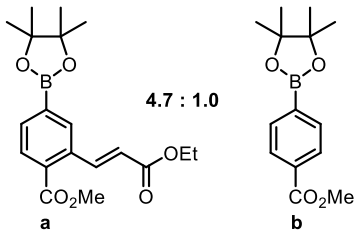
^{1}H NMR (400 MHz, Chloroform-*d*) δ 8.52 – 8.41 (m, 1H, **a**, **b**, and **c**), 8.38 (d, *J* = 1.3 Hz, 1H, **b**), 8.29 (t, *J* = 1.8 Hz, 1H, **a**), 8.16 (t, *J* = 1.4 Hz, 1H, **a** and **c**), 8.00 (dt, *J* = 7.4, 1.3 Hz, 1H, **c**), 7.96 (dd, *J* = 7.7, 1.3 Hz, 1H, **b**), 7.75 (d, *J* = 16.0 Hz, 1H, **a**), 7.62 (d, *J* = 7.8 Hz, 1H, **b**), 7.47 (t, *J* = 7.6 Hz, 1H, **c**), 6.59 (d, *J* = 16.0 Hz, 1H, **a**), 6.36 (d, *J* = 15.9 Hz, 1H, **b**), 4.29 (q, *J* = 7.2 Hz, 2H, **a** and **b**), 3.98 – 3.91 (m, 3H, **a**, **b**, and **c**), 1.47 – 1.26 (m, 15H, **a**, **b**, and **c**).

^{13}C NMR (101 MHz, Chloroform-*d*) δ 166.7 (**a**), 166.6 (**a**), 143.5 (**b**), 143.4 (**a**), 139.2 (**b**), 138.4 (**a**), 137.2 (**a**), 137.0 (**b**), 135.8 (**b**), 134.3 (**a**), 131.6 **(a)**, 130.4 (**a**), 119.6 (**a**), 84.4 (**a** and **b**), 84.3 (**c**), 60.6 (**a** and **b**), 52.3 (**a** and **b**), 24.9 (**a**, **b**, and **c**), 14.3 (**a** and **b**). Unable to fully characterise ^{13}C for **b** and **c**.

^{11}B NMR (128 MHz, Chloroform-*d*) δ 30.5.

The characterisation data for **c** is in agreement with that reported in the literature (*Angew. Chem. Int. Ed.* 2018, 57, 16721-16726).

Methyl (*E*)-2-(3-ethoxy-3-oxoprop-1-en-1-yl)-4-(4,4,5,5-tetramethyl-1,3,2-dioxaborolan-2-yl)benzoate (338)



General procedure F: The corresponding alkenylated boronic acid MIDA-DG ester (0.07 mmol) was used as a mixture of regioisomers to yield the pinacol boronate ester as clear glassy solids. The ratio of product (**a**) : non-alkenylated material (**b**) in the isolated mixture was 4.7 : 1.0 (15 mg, 0.04 mmol (**a**), 51%).

HRMS (APCI +) Calcd. for $C_{19}H_{26}O_6B$ ([M + H]$^+$): 361.1817. Found: 361.1809.

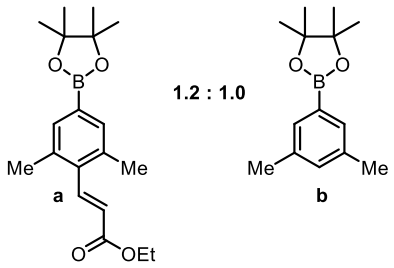
^{1}H NMR (400 MHz, Chloroform-*d*) δ 8.43 (d, *J* = 15.9 Hz, 1H, **a**), 8.06 (s, 1H, **a**), 8.04 (d, *J* = 8.4 Hz, 2H, **b**), 7.95 (d, *J* = 7.7 Hz, 1H, **a**), 7.89 (d, *J* = 8.3 Hz, 2H, **b**), 7.86 (dd, *J* = 7.8, 1.2 Hz, 1H, **a**), 6.43 (d, *J* = 15.9 Hz, 1H, **a**), 4.29 (q, *J* = 7.1 Hz, 2H, **a**), 3.96 (s, 3H, **a**), 3.94 (s, 3H, **b**), 1.41 – 1.33 (m, 15H, **a** and 12H, **b**).

^{13}C NMR (101 MHz, Chloroform-*d*) δ 167.3 (**a**), 166.7 (**a**), 143.5 (**a**), 135.4 (**a**), 135.3 (**a**), 134.7 (**b**), 134.3 (**a**), 132.0 (**a**), 129.8 (**a**), 128.6 (**b**), 121.2 (**a**), 84.4 (**a**), 60.5 (**a**), 52.4 (**a**), 24.9 (**a**), 14.3 (**a**).

^{11}B NMR (128 MHz, Chloroform-*d*) δ 30.9.

The characterisation data for **b** is in agreement with that reported in the literature (*J. Am. Chem. Soc*. 2017, 139, 607-610).

Ethyl (*E*)-3-(2,6-dimethyl-4-(4,4,5,5-tetramethyl-1,3,2-dioxaborolan-2-yl)phenyl)acrylate (345)



General procedure F: The corresponding alkenylated boronic acid MIDA-DG ester (0.12 mmol) was used as a mixture with the non-alkenylated starting material to yield the pinacol boronate esters as a clear glassy solid. The ratio of product (**a**) : non-alkenylated material (**b**) in the isolated mixture was 1.2 : 1.0 (38 mg, 0.06 mmol (**a**), 50%).

HRMS (APCI +) Calcd. for $C_{19}H_{28}O_4B$ ([M + H]$^+$): 331.2075. Found: 331.2074.

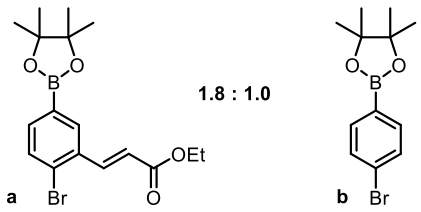
^{1}H NMR (400 MHz, Chloroform-*d*) δ 7.87 (d, *J* = 16.4 Hz, 1H, **a**), 7.54 (s, 2H, **a**), 7.47 (s, 2H, **b**), 7.13 (s, 1H, **b**), 6.11 (d, *J* = 16.4 Hz, 1H, **a**), 4.31 (q, *J* = 7.2 Hz, 2H, **a**), 2.38 (s, 6H, **a**), 2.35 (s, 6H, **b**), 1.37 (d, *J* = 1.6 Hz, 15H, **a** and 12H, **b**).

^{13}C NMR (101 MHz, Chloroform-*d*) δ 166.7 (**a**), 143.2 (**a**), 137.2 (**b**), 137.0 (**a**), 135.8 (**a**), 134.4 (**a**), 133.0 (**b**), 132.4 (**b**), 124.3 (**a**), 83.9 (**a**), 83.7 (**b**), 60.6 (**a**), 24.9 (**a** and **b**), 21.2 (**b**), 20.8 (**a**)f, 14.3 (**a**).

^{11}B NMR (128 MHz, Chloroform-*d*) δ 31.1.

The characterisation data for **b** is in agreement with that reported in the literature (*Org. Lett.* 2018, 20, 5564-5568).

Ethyl (*E*)-3-(2-bromo-5-(4,4,5,5-tetramethyl-1,3,2-dioxaborolan-2-yl)phenyl)acrylate (341)



General procedure F: The corresponding alkenylated boronic acid MIDA-DG ester (0.17 mmol) was used as a mixture with the non-alkenylated starting material to yield the pinacol boronate esters as a clear glassy solid. The ratio of product (**a**) : non-alkenylated material (**b**) in the isolated mixture was 1.8 : 1.0 (28 mg, 0.05 mmol (**a**), 29%). The mixture also contained a small impurity believed to correspond to *ortho* alkenylated 4-bromophenylboronic acid, that could not be fully characterised.

HRMS (TOF ES-) Calcd. for $C_{17}H_{21}O_4BBr$ ([M − H]$^-$): 379.0716. Found: 379.0735.

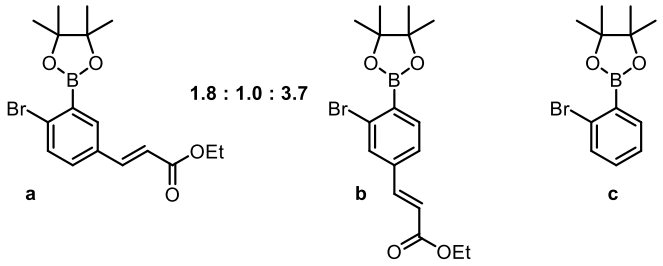
^{1}H NMR (400 MHz, Chloroform-*d*) δ 8.12 – 8.02 (m, 2H, **a**), 7.68 (d, *J* = 8.3 Hz, 2H, **b**), 7.63 (m, 2H, **a**), 7.55 – 7.50 (m, 2H, **b**), 6.52 (d, *J* = 16.0 Hz, 1H, **a**), 4.30 (q, *J* = 7.1 Hz, 2H, **a**), 1.36 (d, *J* = 3.7 Hz, 15H, **a** and 12H **b**).

^{13}C NMR (101 MHz, Chloroform-*d*) δ 166.5 (**a**), 142.9, 142.8 (**a**), 137.1 (**a**), 136.3 (**b**), 134.2 (**a**), 134.0 (**a**), 133.4, 132.9 (**a**), 131.1, 131.0 (**b**), 128.7 (**a**), 127.8, 127.7, 126.2 (**b**), 121.3 (**a**), 121.1, 84.3 (**a**), 84.0 (**b**), 60.7 (**a**), 24.9 (**a** and **b**), 14.3 (**a**). Peaks that are unassigned are believed to correspond to the 2-alkenylated 4-bromophenylboronic acid pinacol ester.

^{11}B NMR (128 MHz, Chloroform-*d*) δ 30.9.

The characterisation data for **b** is in agreement with that reported in the literature (*J. Org. Chem.* 2018, 83, 12831-12837).

Ethyl (*E*)-3-(2-bromo-5-(4,4,5,5-tetramethyl-1,3,2-dioxaborolan-2-yl)phenyl)acrylate (340)



General procedure F: The corresponding alkenylated boronic acid MIDA-DG ester (0.14 mmol) was used as a mixture with the non-alkenylated starting material to yield the pinacol boronate esters as a clear glassy solid. The ratio of product (**a**) : non-alkenylated material (**b**) : starting material (**c**) in the isolated mixture was 1.8 : 1.0 : 3.0 (13 mg, 0.01 mmol (**a**), 0.01 (**b**), 12% yield).

HRMS (APCI +) Calcd. for $C_{19}H_{26}O_6B$ ([M + H]$^+$): 381.0867. Found: 381.0869.

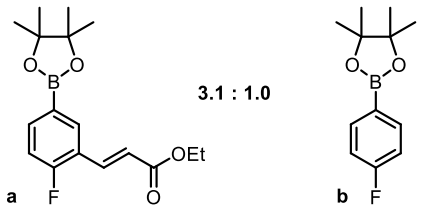
^{1}H NMR (400 MHz, Chloroform-*d*) δ 8.07 (d, *J* = 15.9 Hz, 1H, **b**), 7.68 – 7.60 (m, 2H, **a** and 1H, **c**), 7.59 – 7.52 (m, 1H, **a,** 1H, **b** and 1H, **c**), 7.44 – 7.38 (m, 1H, **a** and 2H, **b**), 7.31 (m, 1H, **c**), 7.26 (m, 1H, **c**), 6.47 (d, *J* = 16.0 Hz, 1H, **a**), 6.41 (d, *J* = 15.9 Hz, 1H, **b**), 4.30 (app. p, *J* = 7.3 Hz, 2H, **a** and **b**), 1.40 (s, 12H, **a, b**, and **c**), 1.38 – 1.34 (m, 3H, **a** and **b**).

^{13}C NMR (101 MHz, Chloroform-*d*) δ 167.3 (**a**), 143.2 (**a**), 136.4 (**c**), 132.6 (**c**), 132.1 (**a**), 131.9 (**c**), 129.4 (**a**), 128.0 (**c**), 127.8 (**b**), 127.7 (**a**), 126.3 (**c**), 121.2 (**b**), 119.0 (**a**), 84.3 (**a**, **b**, and **c**), 60.7 (**b**), 60.7 (**a**), 24.8 (**a**, **b**, and **c**), 14.3 (**a** and **b**). Unable to fully characterise the ^{13}C data for **b**.

^{11}B NMR (128 MHz, Chloroform-*d*) δ 30.8.

The characterisation data for **c** is in agreement with that reported in the literature (*Angew. Chem. Int. Ed.* 2017, 56, 7078-7082).

Ethyl (*E*)-3-(2-fluoro-5-(4,4,5,5-tetramethyl-1,3,2-dioxaborolan-2-yl)phenyl)acrylate (342)



General procedure F: The corresponding alkenylated boronic acid MIDA-DG ester (0.13 mmol) was used as a mixture with the non-alkenylated starting material to yield the pinacol boronate esters as a clear glassy solid. The ratio of product (**a**) : non-alkenylated material (**b**) in the isolated mixture was 3.1 : 1.0 (27 mg, 0.07 mmol (**a**), 54%).

HRMS (APCI +) Calcd. for $C_{17}H_{23}O_4B$ ([M + H]$^+$): 321.1668. Found: 321.1671.

^{1}H NMR (400 MHz, Chloroform-*d*) δ 8.04 (dd, *J* = 8.0, 1.7 Hz, 1H, **a**), 7.85 (d, *J* = 16.3 Hz, 1H, **a**), 7.81 (m, 1H, **a** and 2H, **b**), 7.14 – 7.04 (m, 1H, **a** and 2H, **b**), 6.63 (d, *J* = 16.2 Hz, 1H, **a**), 4.29 (q, *J* = 7.1 Hz, 2H, **a**), 1.36 (m, 15H, **a** and 12H, **b**).

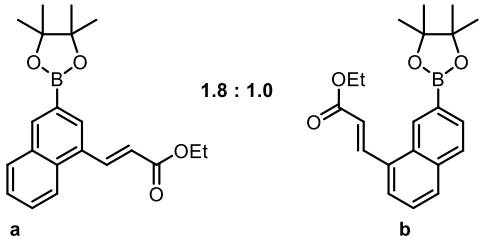
^{13}C NMR (101 MHz, Chloroform-*d*) δ 166.8 (**a**), 165.1 (d, *J* = 250.4 Hz, **b**), 163.4 (d, *J* = 258.2 Hz, **a**), 138.3 (d, *J* = 9.0 Hz, **a**), 137.0 (m, **a** and **b**), 136.0 (d, *J* = 3.1 Hz, **a**), 122.0 (d, *J* = 11.2 Hz, **a**), 120.9 (d, *J* = 6.0 Hz, **a**), 115.7 (d, *J* = 21.2 Hz, **a**), 114.8 (d, *J* = 20.2 Hz, **b**), 84.2 (**a**), 83.9 (**b**), 60.6 (**a**), 24.9 (**a** and **b**), 14.3 (**a**).

^{19}F NMR (377 MHz, Chloroform-*d*) δ -108.4 (**b**), -110.5 (**a**).

^{11}B NMR (128 MHz, Chloroform-*d*) δ 30.6.

The characterisation data for **b** is in agreement with that reported in the literature (*Angew. Chem. Int. Ed.* 2018, 57, 16832-16836).

Ethyl (*E*)-3-(3-(4,4,5,5-tetramethyl-1,3,2-dioxaborolan-2-yl)naphthalen-1-yl)acrylate (344)



General procedure F: The corresponding alkenylated boronic acid MIDA-DG ester (0.3 mmol) was used as a mixture of regioisomers to yield the mono-alkenylated pinacol boronate esters as a colourless solid. The ratio of *meta* (**a**) : *para* (**b**) in the isolated mixture was 1.8 : 1.0, **a** : **b** (22 mg, 0.06 mmol, 21% over 2 steps from the 2-naphtylboronic acid MIDA-DG ester).

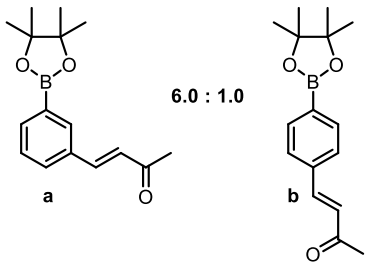
HRMS (TOF ES+) Calcd. for $C_{21}H_{26}O_4B$ ([M + H]$^+$): 353.1924. Found: 353.1931.

^{1}H NMR (400 MHz, Chloroform-*d*) δ 8.70 (s, 1H, **b**), 8.68 (d, *J* = 15.7 Hz, 1H, **b**), 8.54 (d, *J* = 15.7 Hz, 1H, **a**), 8.42 (s, 1H, **a**), 8.22 (dd, *J* = 8.6, 1.1 Hz, 1H, **a**), 8.17 (t, *J* = 0.9 Hz, 1H, **a**), 7.96 – 7.86 (m, 1H, **a** and 2H, **b**), 7.78 (dt, *J* = 7.2, 0.9 Hz, 1H, **b**), 7.64 (ddd, *J* = 8.4, 6.8, 1.4 Hz, 1H, **a**), 7.59 – 7.49 (m, 1H, **a** and **b**), 6.66 (d, *J* = 15.7 Hz, 1H, **a**), 6.57 (d, *J* = 15.7 Hz, 1H, **b**), 4.39 – 4.30 (m, 2H, **a** and **b**), 1.42 (s, 12H, **a** and **b**), 1.41 – 1.38 (m, 3H, **a** and **b**).

^{13}C NMR (101 MHz, Chloroform-*d*) δ 167.0 (**a** and **b**), 141.9 (**a**), 141.6 (**a**), 138.5 (**a**), 135.2 (**b**), 133.0 (**b**), 132.9 (**b**), 132.6 (**a**), 131.5 (**b**), 131.3 (**b**), 130.9 (**a**), 130.3 (**b**), 129.8 (**a**), 129.5 (**a**), 128.0 (**a**), 127.8 (**b**), 126.5 (**b**), 126.2 (**a**), 124.9 (**b**), 123.3 (**a**), 122.5 (**b**), 121.0 (**a** and **b**), 84.2 (**a**), 84.1 (**b**), 60.6 (**b**), 60.6 (**a**), 24.9 (**a** and **b**), 14.4 (**a** and **b**).

^{11}B NMR (128 MHz, Chloroform-*d*) δ 31.2.

(*E*)-4-(3-(4,4,5,5-Tetramethyl-1,3,2-dioxaborolan-2-yl)phenyl)but-3-en-2-one (331)

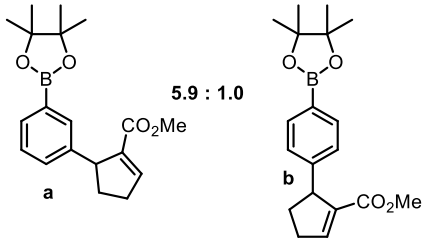


General procedure F: The corresponding alkenylated boronic acid MIDA-DG ester (0.20 mmol) was used as a mixture of regioisomers to yield the mono-alkenylated pinacol boronate esters as a white solid. The ratio of *meta* (**a**) : *para* (**b**) in the isolated mixture was 6.0 : 1.0 (26 mg, 0.10 mmol, 50%).

HRMS (APCI +) Calcd. for $C_{16}H_{22}O_3B$ ([M + H]$^+$): 273.1657. Found: 273.1657.

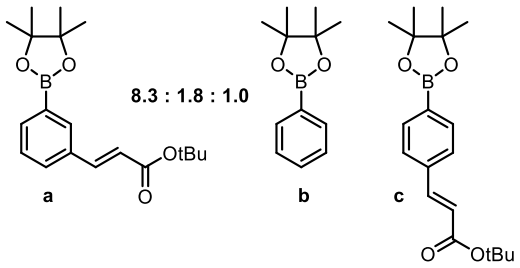
^{1}H NMR (400 MHz, Chloroform-*d*) δ 8.05 – 7.99 (m, 1H, **a**), 7.85 (dt, *J* = 7.3, 1.2 Hz, 1H, **a**), 7.65 (dt, *J* = 8.0, 1.7 Hz, 1H, **a** and 2H, **b**), 7.60 – 7.50 (m, 1H, **a** and 3H, **b**), 7.43 (t, *J* = 7.5 Hz, 1H, **a**), 6.79 (d, *J* = 16.4 Hz, 1H, **a**), 6.78 (d, *J* = 16.1 Hz, 1H, **b**), 2.41 (s, 3H, **b**), 2.40 (s, 3H, **a**), 1.38 (s, 12H, **a** and **b**).
^{13}C NMR (101 MHz, Chloroform-*d*) δ 198.4 (**a**), 198.4 (**b**), 143.4 (**a**), 143.3 (**b**), 136.8 (**a** and **b**), 135.3 (**b**), 134.8 (**a**), 133.8 (**a**), 130.9 (**a**), 128.4 (**a**), 127.9 (**b**), 127.4 (**b**), 127.3 (**a**), 84.1 (**a**), 84.1 (**b**), 27.6 (**b**), 27.5 (**a**), 24.9 (**a** and **b**).
^{11}B NMR (128 MHz, Chloroform-*d*) δ 30.6.
The characterisation data for **b** is in agreement with that reported in the literature (*Angew. Chem. Int. Ed.* 2017, 56, 2022-2025).

Methyl 5-(3-(4,4,5,5-tetramethyl-1,3,2-dioxaborolan-2-yl)phenyl)cyclopent-1-ene-1-carboxylate (350)



General procedure F: The corresponding alkenylated boronic acid MIDA-DG ester (0.20 mmol) was used as a mixture of regioisomers to yield the mono-alkenylated pinacol boronate esters as a white solid. The ratio of *meta* (**a**) : *para* (**b**) in the isolated mixture was 5.9 : 1.0 (28 mg, 0.09 mmol, 45%).
HRMS (APCI +) Calcd. for $C_{19}H_{26}O_4B$ ($[M + H]^+$): 329.1919. Found: 329.1903.
^{1}H NMR (400 MHz, Chloroform-*d*) δ 7.77 – 7.74 (m, 2H, **b**), 7.66 (dt, *J* = 8.2, 1.3 Hz, 2H, **a**), 7.33 – 7.27 (m, 1H, **a**), 7.25 (dt, *J* = 7.7, 1.7 Hz, 1H, **a**), 7.20 (d, *J* = 8.1 Hz, 2H, **b**), 7.03 (td, *J* = 2.4, 1.6 Hz, 1H, **a** and **b**), 4.18 (ddq, *J* = 8.2, 4.3, 2.3, 1.8 Hz, 1H, **a** and **b**), 3.61 (d, *J* = 2.1 Hz, 3H, **a** and **b**), 2.79 – 2.63 (m, 1H, **a** and **b**), 2.62 – 2.47 (m, 2H, **a** and **b**), 2.01 – 1.85 (m, 1H, **a** and **b**), 1.36 (d, *J* = 5.5 Hz, 12H, **a** and **b**).
^{13}C NMR (101 MHz, Chloroform-*d*) δ 165.2 (**a**), 165.1 (**b**), 148.5 (**b**), 145.2 (**a** and **b**), 144.3 (**a**), 139.1 (**a**), 139.0 (**b**), 135.0 (**b**), 133.6 (**a**), 132.8 (**a**), 129.7 (**a**), 127.8 (**a**), 126.4 (**b**), 83.7 (**a**), 83.6 (**b**), 51.3 (**a** and **b**), 50.3 (**b**), 50.1 (**a**), 34.2 (**a**), 34.1 (**b**), 32.3 (**b**), 32.2 (**a**), 24.9 (**b**), 24.9 (**a**).
^{11}B NMR (128 MHz, Chloroform-*d*) δ 30.9.

***tert*-Butyl (*E*)-3-(3-(4,4,5,5-tetramethyl-1,3,2-dioxaborolan-2-yl)phenyl)acrylate (343)**



General procedure F: The corresponding alkenylated boronic acid MIDA-DG ester (0.15 mmol) was used as a mixture of regioisomers to yield the mono-alkenylated pinacol boronate esters as a white solid. The ratio of *meta* (**a**) : phenylboronic acid pinacol ester (**b**) : *para* (**c**) in the isolated mixture was 8.3 : 1.8 : 1.0 (36 mg, 0.10 mmol, 65%).

HRMS (APCI +) Calcd. for $C_{19}H_{28}O_4B$ ($[M + H]^+$): 331.2080. Not found. Found: 257.1334 corresponding to loss of *tert*-butanol anion fragment C_4H_9O. Calcd. for $C_{15}H_{18}O_3B$ ($[M-C_4H_9O]^+$):257.1344.

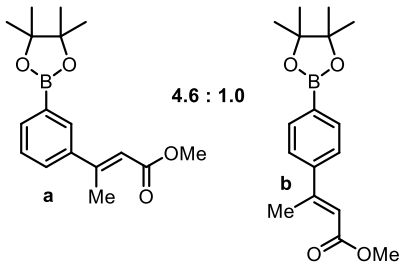
^{1}H NMR (400 MHz, Chloroform-*d*) δ 8.02 – 7.97 (m, 1H, **a**), 7.86 – 7.79 (m, 2H, **a, b** and **c**), 7.66 – 7.58 (m, 2H, **a**), 7.55 – 7.51 (d, *J* = 7.9 Hz, 2H, **c**), 7.51 – 7.45 (m, 1H, **b**), 7.43 – 7.36 (m, 1H, **a** and **b**), 6.45 (d, *J* = 16.0 Hz, 1H, **a** and **c**), 1.55 (s, 9H, **a** and **c**), 1.37 (d, *J* = 2.2 Hz, 15H, **a**, **b**, and **c**).

^{13}C NMR (101 MHz, Chloroform-*d*) δ 166.3 (**a** and **c**), 143.5 (**a**), 143.4 (**c**), 137.2 (**c**), 136.3 (**a**), 135.2 (**c**), 134.7 (**b**), 134.2 (**a**), 134.0 (**a**), 131.3 (**b**), 130.8 (**a**), 128.2 (**a**), 127.7 (**b**), 127.2 (**c**), 121.1 (**c**), 120.3 (**a**), 84.0 (**a** and **c**), 83.8 (**b**), 80.6 (**c**), 80.4 (**a**), 28.2 (**a** and **c**), 24.9 (**a**, **b**, and **c**).

^{11}B NMR (128 MHz, Chloroform-*d*) δ 31.0.

The characterisation data for **b** is in agreement with that reported in the literature (*Chem. Comm.*, 2018, 54, 13969-13972).

Methyl (*E*)-3-(3-(4,4,5,5-tetramethyl-1,3,2-dioxaborolan-2-yl)phenyl)but-2-enoate (347)



General procedure F: The corresponding alkenylated boronic acid MIDA-DG ester (0.05 mmol) was used as a mixture of regioisomers to yield the mono-alkenylated pinacol boronate esters as a white solid. The ratio of *meta* (**a**) : *para* (**b**) in the isolated mixture was 4.6 : 1.0 (4 mg, 0.01 mmol, 20%).

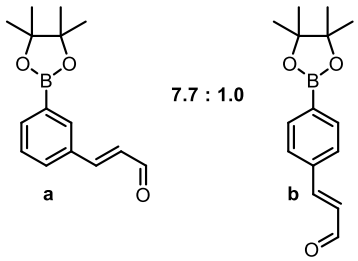
HRMS (APCI +) Calcd. for $C_{17}H_{24}O_4B$ ($[M + H]^+$): 303.1762. Found: 303.1762.

^{1}H NMR (400 MHz, Chloroform-*d*) δ 7.97 – 7.91 (m, 1H, **a**), 7.86 – 7.79 (m, 1H, **a** and 2H, **b**), 7.58 (ddd, *J* = 7.9, 2.1, 1.3 Hz, 1H, **a**), 7.52 – 7.47 (m, 2H, **b**), 7.41 (ddd, *J* = 7.9, 7.3, 0.6 Hz, 1H, **a**), 6.19 (q, *J* = 1.3 Hz, 1H, **a** and **b**), 3.78 (s, 3H, **a** and **b**), 2.62 (d, *J* = 1.3 Hz, 3H, **a**), 2.60 (d, *J* = 1.3 Hz, 3H, **b**), 1.38 (d, *J* = 1.4 Hz, 12H, **a** and **b**).

^{13}C NMR (101 MHz, Chloroform-*d*) δ 167.3 (**a**), 156.1 (**a**), 141.5 (**a**), 135.4 (**a**), 134.9 (**b**), 134.7 (**b**), 132.6 (**a**), 129.2 (**a**), 127.9 (**a**), 125.6 (**b**), 117.2 (**b**), 116.7 (**a**), 84.0 (**a**), 51.1 (**a**), 24.9 (**a**), 18.1 (**a**). Unable to fully characterise ^{13}C for **b**.

^{11}B NMR (128 MHz, Chloroform-*d*) δ 30.9.

(*E*)-3-(3-(4,4,5,5-Tetramethyl-1,3,2-dioxaborolan-2-yl)phenyl)acrylaldehyde (348)



General procedure F: The corresponding alkenylated boronic acid MIDA-DG ester (0.19 mmol) was used as a mixture of regioisomers to yield the mono-alkenylated pinacol boronate esters as a white solid. The ratio of *meta* (**a**) : *para* (**b**) in the isolated mixture was 7.7 : 1.0 (24 mg, 0.09 mmol, 47%).

HRMS (APCI +) Calcd. for $C_{15}H_{21}O_3B$ ([M + H]$^+$): 259.1500. Found: 259.1506.

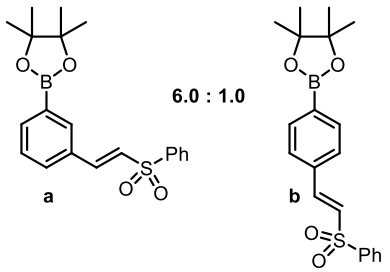
^{1}H NMR (400 MHz, Chloroform-*d*) δ 9.74 (d, *J* = 7.7 Hz, 1H, **b**), 9.72 (d, *J* = 7.7 Hz, 1H, **a**), 8.03 (s, 1H, **a**), 7.92 – 7.84 (m, 1H, **a** and 2H, **b**), 7.68 (dt, *J* = 7.8, 1.6 Hz, 1H, **a**), 7.61 – 7.55 (m, 2H, **b**), 7.51 (d, *J* = 16.0 Hz, 1H, **a** and **b**), 7.46 (t, *J* = 7.6 Hz, 1H, **a**), 6.79 (dd, *J* = 16.0, 7.7 Hz, 1H, **a** and **b**), 1.38 (d, *J* = 2.5 Hz, 12H, **a** and **b**).

^{13}C NMR (101 MHz, Chloroform-*d*) δ 193.7 (**a** and **b**), 152.8 (**a**), 152.5 (**b**), 137.6 (**a**), 136.4 (**b**), 135.4 (**b**), 135.2 (**a**), 133.4 (**a**), 130.9 (**a**), 129.3 (**b**), 128.6 (**a**), 128.5 (**a**), 127.6 (**b**), 84.2 **(a** and **b**), 24.9 **(a** and **b**).

^{11}B NMR (128 MHz, Chloroform-*d*) δ 30.8.

The characterisation data for **b** is in agreement with that reported in the literature (*Angew. Chem. Int. Ed.* 2018, 57, 12819-12823).

(*E*)-4,4,5,5-Tetramethyl-2-(3-(2-(phenylsulfonyl)vinyl)phenyl)-1,3,2-dioxaborolane (335)



General procedure F: The corresponding alkenylated boronic acid MIDA-DG ester (0.11 mmol) was used as a mixture of regioisomers to yield the mono-alkenylated pinacol boronate esters as a white solid. The ratio of *meta* (**a**) : *para* (**b**) in the isolated mixture was 6.0 : 1.0 (15 mg, 0.04 mmol, 36%).

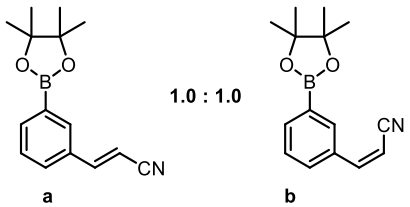
HRMS (APCI +) Calcd. for $C_{20}H_{24}O_4BS$ ([M + H]$^+$): 371.1483. Found: 371.1481.

^{1}H NMR (400 MHz, Chloroform-*d*) δ 7.97 (m, 3H, **a**, 2H, **b**), 7.89 – 7.81 (m, 1H, **a**, 2H, **b**), 7.72 (d, *J* = 15.4 Hz, 1H, **a** and **b**), 7.67 – 7.61 (m, 1H, **a**), 7.61 – 7.54 (m, 3H, **a** and **b**), 7.52 – 7.47 (m, 2H, **b**), 7.43 (t, *J* = 7.6 Hz, 1H, **a**), 6.94 (d, *J* = 15.5 Hz, 1H, **a**), 6.93 (d, *J* = 15.5 Hz, 1H, **b**), 1.36 (s, 12H, **a** and **b**).

^{13}C NMR (101 MHz, Chloroform-*d*) δ 142.4 (**a**), 142.3 (**b**), 140.8 (**b**), 137.4 (**a**), 135.4 (**b**), 134.5 (**a**), 133.5 (**b**), 133.4 (**a**), 131.8 (**a**), 131.6 (**a**), 129.4 (**a**), 129.3 (**a**), 128.5 (**a**), 128.1 (**b**), 127.7 (**a**), 127.4 (**a**), 84.2 (**a** and **b**), 24.9 (**a** and **b**). Unable to assign all carbons for **b**.

^{11}B NMR (128 MHz, Chloroform-*d*) δ 30.6.

(*E*)-3-(3-(4,4,5,5-Tetramethyl-1,3,2-dioxaborolan-2-yl)phenyl)acrylonitrile (349)



General procedure F: The corresponding alkenylated boronic acid MIDA-DG ester (0.17 mmol) was used as a mixture of regioisomers to yield the mono-alkenylated pinacol boronate esters as a white solid. The ratio of *cis* (**a**) : *trans* (**b**) in the isolated mixture was 1.0 : 1.0 (30 mg, 0.12 mmol, 69%). The products contained some small impurities corresponding to the *para*-alkenylated pinacol esters.

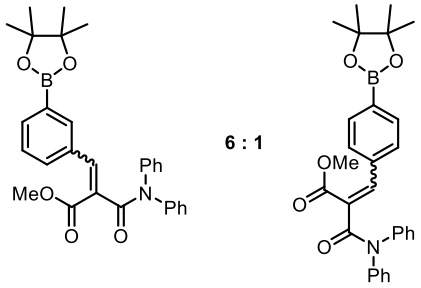
HRMS (TOF ES+) Calcd. for $C_{15}H_{19}NO_2B$ ([M + H]$^+$): 256.1503. Found: 256.1507.

^{1}H NMR (400 MHz, Chloroform-*d*) δ 8.19 (dt, *J* = 7.8, 1.7 Hz, 1H, **b**), 8.01 – 7.95 (m, 1H, **b**), 7.90 (dddd, *J* = 9.8, 5.2, 2.2, 1.2 Hz, 2H, **a and b**), 7.86 – 7.78 (m, 1H, **a**), 7.55 (dt, *J* = 7.7, 1.7 Hz, 1H, **a**), 7.49 (t, *J* = 7.7 Hz, 1H, **a**), 7.47 – 7.38 (m, 2H, **a and b**), 7.18 (d, *J* = 12.1 Hz, 1H, **b**), 5.97 (d, *J* = 16.7 Hz, 1H, **a**), 5.47 (d, *J* = 12.1 Hz, 1H, **b**), 1.38 (d, *J* = 3.4 Hz, 24H, **a and b**).

^{13}C NMR (101 MHz, Chloroform-*d*) δ 150.6 (**a**), 148.8 (**b**), 137.5 (**a or b**), 137.2 (**a or b**), 136.6 (**b**), 134.7 (**a**), 133.6 (**a**), 133.0 (**b**), 132.9 (**a**), 130.3 (**a or b**), 130.1 (**a or b**), 128.5 (**a or b**), 128.4 (**a or b**), 118.2 (**a**), 117.3 (**b**), 96.4 (**b**), 95.1 (**a**), 84.2 (**a or b**), 84.2 (**a or b**), 24.9 (**a and b**). Not all ^{13}C peaks could be exactly assigned to **a or b**.

^{11}B NMR (128 MHz, Chloroform-*d*) δ 30.8.

Methyl 2-(diphenylcarbamoyl)-3-(3-(4,4,5,5-tetramethyl-1,3,2-dioxaborolan-2-yl)phenyl)acrylate (339)



General procedure F: The corresponding alkenylated boronic acid MIDA-DG ester (0.24 mmol) was used as a mixture of regioisomers to yield the mono-alkenylated pinacol boronate esters as a white solid (42 mg, 0.04 mmol, 36%). The product contained a 15% impurity consisting of the *para* substituted isomer (not characterised). The geometry of the double bond is unknown but presumed to be cis.

HRMS (TOF ES+) Calcd. for $C_{29}H_{31}NO_5B$ ([M + H]$^+$): 484.2290. Found: 484.2303

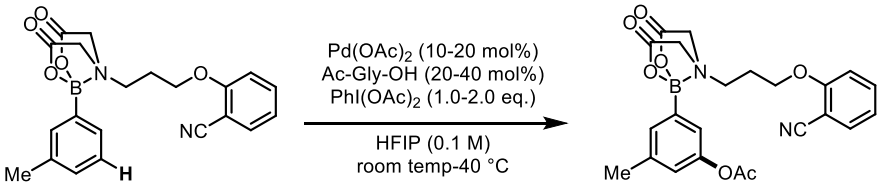
^{1}H NMR (400 MHz, Chloroform-*d*) δ 8.06 – 8.02 (m, 1H), 7.88 (dt, *J* = 7.4, 1.3 Hz, 1H), 7.62 (dt, *J* = 7.9, 1.6 Hz, 1H), 7.48 (s, 1H), 7.45 (dd, *J* = 8.5, 1.4 Hz, 2H), 7.41 – 7.33 (m, 2H), 7.28 – 7.17 (m, 2H), 7.15 – 7.09 (m, 2H), 6.85 – 6.81 (m, 2H), 3.87 (d, *J* = 1.2 Hz, 3H), 1.39 (s, 12H).

^{13}C NMR (101 MHz, Chloroform-*d*) δ 166.2, 165.2, 143.5, 141.9, 141.3, 136.8, 136.3, 135.9, 133.0, 132.4, 128.9, 127.6, 126.4, 84.1, 52.5, 25.0.

^{11}B NMR (128 MHz, Chloroform-*d*) δ 30.9.

Chapter 5

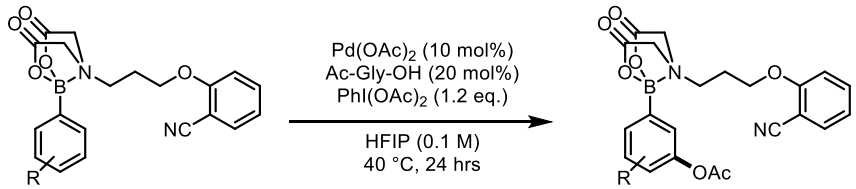
General procedure G for DOE Optimisation of C–H Acetoxylations



295 351

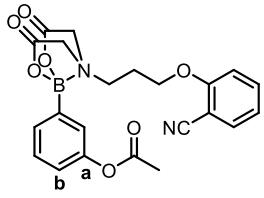
PhB(MIDA-DG) (0.05 mmol, 19 mg), $Pd(OAc)_2$ (X eq.), Ac-gly-OH (X eq.) and $PhI(OAc)_2$ (X eq.) were added to a one dram (4 mL) vial. HFIP (1 mL) and CH_2Br_2 (internal standard, 1 eq., 3.5 mL) were then added and the vial sealed. The reaction mixture was added to a hot plate at the desired temperature and stirred for the desired time. On completion, a 0.1 mL aliquot was taken, diluted with MeCN-d_3, filtered and a ^1H NMR taken. The yield was calculated by comparison of integrals between the product and the CH_2Br_2 internal standard.

General Procedure H for the C–H Acetoxylation of aryl boronic acid MIDA-DG esters



A vial was charged with arylboronic acid MIDA-DG ester (1.0 eq.), $PhI(OAc)_2$ (1.2 eq.), Ac-Gly-OH (20 mol%), $Pd(OAc)_2$ (10 mol%) and HFIP (0.1 M). The vial was sealed and stirred at 40 °C for 24 hours. The reaction mixture was diluted with MeCN (~5 mL), dry loaded onto a silica column and purified via 'catch and release' purification: washing with copious Et_2O to remove by-products then eluting using EtOAc as eluent.

3-Acetoxyphenylboronic acid MIDA-DG ester (364) and Isomers



General Procedure H: Phenylboronic acid MIDA-DG ester (113 mg, 0.3 mmol) was employed to yield the product as an off-white solid (100 mg, total yield: 70% **a**: 61% **b**: 9% with 7% SM remaining, as determined by ^1H NMR).

Characterisation data for major isomer:

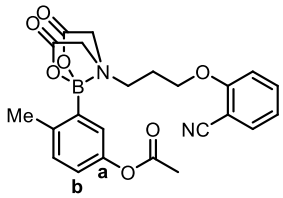
HRMS (TOF ES+) Calcd. for $C_{22}H_{22}N_2O_7B$ ($[M+H]^+$): 437.1520. Found: 437.1536.

^{1}H NMR (400 MHz, Acetonitrile-d_3) δ 7.64 – 7.55 (m, 2H), 7.46 – 7.36 (m, 2H), 7.23 (dd, J = 2.6, 1.1 Hz, 1H), 7.15 – 7.10 (m, 1H), 7.07 (td, J = 7.6, 0.9 Hz, 1H), 7.03 – 6.96 (m, 1H), 4.10 (d, J = 17.1 Hz, 2H), 4.03 (d, J = 17.1 Hz, 2H), 3.97 (t, J = 6.2 Hz, 2H), 2.90 – 2.81 (m, 2H), 2.25 (s, 3H), 2.15 – 2.06 (m, 2H).

^{13}C NMR (101 MHz, Acetonitrile-d_3) δ 169.6, 168.4, 159.9, 150.9, 134.8, 133.8, 133.6, 132.5, 129.9, 129.3, 128.0, 125.7, 122.8, 121.3, 116.1, 112.8, 101.4, 65.8, 59.0, 56.1, 55.9, 23.8, 20.3. Unable to distinguish ^{13}C peaks between regioisomers.

^{11}B NMR (128 MHz, Acetonitrile-d_3) δ 11.6.

2-Methyl-5-acetoxyphenylboronic acid MIDA-DG ester (355) and Isomers



General Procedure H: 2-Methylphenylboronic acid MIDA-DG ester (78 mg, 0.2 mmol) was employed to yield the products as a yellow mixture of solids (43 mg, total yield: 48% **a**: 38%, **b**: 10% as determined by ^{1}H NMR).

Characterisation data for major isomer:

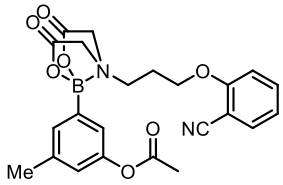
HRMS (TOF ES+) Calcd. for $C_{23}H_{24}N_2O_7B$ ([M+H]$^+$): 451.1677. Found: 451.1674.

^{1}H NMR (400 MHz, Acetonitrile-d_3) δ 7.64 – 7.55 (m, 2H), 7.22 – 7.18 (m, 1H), 7.14 (d, J = 2.5 Hz, 1H), 7.07 (td, J = 7.5, 0.8 Hz, 1H), 7.02 – 6.97 (m, 2H), 4.11 (d, J = 17.2 Hz, 2H), 4.07 – 3.98 (m, 4H), 2.90 – 2.83 (m, 2H), 2.40 (s, 3H), 2.23 (s, 3H), 2.18 – 2.10 (m, 2H).

^{13}C NMR (101 MHz, Acetonitrile-d_3) δ 169.7, 168.4, 159.9, 148.7, 139.9, 135.5, 134.8, 133.6, 132.2, 127.0, 124.0, 122.6, 121.3, 118.5, 116.1, 112.7, 101.4, 65.7, 59.8, 56.1, 24.0, 22.1, 21.5, 20.3. Unable to distinguish ^{13}C peaks between regioisomers.

^{11}B NMR (128 MHz, Acetonitrile-d_3) δ 12.3.

3-Methyl-5-acetoxyphenylboronic acid MIDA-DG ester (351)



General Procedure H: 3-Methylphenyl5boronic acid MIDA-DG ester (78 mg, 0.2 mmol) was employed to yield the product as a white solid (56 mg, 62%).

ν_{max}/cm^{-1} 2956, 2225, 1748, 1599, 1491, 1445, 1282, 1208, 1178, 1014, 945, 865, 757, 708.

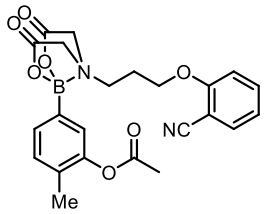
HRMS (TOF ES+) Calcd. for $C_{23}H_{24}N_2O_7B$ ([M+H]$^+$): 451.1677. Found: 451.1674.

^{1}H NMR (400 MHz, Acetonitrile-d_3) δ 7.63 – 7.55 (m, 2H), 7.21 (dt, *J* = 1.8, 0.9 Hz, 1H), 7.07 (td, *J* = 7.6, 0.9 Hz, 1H), 7.03 – 6.97 (m, 2H), 6.93 (ddd, *J* = 2.3, 1.6, 0.8 Hz, 1H), 4.09 (d, *J* = 17.1 Hz, 2H), 4.03 (d, *J* = 17.1 Hz, 2H), 3.98 (t, *J* = 6.2 Hz, 2H), 2.89 – 2.82 (m, 2H), 2.35 (s, 3H), 2.23 (s, 3H), 2.15 – 2.06 (m, 2H).

^{13}C NMR (101 MHz, Acetonitrile-d_3) δ 169.6, 168.4, 159.9, 150.9, 139.5, 134.8, 133.6, 130.6, 123.3, 122.6, 121.3, 116.2, 112.8, 101.4, 65.8, 59.0, 56.1, 23.8, 20.4, 20.3.

^{11}B NMR (128 MHz, Acetonitrile-d_3) δ 11.6.

4-Methyl-3-acetoxyphenylboronic acid MIDA-DG ester (356)



General Procedure H: 4-Methylphenylboronic acid MIDA-DG ester (78 mg, 0.2 mmol) was employed to yield the product as an off-white mixture with the remaining starting material (26 mg, 12%, **SM**: 11% as determined by ^{1}H NMR). The isolated mixture also contained an unknown impurity that was removed after deprotection and oxidation of the boronic acid.

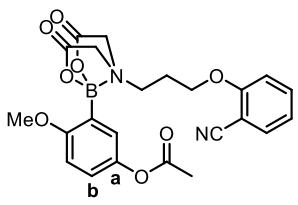
HRMS (TOF ES+) Calcd. for $C_{23}H_{24}N_2O_7B$ ([M+H]$^+$): 451.1677. Found: 451.1672.

^{1}H NMR (400 MHz, Acetonitrile-d_3) δ 7.64 – 7.54 (m, 2H), 7.42 – 7.37 (m, 1H), 7.26 – 7.22 (m, 1H), 7.15 (s, 1H), 7.08 (ddt, *J* = 8.2, 6.7, 0.8 Hz, 1H), 7.00 (d, *J* = 8.5 Hz, 1H), 4.08 (d, *J* = 17.1 Hz, 2H), 4.02 (d, *J* = 17.1 Hz, 2H), 3.99 – 3.96 (m, 2H), 2.88 – 2.81 (m, 2H), 2.19 (s, 3H), 2.16 (s, 3H), 2.13 – 2.07 (m, 2H).

^{13}C NMR (101 MHz, Acetonitrile-d_3) δ 168.6, 168.4, 159.9, 149.6, 139.1, 134.8, 133.7, 132.6, 130.9, 130.1, 126.0, 121.3, 112.8, 65.8, 58.9, 56.0, 26.7, 23.8.

^{11}B NMR (128 MHz, Acetonitrile-d_3) δ 11.9.

2-Methoxy-5-acetoxyphenylboronic acid MIDA-DG ester (352) and Isomers



General Procedure H: 2-Methoxyphenylboronic acid MIDA-DG ester (82 mg, 0.2 mmol) was employed to yield the products as a yellow mixture of solids (35.3 mg, total yield: 28% **a**: 17%, **b**: 11% **SM:** 18% as determined by ^{1}H NMR).

Characterisation data for major isomer:

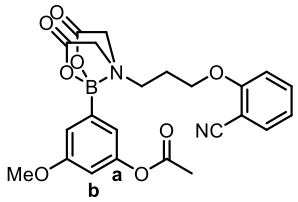
HRMS (TOF ES+) Calcd. for $C_{23}H_{24}N_2O_8B$ ([M+H]$^+$): 467.1626. Found: 451.1627.

^{1}H NMR (400 MHz, Acetonitrile-d_3) δ 7.62 – 7.54 (m, 2H), 7.10 – 7.03 (m, 2H), 7.00 – 6.92 (m, 2H), 6.73 – 6.70 (m, 1H), 4.15 (d, *J* = 17.0 Hz, 2H), 4.06 – 3.97 (m, 4H), 3.78 (s, 3H), 3.09 – 2.99 (m, 2H), 2.26 (s, 3H), 2.17 – 2.07 (m, 2H).

^{13}C NMR (101 MHz, Acetonitrile-d_3) δ 169.3, 168.8, 168.7, 163.2, 162.3, 159.8, 153.5, 139.5, 135.0, 134.8, 134.5, 134.3, 133.7, 131.0, 127.3, 123.7, 121.2, 120.5, 116.1, 113.7, 112.6, 112.5, 111.1, 110.3, 104.8, 101.2, 65.8, 59.2, 55.7, 55.6, 55.5, 55.2, 55.0, 54.6, 23.9, 23.8, 20.3, 20.3. Unable to distinguish ^{13}C peaks between regioisomers.

^{11}B NMR (128 MHz, Acetonitrile-d_3) δ 11.6.

3-Methoxy-5-acetoxyphenylboronic acid MIDA-DG ester (353) and Isomers



General Procedure H: 3-Methoxyphenylboronic acid MIDA-DG ester (122 mg, 0.3 mmol) was employed to yield the products as a yellow mixture of solids (76 mg, Total yield: 54% **a:** 35%, **b**: 19% as determined by ^{1}H NMR).

Characterisation data for major isomer:

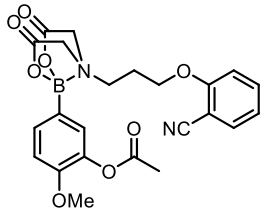
HRMS (TOF ES+) Calcd. for $C_{23}H_{24}N_2O_8B$ ([M+H]$^+$): 467.1626. Found: 467.1624.

^{1}H NMR (400 MHz, Acetonitrile-d_3) δ 7.64 – 7.55 (m, 2H), 7.08 (td, *J* = 7.1, 6.7, 0.9 Hz, 1H), 7.01 (dd, *J* = 8.8, 2.5 Hz, 1H), 6.92 (dd, *J* = 2.4, 1.0 Hz, 1H), 6.80 (dd, *J* = 2.1, 1.0 Hz, 1H), 6.70 (t, *J* = 2.3 Hz, 1H), 4.09 (d, *J* = 17.1 Hz, 2H), 4.04 – 3.97 (m, 4H), 3.80 (s, 3H), 2.88 (dt, *J* = 11.4, 4.4 Hz, 2H), 2.24 (s, 3H), 2.16 – 2.07 (m, 2H).

^{13}C NMR (101 MHz, Acetonitrile-d_3) δ 168.4, 159.9, 134.8, 133.6, 129.3, 125.0, 122.6, 121.3, 117.8, 116.2, 116.2, 114.8, 112.8, 112.8, 109.0, 65.8, 59.0, 58.9, 56.0, 55.9, 55.5, 55.1, 23.9, 23.8, 20.3, 19.8. Unable to distinguish ^{13}C peaks between regioisomers.

^{11}B NMR (128 MHz, Acetonitrile-d_3) δ 11.3.

4-Methoxy-3-acetoxyphenylboronic acid MIDA-DG ester (354)



General Procedure H: 4-Methoxyphenylboronic acid MIDA-DG ester (122 mg, 0.3 mmol) was employed to yield the products as a yellow solid (62 mg, 0.04 mmol, 44%).

ν_{max}/cm^{-1} 2926, 2225, 1752, 1599, 1513, 1449, 1290, 1260, 1200, 1126, 1044, 1006, 591, 865, 813, 757.

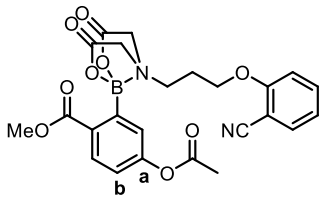
HRMS (TOF ES+) Calcd. for $C_{23}H_{24}N_2O_8B$ ([M+H]$^+$): 467.1626. Found: 467.1642.

^{1}H NMR (400 MHz, Acetonitrile-d_3) δ 7.64 – 7.54 (m, 2H), 7.36 (dd, *J* = 8.2, 1.8 Hz, 1H), 7.16 (d, *J* = 1.8 Hz, 1H), 7.11 – 7.05 (m, 2H), 7.01 (dd, *J* = 8.5, 0.8 Hz, 1H), 4.07 (d, *J* = 17.1 Hz, 2H), 4.03 – 3.96 (m, 4H), 3.81 (s, 3H), 2.89 – 2.81 (m, 2H), 2.24 (s, 3H), 2.16 – 2.05 (m, 2H).

^{13}C NMR (101 MHz, Acetonitrile-d_3) δ 168.9, 168.4, 159.9, 152.2, 139.7, 134.8, 133.7, 131.4, 126.8, 121.3, 116.1, 112.8, 112.4, 101.4, 65.8, 58.9, 56.0, 55.4, 23.8, 19.8.

^{11}B NMR (128 MHz, Acetonitrile-d_3) δ 11.8.

2-Methoxycarbonyl-5-acetoxyphenylboronic acid MIDA-DG ester (357) and Isomers



General Procedure H: 2-Methoxycarbonylphenylboronic acid MIDA-DG ester (44 mg, 0.1 mmol) was employed to yield the products as a yellow mixture of solids after an extended reaction time of 48 hours (35 mg, total yield: 40% **a**: 33%, **b**: 7% **SM:** 36% as determined by ^{1}H NMR).

Characterisation data for major isomer:

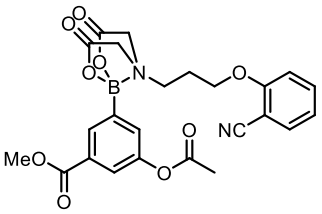
HRMS (TOF ES+) Calcd. for $C_{24}H_{24}N_2O_9B$ ([M+H]$^+$): 495.1575. Found: 495.1574.

^{1}H NMR (400 MHz, Acetonitrile-d_3) δ 7.72 (d, *J* = 8.4 Hz, 1H), 7.65 – 7.51 (m, 2H), 7.42 (d, *J* = 2.4 Hz, 1H), 7.21 (dd, *J* = 8.4, 2.4 Hz, 1H), 7.06 (m, 1H), 7.00 (m, 1H), 4.29 (d, *J* = 17.1 Hz, 2H), 4.07 – 3.98 (m, 4H), 3.82 (s, 3H), 3.25 – 3.14 (m, 2H), 2.28 (s, 3H), 2.25 – 2.18 (m, 2H).

^{13}C NMR (101 MHz, Acetonitrile-d_3) δ 171.4, 170.5, 169.3, 168.9, 168.8, 168.6, 159.8, 152.5, 137.1, 136.4, 134.7, 134.3, 133.7, 131.6, 130.5, 130.4, 130.2, 129.3, 128.5, 128.1, 124.3, 122.6, 121.3, 116.1, 112.7, 101.4, 101.3, 65.8, 61.5, 61.3, 60.4, 57.9, 57.6, 52.4, 24.2, 20.4, 19.9. Unable to distinguish ^{13}C peaks between regioisomers.

^{11}B NMR (128 MHz, Acetonitrile-d_3) δ 12.0.

3-Methoxycarbonyl-5-acetoxyphenylboronic acid MIDA-DG ester (358)



General Procedure H: 3-Methoxycarbonylphenylboronic acid MIDA-DG ester (44 mg, 0.1 mmol) was employed to yield the products as a yellow mixture of solids after an extended reaction time of 48 hours (40 mg, **product**: 36%, **SM**: 50% as determined by ^{1}H NMR).

Characterisation data for major isomer:

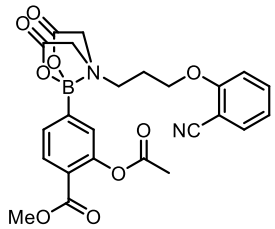
HRMS (TOF ES+) Calcd. for $C_{24}H_{24}N_2O_9B$ ([M+H]$^+$): 495.1575. Found: 495.1572.

^{1}H NMR (400 MHz, Acetonitrile-d_3) δ 8.01 – 7.99 (m, 1H), 7.72 (dd, *J* = 2.4, 1.5 Hz, 1H), 7.62 – 7.53 (m, 2H), 7.48 – 7.46 (m, 1H), 7.05 (tdd, *J* = 7.6, 2.6, 0.9 Hz, 1H), 6.97 (d, *J* = 8.3 Hz, 1H), 4.13 (d, *J* = 17.2 Hz, 2H), 4.06 (d, *J* = 17.2 Hz, 2H), 3.98 (t, *J* = 6.1 Hz, 2H), 3.89 (s, 3H), 2.90 – 2.79 (m, 2H), 2.27 (s, 3H), 2.11 (dddd, *J* = 11.1, 9.6, 7.2, 4.9 Hz, 2H).

^{13}C NMR (101 MHz, Acetonitrile-d_3) δ 169.5, 168.4, 168.3, 166.9, 166.1, 159.9, 159.8, 150.9, 137.2, 134.7, 133.6, 133.6, 133.3, 131.4, 130.5, 130.4, 130.2, 129.8, 128.3, 123.6, 123.5, 121.3, 116.1, 116.0, 112.7, 112.7, 101.4, 101.4, 65.7, 59.2, 59.1, 56.3, 56.2, 51.9, 51.7, 23.9, 23.8, 20.3. Unable to distinguish ^{13}C peaks between regioisomers.

^{11}B NMR (128 MHz, Acetonitrile-d_3) δ 11.46.

4-Methoxycarbonyl-3-acetoxyphenylboronic acid MIDA-DG ester (359)



General Procedure H: 4-Methoxycarbonylphenylboronic acid MIDA-DG ester (44 mg, 0.1 mmol) was employed to yield the products as a yellow mixture of solids after an extended reaction time of 48 hours (31 mg, **product**: 21%, **SM**: 48% as determined by ^{1}H NMR).

Characterisation data for major isomer:

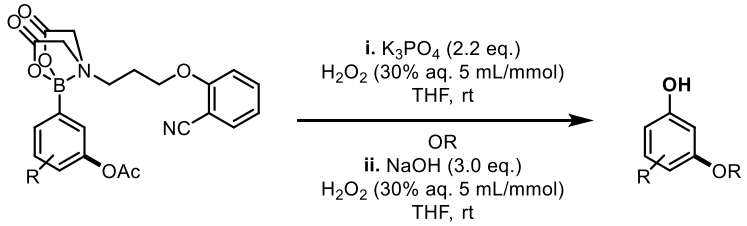
HRMS (TOF ES+) Calcd. for $C_{24}H_{23}N_2O_9BNa$([M+Na]$^+$): 517.1394. Found: 517.1407.

^{1}H NMR (400 MHz, Acetonitrile-d_3) δ 7.94 (d, *J* = 7.7 Hz, 1H), 7.60 – 7.53 (m, 2H), 7.50 (dd, *J* = 7.7, 1.3 Hz, 1H), 7.30 (d, *J* = 1.3 Hz, 1H), 7.06 (td, *J* = 7.6, 0.8 Hz, 1H), 6.98 (d, *J* = 9.0 Hz, 1H), 4.13 (d, *J* = 17.1 Hz, 2H), 4.07 (d, *J* = 14.2 Hz, 2H), 3.98 (t, *J* = 6.3 Hz, 2H), 3.84 (s, 3H), 2.90 – 2.84 (m, 2H), 2.28 (s, 3H), 2.10 (m, 2H).

^{13}C NMR (101 MHz, Acetonitrile-d_3) δ 170.7, 169.6, 168.4, 168.3, 166.8, 159.9, 159.8, 150.0, 134.7, 133.6, 133.6, 132.7, 130.9, 130.9, 130.2, 128.6, 128.4, 127.8, 124.2, 123.6, 121.3, 121.3, 116.2, 116.1, 112.8, 112.7, 101.4, 65.6, 60.0, 59.1, 59.0, 56.2, 56.1, 51.9, 51.7, 23.8, 23.8, 20.2, 20.2, 13.5. Unable to distinguish ^{13}C peaks between regioisomers.

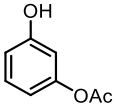
^{11}B NMR (128 MHz, Acetonitrile-d_3) δ 11.4.

General Procedure I for the oxidation of C–H Acetoxylated Products



To a 20 mL vial was added the acetoxylated boronic acid MIDA-DG mixture (1 eq.), K_3PO_4 (2.2 eq.) or NaOH (3 eq.). The mixture was dissolved in THF (0.05 M), and H_2O_2 (30% v/v aq., 5 mL / mmol) added. The reaction mixture was stirred at room temperature until complete conversion of the SM (checked by TLC). The reaction mixture was diluted with brine (5.0 mL) and DCM (10 mL). The organic layer was separated, concentrated under vacuum and purified via preparative TLC to yield the desired product.

3-Hydroxyphenyl acetate (367)



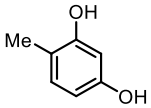
General Procedure I: The corresponding acetoxylated boronic acid MIDA-DG ester (0.3 mmol) (as a mixture of regioisomers) and K_3PO_4 were employed to yield the desired phenol as a clear glassy solid (8 mg, 0.05 mmol, 18%).

^{1}H NMR (400 MHz, Chloroform-*d*) δ 7.24 (t, *J* = 8.1 Hz, 1H), 6.69 (dddd, *J* = 12.2, 8.1, 2.3, 0.9 Hz, 2H), 6.61 (t, *J* = 2.3 Hz, 1H), 5.48 (s, 1H), 2.32 (s, 3H).

^{13}C NMR (101 MHz, Chloroform-*d*) δ 169.8, 156.6, 151.5, 130.1, 113.7, 109.2, 105.4, 21.2.

The characterisation data for the compound is in agreement with that reported in the literature (*Org. Biomol. Chem.,* 2011, 9, 8119-8121).

2,4-Dihydroxytoluene (368)



Methyl 2,4-dihydroxytoluene was synthesised by oxidation/de-acetoxylation of 2-methyl-5-acetoxyphenylboronic acid MIDA-DG ester and 4-methyl-3-acetoxyphenylboronic acid MIDA-DG ester.

From 2-methyl-5-acetoxyphenylboronic acid MIDA-DG ester (368)

General Procedure I: The corresponding acetoxylated boronic acid MIDA-DG ester (0.07 mmol) (as a mixture of regioisomers) and NaOH were employed to yield the desired phenol as a glassy solid (2.5 mg, 0.02 mmol, 29%).

From 4-methyl-3-acetoxyphenylboronic acid MIDA-DG ester (370)

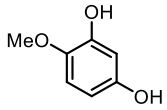
General Procedure I: The corresponding acetoxylated boronic acid MIDA-DG ester (0.02 mmol) (as a mixture of regioisomers) and NaOH were employed to yield the desired phenol as a glassy solid (1.6 mg, 0.01 mmol, 65%).

^{1}H NMR (400 MHz, Chloroform-*d*) δ 6.95 (d, *J* = 9.0 Hz, 1H), 6.33 (dq, *J* = 5.1, 2.5 Hz, 2H), 2.16 (s, 3H).

^{13}C NMR (101 MHz, Chloroform-*d*) δ 154.8, 154.6, 131.4, 115.7, 107.5, 102.6, 14.9.

The characterisation data for the compound is in agreement with that reported in the literature (*Eur. J. Med. Chem.* 143, 2018, 1428-1435).

2,4-Dihydroxyanisole (365)



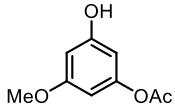
General Procedure I: The corresponding acetoxylated 2-methoxyphenylboronic acid MIDA-DG ester (0.03 mmol) (as a mixture of regioisomers) was used as a mixture of regioisomers to yield the desired phenol as a clear oil (1.5 mg, 0.01 mmol, 33%).

^{1}H NMR (400 MHz, Methanol-d_4) δ 6.74 (d, *J* = 8.7 Hz, 1H), 6.34 (d, *J* = 2.8 Hz, 1H), 6.23 (dd, *J* = 8.7, 2.8 Hz, 1H), 3.77 (s, 3H).

^{13}C NMR (101 MHz, Methanol-d_4) δ 153.0, 148.5, 142.5, 114.5, 106.5, 104.4, 57.4.

The characterisation data for the compound is in agreement with that reported in the literature (*J. Agric. Food Chem.* 2008, 56, 6809-6817).

3-Hydroxy-5-methoxyphenyl acetate (366)



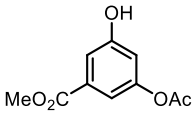
General Procedure I: The corresponding acetoxylated boronic acid MIDA-DG ester (0.21 mmol) (as a mixture of regioisomers) and K_3PO_4 were employed to yield the desired phenol as a clear oil (20 mg, 0.11 mmol, 52%).

HRMS (TOF ES+) Calcd. for $C_9H_{11}O_4$ ([M+H]$^+$): 183.0652. Found: 183.0655.

^{1}H NMR (400 MHz, Chloroform-*d*) δ 6.30 (t, *J* = 2.2 Hz, 1H), 6.26 (t, *J* = 2.1 Hz, 1H), 6.23 (t, *J* = 2.1 Hz, 1H), 5.21 (s, 1H), 3.78 (s, 3H), 2.30 (s, 3H).

^{13}C NMR (101 MHz, Chloroform-*d*) δ 169.4, 161.3, 157.0, 152.2, 101.9, 100.3, 99.4, 55.5, 21.2.

Methyl 3-acetoxy-5-hydroxybenzoate (369)



General Procedure I: The corresponding acetoxylated boronic acid MIDA-DG ester (0.04 mmol) (as a mixture of regioisomers) and K_3PO_4 were employed to yield the desired phenol as a clear oil (4 mg, 0.02 mmol, 50%).

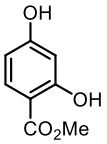
^{1}H NMR (400 MHz, Chloroform-*d*) δ 7.39 (dd, *J* = 2.4, 1.3 Hz, 1H), 7.34 (dd, *J* = 2.1, 1.3 Hz, 1H), 6.82 (t, *J* = 2.3 Hz, 1H), 5.63 (s, 1H), 3.90 (s, 3H), 2.31 (s, 3H).

^{1}H NMR (400 MHz, Methanol-d_4) δ 7.31 (dd, *J* = 2.4, 1.4 Hz, 1H), 7.19 (dd, *J* = 2.2, 1.4 Hz, 1H), 6.76 (t, *J* = 2.3 Hz, 1H), 3.88 (s, 4H), 2.27 (s, 3H).

^{13}C NMR (101 MHz, Methanol-d_4) δ 170.8, 167.7, 159.9, 153.1, 133.2, 114.8, 114.7, 52.8, 20.9.

The characterisation data for the compound is in agreement with that reported in the literature (*ChemMedChem*, 2015, 10, 116-133).

Methyl 2,4-dihydroxybenzoate



Methyl 2,4-dihydroxybenzoate was synthesised by oxidation/de-acetoxylation of 2-methoxycarbonyl-5-acetoxyphenylboronic acid MIDA-DG ester and 4-methoxycarbonyl-3-acetoxyphenylboronic acid MIDA-DG ester.

From 2-methoxycarbonyl-5-acetoxyphenylboronic acid MIDA-DG ester (371)

General Procedure I: The corresponding acetoxylated boronic acid MIDA-DG ester (0.04 mmol) (as a mixture of regioisomers) and K_3PO_4 were employed to yield the desired phenol as a glassy solid (2.2 mg, 0.01 mmol, 33%).

From 4-methoxycarbonyl-3-acetoxyphenylboronic acid MIDA-DG ester (372)

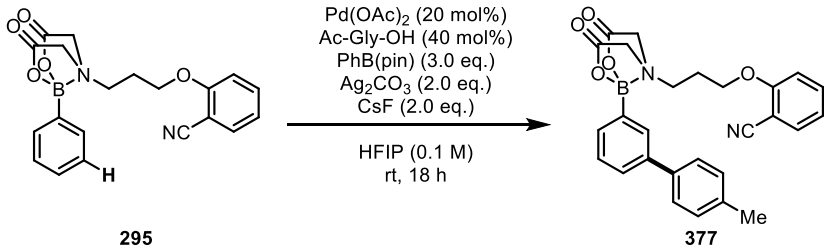
General Procedure I: The corresponding acetoxylated boronic acid MIDA-DG ester (0.21 mmol) (as a mixture of regioisomers) and K_3PO_4 were employed to yield the desired phenol as a glassy solid (12 mg, 0.07 mmol, 34%).

^{1}H NMR (400 MHz, DMSO-d_6) δ 10.72 (s, 1H), 10.48 (s, 1H), 7.64 (d, J = 8.8 Hz, 1H), 6.37 (dd, J = 8.8, 2.3 Hz, 1H), 6.30 (d, J = 2.3 Hz, 1H), 3.84 (s, 3H).

^{13}C NMR (101 MHz, DMSO-d_6) δ 170.01, 164.67, 163.13, 132.07, 108.82, 104.42, 102.94, 52.49.

The characterisation data for the compound is in agreement with that reported in the literature (*Org. Lett.* 2018, 20, 708-711).

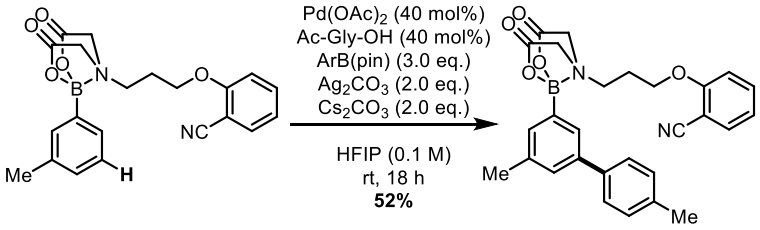
General Procedure J for the Screening of C–H Arylation Conditions:



295 377

A 4 mL vial was charged with aryl boronic acid MIDA-DG ester (0.05 mmol), aryl boronic acid pinacol ester (3.0 eq.), Ag_2CO_3 (2.0 eq.), Cs_2CO_3 (2.0 eq.), Ac-Gly-OH (40 mol%) and $Pd(OAc)_2$ (20 mol%). HFIP (0.1 M) was then added, the vial sealed and the suspension stirred at room temperature for 18 hours. After this time, CH_2Br_2 (1.0 eq.) was added as an internal standard and an aliquot (approximately 0.1 mL) taken. The aliquot was diluted with MeCN-d_3 and a ^{1}H NMR taken. The yield and remaining SM was calculated from comparison of the CH_2Br_2 peak with the middle methylene (-CH_2-) peak of the propylene linker.

3-Methyl-5-(4-methylphenyl)phenylboronic acid MIDA-DG ester



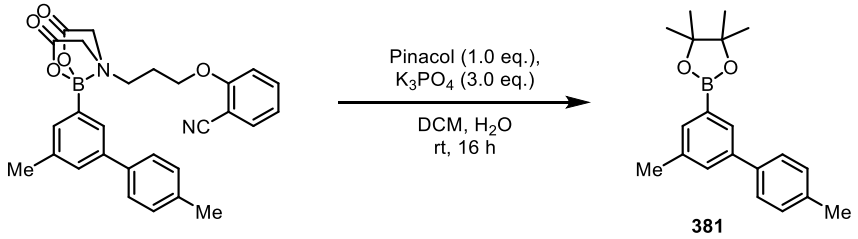
295

A 20 mL vial was charged with 3-methylphenylboronic acid MIDA-DG ester (78.4 mg, 0.20 mmol), 4-methylphenylboronic acid pinacol ester (90.3 mg, 2.0 eq.), Ag_2CO_3 (110 mg, 2.0 eq.), Cs_2CO_3 (130 mg, 2.0 eq.), Ac-Gly-OH (9.4 mg, 40 mol%) and $Pd(OAc)_2$ (9.0 mg, 20 mol%). HFIP (2.0 mL, 0.1 M) was then added, the vial sealed and the suspension stirred at room temperature for 4 hours. After this time, further $Pd(OAc)_2$ (9.0 mg, 20 mol%) was added, the vial resealed and stirring continued for 14 further hours. The reaction mixture was diluted with MeCN (~5 mL) and dry loaded onto a silica column. The column was washed with Et_2O (50 mL) before the products were eluted with MeCN:Et_2O (1:1) (50 mL). The solvent was removed to yield the crude

product/starting material mixture as an off white solid (71 mg, crude yield, calculated from ^{1}H NMR: **product:** 52%, **SM**: 26%).

HRMS (TOF ES+) Calcd. for $C_{28}H_{28}N_2O_5B$ ([M+H]$^+$): 483.2086. Found: 483.2098.

2-(4',5-Dimethyl-[1,1'-biphenyl]-3-yl)-4,4,5,5-tetramethyl-1,3,2-dioxaborolane (381)



A 20 mL vial was charged with the crude 3-methyl-5-(4-methylphenyl)phenylboronic acid MIDA-DG ester product (0.155 mmol from ^{1}H NMR) mixture and K_3PO_4 (99 mg, 3.0 eq.) and pinacol (18 mg, 1.0 eq.) were added. The solids were dissolved in DCM (1.55 mL), H_2O (0.8 mL) and THF (0.15 mL) and the biphasic mixture stirred overnight. The reaction mixture was diluted with brine (5 mL) and DCM (5 mL), the phases separated and the aqueous further extracted with DCM (2 × 5 mL). The organic phases were combined, dried over MgSO4, filtered and concentrated in vacuo. The crude product was purified using FCC (10% Et2O in hexanes) to yield the product as a white solid **381** (19 mg, 0.06 mmol, 40% yield, 32% over two steps). *The reaction mixture contained a 10% inseparable impurity believed to correspond to the 3-methyl-4-(4-phenylmethyl)phenylboronic acid pinacol ester.*

HRMS (TOF ES+) Calcd. for $C_{20}H_{26}O_2B$ ([M+H]$^+$): 309.2020. Found: 309.2032.

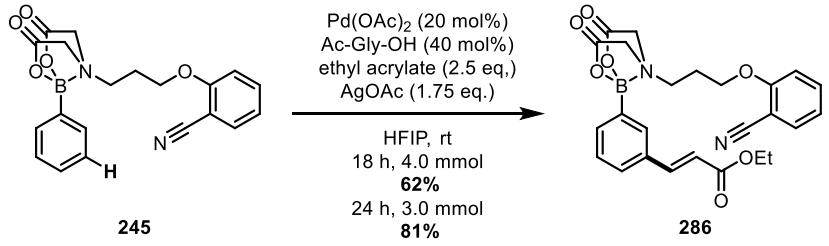
^{1}H NMR (400 MHz, Chloroform-*d*) δ 7.88 (dt, *J* = 1.8, 0.8 Hz, 1H), 7.64 (qd, *J* = 1.8, 1.2 Hz, 1H), 7.56 (d, *J* = 8.1 Hz, 2H), 7.53 (td, *J* = 1.9, 0.8 Hz, 1H), 7.28 – 7.24 (m, 3H), 2.45 (d, *J* = 0.7 Hz, 3H), 2.42 (s, 3H), 1.39 (d, *J* = 1.0 Hz, 15H).

^{13}C NMR (101 MHz, Chloroform-*d*) δ 138.3, 137.6, 136.8, 135.4, 134.1, 130.7, 130.5, 129.3, 127.1, 83.8, 24.9, 21.4, 21.1. ^{13}C NMR peaks were unambiguously assigned using HMBC and HSQC.

^{11}B NMR (128 MHz, Chloroform-*d*) δ 31.0.

Chapter 6

Large Scale Syntheses of 3-(Ethyl prop-2-enoate)phenylboronic acid MIDA-DG ester (286)



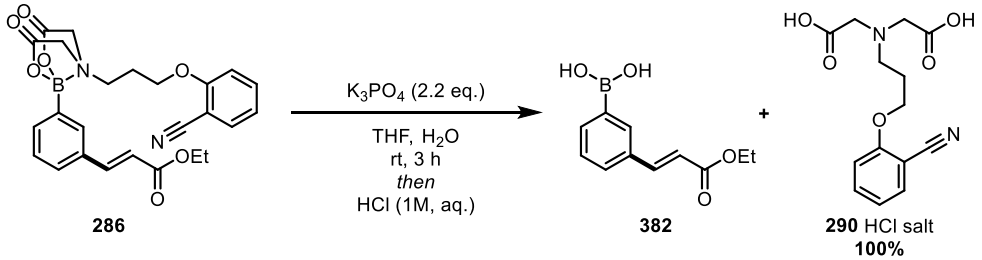
A 100 mL round-bottomed flask was charged with phenylboronic acid MIDA-DG ester (1.51 g, 4.00 mmol), AgOAc (1.17 g, 1.75 eq.), Ac-Gly-OH (187 mg, 40 mol%) and $Pd(OAc)_2$ (180 mg, 20 mol%). The flask was evacuated and flushed with nitrogen three times before HFIP (40 mL, 0.1 M) and the corresponding alkene coupling partner (1.09 mL, 2.5 eq.) were added. The vial was sealed and stirred at room temperature for 18 hours. The reaction mixture was diluted with MeCN (40 mL) and dry loaded onto a silica column. The column was washed with copius Et_2O before the products were subsequently eluted with MeCN:Et_2O (1:1, 250 mL). The solvent was removed under vacuum to yield the desired product as a crystalline white solid (1.45g, 62% total yield, **a**: 43%, **b**: 7%, **a+a:** 7%, **a+b:** 5%, **SM:** 15%).

The reaction was repeated on a 3 mmol scale, and left for 24 hours to drive the reaction to completion. The product was isolated as a crystalline white solid (1.25 g, 81% total yield, **a**: 56%, **b**: 8%, **a+a:** 10%, **a+b:** 7%).

The average yield for the two repeats was: 72% total yield

The characterisation data was in agreement with that reported within this experimental.

General procedure K for the removal and recovery of the MIDA-DG HCl Salt (290):

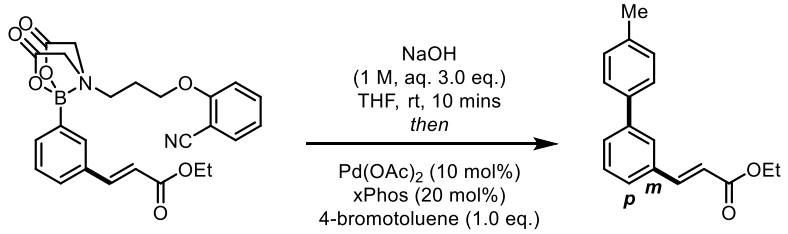


To a mixture of C–H alkenylated products [168 mg, 0.36 mmol (0.20 mmol *meta*, 0.16 mmol *para, meta-meta di, meta-para di* and *non-alkenylated*)] was added THF (3.25 mL) and NaOH (1 M aq., 1.1 mL, 3 eq.). The mixture was stirred for 10 minutes at room temperature until no starting materials were observed by TLC (EtOAc). The reaction was acidified using HCl (1 M, aq.) (2.2 mL), the THF removed under reduced pressure at 30 °C for 10 minutes and the resulting suspension diluted with H_2O (11 mL) and Et_2O (13 mL). The layers were separated and the aqueous phase further extracted with Et_2O (2 × 13 mL). The combined organic phases were dried with $MgSO_4$

and concentrated to give a crude mixture of boronic acids that were immediately used in the next step.

The aqueous phase was collected and concentrated under a steady stream of nitrogen overnight. The resulting solid was dissolved in MeCN, filtered to remove the NaCl and concentrated under vacuo to yield the MIDA-DG hydrochloride (118 mg, 0.36 mmol, 100%) as an off-white solid.

Ethyl (*E*)-3-(4'-methyl-[1,1'-biphenyl]-3-yl)acrylate (385)



286 **385**

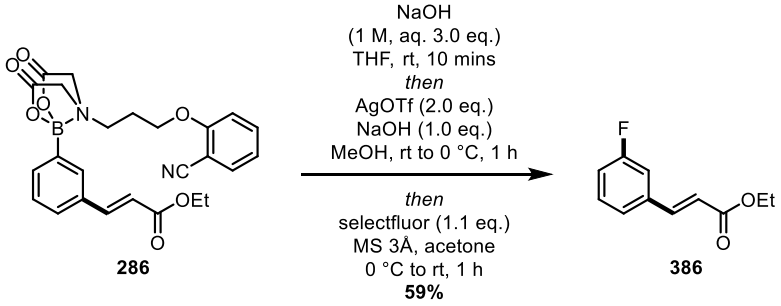
Following the **general procedure K for removal and recovery of the MIDA-DG** (84 mg, 0.18 mmol, 0.10 mmol *meta*), the crude boronic acid (1.2 eq.), $Pd(OAc)_2$ (3.3 mg, 10 mol%), xphos (14.1 mg, 20 mol%) and K_3PO_4 (94 mg, 3.0 eq.) were added to a 20 mL vial and placed under an atmosphere of nitrogen. Degassed 1,4-dioxane (1.5 mL) and 4-bromotoluene (18 □L, 0.15 mmol, 1.0 eq.) were then added and the reaction mixture stirred under N_2 at 75 °C for 18 hours. The reaction mixture was dry loaded on to silica and purified via FCC (5% EtOAc in hexane) to yield the desired product (13.0 mg, 0.05 mmol, 48%) as a colourless oil. *The product contains a 6% impurity believed to be ethyl (E)-3-(4'-methyl-[1,1'-biphenyl]-4-yl)acrylate.*

^{1}H NMR (400 MHz, Chloroform-*d*) δ 7.75 (d, *J* = 16.1 Hz, 1H), 7.72 (t, *J* = 1.8 Hz, 1H), 7.62 – 7.57 (m, 1H), 7.51 – 7.43 (m, 4H), 7.29 – 7.25 (m, 2H), 6.50 (d, *J* = 16.0 Hz, 1H), 4.28 (q, *J* = 7.1 Hz, 2H), 2.41 (s, 3H), 1.35 (t, *J* = 7.1 Hz, 3H).

^{13}C NMR (101 MHz, Chloroform-*d*) δ 167.0, 144.6, 141.9, 137.5, 134.9, 129.6, 129.3, 128.9, 127.0, 126.7, 126.5, 118.5, 60.6, 21.1, 14.4.

The characterisation data for the compound is in agreement with that reported in the literature (*J. Am. Chem. Soc.* 2019, 141, 1903-1907).

Ethyl (*E*)-3-(3-fluorophenyl)acrylate (386)



The method described in *Org. Lett.* 2009, **11**, 2860-2863 was used for the fluorination of the boronic acid.

Following the **general procedure K for removal and recovery of the MIDA-DG** (168.0 mg, 0.36 mmol, 0.20 mmol *meta*), the crude boronic acid (1.0 eq.) and NaOH (14.2 mg, 1.0 eq.) were dissolved in MeOH (1.8 mL) and stirred at room temperature for 15 minutes. The mixture was then cooled to 0 °C and AgOTf (182.5 mg, 2.0 eq.) added. The reaction mixture was then stirred for 30 minutes at 0 °C then concentrated under a stream of nitrogen, still at 0 °C. The MeOH was further removed by azeotroping with acetone (2 × 1.8 mL) at 0 °C. Once dry, molecular sieves (3 Å, 180 mg) and selectfluor (132.0 mg, 1.05 eq.) were added, dissolved in acetone (3.6 mL), stirred at 0 °C for 5 minutes then warmed to room temperature. The reaction mixture was dry loaded onto silica and purified via FCC (5% EtOAc in hexane). The appropriate fractions were combined and concentrated to yield the desired product (23.0 mg, 0.12 mmol, 59%) as a colourless oil. *The product contains a 10% impurity believed to be ethyl cinnamate from protodeboronation during the reaction.*

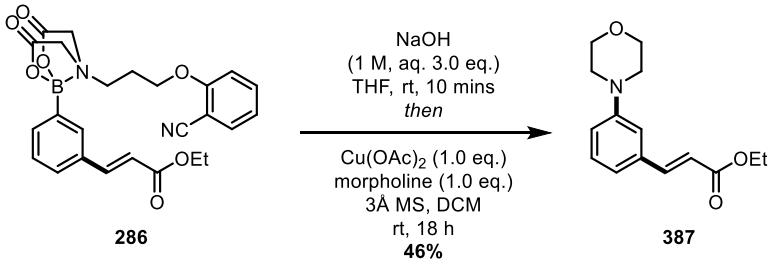
^{1}H NMR (400 MHz, Chloroform-*d*) δ 7.63 (d, *J* = 16.0 Hz, 1H), 7.39 – 7.31 (m, 1H), 7.29 (dt, *J* = 7.8, 1.3 Hz, 1H), 7.24 – 7.18 (m, 1H), 7.07 (tdd, *J* = 8.1, 2.5, 1.0 Hz, 1H), 6.42 (d, *J* = 16.0 Hz, 1H), 4.27 (q, *J* = 7.1 Hz, 2H), 1.34 (t, *J* = 7.1 Hz, 3H).

^{19}F NMR (377 MHz, Chloroform-*d*) δ -112.6 (q, *J* = 8.6 Hz).

^{13}C NMR (101 MHz, Chloroform-*d*) δ 166.6, 163.0 (d, *J* = 246.8 Hz), 143.2 (d, *J* = 1.9 Hz), 136.7 (d, *J* = 7.7 Hz), 130.4 (d, *J* = 8.1 Hz), 124.0, 119.7, 117.1 (d, *J* = 21.6 Hz), 114.3 (d, *J* = 22.3 Hz), 60.7, 14.3.

The characterisation data for the compound is in agreement with that reported in the literature (*Synth. Commun.* 2018, 48, 1482-1486).

Ethyl (*E*)-3-(3-morpholinophenyl)acrylate (387)



Following the **general procedure K for removal and recovery of the MIDA-DG** (168.0 mg, 0.36 mmol, 0.20 mmol *meta*), the crude boronic acid (1.2 eq.), $Cu(OAc)_2$ (27.3 mg, 1 eq.) and molecular sieves (3 Å, 50 mg) were added to a 4 mL vial. The solids were dissolved in DCM (1 mL) and morpholine (13 mL, 1 eq.) added. The reaction mixture was stirred under air, at room temperature, overnight. After completion, the reaction mixture was dry loaded onto silica and purified via FCC (15% EtOAc in hex) to yield the product (24.0 mg, 0.09 mmol, 46%) as a colourless oil.

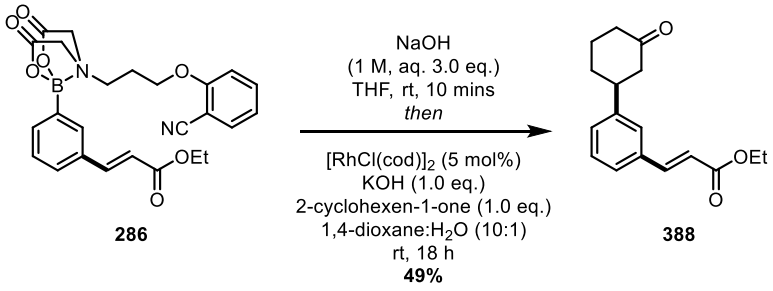
ν_{max}/cm^{-1} 2974, 1707, 1636, 1595, 1491, 1446, 1305, 1267, 1238, 1174, 1122, 1036, 980, 891, 857, 783, 682

HRMS (TOF ES+) Calcd. for $C_{15}H_{20}NO_3$ ($[M+H]^+$): 262.1438. Found: 262.1445.

^{1}H NMR (400 MHz, Acetonitrile-d_3) δ 7.63 (d, *J* = 16.0 Hz, 1H), 7.31 – 7.24 (m, 1H), 7.15 (t, *J* = 2.1 Hz, 1H), 7.11 – 7.07 (m, 1H), 6.98 (ddd, *J* = 8.3, 2.6, 0.9 Hz, 1H), 6.49 (d, *J* = 16.0 Hz, 1H), 4.21 (q, *J* = 7.1 Hz, 2H), 3.80 – 3.74 (m, 4H), 3.19 – 3.11 (m, 4H), 1.28 (t, *J* = 7.1 Hz, 3H).

^{13}C NMR (101 MHz, Acetonitrile-d_3) δ 166.6, 152.0, 144.8, 144.1, 135.2, 129.6, 119.2, 118.1, 114.9, 66.4, 60.2, 48.8, 13.6.

Ethyl (*E*)-3-(3-(3-oxocyclohexyl)phenyl)acrylate (388)



Following the **general procedure K for removal and recovery of the MIDA-DG** (84.0 mg, 0.18 mmol, 0.1 mmol *meta*), the crude boronic acid (1.2 eq.) and $[RhCl(cod)]_2$ (3.7 mg, 5 mol%) were place under a nitrogen atmosphere. A solution of 1,4-dioxane:H_2O (10:1, 1.5 mL) and KOH (8.4 mg, 1.0 eq.) was degassed for 15 minutes using nitrogen before being added to the boronic acid and catalyst. 2-Cyclohexen-1-one (14.5 ?l, 1.0 eq.) was added and the mixture stirred at room temperature overnight. After completion, the reaction mixture was dry loaded directly onto silica

and purified via FCC (30% EtOAc in hexanes). The appropriate fractions were combined and concentrated to yield the product (20 mg, 0.07 mmol, 49%) as a colourless oil.

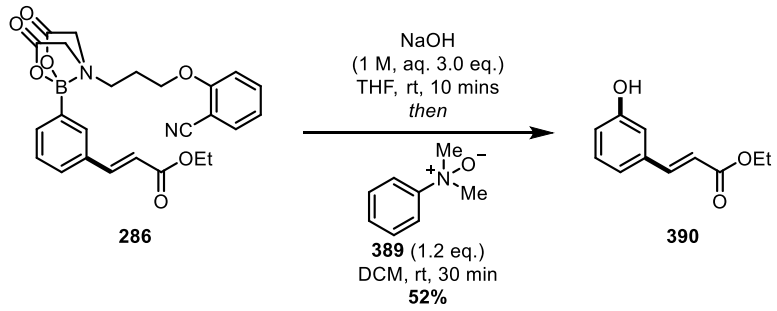
ν_{max}/cm^{-1} 2933, 1703, 1636, 1446, 1368, 1312, 1264, 1223, 1163, 1096, 1036, 984, 865, 798, 693

HRMS (TOF ES+) Calcd. for $C_{17}H_{21}O_3$ ([M+H]$^+$): 273.1485. Found: 273.1488.

^{1}H NMR (400 MHz, Chloroform-*d*) δ 7.70 (d, *J* = 16.0 Hz, 1H), 7.43 (dt, *J* = 7.8, 1.5 Hz, 1H), 7.41 – 7.34 (m, 2H), 7.26 (dt, *J* = 7.6, 1.5 Hz, 1H), 6.46 (d, *J* = 16.1 Hz, 1H), 4.29 (q, *J* = 7.1 Hz, 2H), 3.05 (tt, *J* = 11.7, 4.0 Hz, 1H), 2.67 – 2.34 (m, 4H), 2.24 – 2.07 (m, 2H), 1.98 – 1.71 (m, 2H), 1.36 (t, *J* = 7.1 Hz, 3H).

^{13}C NMR (101 MHz, Chloroform-*d*) δ 210.6, 166.9, 145.0, 144.4, 134.9, 129.3, 128.6, 126.4, 126.3, 118.5, 60.6, 48.8, 44.6, 41.2, 32.7, 25.5, 14.3.

Ethyl (*E*)-3-(3-hydroxyphenyl)acrylate (390)



Following the **general procedure K for removal and recovery of the MIDA-DG** (84.0 mg, 0.18 mmol, 0.1 mmol *meta*), the crude boronic acid (1 eq.) and *N,N*-dimethylaniline-*N*-oxide (29.6 mg, 1.2 eq.) were dissolved in DCM (1 mL) and stirred at room temperature. After completion by TLC (15% EtOAc in hexane), roughly 30 minutes, the reaction mixture was dry loaded onto silica and purified via FCC (15% EtOAc in hexane). The appropriate fractions were combined and concentrated to yield the product (10 mg, 0.05 mmol, 52%) as a colourless oil.

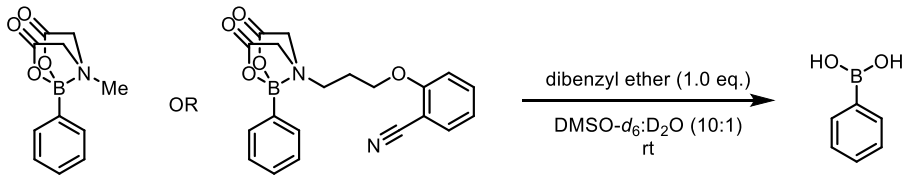
^{1}H NMR (400 MHz, Chloroform-*d*) δ 7.63 (d, *J* = 16.0 Hz, 1H), 7.30 – 7.21 (m, 1H), 7.09 (dt, *J* = 8.0, 1.3 Hz, 1H), 7.02 (t, *J* = 2.0 Hz, 1H), 6.91 – 6.85 (m, 1H), 6.41 (d, *J* = 16.1 Hz, 1H), 5.75 (br. s, 1H), 4.27 (q, *J* = 7.2 Hz, 2H), 1.34 (t, *J* = 7.2 Hz, 3H).

^{13}C NMR (101 MHz, Chloroform-*d*) δ 167.3, 156.2, 144.6, 135.9, 130.1, 120.7, 118.5, 117.5, 114.6, 60.8, 14.3.

The characterisation data for the compound is in agreement with that reported in the literature (*J. Am. Chem. Soc.* 2019, 141, 1903-1907).

Comparison of PhB(MIDA-DG) (245) and PhB(MIDA) (127) stabilities to hydrolysis.

The stability of phenylboronic acid MIDA-DG ester to hydrolysis compared to phenylboronic acid MIDA ester and other boronate esters was performed using the same method as Suginome et al. (*Org. Lett.* 2011, **13**, 2662-2665) to allow for comparison of results.

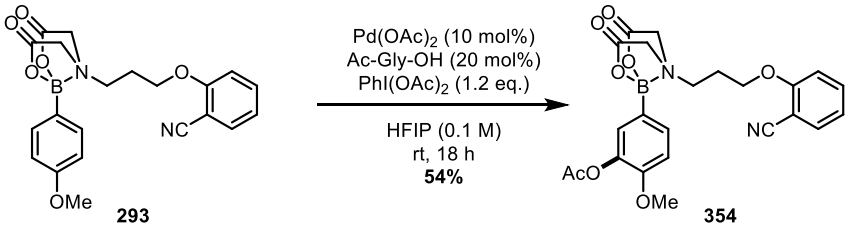


127 **245** **108**

For the PhB(MIDA): 127 A solution of PhB(MIDA) (5.0 mg, 0.02 mmol) and dibenzyl ether (3.8 μL, 0.02 mmol) in DMSO-d_6 (0.7 mL) and D_2O (0.07 mL) and ^1H NMR spectra taken at intervals of 24 hours starting at 0 hours.

For the PhB(MIDA-DG) 245: A solution of PhB(MIDA-DG) (8.1 mg, 0.02 mmol) and dibenzyl ether (3.8 μL, 0.02 mmol) in DMSO-d_6 (0.7 mL) and D_2O (0.07 mL) and ^1H NMR spectra taken at intervals of 24 hours starting at 0 hours for 72 hours.

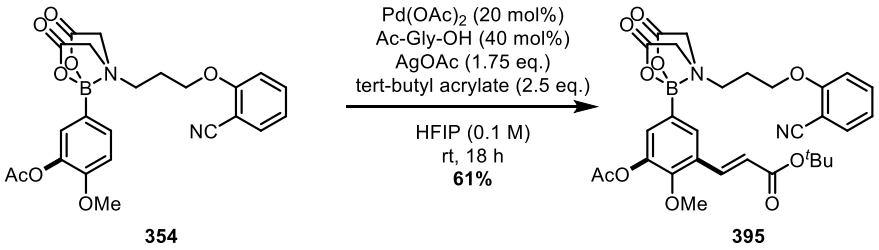
4-Methoxy-3-acetoxyphenylboronic acid MIDA-DG ester (354)



293 **354**

A 20 mL vial was charged with arylboronic acid MIDA-DG ester (354 mg, 0.87 mmol), $PhI(OAc)_2$ (335 mg, 1.2 eq.), Ac-Gly-OH (20 mg, 20 mol%), $Pd(OAc)_2$ (20 mg, 10 mol%) and HFIP (8.7 mL). The vial was sealed and stirred at room temperature for 18 hours. The reaction mixture was diluted with MeCN (~5 mL), dry loaded onto a silica column and purified via 'catch and release' purification (washed with copious Et_2O, then elute with a similar amount of EtOAc) to yield the acetoxylated product as an off-white solid (218 mg, 0.47 mmol, 54%). The characterisation data was in agreement with that reported for the same compound above.

3-Acetoxy-4-methoxy-5-(*tert*-butyl prop-2-enoate)phenylboronic acid MIDA-DG ester (395)



354 395

A 20 mL vial was charged with the acetoxylated arylboronic acid MIDA-DG ester (161 mg, 0.35 mmol), AgOAc (100 mg, 1.75 eq.), Ac-Gly-OH (16 mg, 40 mol%) and $Pd(OAc)_2$ (16 mg, 20 mol%). The vial was evacuated and flushed with nitrogen three times before HFIP (3.45 mL) and the *tert*-butyl acrylate (125 □L, 2.5 eq.) were added. The vial was sealed and stirred at room temperature for 23 hours. The reaction mixture was diluted with MeCN (~5 mL) and dry loaded onto a silica column. The column was washed with Et_2O (100 mL) before the products were subsequently eluted with copious EtOAc. The EtOAc was removed under vacuum to yield the alkenylated products as an off white solid (158 mg, 0.209 mmol, 61%). The isolated product contained a 21% (0.07 mmol) impurity corresponding to the starting material that could not be separated from the product.

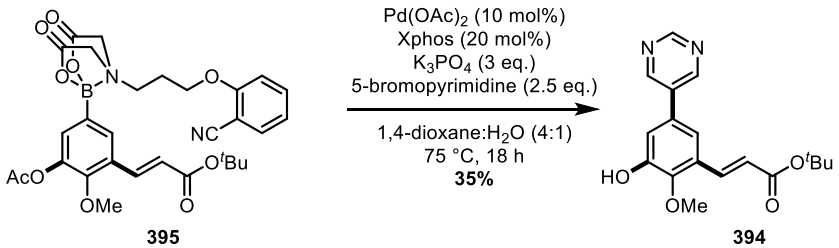
HRMS (TOF ES+) Calcd. for $C_{30}H_{33}N_2O_{10}BNa$ ([M+Na]$^+$): 615.2126. Found: 615.2128.

^{1}H NMR (400 MHz, Acetonitrile-d_3) δ 7.81 – 7.74 (m, 1H), 7.64 – 7.54 (m, 3H), 7.27 (d, J = 1.7 Hz, 1H), 7.10 – 7.05 (m, 1H), 7.00 (d, J = 8.5 Hz, 1H), 6.50 (d, J = 16.2 Hz, 1H), 4.11 (d, J = 17.1 Hz, 2H), 4.06 – 3.96 (m, 4H), 3.82 (s, 3H), 2.92 – 2.82 (m, 2H), 2.31 (s, 3H), 2.11 (dtd, J = 11.6, 4.0, 2.2 Hz, 2H), 1.53 (s, 9H).

^{13}C NMR (101 MHz, Acetonitrile-d_3) δ 169.1, 168.3, 165.9, 160.0, 151.6, 143.9, 137.4, 134.8, 133.6, 129.8, 129.4, 129.0, 122.1, 121.3, 116.1, 112.8, 101.4, 80.2, 65.9, 61.4, 59.1, 56.2, 27.4, 23.9, 20.1.

^{11}B NMR (128 MHz, Acetonitrile-d_3) δ 11.4.

tert-Butyl (*E*)-3-(3-hydroxy-2-methoxy-5-(pyrimidin-5-yl)phenyl)acrylate (394)



395 394

A 20 mL vial was charged with the acetoxylated and alkenylated boronic acid MIDA-DG (0.28 mmol, 0.209 acetoxylated and alkenylated product, 0.07 mmol acetoxylated material, 1.2 eq.). $Pd(OAc)_2$ (5.3 mg, 10 mol%), XPhos (22.4 mg, 20 mol%) and 5-bromopyrimidine (37.5 mg, 1.0 eq.) were added and the vial sealed and placed under a nitrogen atmosphere. The mixture was

suspended in degassed 1,3-dioxane (0.24 mL) and a degassed solution of K_3PO_4 (150 mg, 3.0 eq.) in H_2O (0.6 mL) subsequently added. The mixture was heated to 75 °C for 18 hours. On completion, the mixture was diluted with brine (3 mL) and extracted with DCM (3 × 6 mL). The organic phases were combined, dried over $MgSO_4$, filtered and concentrated in vacuo. The crude product was purified using preparative TLC (50% Et2O in hexanes) to yield the desired product (27 mg, 0.082 mmol, 35%) as a clear glassy solid.

ν_{max}/cm^{-1} 2930m 1703, 1636, 1580, 1416, 1368, 1312, 1252, 1215, 1152, 992, 902, 854, 992

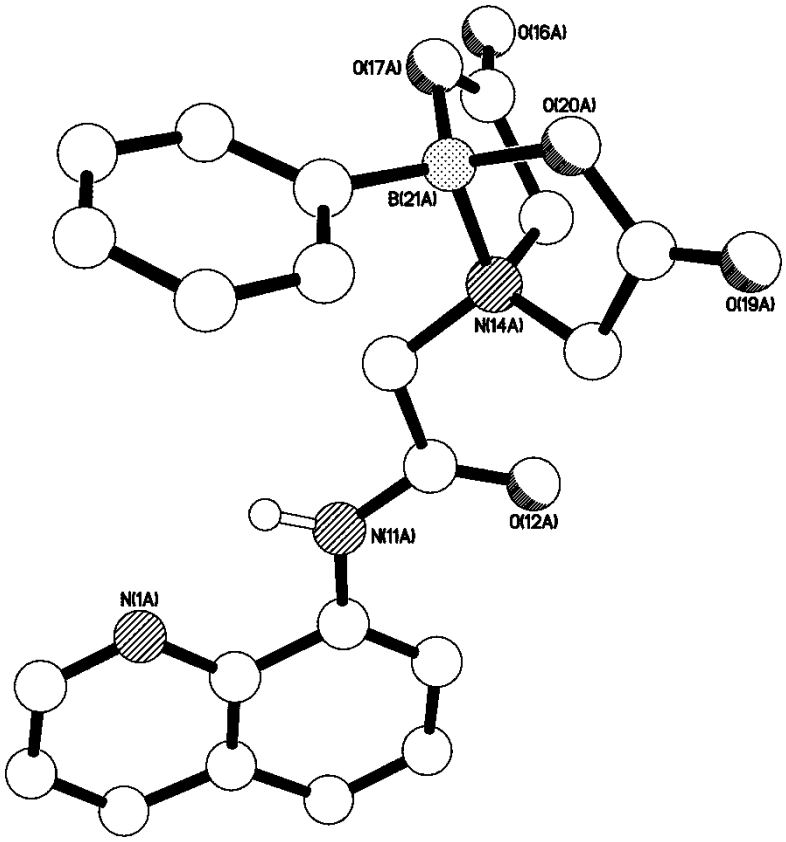
HRMS (APCI +) Calcd. for $C_{18}H_{21}N_2O_4$ ($[M+H]^+$): 329.1496. Found: 329.1495.

^{1}H NMR (400 MHz, Chloroform-*d*) δ 9.24 (s, 1H), 8.95 (s, 3H), 7.85 (d, *J* = 16.1 Hz, 1H), 7.28 (s, 1H), 7.22 (d, *J* = 2.2 Hz, 1H), 6.54 (d, *J* = 16.1 Hz, 1H), 6.10 (s, 1H), 3.91 (s, 3H), 1.58 (s, 10H).

^{13}C NMR (101 MHz, Chloroform-*d*) δ 166.0, 157.6, 154.8, 150.2, 136.9, 133.5, 131.3, 129.1, 123.1, 117.9, 115.4, 115.0, 81.0, 62.6, 28.2.

X-Ray Crystallisation Data

X-ray data for 187:



Formula	C21 H18 B N3 O5, 1.5(C4 H8 O)	
Formula weight	511.35	
Temperature	293(2) K	
Diffractometer, wavelength	Agilent Xcalibur 3 E, 0.71073 Å	
Crystal system, space group	Triclinic, P-1	
Unit cell dimensions	a = 13.2920(8) Å	α = 93.193(4)°
	b = 14.1645(7) Å	β = 97.190(4)°
	c = 14.9222(6) Å	γ = 111.082(5)°
Volume, Z	2585.4(2) $Å^3$, 4	
Density (calculated)	1.314 Mg/m^3	
Absorption coefficient	0.094 mm^{-1}	
F(000)	1080	
Crystal colour / morphology	Colourless blocks	
Crystal size	0.76 x 0.50 x 0.35 mm^3	
□ range for data collection	2.660 to 28.307°	
Index ranges	-17<=h<=17, -12<=k<=18, -18<=l<=19	

Reflns collected / unique	14864 / 10172 [R(int) = 0.0163]
Reflns observed [F>4σ(F)]	6706
Absorption correction	Analytical
Max. and min. transmission	0.974 and 0.960
Refinement method	Full-matrix least-squares on F^2
Data / restraints / parameters	10172 / 33 / 550
Goodness-of-fit on F^2	1.037
Final R indices [F>4σ(F)]	R1 = 0.0666, wR2 = 0.1666
R indices (all data)	R1 = 0.1001, wR2 = 0.1905
Largest diff. peak, hole	0.626, -0.328 $eÅ^{-3}$
Mean and maximum shift/error	0.000 and 0.002

Bond lengths [Å] and angles [°] for **187**:

N(1A)-C(10A)	1.312(4)
N(1A)-C(2A)	1.360(4)
C(2A)-C(7A)	1.413(4)
C(2A)-C(3A)	1.432(4)
C(3A)-C(4A)	1.359(4)
C(3A)-N(11A)	1.405(3)
C(4A)-C(5A)	1.406(4)
C(5A)-C(6A)	1.361(5)
C(6A)-C(7A)	1.402(5)
C(7A)-C(8A)	1.425(5)
C(8A)-C(9A)	1.344(5)
C(9A)-C(10A)	1.403(5)
N(11A)-C(12A)	1.343(3)
C(12A)-O(12A)	1.220(3)
C(12A)-C(13A)	1.518(3)
C(13A)-N(14A)	1.483(3)
N(14A)-C(18A)	1.490(3)
N(14A)-C(15A)	1.503(3)
N(14A)-B(21A)	1.668(3)
C(15A)-C(16A)	1.509(4)
C(16A)-O(16A)	1.206(3)

C(16A)-O(17A)	1.323(3)
O(17A)-B(21A)	1.464(3)
C(18A)-C(19A)	1.507(3)
C(19A)-O(19A)	1.214(3)
C(19A)-O(20A)	1.319(3)
O(20A)-B(21A)	1.484(3)
B(21A)-C(22A)	1.578(4)
C(22A)-C(23A)	1.385(4)
C(22A)-C(27A)	1.395(3)
C(23A)-C(24A)	1.391(4)
C(24A)-C(25A)	1.367(5)
C(25A)-C(26A)	1.371(4)
C(26A)-C(27A)	1.378(4)
N(1B)-C(10B)	1.316(4)
N(1B)-C(2B)	1.361(4)
C(2B)-C(3B)	1.397(4)
C(2B)-C(7B)	1.439(4)
C(3B)-C(4B)	1.375(4)
C(3B)-N(11B)	1.409(4)
C(4B)-C(5B)	1.383(5)
C(5B)-C(6B)	1.330(5)
C(6B)-C(7B)	1.394(5)
C(7B)-C(8B)	1.378(5)
C(8B)-C(9B)	1.345(6)
C(9B)-C(10B)	1.418(5)
N(11B)-C(12B)	1.344(3)
C(12B)-O(12B)	1.216(3)
C(12B)-C(13B)	1.513(4)
C(13B)-N(14B)	1.487(3)
N(14B)-C(18B)	1.498(3)
N(14B)-C(15B)	1.498(3)
N(14B)-B(21B)	1.660(4)
C(15B)-C(16B)	1.523(4)
C(16B)-O(16B)	1.204(3)
C(16B)-O(17B)	1.310(4)
O(17B)-B(21B)	1.466(4)

C(18B)-C(19B)	1.491(4)
C(19B)-O(19B)	1.203(3)
C(19B)-O(20B)	1.320(3)
O(20B)-B(21B)	1.475(4)
B(21B)-C(22B)	1.603(4)
B(21B)-C(22")	1.608(9)
C(22B)-C(23B)	1.3900
C(22B)-C(27B)	1.3900
C(23B)-C(24B)	1.3900
C(24B)-C(25B)	1.3900
C(25B)-C(26B)	1.3900
C(26B)-C(27B)	1.3900
C(22")-C(23")	1.3900
C(22")-C(27")	1.3900
C(23")-C(24")	1.3900
C(24")-C(25")	1.3900
C(25")-C(26")	1.3900
C(26")-C(27")	1.3900

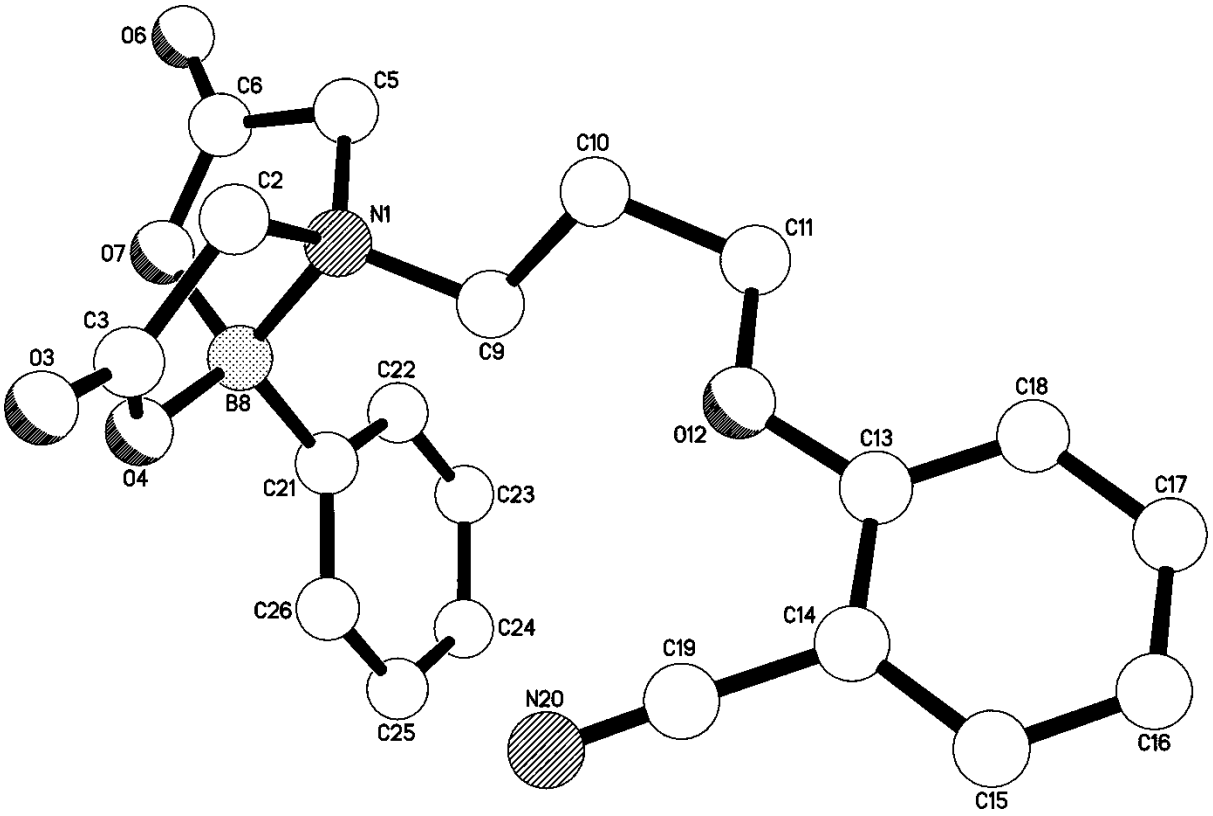
C(10A)-N(1A)-C(2A)	117.4(3)
N(1A)-C(2A)-C(7A)	123.7(3)
N(1A)-C(2A)-C(3A)	117.6(2)
C(7A)-C(2A)-C(3A)	118.7(3)
C(4A)-C(3A)-N(11A)	125.8(2)
C(4A)-C(3A)-C(2A)	120.2(2)
N(11A)-C(3A)-C(2A)	113.9(2)
C(3A)-C(4A)-C(5A)	120.2(3)
C(6A)-C(5A)-C(4A)	120.9(3)
C(5A)-C(6A)-C(7A)	120.6(3)
C(6A)-C(7A)-C(2A)	119.4(3)
C(6A)-C(7A)-C(8A)	124.9(3)
C(2A)-C(7A)-C(8A)	115.7(3)
C(9A)-C(8A)-C(7A)	120.2(3)
C(8A)-C(9A)-C(10A)	119.4(3)
N(1A)-C(10A)-C(9A)	123.6(4)
C(12A)-N(11A)-C(3A)	128.4(2)

O(12A)-C(12A)-N(11A)	124.9(2)
O(12A)-C(12A)-C(13A)	122.8(2)
N(11A)-C(12A)-C(13A)	112.3(2)
N(14A)-C(13A)-C(12A)	112.87(19)
C(13A)-N(14A)-C(18A)	113.85(17)
C(13A)-N(14A)-C(15A)	112.07(18)
C(18A)-N(14A)-C(15A)	112.87(18)
C(13A)-N(14A)-B(21A)	112.34(17)
C(18A)-N(14A)-B(21A)	103.20(17)
C(15A)-N(14A)-B(21A)	101.50(17)
N(14A)-C(15A)-C(16A)	105.4(2)
O(16A)-C(16A)-O(17A)	124.2(3)
O(16A)-C(16A)-C(15A)	124.3(3)
O(17A)-C(16A)-C(15A)	111.5(2)
C(16A)-O(17A)-B(21A)	113.42(19)
N(14A)-C(18A)-C(19A)	104.73(18)
O(19A)-C(19A)-O(20A)	123.8(2)
O(19A)-C(19A)-C(18A)	124.6(2)
O(20A)-C(19A)-C(18A)	111.6(2)
C(19A)-O(20A)-B(21A)	113.81(18)
O(17A)-B(21A)-O(20A)	111.67(19)
O(17A)-B(21A)-C(22A)	114.2(2)
O(20A)-B(21A)-C(22A)	113.2(2)
O(17A)-B(21A)-N(14A)	101.60(19)
O(20A)-B(21A)-N(14A)	98.96(18)
C(22A)-B(21A)-N(14A)	115.77(18)
C(23A)-C(22A)-C(27A)	116.5(2)
C(23A)-C(22A)-B(21A)	122.6(2)
C(27A)-C(22A)-B(21A)	120.9(2)
C(22A)-C(23A)-C(24A)	121.4(3)
C(25A)-C(24A)-C(23A)	120.3(3)
C(24A)-C(25A)-C(26A)	119.8(3)
C(25A)-C(26A)-C(27A)	119.7(3)
C(26A)-C(27A)-C(22A)	122.3(3)
C(10B)-N(1B)-C(2B)	115.9(3)
N(1B)-C(2B)-C(3B)	117.7(3)

N(1B)-C(2B)-C(7B)	123.5(3)
C(3B)-C(2B)-C(7B)	118.7(3)
C(4B)-C(3B)-C(2B)	119.3(3)
C(4B)-C(3B)-N(11B)	123.9(3)
C(2B)-C(3B)-N(11B)	116.8(3)
C(3B)-C(4B)-C(5B)	121.2(4)
C(6B)-C(5B)-C(4B)	120.9(4)
C(5B)-C(6B)-C(7B)	121.2(3)
C(8B)-C(7B)-C(6B)	124.2(4)
C(8B)-C(7B)-C(2B)	117.1(3)
C(6B)-C(7B)-C(2B)	118.7(3)
C(9B)-C(8B)-C(7B)	119.7(4)
C(8B)-C(9B)-C(10B)	119.8(3)
N(1B)-C(10B)-C(9B)	123.9(4)
C(12B)-N(11B)-C(3B)	126.4(2)
O(12B)-C(12B)-N(11B)	123.9(3)
O(12B)-C(12B)-C(13B)	121.8(2)
N(11B)-C(12B)-C(13B)	114.3(2)
N(14B)-C(13B)-C(12B)	112.2(2)
C(13B)-N(14B)-C(18B)	111.2(2)
C(13B)-N(14B)-C(15B)	112.9(2)
C(18B)-N(14B)-C(15B)	111.9(2)
C(13B)-N(14B)-B(21B)	114.95(18)
C(18B)-N(14B)-B(21B)	102.6(2)
C(15B)-N(14B)-B(21B)	102.56(19)
N(14B)-C(15B)-C(16B)	105.1(2)
O(16B)-C(16B)-O(17B)	124.5(3)
O(16B)-C(16B)-C(15B)	123.8(3)
O(17B)-C(16B)-C(15B)	111.7(2)
C(16B)-O(17B)-B(21B)	113.5(2)
C(19B)-C(18B)-N(14B)	105.1(2)
O(19B)-C(19B)-O(20B)	124.0(3)
O(19B)-C(19B)-C(18B)	124.8(3)
O(20B)-C(19B)-C(18B)	111.1(2)
C(19B)-O(20B)-B(21B)	114.4(2)
O(17B)-B(21B)-O(20B)	111.5(2)

O(17B)-B(21B)-C(22B)	115.8(2)
O(20B)-B(21B)-C(22B)	113.5(3)
O(17B)-B(21B)-C(22")	110.2(5)
O(20B)-B(21B)-C(22")	111.2(6)
O(17B)-B(21B)-N(14B)	101.2(2)
O(20B)-B(21B)-N(14B)	99.4(2)
C(22B)-B(21B)-N(14B)	113.6(2)
C(22")-B(21B)-N(14B)	122.5(6)
C(23B)-C(22B)-C(27B)	120.0
C(23B)-C(22B)-B(21B)	120.8(2)
C(27B)-C(22B)-B(21B)	119.2(2)
C(24B)-C(23B)-C(22B)	120.0
C(23B)-C(24B)-C(25B)	120.0
C(26B)-C(25B)-C(24B)	120.0
C(25B)-C(26B)-C(27B)	120.0
C(26B)-C(27B)-C(22B)	120.0
C(23")-C(22")-C(27")	120.0
C(23")-C(22")-B(21B)	118.2(8)
C(27")-C(22")-B(21B)	121.8(8)
C(22")-C(23")-C(24")	120.0
C(23")-C(24")-C(25")	120.0
C(26")-C(25")-C(24")	120.0
C(25")-C(26")-C(27")	120.0
C(26")-C(27")-C(22")	120.0

X-ray data for 245:



Formula	C20 H19 B N2 O5	
Formula weight	378.18	
Temperature	173(2) K	
Diffractometer, wavelength	Agilent Xcalibur 3 E, 0.71073 Å	
Crystal system, space group	Monoclinic, $P2_1/c$	
Unit cell dimensions	a = 9.8085(5) Å	α = 90°
	b = 8.9262(4) Å	β = 99.222(5)°
	c = 21.7277(9) Å	γ = 90°
Volume, Z	1877.72(16) $Å^3$, 4	
Density (calculated)	1.338 Mg/m^3	
Absorption coefficient	0.096 mm^{-1}	
F(000)	792	
Crystal colour / morphology	Colourless blocky needles	
Crystal size	0.756 x 0.225 x 0.125 mm^3	
□ range for data collection	2.471 to 28.211°	
Index ranges	-13<=h<=13, -7<=k<=11, -18<=l<=28	
Reflns collected / unique	6389 / 3720 [R(int) = 0.0233]	
Reflns observed [F>4□(F)]	2805	

Absorption correction	Analytical
Max. and min. transmission	0.990 and 0.954
Refinement method	Full-matrix least-squares on F^2
Data / restraints / parameters	3720 / 0 / 254
Goodness-of-fit on F^2	1.044
Final R indices [F>4□(F)]	R1 = 0.0439, wR2 = 0.0895
R indices (all data)	R1 = 0.0648, wR2 = 0.1012
Largest diff. peak, hole	0.239, -0.203 $eÅ^{-3}$
Mean and maximum shift/error	0.000 and 0.000

Bond lengths [Å] and angles [°] for **245:**

N(1)-C(5)	1.4899(18)
N(1)-C(2)	1.4964(19)
N(1)-C(9)	1.5001(19)
N(1)-B(8)	1.662(2)
C(2)-C(3)	1.506(2)
C(3)-O(3)	1.2027(19)
C(3)-O(4)	1.334(2)
O(4)-B(8)	1.462(2)
C(5)-C(6)	1.513(2)
C(6)-O(6)	1.2025(18)
C(6)-O(7)	1.3272(19)
O(7)-B(8)	1.486(2)
B(8)-C(21)	1.581(2)
C(9)-C(10)	1.520(2)
C(10)-C(11)	1.508(2)
C(11)-O(12)	1.4361(18)
O(12)-C(13)	1.3564(18)
C(13)-C(18)	1.390(2)
C(13)-C(14)	1.398(2)
C(14)-C(15)	1.388(2)
C(14)-C(19)	1.441(3)
C(15)-C(16)	1.380(3)
C(16)-C(17)	1.376(3)

C(17)-C(18)	1.389(2)
C(19)-N(20)	1.142(2)
C(21)-C(26)	1.392(2)
C(21)-C(22)	1.394(2)
C(22)-C(23)	1.383(2)
C(23)-C(24)	1.374(3)
C(24)-C(25)	1.370(3)
C(25)-C(26)	1.388(3)

C(5)-N(1)-C(2)	112.35(12)
C(5)-N(1)-C(9)	113.28(12)
C(2)-N(1)-C(9)	111.81(11)
C(5)-N(1)-B(8)	103.61(11)
C(2)-N(1)-B(8)	101.62(11)
C(9)-N(1)-B(8)	113.34(11)
N(1)-C(2)-C(3)	106.04(13)
O(3)-C(3)-O(4)	123.93(15)
O(3)-C(3)-C(2)	125.19(16)
O(4)-C(3)-C(2)	110.88(13)
C(3)-O(4)-B(8)	113.31(12)
N(1)-C(5)-C(6)	105.31(12)
O(6)-C(6)-O(7)	124.21(16)
O(6)-C(6)-C(5)	124.95(16)
O(7)-C(6)-C(5)	110.82(13)
C(6)-O(7)-B(8)	114.22(12)
O(4)-B(8)-O(7)	111.31(13)
O(4)-B(8)-C(21)	113.85(13)
O(7)-B(8)-C(21)	112.02(13)
O(4)-B(8)-N(1)	102.13(12)
O(7)-B(8)-N(1)	99.32(12)
C(21)-B(8)-N(1)	117.01(13)
N(1)-C(9)-C(10)	113.98(12)
C(11)-C(10)-C(9)	111.44(13)
O(12)-C(11)-C(10)	106.40(12)
C(13)-O(12)-C(11)	118.78(12)
O(12)-C(13)-C(18)	125.14(15)

O(12)-C(13)-C(14)	115.40(14)
C(18)-C(13)-C(14)	119.46(15)
C(15)-C(14)-C(13)	120.32(16)
C(15)-C(14)-C(19)	120.40(16)
C(13)-C(14)-C(19)	119.28(14)
C(16)-C(15)-C(14)	120.00(17)
C(17)-C(16)-C(15)	119.62(17)
C(16)-C(17)-C(18)	121.44(18)
C(17)-C(18)-C(13)	119.15(17)
N(20)-C(19)-C(14)	178.1(2)
C(26)-C(21)-C(22)	116.91(16)
C(26)-C(21)-B(8)	122.58(15)
C(22)-C(21)-B(8)	120.49(14)
C(23)-C(22)-C(21)	121.91(17)
C(24)-C(23)-C(22)	119.79(18)
C(25)-C(24)-C(23)	119.73(18)
C(24)-C(25)-C(26)	120.50(18)
C(25)-C(26)-C(21)	121.14(17)

References

(1) Chen, X.; Engle, K. M.; Wang, D. H.; Jin-Quan, Y. *Angew. Chem. Int. Ed.* **2009**, *48* (28), 5094–5115.

(2) Wencel-Delord, J.; Glorius, F. *Nat. Chem.* **2013**, *5*, 369.

(3) Johansson Seechurn, C. C. C.; Kitching, M. O.; Colacot, T. J.; Snieckus, V. *Angew. Chem. Int. Ed.* **2012**, *51* (21), 5062–5085.

(4) Roy, D.; Uozumi, Y. *Adv. Synth. Catal.* **2018**, *360* (4), 602–625.

(5) Lyons, T. W.; Sanford, M. S. *Chem. Rev.* **2010**, *110* (2), 1147–1169.

(6) Torborg, C.; Beller, M. *Adv. Synth. Catal.* **2009**, *351* (18), 3027–3043.

(7) Yamaguchi, J.; Yamaguchi, A. D.; Itami, K. *Angew. Chem. Int. Ed.* **2012**, *51* (36), 8960–9009.

(8) McMurray, L.; O'Hara, F.; Gaunt, M. J. *Chem. Soc. Rev.* **2011**, *40* (4), 1885–1898.

(9) Sambiagio, C.; Schönbauer, D.; Blieck, R.; Dao-Huy, T.; Pototschnig, G.; Schaaf, P.; Wiesinger, T.; Zia, M. F.; Wencel-Delord, J.; Besset, T.; Maes, B. U. W.; Schnürch, M. *Chem. Soc. Rev.* **2018**, *47* (17), 6603–6743.

(10) Neufeldt, S. R.; Sanford, M. S. *Acc. Chem. Res.* **2012**, *45* (6), 936–946.

(11) Blanksby, S. J.; Ellison, G. B. *Acc. Chem. Res.* **2003**, *36* (4), 255–263.

(12) Cope, A. C.; Siekman, R. W. *J. Am. Chem. Soc.* **1965**, *87* (4), 3272–3273.

(13) Sigman, M. S.; Schultz, M. J. *Org. Biomol. Chem.* **2004**, *2* (18), 2551–2554.

(14) Dick, A. R.; Hull, K. L.; Sanford, M. S. *J. Am. Chem. Soc.* **2004**, *126* (8), 2300–2301.

(15) Kalyani, D.; Sanford, M. S. *Org. Lett.* **2005**, *7* (19), 4149–4152.

(16) Stowers, K. J.; Sanford, M. S. *Org. Lett.* **2009**, *11* (20), 4584–4587.

(17) Racowski, J. M.; Dick, A. R.; Sanford, M. S. *J. Am. Chem. Soc.* **2009**, *131* (31), 10974–10983.

(18) Kalyani, D.; Deprez, N. R.; Desai, L. V; Sanford, M. S. *J. Am. Chem. Soc.* **2005**, *127* (20), 7330–7331.

(19) Deprez, N. R.; Sanford, M. S. *Inorg. Chem.* **2007**, *46* (6), 1924–1935.

(20) Deprez, N. R.; Sanford, M. S. *J. Am. Chem. Soc.* **2009**, *131* (31), 11234–11241.

(21) Cotton, F. A.; Gu, J.; Murillo, C. A.; Timmons, D. J. *J. Am. Chem. Soc.* **1998**, *120* (50), 13280–

13281.

(22) Cotton, F. A.; Koshevoy, I. O.; Lahuerta, P.; Murillo, C. A.; Sanaú, M.; Ubeda, M. A.; Zhao, Q. *J. Am. Chem. Soc.* **2006**, *128* (42), 13674–13675.

(23) Powers, D. C.; Ritter, T. *Nat. Chem.* **2009**, *1*, 302.

(24) Powers, D. C.; Xiao, D. Y.; Geibel, M. A. L.; Ritter, T. *J. Am. Chem. Soc.* **2010**, *132* (41), 14530–14536.

(25) Shi, Z.; Li, B.; Wan, X.; Cheng, J.; Fang, Z.; Cao, B.; Qin, C.; Wang, Y. *Angew. Chem. Int. Ed.* **2007**, *46* (29), 5554–5558.

(26) Wang, D. H.; Mei, T. S.; Yu, J. Q. *J. Am. Chem. Soc.* 2008, *130* (52), 17676–17677.

(27) Cai, G.; Fu, Y.; Li, Y.; Wan, X.; Shi, Z. *J. Am. Chem. Soc.* **2007**, *129* (24), 7666–7673.

(28) Tsang, W. C. P.; Zheng, N.; Buchwald, S. L. *J. Am. Chem. Soc.* **2005**, *127* (42), 14560–14561.

(29) Brasche, G.; García-Fortanet Jorge; Buchwald, S. L. *Org. Lett.* **2008**, *10* (11), 2207–2210.

(30) Bay, K. L.; Yang, Y.-F.; Houk, K. N. *J. Organomet. Chem.* **2018**, *864*, 19–25.

(31) Giri, R.; Maugel, N.; Li, J.-J.; Wang, D.-H.; Breazzano, S. P.; Saunders, L. B.; Yu, J.-Q. *J. Am. Chem. Soc.* **2007**, *129* (12), 3510–3511.

(32) Zhou, H.; Xu, Y.-H.; Chung, W.-J.; Loh, T.-P. *Angew. Chem. Int. Ed.* **2009**, *48* (29), 5355–5357.

(33) Chiong, H. A.; Pham, Q.-N.; Daugulis, O. *J. Am. Chem. Soc.* **2007**, *129* (32), 9879–9884.

(34) Dogan, Ö.; Gürbüz, N.; Özdemir, İ.; Çetinkaya, B. *Heteroat. Chem.* **2008**, *19* (6), 569–574.

(35) Ryabov, A. D.; Sakodinskaya, I. K.; Yatsimirsky, A. K. *J. Chem. Soc. Dalt. Trans.* **1985**, No. 12, 2629–2638.

(36) Lane, B. S.; Brown, M. A.; Sames, D. *J. Am. Chem. Soc.* **2005**, *127* (22), 8050–8057.

(37) Park, C.-H.; Ryabova, V.; Seregin, I. V; Sromek, A. W.; Gevorgyan, V. *Org. Lett.* **2004**, *6* (7), 1159–1162.

(38) Okazawa, T.; Satoh, T.; Miura, M.; Nomura, M. *J. Am. Chem. Soc.* **2002**, *124* (19), 5286–5287.

(39) Glover, B.; Harvey, K. A.; Liu, B.; Sharp, M. J.; Tymoschenko, M. F. *Org. Lett.* **2003**, *5* (3), 301–304.

(40) García-Cuadrado, D.; Braga, A. A. C.; Maseras, F.; Echavarren, A. M. *J. Am. Chem. Soc.* **2006**, *128* (4), 1066–1067.

(41) Davies, D. L.; Donald, S. M. A.; Macgregor, S. A. *J. Am. Chem. Soc.* **2005**, *127* (40), 13754–13755.

(42) Balcells, D.; Clot, E.; Eisenstein, O. *Chem. Rev.* **2010**, *110* (2), 749–823.

(43) Ryabov, A. D. *Chem. Rev.* **1990**, *90* (2), 403–424.

(44) Boutadla, Y.; Davies, D. L.; Macgregor, S. A.; Poblador-Bahamonde, A. I. *Dalt. Trans.* **2009**, No. 30, 5820–5831.

(45) García-Cuadrado, D.; de Mendoza, P.; Braga, A. A. C.; Maseras, F.; Echavarren, A. M. *J. Am. Chem. Soc.* **2007**, *129* (21), 6880–6886.

(46) Gorelsky, S. I.; Lapointe, D.; Fagnou, K. *J. Am. Chem. Soc.* **2008**, *130* (33), 10848–10849.

(47) Lafrance, M.; Rowley, C. N.; Woo, T. K.; Fagnou, K. *J. Am. Chem. Soc.* **2006**, *128* (27), 8754–8756.

(48) Pinto, A.; Neuville, L.; Retailleau, P.; Zhu, J. *Org. Lett.* **2006**, *8* (21), 4927–4930.

(49) Lafrance, M.; Fagnou, K. *J. Am. Chem. Soc.* **2006**, *128* (51), 16496–16497.

(50) Nishikata, T.; Abela, A. R.; Huang, S.; Lipshutz, B. H. *Beilstein J. Org. Chem.* **2016**, *12*, 1040–1064.

(51) Bosque, R.; Maseras, F. *Eur. J. Inorg. Chem.* **2005**, *2005* (20), 4040–4047.

(52) Frutos-Pedreño, R.; García-Sánchez, E.; Oliva-Madrid, M. J.; Bautista, D.; Martínez-Viviente, E.; Saura-Llamas, I.; Vicente, J. *Inorg. Chem.* **2016**, *55* (11), 5520–5533.

(53) Yang, J. *Org. Biomol. Chem.* **2015**, *13* (7), 1930–1941.

(54) Chatani, N.; Ie, Y.; Kakiuchi, F.; Murai, S. *J. Org. Chem.* **1997**, *62* (8), 2604–2610.

(55) Shabashov, D.; Daugulis, O. *Org. Lett.* **2005**, *7* (17), 3657–3659.

(56) Taylor, R. D.; MacCoss, M.; Lawson, A. D. G. *J. Med. Chem.* **2014**, *57* (14), 5845–5859.

(57) Schröter, S.; Stock, C.; Bach, T. *Tetrahedron* **2005**, *61* (9), 2245–2267.

(58) Desai, L. V; Stowers, K. J.; Sanford, M. S. *J. Am. Chem. Soc.* **2008**, *130* (40), 13285–13293.

(59) Yu, W.-Y.; Sit, W. N.; Zhou, Z.; Chan, A. S.-C. *Org. Lett.* **2009**, *11* (15), 3174–3177.

(60) Kalyani, D.; Dick, A. R.; Anani, W. Q.; Sanford, M. S. *Org. Lett.* **2006**, *8* (12), 2523–2526.

(61) Zhang, G.; Sun, S.; Yang, F.; Zhang, Q.; Kang, J.; Wu, Y.; Wu, Y. *Adv. Synth. Catal.* **2015**, *357* (2-3), 443–450.

(62) Hull, K. L.; Anani, W. Q.; Sanford, M. S. *J. Am. Chem. Soc.* **2006**, *128* (22), 7134–7135.

(63) Chen, Z.-B.; Zhang, F.-L.; Yuan, Q.; Chen, H.-F.; Zhu, Y.-M.; Shen, J.-K. *RSC Adv.* **2016**, *6* (69), 64234–64238.

(64) Yu, W.-Y.; Sit, W. N.; Lai, K.-M.; Zhou, Z.; Chan, A. S. C. *J. Am. Chem. Soc.* **2008**, *130* (11), 3304–3306.

(65) Wang, Z.; Li, Y.; Zhu, F.; Wu, X.-F. *Adv. Synth. Catal.* **2016**, *358* (17), 2855–2859.

(66) Zhao, X.; Dimitrijević, E.; Dong, V. M. *J. Am. Chem. Soc.* **2009**, *131* (10), 3466–3467.

(67) Zhou, F.; Wang, D.-S.; Guan, X.; Driver, T. G. *Angew. Chem.* **2017**, *129* (16), 4601–4605.

(68) Jia, X.; Zhang, S.; Wang, W.; Luo, F.; Cheng, J. *Org. Lett.* **2009**, *11* (14), 3120–3123.

(69) Bao, Y.-S.; Zhang, D.; Jia, M.; Zhaorigetu, B. *Green Chem.* **2016**, *18* (7), 2072–2077.

(70) Liu, X.; Yi, Z.; Wang, J.; Liu, G. *RSC Adv.* **2015**, *5* (14), 10641–10646.

(71) Xiao, F.; Chen, S.; Huang, H.; Deng, G.-J. *Eur. J. Org. Chem.* **2015**, *2015* (36), 7919–7925.

(72) Chu, J.-H.; Lin, P.-S.; Wu, M.-J. *Organometallics* **2010**, *29* (18), 4058–4065.

(73) Kinuta, H.; Tobisu, M.; Chatani, N. *J. Am. Chem. Soc.* **2015**, *137*, 1593.

(74) Tobisu, M.; Zhao, J.; Kinuta, H.; Furukawa, T.; Igarashi, T.; Chatani, N. *Adv. Synth. Catal.* **2016**, *358* (15), 2417–2421.

(75) Li, J.; Wang, Z.-X. *Org. Lett.* **2017**, *19* (14), 3723–3726.

(76) Richter, H.; Beckendorf, S.; Mancheño, O. G. *Adv. Synth. Catal.* **2011**, *353* (2-3), 295–302.

(77) García-Rubia, A.; Fernández-Ibáñez, M. Á.; Gómez Arrayás, R.; Carretero, J. C. *Chem. – A Eur. J.* **2011**, *17* (13), 3567–3570.

(78) Sun, M.; Wang, Z.; Wang, J.; Guo, P.; Chen, X.; Li, Y.-M. *Org. Biomol. Chem.* **2016**, *14* (45), 10585–10588.

(79) Huang, C.; Chernyak, N.; Dudnik, A. S.; Gevorgyan, V. *Adv. Synth. Catal.* **2011**, *353* (8), 1285–1305.

(80) Denmark, S. E.; Ober, M. H. *Adv. Synth. Catal.* **2004**, *346* (13-15), 1703–1714.

(81) Zhang, Y.; Jiang, H.; Chen, D.; Zhang, Y. *Org. Biomol. Chem.* **2016**, *14* (20), 4585–4589.

(82) Zaitsev, V. G.; Shabashov, D.; Daugulis, O. *J. Am. Chem. Soc.* **2005**, *127*, 13154–13155.

(83) Daugulis, O.; Roane, J.; Tran, L. D. *Acc. Chem. Res.* **2015**, *48* (4), 1053–1064.

(84) Rouquet, G.; Chatani, N. *Angew. Chem. Int. Ed.* **2013**, *52* (45), 11726–11743.

(85) Canty, A. J. *Dalt. Trans.* **2009**, No. 47, 10409–10417.

(86) Padmavathi, R.; Sankar, R.; Gopalakrishnan, B.; Parella, R.; Babu, S. A. *Eur. J. Org. Chem.* **2015**, *2015* (17), 3727–3742.

(87) Rajkumar, V.; Naveen; Babu, S. A. *ChemistrySelect* **2016**, *1* (6), 1207–1219.

(88) Bisht, N.; Babu, S. A. *Tetrahedron* **2016**, *72* (39), 5886–5897.

(89) Liu, Y.; Zhang, Y.; Huang, M.; Wan, J.-P. *RSC Adv.* **2015**, *5* (57), 46192–46196.

(90) Wang, X.; Niu, S.; Xu, L.; Zhang, C.; Meng, L.; Zhang, X.; Ma, D. *Org. Lett.* **2017**, *19* (1), 246–249.

(91) Zhang, S.-Y.; Li, Q.; He, G.; Nack, W. A.; Chen, G. *J. Am. Chem. Soc.* **2015**, *137* (1), 531–539.

(92) Shao, C.; Shi, G.; Zhang, Y. *Eur. J. Org. Chem.* **2016**, *2016* (33), 5529–5538.

(93) Li, Z.; Sun, S.; Qiao, H.; Yang, F.; Zhu, Y.; Kang, J.; Wu, Y.; Wu, Y. *Org. Lett.* **2016**, *18* (18), 4594–4597.

(94) Gui, Q.; Chen, X.; Hu, L.; Wang, D.; Liu, J.; Tan, Z. *Adv. Synth. Catal.* **2016**, *358* (4), 509–514.

(95) Chabrier, A.; Bruneau, A.; Benmahdjoub, S.; Benmerad, B.; Belaid, S.; Brion, J.-D.; Alami, M.; Messaoudi, S. *Chem. – A Eur. J.* **2016**, *22* (42), 15006–15010.

(96) Engle, K. M.; Mei, T.-S.; Wasa, M.; Yu, J.-Q. *Acc. Chem. Res.* **2012**, *45* (6), 788–802.

(97) Li, G.; Wan, L.; Zhang, G.; Leow, D.; Spangler, J.; Yu, J. Q. *J. Am. Chem. Soc.* **2015**, *137* (13), 4391–4397.

(98) Engle, K. M.; Yu, J.-Q. *J. Org. Chem.* **2013**, *78* (18), 8927–8955.

(99) Dey, A.; Sinha, S. K.; Achar, T. K.; Maiti, D. *Angew. Chem. Int. Ed.* **2019**, *58* (32), 10820–10843.

(100) Mo, F.; Trzepkowski, L. J.; Dong, G. *Angew. Chem. Int. Ed.* **2012**, *51* (52), 13075–13079.

(101) Sun, X.; Shan, G.; Sun, Y.; Rao, Y. *Angew. Chem. Int. Ed.* **2013**, *52* (16), 4440–4444.

(102) Mei, T.-S.; Giri, R.; Maugel, N.; Yu, J.-Q. *Angew. Chem. Int. Ed.* **2008**, *47* (28), 5215–5219.

(103) Giri, R.; Yu, J.-Q. *J. Am. Chem. Soc.* **2008**, *130* (43), 14082–14083.

(104) Zhang, Y.-H.; Yu, J.-Q. *J. Am. Chem. Soc.* **2009**, *131* (41), 14654–14655.

(105) Zhang, Y.-H.; Shi, B.-F.; Yu, J.-Q. *Angew. Chem. Int. Ed.* **2009**, *48* (33), 6097–6100.

(106) Yoo, E. J.; Ma, S.; Mei, T.-S.; Chan, K. S. L.; Yu, J.-Q. *J. Am. Chem. Soc.* **2011**, *133* (20), 7652–7655.

(107) Chan, K. S. L.; Wasa, M.; Wang, X.; Yu, J.-Q. *Angew. Chem. Int. Ed.* **2011**, *50* (39), 9081–9084.

(108) Lu, Y.; Wang, D.-H.; Engle, K. M.; Yu, J.-Q. *J. Am. Chem. Soc.* **2010**, *132* (16), 5916–5921.

(109) Wang, X.; Lu, Y.; Dai, H.-X.; Yu, J.-Q. *J. Am. Chem. Soc.* **2010**, *132* (35), 12203–12205.

(110) Li, J.-J.; Mei, T.-S.; Yu, J.-Q. *Angew. Chem. Int. Ed.* **2008**, *47* (34), 6452–6455.

(111) Mei, T.-S.; Wang, X.; Yu, J.-Q. *J. Am. Chem. Soc.* **2009**, *131* (31), 10806–10807.

(112) Wang, D.-H.; Wasa, M.; Giri, R.; Yu, J.-Q. *J. Am. Chem. Soc.* **2008**, *130* (23), 7190–7191.

(113) Ping, Y.; Wang, L.; Ding, Q.; Peng, Y. *Adv. Synth. Catal.* **2017**, *359* (19), 3274–3291.

(114) Li, G.; Leow, D.; Wan, L.; Yu, J.-Q. *Angew. Chem. Int. Ed.* **2013**, *52* (4), 1245–1247.

(115) Engle, K. M.; Wang, D.-H.; Yu, J.-Q. *J. Am. Chem. Soc.* **2010**, *132* (40), 14137–14151.

(116) Gensch, T.; Hopkinson, M. N.; Glorius, F.; Wencel-Delord, J. *Chem. Soc. Rev.* **2016**, *45* (10), 2900–2936.

(117) Cong, X.; Tang, H.; Wu, C.; Zeng, X. *Organometallics* **2013**, *32* (21), 6565–6575.

(118) Cheng, G.-J.; Yang, Y.-F.; Liu, P.; Chen, P.; Sun, T.-Y.; Li, G.; Zhang, X.; Houk, K. N.; Yu, J.-Q.; Wu, Y.-D. *J. Am. Chem. Soc.* **2014**, *136* (3), 894–897.

(119) Colomer, I.; Chamberlain, A. E. R.; Haughey, M. B.; Donohoe, T. J. *Nat. Rev. Chem.* **2017**, *1*, 0088.

(120) Sinha, S. K.; Bhattacharya, T.; Maiti, D. *React. Chem. Eng.* **2019**, *4* (2), 244–253.

(121) Shi, B.-F.; Zhang, Y.-H.; Lam, J. K.; Wang, D.-H.; Yu, J.-Q. *J. Am. Chem. Soc.* **2010**, *132* (2), 460–461.

(122) Leow, D.; Li, G.; Mei, T.-S.; Yu, J.-Q. *Nature* **2012**, *486* (7404), 518–522.

(123) Bag, S.; Patra, T.; Modak, A.; Deb, A.; Maity, S.; Dutta, U.; Dey, A.; Kancherla, R.; Maji, A.; Hazra, A.; Bera, M.; Maiti, D. *J. Am. Chem. Soc.* **2015**, *137* (37), 11888–11891.

(124) Beesley, R. M.; Ingold, C. K.; Thorpe, J. F. *J. Chem. Soc. Trans.* **1915**, *107* (0), 1080–1106.

(125) Tang, R.-Y.; Li, G.; Yu, J.-Q. *Nature* **2014**, *507*, 215.

(126) Yang, G.; Lindovska, P.; Zhu, D.; Kim, J.; Wang, P.; Tang, R.-Y.; Movassaghi, M.; Yu, J.-Q. *J. Am. Chem. Soc.* **2014**, *136* (30), 10807–10813.

(127) Wan, L.; Dastbaravardeh, N.; Li, G.; Yu, J.-Q. *J. Am. Chem. Soc.* **2013**, *135* (48), 18056–18059.

(128) Yang, Y.-F.; Cheng, G.-J.; Liu, P.; Leow, D.; Sun, T.-Y.; Chen, P.; Zhang, X.; Yu, J.-Q.; Wu, Y.-D.; Houk, K. N. *J. Am. Chem. Soc.* **2014**, *136* (1), 344–355.

(129) Fang, L.; Saint-Denis, T. G.; Taylor, B. L. H.; Ahlquist, S.; Hong, K.; Liu, S.; Han, L.; Houk, K. N.; Yu, J.-Q. *J. Am. Chem. Soc.* **2017**, *139* (31), 10702–10714.

(130) Deng, Y.; Yu, J.-Q. *Angew. Chem. Int. Ed.* **2015**, *54* (3), 888–891.

(131) Bera, M.; Modak, A.; Patra, T.; Maji, A.; Maiti, D. *Org. Lett.* **2014**, *16* (21), 5760–5763.

(132) Li, S.; Ji, H.; Cai, L.; Li, G. *Chem. Sci.* **2015**, *6* (10), 5595–5600.

(133) Li, S.; Cai, L.; Ji, H.; Yang, L.; Li, G. *Nat. Commun.* **2016**, *7*, 10443.

(134) Maity, S.; Hoque, E.; Dhawa, U.; Maiti, D. *Chem. Commun.* **2016**, *52* (97), 14003–14006.

(135) Lee, S.; Lee, H.; Tan, K. L. *J. Am. Chem. Soc.* **2013**, *135* (50), 18778–18781.

(136) Patra, T.; Watile, R.; Agasti, S.; Naveen, T.; Maiti, D. *Chem. Commun.* **2016**, *52* (10), 2027–2030.

(137) Patra, T.; Bag, S.; Kancherla, R.; Mondal, A.; Dey, A.; Pimparkar, S.; Agasti, S.; Modak, A.; Maiti, D. *Angew. Chem. Int. Ed.* **2016**, *55* (27), 7751–7755.

(138) Maji, A.; Guin, S.; Feng, S.; Dahiya, A.; Singh, V. K.; Liu, P.; Maiti, D. *Angew. Chemie Int. Ed.* **2017**, *56* (47), 14903–14907.

(139) Yang, G.; Zhu, D.; Wang, P.; Tang, R.-Y.; Yu, J.-Q. *Chem. – A Eur. J.* **2018**, *24* (14), 3434–3438.

(140) Bera, M.; Maji, A.; Sahoo, S. K.; Maiti, D. *Angew. Chem. Int. Ed.* **2015**, *54* (29), 8515–8519.

(141) Maji, A.; Bhaskararao, B.; Singha, S.; Sunoj, R. B.; Maiti, D. *Chem. Sci.* **2016**, *7* (5), 3147–3153.

(142) Modak, A.; Mondal, A.; Watile, R.; Mukherjee, S.; Maiti, D. *Chem. Commun.* **2016**, *52* (96),

13916–13919.

(143) Zhang, L.; Zhao, C.; Liu, Y.; Xu, J.; Xu, X.; Jin, Z. *Angew. Chem. Int. Ed.* **2017**, *56* (40), 12245–12249.

(144) Modak, A.; Patra, T.; Chowdhury, R.; Raul, S.; Maiti, D. *Organometallics* **2017**, *36* (13), 2418–2423.

(145) Bera, M.; Sahoo, S. K.; Maiti, D. *ACS Catal.* **2016**, *6* (6), 3575–3579.

(146) Chu, L.; Shang, M.; Tanaka, K.; Chen, Q.; Pissarnitski, N.; Streckfuss, E.; Yu, J.-Q. *ACS Cent. Sci.* **2015**, *1* (7), 394–399.

(147) Jin, Z.; Chu, L.; Chen, Y.-Q.; Yu, J.-Q. *Org. Lett.* **2018**, *20* (2), 425–428.

(148) Bag, S.; Jayarajan, R.; Dutta, U.; Chowdhury, R.; Mondal, R.; Maiti, D. *Angew. Chem. Int. Ed.* **2017**, *56* (41), 12538–12542.

(149) Bag, S.; Jayarajan, R.; Mondal, R.; Maiti, D. *Angew. Chem. Int. Ed.* **2017**, *56* (12), 3182–3186.

(150) Jayarajan, R.; Das, J.; Bag, S.; Chowdhury, R.; Maiti, D. *Angew. Chem. Int. Ed.* **2018**, *57* (26), 7659–7663.

(151) Xu, H.; Liu, M.; Li, L.-J.; Cao, Y.-F.; Yu, J.-Q.; Dai, H.-X. *Org. Lett.* **2019**, *21* (12), 4887–4891.

(152) Bag, S.; Petzold, M.; Sur, A.; Bhowmick, S.; Werz, D. B.; Maiti, D. *Chem. – A Eur. J.* **2019**, *25,* 9433-9437.

(153) Brochetta, M.; Borsari, T.; Bag, S.; Jana, S.; Maiti, S.; Porta, A.; Werz, D. B.; Zanoni, G.; Maiti, D. *Chem. – A Eur. J.* **2019**, *25*, 10323-10327.

(154) Xu, J.; Chen, J.; Gao, F.; Xie, S.; Xu, X.; Jin, Z.; Yu, J.-Q. *J. Am. Chem. Soc.* **2019**, *141* (5), 1903–1907.

(155) Ihara, H.; Suginome, M. *J. Am. Chem. Soc.* **2009**, *131* (22), 7502–7503.

(156) Hall, D. G. *Boronic Acids: Preparation, Applications in Organic Synthesis and Medicine*, 1st ed.; Hall, D. G., Ed.; John Wiley & Sons, Ltd, 2006.

(157) Lennox, A. J. J.; Lloyd-Jones, G. C. *Chem. Soc. Rev.* **2014**, *43* (1), 412–443.

(158) Fyfe, J. W. B.; Watson, A. J. B. *Chem* **2017**, *3* (1), 31–55.

(159) Brown, D. G.; Boström, J. *J. Med. Chem.* **2016**, *59* (10), 4443–4458.

(160) Ihara, H.; Ueda, A.; Suginome, M. *Chem. Lett.* **2011**, *40* (9), 916–918.

(161) Yamamoto, T.; Ishibashi, A.; Suginome, M. *Chem. Lett.* **2017**, *46* (8), 1169–1172.

(162) Yamamoto, T.; Ishibashi, A.; Suginome, M. *Org. Lett.* **2017**, *19* (4), 886–889.

(163) Yamamoto, T.; Ishibashi, A.; Suginome, M. *Org. Lett.* **2019**, *21* (16), 6235–6240.

(164) Ihara, H.; Koyanagi, M.; Suginome, M. *Org. Lett.* **2011**, *13* (10), 2662–2665.

(165) Koyanagi, M.; Eichenauer, N.; Ihara, H.; Yamamoto, T.; Suginome, M. *Chem. Lett.* **2013**, *42* (5), 541–543.

(166) Yamamoto, T.; Ishibashi, A.; Koyanagi, M.; Ihara, H.; Eichenauer, N.; Suginome, M. *Bull. Chem. Soc. Jpn.* **2017**, *90* (5), 604–606.

(167) Devaraj, K.; Ingner, F. J. L.; Sollert, C.; Gates, P. J.; Orthaber, A.; Pilarski, L. T. *J. Org. Chem.* **2019**, *84* (9), 5863–5871.

(168) Erb, W.; Hurvois, J.-P.; Roisnel, T.; Dorcet, V. *Organometallics* **2018**, *37* (21), 3780–3790.

(169) Mancilla, T.; Contreras, R.; Wrackmeyer, B. *J. Organomet. Chem.* **1986**, *307* (1), 1–6.

(170) Contreras, R.; García, C.; Mancilla, T.; Wrackmeyer, B. *J. Organomet. Chem.* **1983**, *246* (3), 213–217.

(171) Gillis, E. P.; Burke, M. D. *J. Am. Chem. Soc.* **2008**, *130* (43), 14084–14085.

(172) Dick, G. R.; Knapp, D. M.; Gillis, E. P.; Burke, M. D. *Org. Lett.* **2010**, *12* (10), 2314–2317.

(173) Gonzalez, J. A.; Ogba, O. M.; Morehouse, G. F.; Rosson, N.; Houk, K. N.; Leach, A. G.; Cheong, P. H.-Y.; Burke, M. D.; Lloyd-Jones, G. C. *Nat. Chem.* **2016**, *8* (11), 1067–1075.

(174) Cox, P. A.; Leach, A. G.; Campbell, A. D.; Lloyd-Jones, G. C. *J. Am. Chem. Soc.* **2016**, *138* (29), 9145–9157.

(175) Gillis, E. P.; Burke, M. D. *J. Am. Chem. Soc.* **2007**, *129* (21), 6716–6717.

(176) Lennox, A. J. J.; Lloyd-Jones, G. C. *Angew. Chem. Int. Ed.* **2013**, *52* (29), 7362–7370.

(177) Uno, B. E.; Gillis, E. P.; Burke, M. D. *Tetrahedron* **2009**, *65* (16), 3130–3138.

(178) Struble, J. R.; Lee, S. J.; Burke, M. D. *Tetrahedron* **2010**, *66* (26), 4710–4718.

(179) Woerly, E. M.; Struble, J. R.; Palyam, N.; O'Hara, S. P.; Burke, M. D. *Tetrahedron* **2011**, *67* (24), 4333–4343.

(180) Woerly, E. M.; Miller, J. E.; Burke, M. D. *Tetrahedron* **2013**, *69* (36), 7732–7740.

(181) Ballmer, S.; Gillis, E.; Burke, M. *Org. Synth.* **2009**, *86*, 344.

(182) Lee, S. J.; Gray, K. C.; Paek, J. S.; Burke, M. D. *J. Am. Chem. Soc.* **2008**, *130* (2), 466–468.

(183) Woerly, E. M.; Cherney, A. H.; Davis, E. K.; Burke, M. D. *J. Am. Chem. Soc.* **2010**, *132* (20), 6941–6943.

(184) Lee, S. J.; Anderson, T. M.; Burke, M. D. *Angew. Chem. Int. Ed.* **2010**, *49* (47), 8860–8863.

(185) Palacios, D. S.; Dailey, I.; Siebert, D. M.; Wilcock, B. C.; Burke, M. D. *Proc. Natl. Acad. Sci.* **2011**, *108* (17), 6733–6738.

(186) Fujii, S.; Chang, S. Y.; Burke, M. D. *Angew. Chem. Int. Ed.* **2011**, *50* (34), 7862–7864.

(187) Woerly, E. M.; Roy, J.; Burke, M. D. *Nat Chem* **2014**, *6* (6), 484–491.

(188) Vaz, B.; Pereira, R.; Pérez, M.; Álvarez, R.; de Lera, A. R. *J. Org. Chem.* **2008**, *73* (17), 6534–6541.

(189) Barros, M. P.; Pinto, E.; Colepicolo, P.; Pedersén, M. *Biochem. Biophys. Res. Commun.* **2001**, *288* (1), 225–232.

(190) Endo, M. M.; Cioffi, A. G.; Burke, M. D. *Synlett* **2016**, *27* (03), 337–354.

(191) Merrifield, R. B. *J. Am. Chem. Soc.* **1963**, *85* (14), 2149–2154.

(192) Palomo, J. M. *RSC Adv.* **2014**, *4* (62), 32658–32672.

(193) Maechling, S.; Good, J.; Lindell, S. D. *J. Comb. Chem.* **2010**, *12* (6), 818–821.

(194) Li, J.; Ballmer, S. G.; Gillis, E. P.; Fujii, S.; Schmidt, M. J.; Palazzolo, A. M. E.; Lehmann, J. W.; Morehouse, G. F.; Burke, M. D. *Science* **2015**, *347*, 1221–1226.

(195) Knapp, D. M.; Gillis, E. P.; Burke, M. D. *J. Am. Chem. Soc.* **2009**, *131* (20), 6961–6963.

(196) Dick, G. R.; Woerly, E. M.; Burke, M. D. *Angew. Chem. Int. Ed.* **2012**, *51* (11), 2667–2672.

(197) Li, J.; Burke, M. D. *J. Am. Chem. Soc.* **2011**, *133* (35), 13774–13777.

(198) Mancilla, T.; Alarcon, M. de L.; Carrillo, L. *Heteroat. Chem.* **1994**, *5* (6), 455–462.

(199) Mancilla, T.; Ancona, R. M. F.; Martínez, M. L. *Polyhedron* **2009**, *28* (13), 2771–2775.

(200) Ballmer, S. G.; Gillis, E. P.; Burke, M. D. *Org. Synth.* **2009**, *86*, 344–359.

(201) Close, A. J.; Kemmitt, P.; Emmerson, M. K.; Spencer, J. *Tetrahedron* **2014**, *70* (40), 9125-9131.

(202) Mancilla, T.; Hopfl, H.; Bravo, G.; Carillo, L. *Main Group Metal Chem.* **1997**, *20*, 31-36.

(203) Pérez, J. M.; Cano, R.; McGlacken, G. P.; Ramón, D. J. *RSC Adv.* **2016**, *6* (43), 36932–36941.

(204) Dherbassy, Q.; Schwertz, G.; Chessé, M.; Hazra, C. K.; Wencel-Delord, J.; Colobert, F. *Chem. - A Eur. J.* **2016**, *22* (5), 1735–1743.

(205) Williams, M. A.; Rapoport, H. *J. Org. Chem.* **1993**, *58* (5), 1151–1158.

(206) Murray, P. M.; Bellany, F.; Benhamou, L.; Bučar, D.-K.; Tabor, A. B.; Sheppard, T. D. *Org. Biomol. Chem.* **2016**, *14* (8), 2373–2384.

(207) Yang, Q.; Sheng, M.; Henkelis, J. J.; Tu, S.; Wiensch, E.; Zhang, H.; Zhang, Y.; Tucker, C.; Ejeh, D. E. *Org. Process Res. Dev.* **2019**, *23* (10), 2210-2217.

(208) Kirchhoff, J. H.; Netherton, M. R.; Hills, I. D.; Fu, G. C. *J. Am. Chem. Soc.* **2002**, *124* (46), 13662–13663.

(209) Wan, L.; Dastbaravardeh, N.; Li, G.; Yu, J. Q. *J. Am. Chem. Soc.* **2013**, *135* (48), 18056–18059.

(210) Shimizu, M.; Hiyama, T. *Angew. Chem. Int. Ed.* **2005**, *44* (2), 214–231.

(211) Furuya, T.; Ritter, T. *Org. Lett.* **2009**, *11* (13), 2860–2863.

(212) Zhu, C.; Wang, R.; Falck, J. R. *Org. Lett.* **2012**, *14* (13), 3494–3497.

(213) Gupta, S.; Sureshbabu, P.; Singh, A. K.; Sabiah, S.; Kandasamy, J. *Tetrahedron Lett.* **2017**, *58* (10), 909–913.

(214) Dey, A.; Agasti, S.; Maiti, D. *Org. Biomol. Chem.* **2016**, *14* (24), 5440–5453.